2005

Population dynamics of Clausocalanus furcatus (Copepoda, Calanoida) in the northern Gulf of Mexico

Hongsheng Bi
Louisiana State University and Agricultural and Mechanical College

POPULATION DYNAMICS OF *CLAUSOCALANUS FURCATUS* (COPEPODA, CALANOIDA) IN THE NORTHERN GULF OF MEXICO

A Dissertation

Submitted to the Graduate Faculty of the
Louisiana State University and
Agricultural and Mechanical College
in partial fulfillment of the
requirements for the degree of
Doctor of Philosophy

in

The Department of Oceanography and Coastal Sciences by

Hongsheng Bi
B.S., Ocean University of Qingdao, 1994
M.S., Institute of Oceanography, Qingdao 1996
May, 2005

ACKNOWLEDGEMENTS

First and foremost, I would like to thank my major advisor Dr. Mark Benfield for his support throughout the project. His guidance, encouragement and patience have been an inspiration, which helped me tremendously in completing this dissertation. I would also like to thank my committee members, Dr. Kenneth Rose, Dr. Robert Downer, Dr. Michael Dagg, and Dr. Richard Shaw for their support, valuable comments and advice.

This project would not have been possible, without the help of the crew on South Timbalier 151. I want to thank Dr. Richard Shaw and Dr. Michael Dagg for use of their equipment. I also want to thank Dr. Samuel Bentley for the help with the particulate organic carbon measurements, Dr. Gregory Stone for providing the wind and water level data, Dr. Nan Walker for providing the satellite images, and Dr. Lawrence Rouse for advice on analyzing wind and tidal data.

Additionally, I would like to thank Sean Keenan for the help with field work and reading through my drafts. I also want to thank Shaye Sable, Aaron Adamack, Harmon Brown and Nicole Smith for their help and encouragements throughout the years. Special thank goes to the zooplankton research group, Mark Benfield, Sean Keenan, Malinda Sutor and Harmon Brown.

Finally, I want to thank my parents for their understanding and support.

TABLE OF CONTENTS

LIST OF TABLES

LIST OF FIGURES

ABSTRACT

Copepods are important components of marine ecosystems. Understanding copepod population dynamics can help interpret variations in both primary producers and higher trophic levels. Egg production, stage duration, and stage–specific mortality rates are key parameters describing copepod population dynamics. Estimation of stage–specific mortality is complicated due to a complex life history, patchiness, and sampling biases. This study was undertaken to quantify the population dynamics of the copepod *Clausocalanus furcatus* in the northern Gulf of Mexico and to assess the utility of available mortality estimation methods in a highly advective environment. Zooplankton samples were taken every 12h from March 18–April 6, and May 15–June 9, 2003 from an offshore petroleum platform using a 153μm net and a 30L Niskin bottle to characterize the mesozooplankton assemblage. Incubation experiments were conducted during June–July 2002, March–April 2003, and May–June 2003 to measure egg production rates and stage durations. Stage–specific mortality rates were estimated using the horizontal life table (HTL), vertical life table (VTL), quadratic programming method (QPM) and inverse matrix method (IMM). Mesozooplankton communities in the study area were influenced by the Mississippi River plume. Field estimates of the mean egg production rate of *C. furcatus* were lower than measurements from lab incubation experiments. Egg production rates did not appear to be limited by food availability. A complete generation time ranged from ~13–20d. Early naupliar stages had shorter durations than late copepodite stages. Comparisons among HTL, VTL, QPM and IMM showed that the HTL and VTL had the disadvantage of producing negative mortality estimates, while the QPM likely overestimated mortality rates. Simulation experiments indicated that variability in stage abundances was a key factor affecting estimates of copepod mortality by the QPM and IMM techniques. Neither the QPM nor the IMM performed well when stage abundance variability was high. IMM estimates of instantaneous egg mortality rates were 1.30d^{-1} in March–April and 1.60d^{-1} in May–June. While instantaneous

mortality rates for NI–CIV stages ranged from 0.02 to 0.18d^{-1}. Simulated populations using the mortality rates estimated from the IMM technique were consistent with observed field population trajectories.

CHAPTER 1 INTRODUCTION

Copepods are the most abundant taxon of mesozooplankton in the marine ecosystems (Longhurst 1985) and they are key components of pelagic systems because of their small size range, numerical abundance and the pivotal roles they play in shaping ecosystem structure. They are important food sources for higher trophic levels in the pelagic systems (Runge and De Lafontaine 1996; Cushing 1990; Kiørboe et al. 1988). Grazing by copepods not only regulates primary production in the open ocean (Kiørboe 1997; Banse 1995), but also largely determines the amount and composition of vertical particle flux (Lenz 2000). Thus, better understanding of biogeochemical cycles and estimation of secondary production requires more knowledge of copepod population dynamics.

Natural copepod populations have the potential for high population growth; however, they are limited by physical and biological constraints. Three general factors govern copepod population dynamics: (a) the species itself, i.e., the optimum range of environmental conditions and life history traits (Cervetto et al. 1999;Mauchline 1998; Aksnes et al. 1997), (b) the physical environment, e.g., temperature, salinity and hydrology (Halsband-Lenk et al. 2002; Hall and Burns 2001); and (c) the biological environment, comprising the effects of interspecific competition, food regime and predation. Differentiating the relative importance of the three factors may be complicated by their patchy distributions and vertical migration patterns (Omori and Hammer 1982).

Biotic factors regulating copepod population dynamics are usually density-dependent, whereas abiotic factors are independent of population density. Density-dependent feedback mechanisms have been considered as a central process regulating copepod population dynamics (Ohman and Wood 1996; Peterson and Kimmerer 1994). Food availability (Hansen and Hairston 1998), cannibalism (Ohman et al. 2002; Peterson and Kimmerer 1994), and predation (Steele

and Henderson 1995; Purcell et al. 1994; Ohman 1986) are among these key biotic factors and regulate population recruitment and vital rates.

Changes in copepods population dynamics are determined by the rates at which adults are producing eggs, and mortality among different developmental stages. Possible causes for population changes include: (a) a decrease in the number of eggs produced or hatched; (b) death of adults and later stages from adverse physical conditions; (c) mortality from predators or diseases; (d) reductions in food quantity and quality; (e) unsuccessful competition for food and (f) cannibalism. To describe these changes requires a number of equations relating to egg production, hatching success, mortality and state-to-stage development time. Mathematically, a closed copepod population can be described using differential equations and the changes of these rates will reflect variations in either recruitment or death (Equation 1.1; Wood and Nisbet 1991).

$$\frac{d\eta(t)}{dt} = R_j(t) - M_j(t) - \mu_j(t)\eta_j(t) \tag{1.1}$$

where, $R_j(t)$ is the recruitment rate to the stage j at time t, $M_j(t)$ is the maturation rate from stage j at time t, $\mu_j(t)$ is per capita death rate in stage j at time t, and $\eta_j(t)$ is the number of stage j at time t.

The study of copepod population dynamics faces three major difficulties: (1) accurate estimation of mortality and growth rates; (2) a complex life history; and (3) various physical factors that potentially influence copepod population dynamics. To understand population dynamics and productivity, properly estimating population parameters and understanding how physical factors influence populations mechanistically, are essential.

Accurate estimation of mortality and growth rates requires an intensive time series of samples with a complete temporal coverage, e.g., three or four samples per day over three to five

weeks considering the shortest stage duration and the time for one generation (Wood and Nisbet 1991). Field data frequently show large variability due to different physical factors on various temporal and spatial scales (Planque and Fromentin 1996; Daly and Smith Jr. 1993). Furthermore, it's almost impossible to sample the same population during the whole study period, and time series data from the ocean frequently fail to show the changes in abundance for each stage over time (Aksnes et al. 1997; Huntley and Niiler 1995).

There are 13 distinguishable development stages including the egg, six naupliar stages and six copepodite stages; however, individuals can not be aged clearly within a stage. Copepodids are more mobile than nauplii, so that sampling efficiency will vary for the different stages (Aksnes et al. 1997). Different development stages may utilize different vertical stratum (Huang et al. 1993). Naupliar stages were normally confined near the surface and experienced greater dispersion than later stages (Aksnes et al. 1997). Consequently, depth–integrated net samples may underestimate the abundance of early stages (Herman et al. 1991; Aksnes and Magnesen 1983). Miller and Tande (1993) indicated that pump sampling may underestimate the abundance of copepodite stages. As a result, biased samples may not be able to reflect stage composition for a population. In addition, diapause is a common life strategy in many copepod species to deal with unfavorable conditions (Mauchline 1998). When environments become unfavorable, some species can cease their development at copepodite IV or V and such species may experience different mortality rates (Tarling et al. 2004) and generation times that are much longer than under normal (non–diapause) conditions.

Physical processes can influence population dynamics on various temporal and spatial scales. For example, the annual average abundance of the copepod *Calanus finmarchicus* in the North Sea was correlated with the North Atlantic Oscillation index between 1960 and 1996 (Fromentin and Planque 1996; Planque and Fromentin 1996). McGowan and Walker (1985) found an 80% decrease in zooplankton biomass in waters off Southern California since 1951.

During this period surface waters warmed by as much as 1.5°C and this enhanced stratification of the water column. The stratification reduced wind–driven upwelling, which reduced nutrient delivery to the upper waters; and hence lowered the phytoplankton production, which appeared to be the cause of the reduction in zooplankton biomass. Local physical processes could also be important in shaping the spatial and temporal occurrence of zooplankton populations. Resgalla Jr. et al. (2001) found cross– and long–shelf Ekman transport were correlated with the variability of zooplankton biomass from 1977 to 1990 off the southern Brazilian coast.

1.1 Egg Production Rate

In copepods, the egg production rate is a main factor determining the upper limit of the population size. The egg production rate also provides a key index for secondary production estimates, e.g., total egg production is potentially an important food source for fish larvae (Kiørboe et al. 1988). Hirst and Kiørboe (2002), Hirst and McKinnon (2001) and Mauchline (1998) have reviewed egg production rates for the copepod species that have been studied.

Most pelagic calanoid copepods broadcast their eggs freely into the water column, but some species carry eggs attached to the ventral side of the genital somite until nauplii hatch. Egg production is not only a function of spawning frequency, but also a function of clutch size (Runge and Roff 2000). Spawning frequency can be influenced by environmental conditions (Carlotti and Hirche 1997; Hirche et al. 1997) and clutch size can vary by a factor of two or three among adult females based on upon their conditions (Niehoff 2000; Niehoff et al. 1999). The interclutch duration for egg–carrying species is normally longer than broadcasting species because the latter species generally produce relatively smaller eggs (Mauchline 1998). Kiørboe and Sabatini (1995) reported that egg production rates in free–spawning species were about 7.5 times higher than those with egg masses. Copepods are exposed to fluctuating environmental factors, thus egg production may show substantial variability in the field (Runge et al. 1997).

Egg–carrying species may show less variability in nature than free–spawning species (Sabatini and Kiørboe 1994).

1.1.1 Factors Influencing Egg Production Rates

Food limitation has been considered as one of the main factors controlling recruitment of individuals to copepod populations (Mauchline 1998). Food concentration can influence both clutch size (Makino and Ban 2000; Smyly 1973) and interclutch duration (Ban 1994). Copepods generally increase their egg production rates as food availability increases (Dam et al. 1994; Durbin et al. 1983). In the field, the egg reproduction rates of free-spawning species have been frequently used as an indication of food availability (Plourde and Runge 1993; Peterson 1988) and some studies have shown that egg production was coincident with the onset of phytoplankton blooms (Nielsen and Hansen 1995; Diel and Tande 1992; Kiørboe and Nielsen 1990; Runge 1985; Williams and Lindley 1980). Feeding history immediately prior to egg laying can influence egg production rates (Calbet and Alcaraz 1996). When the egg production rate is regulated by food concentration (Ianora and Poulet 1993; Runge 1985), hatching success may also be altered.

Egg production rates are also sensitive to food quality and high quality food can enhance the production of successive egg masses and clutches (Pond et al. 1996; Poulet et al. 1995; Miralot et al. 1995). Diatoms comprise a large proportion of the spring phytoplankton bloom in temperate regions and diatoms are important components of copepod diets (Miralto et al. 1999). Since the 1990s, research has been conducted on the role of diatoms as high quality food for marine calanoid copepods. Paffenhöfer (2002), Miralto et al. (1999), Miralot et al. (1995), and Poulet et al. (1994) indicated diatoms can have injurious effects on egg hatching

success. However, some recent studies either failed to demonstrate such a negative relationship (Ohman et al. 2002) or showed a positive relationship (Irigoien et al. 2002) between egg hatching success and diatom abundance.

As the adult is the only stage capable of reproduction in copepods, the egg production rate is dependent upon the number of adult males, fertile females and their average fecundity. The size distribution of females and stage structure of the female portion of the population may also limit egg production rate. The number of eggs produced in a single spawning event increases with increasing prosome length or weight of the females. The number of eggs in an egg sac or clutch varies seasonally and partially corresponds to seasonal changes in the body size of adult females (reviewed by Mauchline 1998).

The egg production rate is also a function of temperature (Hirche et al. 1997; Runge 1985). Studies analyzing the relationship between egg production rate and temperature have been reviewed extensively by Hirst and Bunker (2003), Mauchline (1998) and Huntley and Lopez (1992). Depending on the range to which the species adapted, temperature may favor one species to bloom at a specific season, or alternatively, it may limit population growth for other species. Egg production rates generally exponentially increase with temperature within an optimum range (Hirche et al. 1997; Runge 1985). Temperature affects on egg production rates are likely associated with ovariogensis, oogensis and the clutch size and spawning interval (Mauchline 1998).

Egg production rates may also be influenced by other environmental factors. When salinity was out of the optimum range, copepods either declined (Miliou and Moraitou-Apostologpoulou 1991) or increased (Hall and Burns 2001) their egg production rates. Copepod egg production rates can also be influenced by organochemical and trace metal contaminants (Buttion 1994; Cowles and Remillard 1983).

1.1.2 Measurements of Egg Production Rates

The egg production rate can be measured by two general approaches: direct measurements from incubation experiments and indirect estimation from preserved field samples. Assuming that egg laying observed immediately after capture reflects the spawning behavior in the field, incubation experiments can be used to estimate egg production rates with gentle capture of the target species, i.e., minimum physiological damage and stress (Runge and Roff 2000). This method has been widely adopted to estimate egg production rates (Gómez-Gutiérrez and Peterson 1999; Runge et al. 1997; Hirche 1990; Runge 1985) since Dagg (1978) described the egg laying of *Centropages typicus*. However, there are concerns about the physiological stress associated with capturing and handling (Marshall and Orr 1955).

The egg production rate can be estimated from preserved field samples using the Edmonson egg ratio method by Equation 1.2 (Edmondson 1968; Edmondson 1960).

$$B_{ER} = \frac{E}{N_f D} \tag{1.2}$$

where, B_{ER} is the egg production rate, E is the egg concentration estimated from field samples, N_f is the female abundance, and D is the egg development time.

Runge (1987) established a quantitative reproductive index based on morphological changes during the reproductive processes. This method can yield an empirical prediction of egg production from preserved samples. However, detail morphological information on the target species is essential. The method has been successful applied on *Calanus finmarchicus* (Niehoff and Runge 2003; Niehoff and Hirche 1996; Runge 1987).

1.2 Stage–specific Development Times

Stage duration is the temporal period measured between successive moults in the life history. Stage–specific development times are key variables to estimate the production of marine

copepods and to calculate the recruitment rate (Huntley and Lopez 1992). Several publications summarize the common features of development among copepods (Peterson 2001; Mauchline 1998; Kiørboe and Sabatini 1995; Hart 1990, Landry 1983). These features include: the non–feeding naupliar stages have shorter development times than later stages; the first feeding nauplius stage, NII or NIII, has an extended duration; and the copepodite stage V generally has an extended duration.

The isochronal rule states that the pattern of postembryonic development is characterized by development stages of equal duration (Miller et al. 1977). However, copepod development frequently shows a sigmoid development (Peterson 1986).

Equiproportional development states that the duration of a given life history occupies a constant proportion of the embryonic development time regardless temperature (Corkett et al. 1984). Equiproportional rule may be extended to include all species in the same genus. However, there are some species, that do not conform to the equiproportional rule (Christou and Verriopoulos 1993; Peterson and Painting 1990).

1.2.1 Factors Influencing Stage Duration

Food availability directly affects growth rates; therefore, stage–specific development time and generation time are influenced by food (Mauchline 1998). Laboratory populations exhibit a longer stage development time at low food concentrations than at high food concentrations (Makino and Ban 2000; Hansen and Hairston 1998; Harris and Paffenhöfer 1976) and field studies showed similar results (Hirche et al. 2001). Food quality may also be an important factor influencing stage duration. Diel and Klein Breteler (1986) found that development and growth can be arrested by changes in quality of available food in both field studies and laboratory studies.

Temperature is a main factor influencing stage–specific development times. The relationship between temperature and growth rate can be described by equation 1.3 (Bělehràdek 1935) or equation 1.4 (Thompson 1982). Numerous studies have been conducted on the relationship between temperature and development times and the Bělehràdek functions for different species were summarized by Mauchline (1998). In conjunction with the development rules, this function is very useful in estimating stage–specific development times. For instance, if one measures stage development times for early stages (e.g., egg) experimentally at multiple temperatures and later stages at one temperature, according to the equiproportional rule or isochronal rule, stage duration for older stage can be predicted at the given temperature. Many studies have showed that unfavorable temperature could lead to an extended stage duration (Hirche et al. 2001; Uye 1988; Corkett and McLaren 1970). Stage–development times can vary up to two times among individuals in the field and the same species from different locations may have different stage–specific development times at the same temperature (Halsband-Lenk et al. 2002).

$$D = a(T - \alpha)^b \tag{1.3}$$

$$\ln D = a - bT \tag{1.4}$$

where a, α and b are fitted constants, T is temperature, and D is stage–specific development time.

Other factors such as body size and life traits can also influence stage duration. Halsband-Lenk et al. (2002) found that *Centropages typicus* tended to develop more quickly in the Mediterranean than in the North Sea. The difference might be explained by different body size, i.e., smaller individuals have shorter stage duration than large ones (Vidal 1980). Gillooly

et al. (2002) developed an emprical equation (Equation 1.5) to describe the relationship between body size and development time, which explained nearly 75% of the variation in post–embryonic development among a diverse sample of zooplankton in the study. Contrarily, Huntley and Lopez (1992) found that development times (data mainly collected from incubation experiments) were size independent. If copepods which have seasonal diapause cease development in copepodite IV or V, the generation time could extend much longer.

$$\frac{t_m}{m^{1/4}} = (4a) \times \frac{1}{\delta^{1/4}} \times \ln[\frac{(1-(m_0/M)^{1/4})}{(1-\delta^{1/4})}] \tag{1.5}$$

where, m is the mass of the embryo, t_m is the time taken to develop to m, M is the asymptotic mass, a is a coefficient related to fundamental cell properties, δ is a coefficient ranging from 0.50–0.90.

1.2.2 Measurements of Stage Duration

Development time can be directly estimated from repeated sampling of a cohort (Landry 1978; Rigler and Cooley 1974) based on cohort analysis (Equation 1.6 and 1.7).

$$M_n = \frac{\sum(days \times animals)}{\sum animals} \tag{1.6}$$

$$M_{n+1} - M_n = \frac{t_{n+1} + t_n}{2} \tag{1.7}$$

where M_n is the mean pulse time of stage n and t_n is the duration for stage n.

Stage duration can also be measured from incubation experiments. The stage–specific development times can be estimated by incubating individuals of known stages. Artificial cohorts (Hopcroft and Roff 1998) can be employed when incubation experiment can only last for short periods. In the field, artificial cohorts of certain stages were created by sieving and these were incubated in water with natural food. Changes in the stage distribution were measured every few hours and then stage durations were calculated.

1.3 Stage–specific Mortality Rates

Mortality, as a removal process, determines the lower limits of the population size given a fixed fecundity rate, thus knowledge of vital rates is essential to understand copepod population processes (Eiane et al. 2002; Twombly and Lewis Jr. 1989). Small changes in mortality rates can have order of magnitude effects on copepod population abundance. How copepod mortality is apportioned among their 13 distinguishable development stages affects the population growth rate and reproductive output (Aksnes et al. 1997; McCauley and Murdoch 1990). Copepod populations experience temporal and spatial variability in temperature, food availability, food quality, and predation, therefore mortality is likely to vary on related scales. Temporal and spatial variations in mortality rates may determine the species abundance and distribution. There are few studies that have attempted to resolve stage–specific mortality rates. Kiørboe (1997) summarized the reported mortality rates prior to 1997. Table 1.1 summarizes results from studies thereafter and two studies (Twombly 1994; Gehers and Roberston 1975) prior to 1997, which were not included in Kiørboe (1997). Eggs normally have a higher mortality rate than other stages and the instantaneous mortality rate can be up to $21d^{-1}$ with an average of $3d^{-1}$, 0–$0.34d^{-1}$ for naupliar stages, and 0–$0.3d^{-1}$ for copepodite stages.

1.3.1 Factors Influencing Mortality Rates

The mortality which occurs at different stages of life–history varies from organism to organism according to its method of reproduction (Hirst and Kiørboe 2002; Ohman et al. 2002). Several studies indicated mortality is usually concentrated in the egg stage for broadcast spawning copepods (Beckman and Peterson 1986; Uye 1982; Landry 1978) or early naupliar stages (Peterson Jr. 1986). Rates of egg mortality for egg-brooding copepods are relative low and high mortality likely occurrs in early naupliar stages (Hirst and Kiørboe 2002; Ohman 1986). For planktonic copepods, the egg mortality appears to be at least an order of magnitude lower in

Table 1.1: Reported copepod mortality for egg, nauplii and copepodite stages (day^{-1}) for *Acartia omnori*, *Centropages abdominalis*, *Calanus finmarchicus*, *Calanus* spp., *Pseudocalanus elongatus*, *P. newmani*, *P. marinus*, *Oithona similis*, *O. amazonica*, *Paracalanus* sp., *Diaptomus negrensis*, and *D. clavipes*.

Species	Location	Egg	Nauplii	Copepodid	Author
C. finmarchicus	Georges Bank, US	0.5	0.03–117	0.06–0.11	Ohman et al. (2004)
	FLEX in North Sea		0–0.34	0–0.14	Same
	Ocean Station M	1.78	0.01–0.03	0.04–0.13	Same
	Lurefjorden, Norway		0.01–0.36	0–0.17	Same
	Sørfjorden, Norwary		0.05 (averaged)	0.07–0.11	Same
C. finmarchicus	FLEX in North Sea		0–0.34	0–0.1	Eiane and Ohman (2004)
P. elongatus	Same		0–0.11	0–0.11	Same
O. similis	Same		0.01–0.07	0.01–0.02	Same
C. finmarchicus	Scotia Sea			0.06	Tarling et al. (2004)
Calanus spp.	Lurefjorden, Norway	0.18	0–0.35	0–0.12	Eiane et al. (2002)
	Sørfjorden, Norwary	0.05 (averaged egg and NI)		0.04–0.11	Same
Broadcasting		1.36	0.14 (averaged nauplii and copepodid)		Hirst and Kiørboe (2002)
Egg–carrying		0.17	0.17 (averaged nauplii and copepodid)		Same
C. finmarchicus	Norwegian Sea	1.76			Ohman and Hirche (2001)
P. marinus	Japan	5–10% eggs entering the adult stage			Liang and Uye (1997)
Paracalanus sp.	Same	5% eggs entering the adult stage			Same
C. abdominalis	Same	1.5% eggs entering the adult stage			Same
A. omnori	Same	1.5% eggs entering the adult stage			Same
P. newmani	Dabob Bay, US	0.05	0.10 (averaged)	0.04–0.12	Ohman and Wood (1996)
	Same	0.07	0.12 (averaged)	0.03–0.17	Same
P. newmani	Dabob Bay, US			0–0.19	Aksnes and Ohman (1996)
	Same			0–0.15	Same
D. negrensis	Venezuela		0–0.79	0–2.04	Twombly (1994)
O. amazonica	Same		0.11	0–1.46	Same
D. clavipes	Laboratory study	0.03–1.26 (Egg and nauplii)		0–0.23	Gehers and Roberston (1975)

egg–carrying than that in egg-broadcasting species (Kiørboe and Sabatini 1994); however, this this strategy may depend on the trade off between the benefits to offspring and the adult stage. The difference in egg mortality may be arributed to brooding eggs reducing egg predation from suspension–feeders as well as sinking loss to the benthos in shallow water (Logerwell and Ohman 1999).

It is important to note that there is usually a strong stage–specific and size–specific component to postembryonic mortality rates (Lynch, 1983). Copepodite stages are more mobile than earlier naupliar stages, consequently mortality rates may decrease with increasing body size. Hirst and Kiørboe (2002) summarized the relationship between mortality and body size with a log–linear regression model (Equation 1.8).

$$\log \beta = -0.325 \times \log W - 2.086 \tag{1.8}$$

where, β is the mortality rate and W is the dry weight.

Copepod mortality rates may also be sex–specific. The ovigerous females are more suceptible to visual predators than non–ovigerous females (Bollens and Frost 1991; Winfield and Townsend 1983). Blais and Maly (1993) indicated the existence of sex–specific vulnerability in a laboratory study. The sex–specific vulnerability may be a result of sex–specific swimming ability (Van Leeuwen and Maly 1991) and different body size between males and females (Mauchline 1998). In egg–carrying species, several studies indicated predation risk increased with clutch size (Svensson 1995; De Stasio Jr. 1993; Winfield and Townsend 1983). Although Svensson (1997) found there was no mortality difference among *Eudiaptomus gracilis* females with, and without eggs, female mortality did exceed male mortality both in the field and in the laboratory with the difference perhaps resulting from different swimming angles in relation to the predatory *Chaoborus* larvae.

Predation and cannibalism have been considered among the main causes for copepod mortality. Predation pressure from visual predators, such as fish, can cause high mortality rates (Möllmann and Köster 2002; Verheye and Richardson 1998), while chaetognaths (Ohman 1986) and jellyfish (Brodeur et al. 2002; Purcell et al. 1994) are among the major nonvisual predators. Hirst and Kiørboe (2002) attributed about 66–75% of the adult copepod mortality to predation and Tarling et al. (2004) attributed over 80% mortality of *Calanoides acutus* during winter to predation. Predation pressure from visual predators and nonvisual predators may vary seasonally (Ohman 1986). In the field prey usually face different predators and trophic linkages may also exist among predators. Seasonal changes in abundance of *Pseudoclanus neumani* in Dabob Bay seem to be followed by seasonal changes in abundance of its main nonvisual predators *Euchaeta elongata* and *Sagitta elegans*. Additionally, fish can visually hunt the two non–visual predators, but also feed on *P. neumani* (Ohman 1986). Cannibalism has also been considered as an important cause for high egg mortality rates (Ohman and Hirche 2001; Peterson and Kimmerer 1994).

As egg, nauplius I and II are not dependent on food, feeding condition for adults prior to reproduction influences their vital rates. Ianora and Poulet (1993) found that *Temora stylifera* produced the maximum number of viable eggs when it fed on dinoflagellates. Egg mortality in *Calanus helgolandicus* shows a large seasonal variation with an average of 30%, while during the diatom bloom egg mortality increased to 75% (Laabir et al. 1995). Egg hatching success and naupliar survival under starvation increased with egg size, whereas egg size is a response of available food (Kleppel et al. 1998, Guisande and Harris 1995). When food availability becomes a limiting factor, feeding conditions over the previous few days could represent the ability to buffer the short starvation period (Bryant et al. 1997; Carlotti and Sciandra 1989).

Other environmental factors such as temperature and salinity can also influence mortality rates. Hirst and Kiørboe (2002) summarized the mortality rates as a function of temperature

with a log–linear regression model (Equation 1.9). Large variation in salinity can also increase mortality rates (Cervetto et al. 1999) and it may largely be determined by the tolerance of the species.

$$\ln\beta = a \times T - b \tag{1.9}$$

where, β is the mortality, T is temperature, a and b are coefficients.

1.3.2 Estimating Mortality

Copepod mortality rates are difficult to measure in oceanic environments. As a population property, mortality rates are also very difficult to estimate from incubation experiments. While enclosure studies may provide a direct way to estimate the death rate by containing an enclosed population, they reduce mobility and large scale patchiness. Furthermore, they also introduce unwanted artifacts such as cannibalism and altered physical conditions. It is also extremely difficult to contain a full suite of potential predators at realistic densities.

Indirect estimation methods include the horizontal life table method (Carey 1993), maximum likelihood method (Manly 1990), vertical life table method (Aksnes and Ohman 1996), generalized linear regression method (Caswell 2000), and surface smooth method (Wood 1994), referred as the quadratic programming method by Caswell (2000), inverse matrix method (Carlotti et al. 2000; Twombly 1994), and life history method (Hirst and Kiørboe 2002). The applications and underlying assumptions of these methods have been discussed in several papers (Ohman et al. 2004; Hirst and Kiørboe 2002; Caswell 2000; Aksnes et al. 1997; Wood 1994; Wood and Nisbet 1991; Manly 1990). Among these techniques, the horizontal life table method, vertical life table method, and surface smooth method are the three most commonly used techniques.

A fundamental problem of mortality estimation lies in sampling variability. For a closed population, changes in stage composition can be explained by population parameters. Whereas,

field data reflect not only the statistical sampling errors, but also the variability imposed by other factors, such as sampling techniques (Miller and Tande 1993; Miller and Judkins 1981), patchiness (Wiebe and Benfield 2003), the influence of a dynamic physical environment (Herman et al. 1991; Aksnes and Magnesen 1983) and biological processes such as vertical migrations and predation (Hall et al. 1976). Biased samples caused by differential gear selectivity have long been a concern in mortality estimation because older stages are more mobile with better developed sensor systems than younger stages (Aksnes et al. 1997; Wood and Nisbet 1991). Vertical migration or swimming ability may also cause bias in the sampled stage composition (Aksnes et al. 1997), since different development stages may utilize different vertical strata (Huang et al. 1993) and thereby experience different physical conditions. The effectiveness of different methods in estimating mortality rates largely depends on how well the methods handle these variabilities.

1.3.2.1 Horizontal Life Table

A horizontal life table is designed to hold stage abundances for the same population over time, and it can produce a detailed description of the mortality and various other statistics at each stage (Pressat 1985). Horizontal life tables are appropriate for a population with discrete cohorts when the sample interval is shorter than the shortest stage–specific development time and samples satisfy complete temporal coverage (Aksnes et al. 1997; Manly 1990). In the life table, the proportion of a cohort surviving from egg to stage x is denoted as l_x. The difference in number of survivors for successive stage x and $x + 1$ is designated d_x (1.10). The periodic mortality rates (q_x) that represent the probability of dying over these respective periods can be defined by equation 1.11.

$$d_x = l_x - l_{x+1} \tag{1.10}$$

$$q_x = \frac{d_x}{l_x} \tag{1.11}$$

To obtain a nonnegative estimation, the abundance of stage $i+1$ at time $t+1$ has to be lower than the abundance of stage i at time t. However, in the field the reverse situation is frequently encountered (Liang and Uye 1997; Hairston and Twombly 1985). Another disadvantage of this method is that this method does not take stage duration, a factor that is correlated with mortality, into consideration (Hairston and Twombly 1985).

1.3.2.2 Vertical Life Table

If a life table holds a snapshot of stage abundances, the vertical life table method can be applied to estimate stage–specific mortality rates. By assuming that the mortality rates of stage i and $i+1$ can be considered equal for a period corresponding to the duration of two consecutive stages, mortality of stage i can be determined from equation 1.12 and equation 1.13 (Aksnes and Ohman 1996).

$$\frac{n_i}{n_{i+1}} = \frac{[\exp(m \times d_i) - 1]}{[1 - \exp(-m \times d_{i+1)}]} \tag{1.12}$$

$$\frac{n_{q-1}}{n_q} = \exp(m_{q-1}) - 1 \tag{1.13}$$

where, n_i is the number of individuals in stage i and q is the adult stage, m is the mortality rate for stage i, and d_i is the stage duration.

The vertical life table method assumes a steady state population (Aksnes and Ohman 1996) and can be applied to either snapshot data, or data averaged over a period (Brinton 1976). By averaging the data over a period and taking stage duration into consideration, this method can reduce the variability inherent in field data. However, in some cases, it may not be able to account for the variability sufficiently to produce positive estimates for all stages (Aksnes and Ohman 1996).

1.3.2.3 Surface Smooth Method

The basic idea for the surface smooth method is that populations can be described by a surface defined by Equation 1.14 (Wood 1994), where abundance can be found by age and time. Mortality rates can be obtained by tracking cohorts across age and time. To obtain a population surface, two schemes of cubic spline interpolation are applied: the first interpolation is associated with sample interval and the second is associated with cohorts accross stage and time. A smooth surface is defined by minimizing the quadratic term and wiggliness term. The quadratic term reflects the difference between the modeled and observation data. The wiggliness term guarantees that the parameters vary smoothly from stage to stage since the consecutive stages are morphologically similar size in most cases. This method has been described in detail by Wood (1994) and not further described here.

$$\frac{\partial \eta}{\partial t} + \frac{\partial \eta}{\partial \alpha} - \mu \times \eta = 0 \tag{1.14}$$

where, $\eta(\alpha, t)$ is the number of individuals at age α, at time t and $\mu(\alpha, t)$ is the death rate for individuals of age α at time t.

There are few assumptions for this method. First, the solution is a smooth function, which means an individual's probability of death changes fairly slowly from one stage to the next. Second, the death rate has to be positive. Finally, identical stage-specific durations are assumed for all individuals born at the same time (Wood and Nisbet 1991).

The surface smooth method can be applied on field data with moderate sampling variability (Ohman and Wood 1996, Wood 1994). However, there are still some limitations for this method. This method is generally applicable in "nearly closed" situations such as small fjords. When applied to spatially averaged data over a large enough area and advective contributions to population change are assumed to be relatively small. Lastly, this method is restricted by its

requirement for stage as a continuous variable, whereas most observed data are discrete–stage frequency data because copepods can not be reliably aged.

1.3.3 Inverse Matrix Method

Matrix projection population models can be used to predict stage abundance. By varying mortality rates, a set of mortality rates that is best fit for observational data can be found (Twombly 1994; Caswell and Twombly 1989). The Gauss–Marquardt–Levenburg algorithm is a standard nonlinear technique that can be applied to find the parameters that minimize the difference between simulated data and observational data (Carlotti et al. 2000). Another potential way to find the best fit parameters is the bootstrap technique. The basic assumption of the inverse matrix method is that the rates of mortality and development are constant within each stage (Carlotti et al. 2000).

1.4 Stage–structured Population Model

A good simulation model is essential to understand population dynamics (Carlotti et al. 2000). The matrix projection models are one of the most common population models and have been widely applied in modeling zooplankton population (Torres-Sorando et al. 2003; Lo et al. 1995; Caswell and Twombly 1989; Levin et al. 1987), as well as estimating mortality rates (Twombly 1994; Hiby and Mullen 1980). To effectively apply a matrix projection model, it is desirable to formulate a specific model based on concrete knowledge of target species, such as reproduction rate and stage–specific development times.

To properly simulate a copepod population, a critical step is to construct a transitional matrix A, defined by Equation 1.15. Then the population can be projected over time. Caswell

(2000) provided detailed information on how to construct the stage-structured population model.

$$A = \begin{bmatrix} P_1 & 0 & \cdots & \cdots & F \\ G_1 & P_2 & 0 & & 0 \\ 0 & G_2 & \ddots & & \vdots \\ \vdots & & \ddots & \ddots & \vdots \\ 0 & \cdots & \cdots & G_{s-1} & P_s \end{bmatrix} \tag{1.15}$$

where, P_s is the probability of individual surviving and staying in the same stage, G_s is the probability of individuals surviving and entering next stage, and F is the recruitment rate from the adult stage.

After constructing the transitional matrix, the stage–structured population can be conveniently described by Equation 1.16. The matrix model can also be useful in estimating population parameters combining with other techniques (e.g., Gauss–Marquardt–Levenburg algorithm).

$$n(t+1) = A \times n(t) \tag{1.16}$$

where $n(t)$ is a vector hold stage composition data.

1.5 Summary

To study copepod population dynamics, accurate estimation of the reproduction rate, stage duration and mortality rates of each stage are necessary. These parameters are intercorrelated with each other. For instance, an increase in adult female mortality would lead to a decrease in reproduction rate (Ohman et al. 1996). Therefore estimation of these parameters is complicated by these interrelationships, particularly in mortality estimation, e.g., how does variability in egg production influence mortality estimation? However, studies of these aspects are rare.

The purpose of this study is to understand the population dynamics of *Clausocalanus furcatus* in the northern Gulf of Mexico. *Clausocalanus furcatus* is widely distributed in the oligotrophic oceanic waters around the world (Lo et al. 2004; Paffenhöfer 1985) and knowledge about its population dynamics is limited (Mazzocchi and Paffenhöfer 1998). The study comprises four parts. I first investigated mesozooplankton communities in the study area for background knowledge. Secondly, I estimated egg production rates and stage duration for the target species. Thirdly I estimated stage–specific mortality rates with four common techniques with an emphasis on the inverse matrix method combined with a Gauss–Marquardt–Levenburg algorithm. Then I investigated how the variability in egg production rate and stage abundances would influence mortality estimation and the simulated population with a stage–structured matrix model.

1.6 Bibliography

Aksnes, D. L. and Magnesen, T. 1983. Distribution, development, and production of *Calanus finmarchicus* (Gunnerus) in Lindåpollene, Western Norway, 1979. *Sarsia*, 68:195–208.

Aksnes, D. L., Miller, C. B., Ohman, M. D., and Wood, S. N. 1997. Estimation techniques used in studies of copepod population dynamics — A review of underlying assumptions. *Sarsia*, 82:279–296.

Aksnes, D. L. and Ohman, M. D. 1996. A vertical life table approach to zooplankton mortality estimation. *Limnol. Oceanogr.*, 41:1461–1469.

Ban, S. 1994. Effect of temperature and food concentration on post–embryonic development, egg production and adult body size of calanoid copepod *Eurytemora affinis*. *J. Plankton Res.*, 15:721–735.

Banse, K. 1995. Zooplankton: Pivotal role in the control of ocean production. *ICES J. Mar. Sci.*, 52:265–277.

Beckman, B. R. and Peterson, W. T. 1986. Egg production by *Acartia tonsa* in Long Island Sound. *J. Plankton Res.*, 8:917–925.

Blais, J. M. and Maly, E. J. 1993. Differential predation by *Chaoborus americanus* on males and females of two species of *Diaptomus*. *Can. J. Fish. Aquat. Sci.*, 50:410–415.

Bollens, S. M. and Frost, B. W. 1991. Ovigerity, selective predation, and variable diel vertical migration in *Euchaeta elongata* (Copepoda, Calanoida). *Oecologia*, 87:155–161.

Brinton, E. 1976. Population biology of *Euphausia pacifica* off Southern California. *Fish. Bull.*, 74:733C–762.

Brodeur, R. D., Sugisaki, H., and Hunt Jr, G. L. 2002. Increases in jellyfish biomass in the Bering Sea: implications for the ecosystem. *Mar. Ecol. Prog. Ser.*, 233:89–103.

Bryant, A. D., Heath, M., Gurney, W., Beare, D. J., and Robertson, W. 1997. The seasonal dynamics of *Calanus finmarchicus*: development of a three–dimensional structured population model and application to the northern North Sea. *Neth. J. Sea Res.*, 38:361–379.

Bělehràdek, J. 1935. Temperature and living matter. *Protoplasma Monogr.*, 8:1–277.

Buttion, I. 1994. The effect of low concentrations of phenol and ammonia on egg production rates, fecal pellet production and egg viability of the calanoid copepod *Acartia clausi*. *Mar. Biol.*, 119:629–634.

Calbet, A. and Alcaraz, M. 1996. Effects of constant and fluctuating food supply on egg production rates of *Acartia grani* (Copepoda: Calanoida). *Mar. Ecol. Prog. Ser.*, 140:33–39.

Carey, J. R. 1993. *Applied Demography for Biologist with Special Emphasis on Insects*. Oxford University Press, Oxford.

Carlotti, F., Gikse, J., and Werners, F. 2000. Modeling zooplankton dynamics. In Harris, R. P., Wiebe, P. H., Lenz, J., Skjoldal, H. R., and Huntley, M., editors, *ICES Zooplankton Methodology Manual*, pages 571–667. Academic Press, London.

Carlotti, F. and Hirche, H. J. 1997. Growth and egg production of female *Calanus finmarchicus*: an individual–based physiological model and experimental validation. *Mar. Ecol. Prog. Ser.*, 149:1–28.

Carlotti, F. and Sciandra, A. 1989. Population dynamics model of *Euterpina acutifrons* (Copepoda: Harpacticoida) coupling individual growth and larval development. *Mar. Ecol. Prog. Ser.*, 56:225–242.

Caswell, H. 2000. *Matrix Population Models: Construction, Analysis, and Interpretation*. Sinauer Associates Inc.

Caswell, H. and Twombly, S. 1989. Estimation of stage–specific demographic parameters for zooplankton populations: methods based on stage–classified matrix projection models. In McDonalds, L. L., Manly, B., Lockwood, J., and Logan, J., editors, *Estimation and analysis of insect populations*, volume 55 of *lecture notes in statistics*, pages 93–107. Springer–Verlag.

Cervetto, G., Gaudy, R., and Pagano, M. 1999. Influence of salinity on the distribution of *Acartia tonsa* (Copepoda, Calanoida). *J. Exp. Mar. Biol. Ecol*, 239:33–45.

Christou, E. D. and Verriopoulos, G. C. 1993. Analysis of the biological cycle of *Acartia clausi* (Copepoda) in in a meso–oligotrophic coastal area of the eastern Mediterranean Sea using time–series analysis. *Mar. Biol.*, 115:643–651.

Corkett, C. J. and McLaren, I. A. 1970. Relationships between development rate of eggs and older copepodite stages of copepods. *J. Mar. Biol. Assoc. UK*, 50:161–168.

Corkett, C. J., McLaren, I. A., and Sevigny, J. M. 1984. The rearing of the marine calanoid copepods *Calanus finmarchicus* (Gunnerus), *C. glacialis* Jaschnov and *C. hyperboreus* kröyer with comment on the equiproportional rule. *Syllogeus*, 58:539–546.

Cowles, T. J. and Remillard, J. F. 1983. Effects of exposure to sublethal concentrations of crude oil on the copepod *Centropages hamatus*. I. Feeding and egg production. *Mar. Biol.*, 78:45–51.

Cushing, D. H. 1990. Plankton production and year–class strength in fish–populations: an update of the match/mismatch hypothesis. *Adv. Mar. Biol.*, 26:249–293.

Dagg, M. 1978. Estimated, *in situ*, rates of egg production for the copepod *Centropages typicus* in the New York Bight. *J. Exp. Mar. Biol. Ecol.*, 34:183–196.

Daly, K. L. and Smith Jr., W. O. 1993. Physical–biological interactions influencing marine plankton production. *Annu. Rev. Ecol. Syst*, 24:555–585.

Dam, H. G., Peterson, W. T., and Bellantoni, D. C. 1994. Seasonal feeding and fecundity of the calanoid copepod *Acartia tonsa* in Long Island Sound: is omnivory important in an egg production? *Hydrobiologia*, 292/293:191–199.

De Stasio Jr., B. T. 1993. Diel vertical and horizontal migration by zooplankton: Population budgets and the diurnal deficit. *Bull. Mar. Sci.*, 53:44–64.

Diel, S. and Klein Breteler, W. C. M. 1986. Growth and development of *Calanus* sp. (Copepoda) during the spring phytoplankton succession in the North Sea. *Mar. Biol.*, 113:21–31.

Diel, S. and Tande, K. S. 1992. Does the spawning of *Calanus finmarchicus* in high latitudes follow a predictable pattern? *Mar. Biol.*, 113:130–446.

Durbin, E. G., Durbin, A. G., Smayda, T. J., and G, V. P. 1983. Food limitation of production by adult *Acartia tonsa* in Narragansett Bay, Rhode Island. *Limnol. Oceanogr.*, 28:1199–1213.

Edmondson, W. T. 1960. Reproductive rates of rotifers in natural populations. *Memorie Ist. Ital. Idrobiol.*, 12:21–77.

Edmondson, W. T. 1968. A graphical method for evaluating the use of the egg ratio technique for measuring birth and death rates. *Oecologica*, 1:1–37.

Eiane, K., Aksnes, D. L., Ohman, M. D., Wood, S., and Martinussen, M. B. 2002. Stage-specific mortality of *Calanus spp.* under different predation regimes. *Limnol. Oceanogr.*, 47:636–645.

Eiane, K. and Ohman, M. D. 2004. Stage-specific mortality of *Calanus finmarchicus, Pseudocalanus elongatus* and *Oithona similis* on Fladen Ground, North Sea, during a spring bloom. *Mar. Ecol. Prog. Ser.*, 268:183–193.

Fromentin, J. M. and Planque, B. 1996. *Calanus* and environment in the eastern North Atlantic. II. Role of the North Atlantic oscillation on *Calanus finmarchicus* and *C. helgolanicus*. *Mar. Ecol. Prog. Ser.*, 134:111–118.

Gehers, W. C. and Roberston, A. 1975. Use of life tables in analyzing the dynamics of copepod populations. *Ecology*, 56:665–672.

Gillooly, J. F., Charnov, E. L., West, G. B., Savage, V. M., and Brown, J. H. 2002. Effects of size and temperature on development time. *Nature*, 417:70–73.

Gómez-Gutiérrez, J. and Peterson, W. T. 1999. Egg production of eight calanoid copepod species during summer 1997 off Newport , Oregon, USA. *J. Plankton Res.*, 21:637–657.

Guisande, C. and Harris, R. 1995. Effect of total organic content of eggs on hatching success and naupliar survival in the copepod *Calanus helgolandicus*. *Limnol. Oceanogr.*, 40:476–482.

Hairston, N. G. and Twombly, S. 1985. Obtaining life table data from cohort analysis: a critique of current methods. *Limnol. Oceanogr.*, 30:431–435.

Hall, C. J. and Burns, C. W. 2001. Effects of salinity and temperature on survival and reproduction of *Boeckella hamata* (Copepoda: Calanoida) from a periodically brackish lake. *J. Plankton Res.*, 23:97–103.

Hall, D. J., Threlkeld, S. T., Burns, C., and Crowley, P. H. 1976. The size–efficiency hypothesis and the size structure of zooplankton communities. *Annu. Rev. Ecol. Syst.*, 7:117–208.

Halsband-Lenk, C., Hirche, H. J., and Carlotti, F. 2002. Temperature impact on reproduction and development of congener copepod populations. *J. Exp. Mar. Biol. Ecol.*, 271:212–153.

Hansen, A. and Hairston, N. G. 1998. Food limitation in a wild cycloid copepod population: direct and indirect life history responses. *Oecologia*, 115:320–330.

Harris, R. P. and Paffenhöfer, G. A. 1976. The effect of food concentration on cumulative ingestion and growth efficiency of two small marine planktonic copepods. *J. Mar. Biol. Assoc. UK*, 56:675–690.

Hart, R. C. 1990. Copepod post–embryonic development: pattern, conformity, and predictability. The realities of isochronal equiproportional development, and trends in the copepodid-naupliar duration ratio. *Hydrobiologia*, 206:175–206.

Herman, A. W., Sameoto, D. D., Shunnian, C., Mitchell, M. R., Petrie, B., and Cochrane, N. 1991. Sources of zooplankton on the Nova Scotia Shelf and their aggregation with deep–shelf basins. *Cont. Shelf Res.*, 11:211–238.

Hiby, A. R. and Mullen, A. J. 1980. Simultaneous determination of fluctuating age structure and mortality from field data. *Theor. Popul. Biol.*, 18:192–203.

Hirche, H. J. 1990. Egg production of *Calanus finmarchicus* at low temperature. *Mar. Biol.*, 106:53–58.

Hirche, H. J., Brey, T., and Niehoff, B. 2001. A high–frequency time series at Ocean Weather Ship Station M (Norwegian Sea): population dynamics of *Calanus finmarchicus*. *Mar. Ecol. Prog. Ser.*, 219:205–219.

Hirche, H. J., Meyer, U., and Niehoff, B. 1997. Egg production of *Calanus finmarchicus*: effect of temperature, food and season. *Mar. Biol.*, 127:609–620.

Hirst, A. G. and Bunker, A. J. 2003. Growth of marine planktonic copepods: Global rates and patterns in relation to chlorophyll α, temperature, and body weight. *Limnol. Oceanogr.*, 48:1988–2010.

Hirst, A. G. and Kiørboe, T. 2002. Mortality in marine planktonic copepods: Global rates and patterns. *Mar. Ecol. Prog. Ser.*, 230:195–209.

Hirst, A. G. and McKinnon, A. D. 2001. Does egg production represent adult female copepod growth? A call to account for body weight changes. *Mar. Ecol. Prog. Ser.*, 223:179–199.

Hopcroft, R. R. and Roff, J. C. 1998. Zooplankton growth rate: the influence of female size and resources on egg production of tropical marine copepods. *Mar. Biol.*, 132:79–86.

Huang, C., Uye, S., and Onbe, T. 1993. Ontogenetic diel vertical migration of the planktonic copepod *Calanus sinicus* in the Inland Sea of Japan. *Mar. biol.*, 117:289–299.

Huntley, M. E. and Lopez, M. D. G. 1992. Temperature–dependent production of marine copepods: A global synthesis. *Am. Nat.*, 140:201–242.

Huntley, M. E. and Niiler, P. P. 1995. Physical control of population dynamics in the Southern Ocean. *ICES J. Mar. Sci.*, 52:457–468.

Ianora, A. and Poulet, S. A. 1993. Egg viability in the copepod *Temora stylifera*. *Limnol. Oceanogr*, 38:1615–1626.

Irigoien, X., Harris, R. P., Verheye, H. M., Joly, P., Runge, J. A., Starr, M., Pond, D., Campbell, R., Shreeve, R., Ward, P., Smith, A. N., Dam, H. G., Peterson, W., Tirelli, V., Koski, M., Smith, T., Harbour, D., and Davidson, R. 2002. Copepod hatching success in marine ecosystem with diatom concentrations. *Nature*, 419:387–389.

Kiørboe, T. 1997. Population regulation and role of mesozooplankton in shaping marine pelagic food webs. *Hydrobiologia*, 363:13–27.

Kiørboe, T., Møhlenberg, F., and Tiselius, P. 1988. Propagation of planktonic copepods: production and mortality of eggs. *Hydrobiologia*, 167/168:219–225.

Kiørboe, T. and Nielsen, T. G. 1990. Effects of wind stress on vertical water column structure, phytoplankton growth, and productivity of planktonic copepods. In Barnes, M. and Gibson, R. N., editors, *Trophic Relationships in the Marine Environment*, pages 28–40. Aberdeen University Press.

Kiørboe, T. and Sabatini, M. 1994. Reproductive and life cycle strategies in egg–carrying cyclopoid and free-spawning calanoid copepods. *J. Plankton Res.*, 16:1353–1366.

Kiørboe, T. and Sabatini, M. 1995. Reproductive and life cycle strategies in egg–carrying cyclopoid and free-spawning calanoid copepods. *J. Plankton Res.*, 16:1353–1366.

Kleppel, G. S., Burkart, C. A., and Houchin, L. 1998. Nutrition and the regulation of egg production in the calanoid copepod *Acartia tonsa*. *Limnol. Oceanogr.*, 43:1000–1007.

Laabir, M., Poulet, S. A., and Ianora, A. 1995. Measuring egg production in *Calanus helgolandicus*. *J. Plankton Res.*, 17:1134–1137.

Landry, M. R. 1978. Population dynamics and production of a planktonic marine copepod, *Acartia clausii*, in a small temperate lagoon on San Juan Island, Washington. *Revue Ges. Hydrobiol.*, 63:77–119.

Landry, M. R. 1983. The development of marine calanoid copepods with comment on the isochronal rule. *Limnol. Oceanogr.*, 28:614–624.

Lenz, J. 2000. Introduction. In Harris, R. P., Wiebe, P. H., Lenz, J., Skjoldal, H. R., and Huntley, M., editors, *ICES Zooplankton Methodology Manual*, pages 1–30. Academic Press, London.

Levin, S. A., Caswell, H., DePatra, K. D., and Creed, E. L. 1987. Demographic consequences of larval development mode: planktontrophy vs. lecithotrophy in *Streblospio benedicti*. *Ecology*, 68:1877–1886.

Liang, D. and Uye, S. 1997. Population dynamics and production of the planktonic copepods in a eutrophic inlet of the Inland Sea of Japan IV. *Pseudodiaptomus marinus*, the egg-carrying calanoid. *Mar. Biol.*, 128:415–421.

Lo, N. C. H., Smith, P. E., and Butler, J. L. 1995. Population growth of northern anchovy and Pacific sardine using stage–specific martic models. *Mar. Ecol. Prog. Ser.*, 127:15–26.

Lo, W., Shih, C., and Hwang, J. 2004. Diel vertical migration of the planktonic copepods at an upwelling station north of Taiwan, western North Pacific. *J. Plankton Res.*, 26:89–97.

Logerwell, E. A. and Ohman, M. D. 1999. Egg-brooding, body size and predation risk in planktonic marine copepods. *Oecologia*, 121:426–431.

Longhurst, A. R. 1985. The structure and evolution of plankton communities. *Prog. Oceanogr.*, 15:1–35.

Makino, W. and Ban, S. 2000. Response of life history traits to food conditions in a cyclopoid copepod from an oligotrophic environment. *Limnol. Oceanogr.*, 45:396–407.

Manly, B. F. 1990. Stage-structured populations: sampling, analysis, and simulation. In *Population and community biology series*, page 187. Chapman and Hall, London; New York.

Marshall, S. M. and Orr, A. P. 1955. *The biology of Calanus finmarchicus*. Oliver & Boyd, Edinburgh.

Mauchline, J. 1998. The biology of calanoid copepods. *Adv. Mar. Biol*, 33:710.

Mazzocchi, M. G. and Paffenhöfer, G. A. 1998. First observations on the biology of *Clausocalanus furcatus* (Copepoda, Calanoida). *J. Plankton Res.*, 20:331–342.

McCauley, E. and Murdoch, W. W. 1990. Predator–prey dynamics in environments rich and poor in nutrients. *Nature*, 343:455–457.

McGowan, J. A. and Walker, P. W. 1985. Dominance and diversity maintenance in an oceanic ecosystem. *Ecol. Monogr.*, 55:103–118.

Miliou, H. and Moraitou-Apostologpoulou, M. 1991. Combined effects of temperature and salinity on the popualtion dynamics of *Tisbe holothuriae* Humes (Copepods: Harpacticoida). *Arch. Hydrobiol.*, 121:289–319.

Miller, C. B., Johnson, J. K., and Heinle, D. R. 1977. Growth rules in the marine copepods genus *Acartia*. *Limnol. Oceanogr.*, 22:326–335.

Miller, C. B. and Judkins, D. C. 1981. Design of pumping systems for sampling zooplankton, with descriptions of two high-capacity samplers for coastal studies. *Biol. Oceanogr.*, 1:29–56.

Miller, C. B. and Tande, K. S. 1993. Stage duration estimation for *Calanus* populations, a modelling study. *Mar. Ecol. Prog. Ser.*, 102:15–34.

Miralot, A., Ianora, A., and Poulet, A. 1995. Food type induces different reproductive responses in the copepod *Centropages typicus*. *J. Plankton Res.*, 17:1521–1534.

Miralto, A., Barone, G., Romano, G., Poulet, S. A., Ianora, A., Russo, G. L., Buttino, I., Mazzarella, G., Laabir, M., Carini, M., and Giacobbe, M. G. 1999. The insidious effect of diatoms on copepod reproduction. *Nature*, 402:173–176.

Möllmann, C. and Köster, F. W. 2002. Population dynamics of calanoid copepods and the implications of their predation by clupeid fish in the Central Baltic Sea. *J. Plankton Res.*, 24:959–977.

Niehoff, B. 2000. The effect of starvation on the reproductive potential of *Calanus finmarchicus*. *ICES J. Mar. Sci.*, 57:1764–1772.

Niehoff, B. and Hirche, H. J. 1996. Oogenesis and gonald maturation in the copepod *Calanus finmarchicus* and the prediction of egg production from preserved samples. *Polar Biol.*, 16:601–612.

Niehoff, B., Klenke, U., Hirche, H. J., Irigoien, X., and Harris, R. 1999. A high frequency time series at Weathership Station M, Norwegian Sea, during the 1997 spring bloom: the reproductive biology of *Calanus finmarchicus*. *Mar. Ecol. Prog. Ser.*, 176:81–92.

Niehoff, B. and Runge, J. A. 2003. A revised methodology for prediction of egg production *Calanus finmarchicus* from preserved samples. *J. Plankton Res.*, 2003:1581–1587.

Nielsen, T. G. and Hansen, B. 1995. Plankton community structure and carbon cycling on the western coast of Greenland during and after the sedimentation of a diatom bloom. *Mar. Ecol. Prog. Ser.*, 125:115–131.

Ohman, M. D. 1986. Predator–limited population growth of the copepod *Pseudocalanus* sp. *J. Plankton Res.*, 8:673–713.

Ohman, M. D., Aksnes, A. J., and Runge, J. A. 1996. The interrelationship of copepod fecundity and mortality. *Limnol. Oceanogr.*, 41:1470–1477.

Ohman, M. D., Eiane, K., Durbin, E. G., Runge, J. A., and Hirche, H. J. 2004. A comparative study of *Calanus finmarchicus* mortality patterns at five localities in the North Atlantic. *ICES J. Mar. Sci.*, 61:687–697.

Ohman, M. D. and Hirche, H. J. 2001. Density–dependent mortality in an oceanic copepod population. *Nature*, 412:638–641.

Ohman, M. D., Runge, J. A., Durbin, E. G., Field, D. B., and Niehoff, B. 2002. On birth and death in the sea. *Hydrobiologia*, 480:55–68.

Ohman, M. D. and Wood, S. N. 1996. Mortality estimation for planktonic copepods: *Pseudocalanus newmani* in a temperate fjord. *Limnol. Oceanogr.*, 41:126–135.

Omori, M. and Hammer, W. M. 1982. Patchy distribution of zooplankton: behavior, population assessment, and sampling problems. *Mar. Biol.*, 72:193–200.

Paffenhöfer, G. A. 1985. The abundance and distribution of zooplankton on the southeastern shelf of the United States. In Atkinson, L. P., Menzel, D. W., and Bush, K. A., editors, *Oceanography of the Southeastern U.S. Continental shelf*, pages 104–117.

Paffenhöfer, G. A. 2002. An assessment of the effects of diatoms on planktonic copepods. *Mari. Ecol. Prog. Ser.*, 227:305–310.

Peterson, W. T. 1986. Development, growth, and survivorship of the copepod *Calanus marshallae* in the laboratory. *Mar. Ecol. Prog. Ser.*, 29:61–72.

Peterson, W. T. 1988. Rates of egg production by the copepod *Calanus marshallae* in the laboratory and in the sea off Oregon, USA. *Mar. Ecol. Prog. Ser.*, 47:229–237.

Peterson, W. T. 2001. Patterns in stage duration and development among marine and freshwater calanoid and cyclopoid copepods: a review of rules, physiological constraints, and evolutionary significance. *Hydrobiologia*, 453/545:91–105.

Peterson, W. T. and Kimmerer, W. J. 1994. Processes controlling recruitment of the marine calanoid copepod *Temora longicornis* in Long Island Sound: Egg production, egg mortality, and cohort survival rates. *Limnol. Oceanogr.*, 39:1594–1605.

Peterson, W. T. and Painting, S. J. 1990. Development rates of the copepods *Calanus australis* and *Calanoides carinatus* in the laboratory, with discussion of methods used for calculation of development time. *J. Plankton. Res.*, 12:283–293.

Peterson Jr., R. C. 1986. In situ particle generation in a southern Swedish stream. *Limnol. Oceanogr.*, 31:432–437.

Planque, B. and Fromentin, J. M. 1996. *Calanus* and environment in the eastern North Atlantic. I. Spatial and temporal patterns of *Calanus finmarchicus* and *C. helgolandicus*. *Mar. Ecol. Prog. Ser.*, 102:101–109.

Plourde, S. and Runge, J. A. 1993. Reproduction of the planktonic copepod *Calanus finmarchicus* in the lower St. Lawrence estuary: Relation to the cycle of phytoplankton production and evidence for a *Calanus* pump. *Mar. Ecol. Prog. Ser.*, 102:217–227.

Pond, D., Harris, R., Head, R., and Harbour, D. 1996. Environmental and nutritional factors determining seasonal variability in the fecundity and egg viability of *Calanus helgolandicus* in coastal waters off Plymouth, UK. *Mar. Ecol. Prog. Ser.*, 143:75–79.

Poulet, S. A., Ianora, A., Laabir, M., and Klein Breteler, W. C. M. 1995. Towards the measurement of secondary production and recruitment in copepods. *ICES J Mar. Sci.*, 52:359–368.

Poulet, S. A., Ianora, A., Miralto, A., and Meijer, L. 1994. Do diatoms arrest embryonic development in copepods. *Mar. Ecol. Prog. Ser.*, 111:79–86.

Pressat, R. 1985. *The Dictionary of Demography*. Bell and Bain, Ltd., Glasgow.

Purcell, J. E., R, W. J., and Roman, M. R. 1994. Predation by gelatinous zooplankton and resource limitation as potential controls of *Acartia tonsa* copepod populations in Chesapeake Bay. *Limnol. Oceanogr.*, 39:263–278.

Resgalla Jr., G., De La Rocha, C., and Montù, M. 2001. The influence of Ekman transport on zooplankton biomass variability off southern Brazil. *J. Plankton Res.*, 23:641–650.

Rigler, F. H. and Cooley, J. M. 1974. The use of field data to derive population statistics of multivoltine copepods. *Limnol. Oceanogr.*, 19:636–655.

Runge, J. A. 1985. Egg production rates of *Calanus finmarchicus* in the sea of Nova Scotia. *Arch. Hydrobiolgia*, 21:33–40.

Runge, J. A. 1987. Measurement of egg production rate of *Calanus finmarchicus* in the sea of Nova Scotia. *Arch. Hydrobiol. Beih. Ergebn. Limnol.*, 21:33–40.

Runge, J. A. and De Lafontaine, Y. 1996. Characterization of the pelagic ecosystem in surface waters of the northern Gulf of St. Lawrence in early summer: The larval redfish–*Calanus*–microplankton interaction. *Fish. Oceanogr.*, 5:21–37.

Runge, J. A., Durbin, E., Plourde, S., and Gratton, Y. 1997. Spatial and temporal variation in egg production of *Calanus finmarchicus* on Georges Bank: implications of the productivity of prey of cod and haddock larvae. In *GLOBEC: Results from Interdisciplinary Programs in the North Atlantic*, Baltimore. ICES Annual Meeting.

Runge, J. A. and Roff, J. C. 2000. The measurement of growth and reproductive rates. In Harris, R., Wiebe, P., Lenz, J., Skjoldal, H. R., and Huntley, M., editors, *ICES Zooplankton Methodology Manual*, pages 401–454. Academic Press, London.

Sabatini, M. and Kiørboe, T. 1994. Egg production, growth and development of the cycloid copepod *Oithona similis*. *J. Plankton Res.*, 16:1329–1351.

Smyly, W. J. P. 1973. Clutch–size in the freshwater cycloid copepod, *Cyclopsstrenuus abyssorum* sars in relation to thoracic volume and food. *J. Nat. Hist.*, 7:545–549.

Steele, J. H. and Henderson, E. W. 1995. Predation control of plankton demography. *ICES J. Mar. Sci.*, 52:565–573.

Svensson, J. E. 1995. Predation risk increases with clutch size in a copepod. *Funct. Ecol.*, 9:774–777.

Svensson, J. E. 1997. *Chaoborus* predation and sex–specific mortality in a copepod. *Limnol. Oceanogr.*, 42:572–577.

Tarling, G. A., Shreeve, R. S., Ward, P., Atkinson, A., and Hirst, G. A. 2004. Life–cycle phenotypic composition and mortality of *Calanoides acutus* (Copepoda: Calanoida) in the Scotia Sea: a modelling approach. *Mar. Ecol. Prog. Ser.*, 272:165–181.

Thompson, B. M. 1982. Growth and development of *Pseudocalanus elongates* and *Calanus* sp. in the laboratory. *J. Mar. Biol. Assoc. U. K.*, 62:359–372.

Torres-Sorando, L. J., Zacarias, de Roa, E. Z., and Rodríguez 2003. Population dynamics of *Oithona hebes* (Copepoda: Cyclopoida) in a coastal estuarine lagoon of Venezuela: a stage-dependent matrix growth model. *Ecol. Model.*, 161:159–168.

Twombly, S. 1994. Comparative demography and population dynamics of two coexisting copepods in a Venezuelan floodplain lake. *Limnol. Oceanogr.*, 39:234–247.

Twombly, S. and Lewis Jr., W. M. 1989. Factors regulating cladoceran dynamics in a Venezuelan floodplain lake. *J. Plankton Res.*, 11:317–333.

Uye, S. I. 1982. Population dynamics and production of *Acartia clausi* Giesbrecht (Copepods: Calanoida) in inlet waters. *J. Exp. Mar. Biol. Ecol.*, 57:55–83.

Uye, S. I. 1988. Temperature–dependent development and growth of *Calanus sinicus* (Copepoda: Calanoida in the laboratory. *Hydrobiologia*, 167/168:285–293.

Van Leeuwen, H. C. and Maly, E. J. 1991. *Chaoborus* prey capture efficiency in the light and dark. *Limnol. Oceanogr.*, 26:461–466.

Verheye, H. M. and Richardson, A. J. 1998. Long–term increase in crustacean zooplankton abundance in the southern Benguela upwelling region (1951–1966): bottom–up or top–down control? *ICES J. Mar. Sci.*, 55:803–807.

Vidal, J. 1980. Physioecology of zooplankton. II Effects of phytoplankton concentration, temperature and body size on the growth of *Calanus pacificus* and *Pseudocalanus* sp. *Mar. Biol.*, 56:111–134.

Wiebe, P. H. and Benfield, M. C. 2003. From the Hensen net toward four-dimensional biological oceanography. *Prog. Oceanogr.*, 56:7–136.

Williams, R. and Lindley, J. A. 1980. Plankton of the Fladen Ground during FLEX 76. I. Spring development of the plankton community. *Mar. Biol.*, 60:47–56.

Winfield, I. J. and Townsend, C. R. 1983. The cost of copepod reproduction: increased susceptibility to fish predation. *Oceanologia*, 60:406–411.

Wood, S. N. 1994. Obtaining birth and mortality patterns from structured population tragjectories. *Ecol. Monogr.*, 64:23–44.

Wood, S. N. and Nisbet, R. M. 1991. Estimation of mortality rates in stage-structured populations. In *Lecture Notes in biomathematics*, volume 90, pages 1–101. Springer–Verlag.

CHAPTER 2 MESOZOOPLANKTON COMMUNITIES

2.1 Introduction

The interactions among physical and biological processes at a wide range of spatial and temporal scales are important in structuring biological communities in marine environments (Daly and Smith Jr. 1993). Physical processes, such as tidal and wind-induced currents can regulate the occurrence and abundance of planktonic species (Hassett and Boehlert 1999; Bailey and Houde 1989; Steele and Frost 1977). Most zooplankton species have small body sizes and are weak swimmers incapable of horizontal control over their positions. Therefore, they tend to be transported horizontally as passive, neutrally buoyant particles (Power 1989; Banse 1986; Hannan 1984). This, combined with their frequent use of vertical migration, makes zooplankton subject to a wide range of environmental conditions in physically heterogenous coastal waters. Physical processes can influence zooplankton population dynamics by changing temperature and salinity on different spatial and temporal scales. Temperature is one of the most important factors regulating the growth rate of poikilothermic organisms such as zooplankton (Huntley and Lopez 1992; Thompson 1982). Large salinity variations may cause high mortality due to osmotic stress (Cervetto et al. 1999). Knowledge about how zooplankton respond to changes in these factors is necessary to interpret zooplankton temporal and spatial variations, food web dynamics, and biogeochemical cycles.

Quantitative samples of zooplankton reflect the influence of biological processes such as recruitment growth, and mortality, as well as physical processes (Huntley and Niiler 1995). In highly advective coastal waters, the distribution patterns of planktonic species can change markedly within a few hours (Ibanez 1976). This large variation may be related to the influence of different physical processes operating on varying spatial and temporal scales (Daly and Smith Jr. 1993). Tidal fluctuations can have a profound influence on zooplankton assemblages

by superimposing a diurnal or a semi–diurnal periodic component to the longer term trend of zooplankton abundance (Kimmerer et al. 1998; Gagnon and Lacroix 1981). Wind forcing can affect both vertical and horizontal distributions of zooplankton, thus influence their population birth, death and growth rates by placing the organisms in different physical and biological environments (Paffenhöfer et al. 1994; Wroblewski 1980).

Since the pioneering work of Hensen (1887), sampling variability has been a concern for biological oceanographers (Wiebe and Benfield 2003). Zooplankton distributions exhibit patchiness over a broad range of temporal and spatial scales (Mackas et al. 1985; Haury et al. 1978), thus high variability among replicate net tows is common. In coastal areas, the mixing processes associated with river outflow and oceanic water can be affected by tides, river input, bathymetry, shoreline geomorphology, and wind-induced and geographic currents. These physical processes can change local coastal hydrographic conditions (e.g., stratification, turbidity) and food availability on different temporal and spatial scales (Johnson and Costello 2002; Orive et al. 1998; Roden et al. 1987; Chelton et al. 1982) consequently altering zooplankton distributional patterns.

How a species responds to environmental changes depends in large part on its own physical tolerance and behavior (McKinney 1997), thus different species may respond to the same environment changes differently. In estuarine environments, salinity may change rapidly within a wide range due to river runoff. For oceanic species that are acclimated to high salinity water, encountering the low salinity of estuaries can cause stress or death due to osmotic changes, consequently the number of species present may also decrease (Vernberg and Vernberg 1972).

The Mississippi River plume influences a large part of the northern Gulf of Mexico. Discharge varies seasonally, being greatest in spring, decreasing through summer and fall to a winter low (Dinnell and Wiseman 1986). The Mississippi river's outflow enhances local primary productivity (Riley 1937), which produces correspondingly high secondary production

and abundances of zooplankton (Dagg and Whitledge 1991; Ortner et al. 1989). The mixing zone associated with Mississippi River outflow follows steep, dynamic, physical boundaries with the Gulf of Mexico continental shelf ecosystem. The mixing zone has important ecological effects on the distribution and survival of estuarine and shelf zooplankton communities (Dagg and Whitledge 1991; Ortner et al. 1989; Minello 1980; Marum 1974).

The aim of this component of my study was to examine variations in the northern Gulf of Mexico zooplankton community in the spring and early summer of 2003. The objectives were to:

- Investigate the variation of zooplankton community structure (total abundance, species composition, species richness) corresponding to tidal and wind-driven currents.
- Study temporal trends for dominant species and identify the physical factors likely controlling their local abundance.

2.2 Methods

2.2.1 Study Site and Zooplankton Sampling

Sampling was conducted at South Timbalier 151 (ST151), a ChevronTexaco offshore petroleum platform complex located 50 km south of Grand Isle, Louisiana (28°37'N, 90°15'W) in 45m water depth (Figure 2.1). Zooplankton samples were collected at 12h intervals from March 18–April 6 and from May 15–June 9, 2003 (the interruption was caused by construction work on the platform). Vertical tows were made from approximately 15m depth to the surface using a 70cm diameter, ring plankton net (2.5m long, 153 μm mesh) hauled vertically at a rate of 20–25 cm s^{-1} by an electrical winch. The net was lowered into the water from approximately 20m above the surface. Depth was determined by lowering the tow cable to a premeasured mark. This mark corresponded to a depth of 15m that was initially verified with a VEMCO temperature and depth data logger in March–April, but was lost during the second sampling

period. The sampling depth error was within 0.7m and the average water volume filtered for each net tow was 5.75 m^3. At each sample time, three replicate net tows were taken over a 30 min period.

Zooplankton were fixed in 5% formalin and transported to the platform's laboratory, where samples were transferred to 70% ethanol before being sorted and identified. A Folsom plankton splitter was used to sub-sample the total plankton sample. Splits were limited so that the most abundant taxonomic group produced over 100 individuals (Postel et al. 2000). Organisms were sorted and identified under a stereo-microscope (50x) down to the lowest possible taxonomic level. The abundance was then calculated as number m^{-3}. Vertical profiles of temperature and salinity were taken every 12h with an YSI 6920 sonde. Surface temperature and surface salinity were extrapolated from the data collected by the sonde at 1m water depth.

Available OCEANSAT satellite images of chlorophyll from Earth Scan Laboratory at Louisiana State University were examined to determine the location and intensity of the Mississippi River plume in relation to ST151. Water level, current velocity, current direction, wind speed and direction were obtained from the Wave-Current-Surge Information System (WAVCIS; CSI station 6, 28°52'N, 90°29'W; Figure 2.1). Hourly WAVCIS water level data were used to investigate tidal patterns during the study period.

2.2.2 Data Analysis

Zooplankton abundance was estimated by taking the mean of three replicate tows for each sample time. The coefficient of variation was calculated as the ratio of standard deviation and mean value from the three replicated net samples. Regression analyses were performed on total abundance versus extrapolated salinity and temperature at 1m. The assumption of normality for residuals were examined with a Kolmogorov-Smirnov test. In this case, the residuals violated the normality assumption, so total abundances were log transformed. No

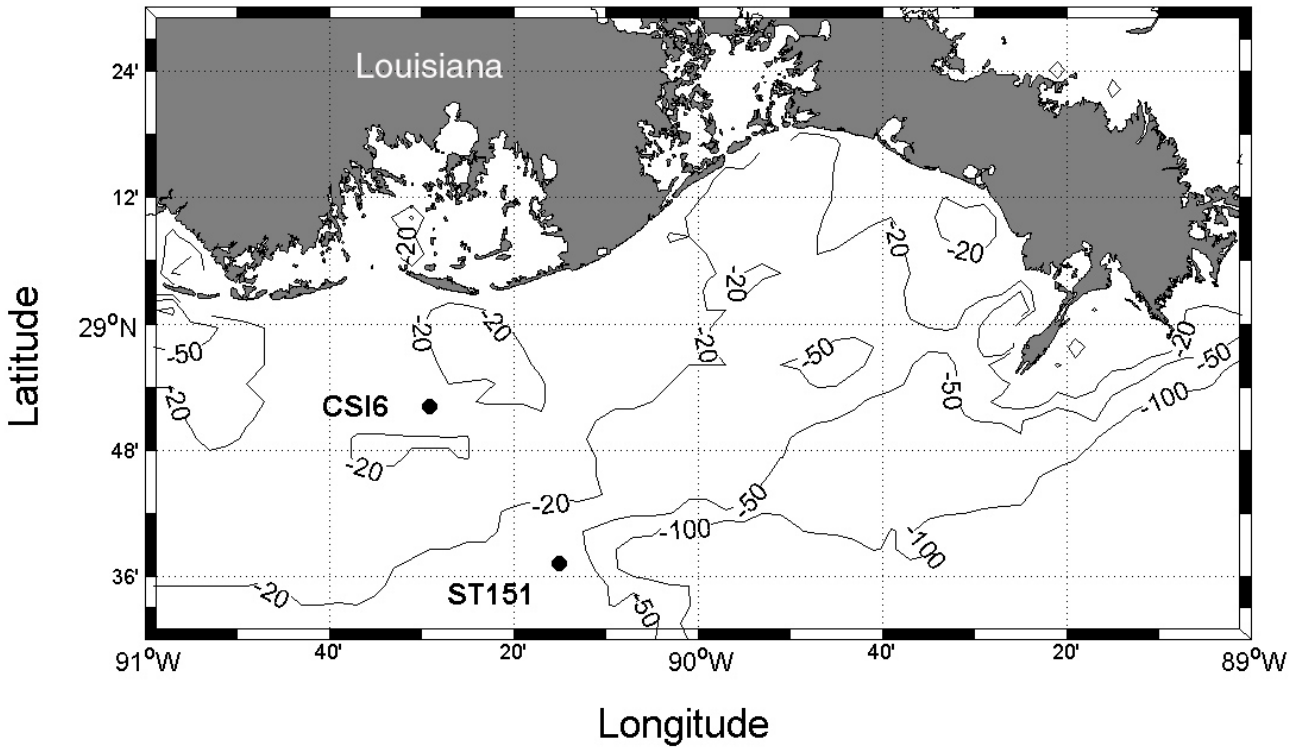

Figure 2.1: Location of the South Timbalier 151 (ST151) study site and the Wave-Current Surge Information System (WAVCIS) observing station (CSI6) in relation to the Mississippi River delta. Depth contours are in meters.

outliers were detected. The hypothesis that both surface salinity and temperature had no effects on log–transformed total abundance was tested by F-test (SAS Institute, 1990).

The total number of species in the community was evaluated by estimating species richness, i.e., the number of species in the community including those that may not have been sampled. The species richness indices were estimated within each sample of three replicates by using the first order jackknife and bootstrap indices (Smith and Belle 1984). These indices are standard descriptors of zooplankton community structure (Postel et al. 2000). Both methods resample the observed species and relate the estimated species richness to an upper sample size as indicated by equation 2.1 and equation 2.2. The analysis included 29 occurring taxonomic groups, which contained 15 copepod species.

$$J_n(S) = S_0 + r_1 \frac{(n-1)}{n} \tag{2.1}$$

$$B_n(S) = S_0 + \sum_{j=1}^{S_O} (1 - p_j)^n \tag{2.2}$$

where $J_n(S)$ is the species richness estimates of the first order jackknife, $B_n(S)$ is bootstrap estimate, the S_0 is the total number of observed species, r_1 is the number of species found only once in the samples, n is the number of samples, p_j is the proportion of replicates in which species j is present.

To study the periodic components in the total abundance variations that corresponded to the frequency and phase of the tidal components, hourly water depth data were used from CSI 6. Hourly wind data were averaged over six hour periods to generate mean wind speed and direction.

To study the shifts in community structure corresponding to the presence of different water masses, surface salinity was adopted as a water mass indicator. Samples were classified as three different groups according to salinity at 1m: low salinity (<25 psu) represented the

Mississippi River plume water mass; intermediate salinity (25–30 psu) represented a mixed river–oceanic water mass; and high salinity (>30 psu) represented an oceanic water mass. A multi–dimensional scaling procedure (MDS; PRIMER, 2000) was applied to examine the similarity among different zooplankton samples and species (contributing more than 15%) using Bray–Curtis similarities. A stress value was calculated to measure goodness–of–fit, where low stress (< 0.2) suggests a good fit (Clarke and Warwick 1994).

A multivariate analysis of variance (MANOVA) procedure was applied on the three different salinity groups by using PROC GLM procedure (SAS, 1990) to test overall salinity effects on community structure. The model contains the abundance of 11 taxa as dependent variables and salinity group as independent variable. Comparisons among the three groups were also performed. The effects included in the model were the dominant species, which account for more than 90% of total abundance. The hypothesis that salinity had no effect in the MANOVA was tested using a Wilks' Lambda test. The assumptions and their screening tests for the MANOVA test were: (1) multinormal distribution, which was examined by testing marginal distribution for each included abundance; (2) homogeneity of variances, which was tested by a variance ratio test (F–test) among different salinity groups for each dependent variable; and (3) the independence of dependent variables, which were examined by partial correlation coefficients. In this case, the MANOVA test violated the assumptions of multinormality and homogeneity of variance. However, the MANOVA is a robust test and it can still reveal the differences among different salinity group and this test was performed as a supportive test for MDS.

To study the temporal abundance trends of individual species and to identify likely factors controlling local abundance, scatter plots were generated to examine the relationship among total abundance, salinity and temperature. Then regression analysis was applied to quantify this relationship. Preliminary analysis indicated the normality assumption for residuals was violated. To satisfy the normality assumption, a $\log(x+1)$ transformation was applied to species

abundances. Since *Clausocalanus furcatus* and *Eucalanus attenuatus* have been reported as typical oceanic species (Ortner et al. 1989; Marum 1974), their abundance may be more related to the volume of high salinity offshore water below the halocline than the surface salinity. Halocline depth, defined as the midpoint of the region of greatest change in salinity over depth, was used as a regressor rather than surface salinity for these two copepods .

2.3 Results

2.3.1 Physical Conditions

The study site ST151 is located in a region that is frequently influenced by the Mississippi River plume. When the River outflow is strong, lighter plume water is represented by a shallow lens of low salinity (~18–25 psu) water overlaying heavier high–salinity Gulf of Mexico shelf water (Figure 2.2a). When the outflow is relative weak, the salinity gradient is relatively weak and the halocline becomes deeper (Figure 2.2b). The predominance of oceanic water is characterized by a weak salinity gradient (Figure 2.2c). Surface salinity showed substantial fluctuations during the entire study period in response to the shifting outflow of the riverine plume; whereas salinity appeared to be constant at ~35 psu below the halocline (Figure 2.3a).

Surface temperature appeared to be constant from mid March to early April, ranging from 18.5˚C–21.7˚C and temperature did not show a strong vertical gradient (Figure 2.3b). When sampling resumed in mid May, temperature had increased to 26.8˚C and gradually increased over the reminder of sampling period, during which time the water column was be more thermally stratified.

The diurnal tide had two spring–neap cycles in each lunar month. The entire study period fell into three cycles: the first part of the sampling period experienced one cycle separately and the latter part experienced two cycles (Figure 2.4). In the first and third cycle, water level potentially was influenced by the prevailing southward wind, since the difference between high

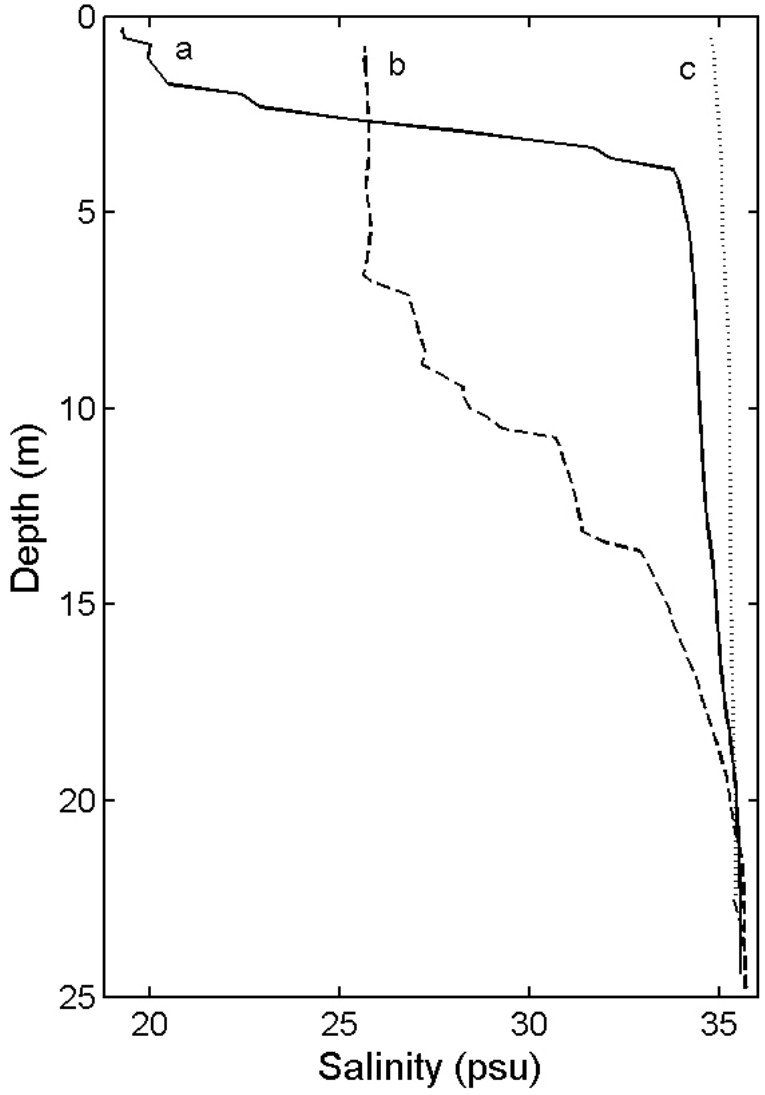

Figure 2.2: Representative salinity profiles at the study site: a) river plume water on top of oceanic water, which typically had a halocline from 2m–5m; b) river plume water mixed with oceanic water with a more gradual halocline extending from below 5m to 15m; and c) oceanic water dominated conditions with little or no halocline.

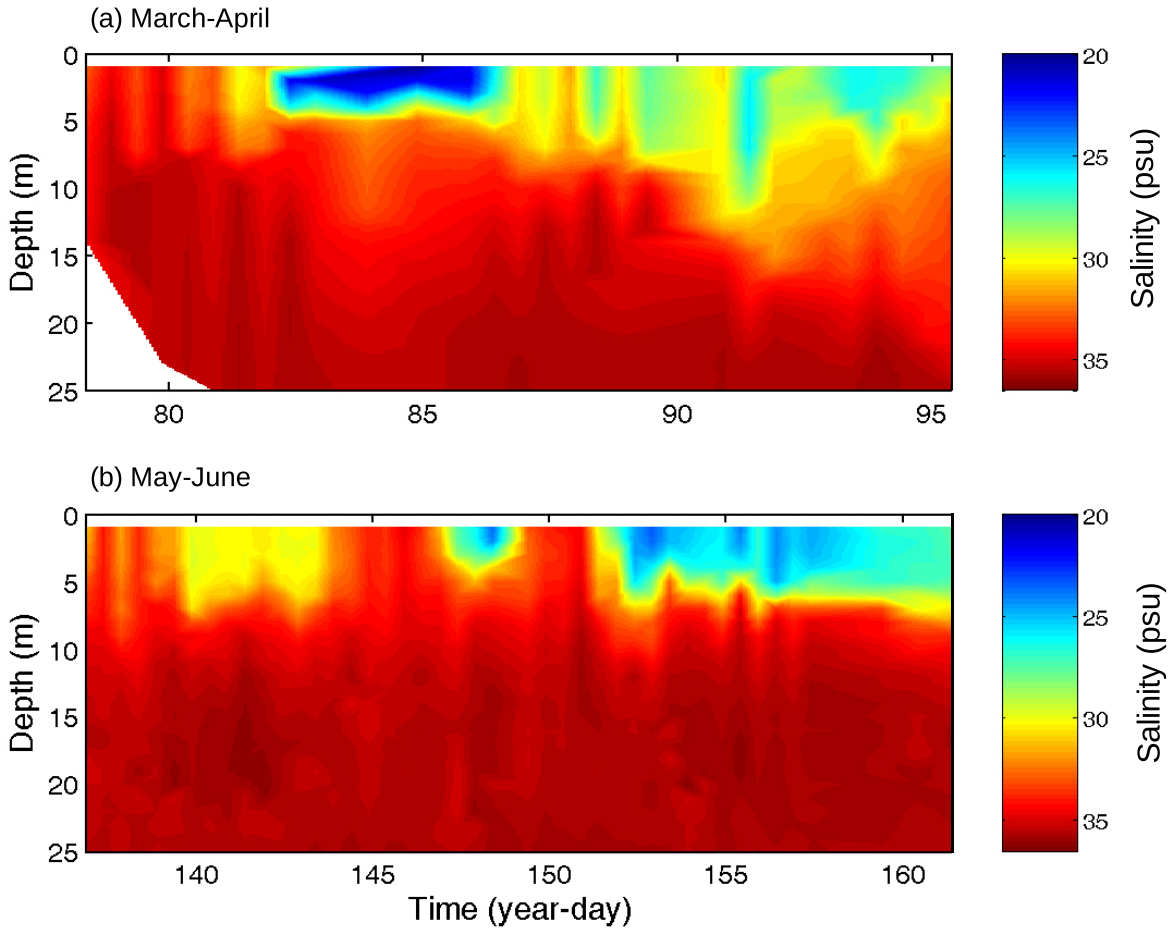

Figure 2.3: Temperature and salinity profiles during the studying period. (a) A salinity profile in March–April 2003 and (b) lower panel showing salinity in May–June 2003; (c) A temperature profile in March–April; and panel (d) temperature profile in May–June. Figure continues on next page.

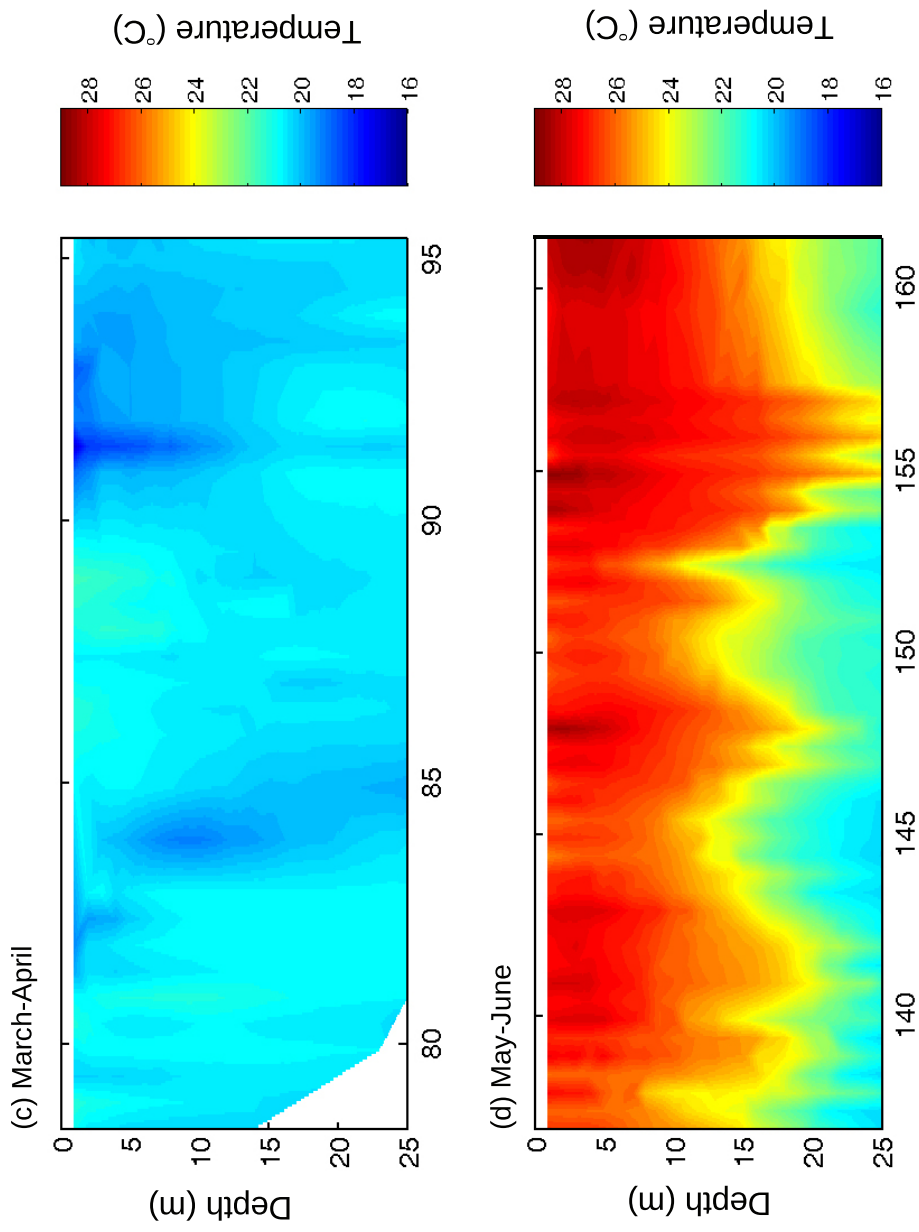

Figure 2.3 (continued)

and mean water level was less than the difference between the mean and low water level. This wind–induced effect was less in the second spring–neap cycle.

The Mississippi River plume generally flowed westward during the study period as observed from satellite imagery (Figure 2.5). A strong plume event was observed from Oceansat satellite images of the surface chlorophyll a on March 22 and 24, which corresponded to a decrease in both the magnitude and variation of surface salinity during those days (Figure 2.3, year day 82–86). At the end of May, the Mississippi River plume flowed southeast due to a prevailing north wind, and then turned back to the study site steered by either ocean currents or some other physical forcing.

2.3.2 Total Abundance of Mesozooplankton and Sampling Variability

Total mesozooplankton abundance showed a large (10x) variation (Figure 2.6) and copepods were the dominant group on all sampling dates, accounting for 68% to 95% of the total abundance. Three maxima occurred during the study period corresponding to large changes in surface salinity. The first peak in total abundance (year day 82–86) can be explained by the influence of Mississippi River plume (Figure 2.6). The second peak (year day 147–150) also corresponded to a local salinity drop, however, satellite images were not available during that period. The third peak (year day 152–162) corresponded to the renewal presence of plume water.

The coefficient of variation based on the three replicates for each sampling interval ranged from 1.7% to 89.6%, with a mean value of 22.2%, and was lower than 50% for more than 70% of samples (Figure 2.7). However, the variations among replicates did not appear to be influenced by salinity changes over the entire study period.

Results from a regression analysis on log total mesozooplankton abundance versus seasonality and salinity, with the test hypothesis of both factors having no effects, showed that

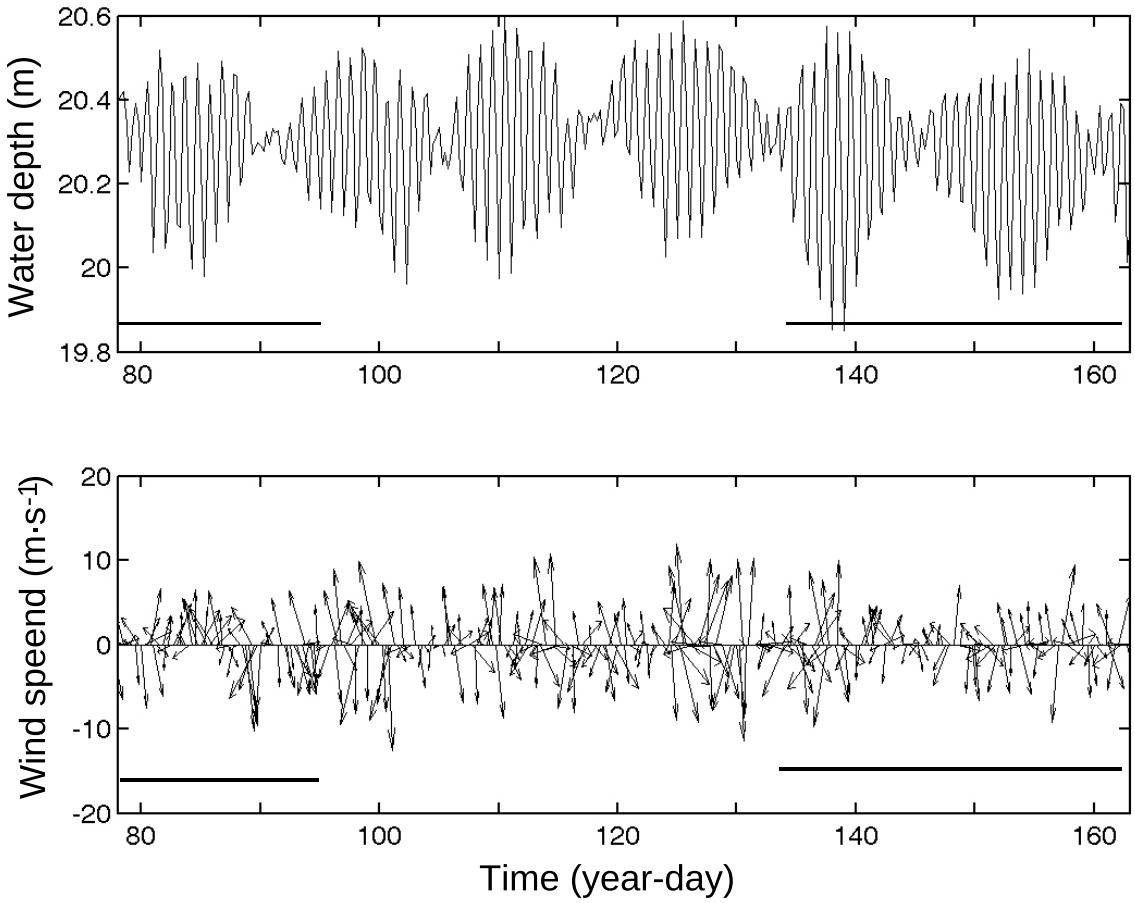

Figure 2.4: Tidal patterns, wind speed and direction from the Wave-Current Surge Information System observing station, CSI 6. The top panel shows the tidal patterns from hourly observing data; lower panel shows wind speed and wind direction from hourly observing data averaged over 6 hours, wind vectors point to the direction from which the wind is blowing. Horizontal line indicates when data collection occurred.

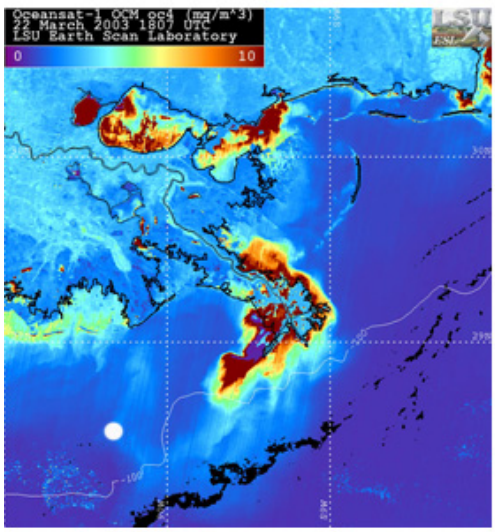

March 22 2003

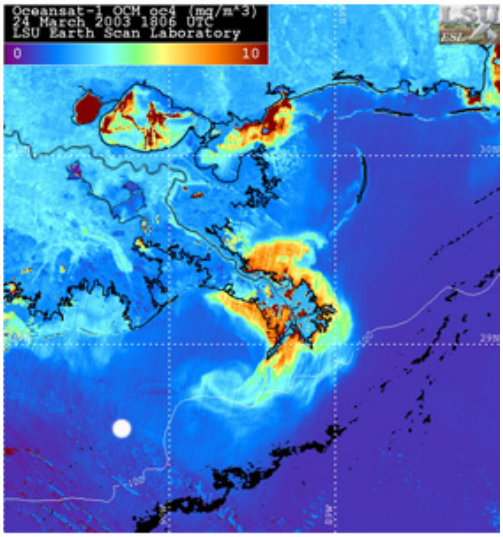

March 24 2003

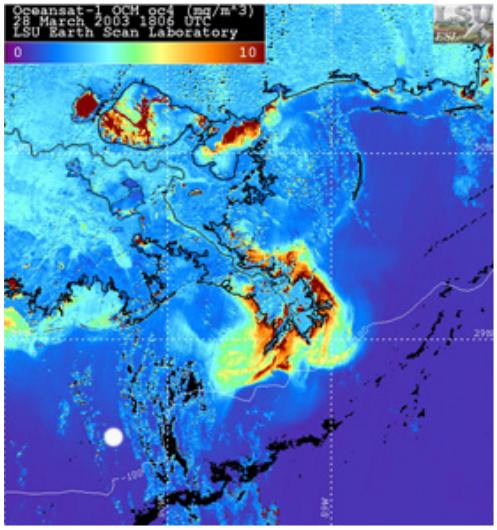

March 28 2003

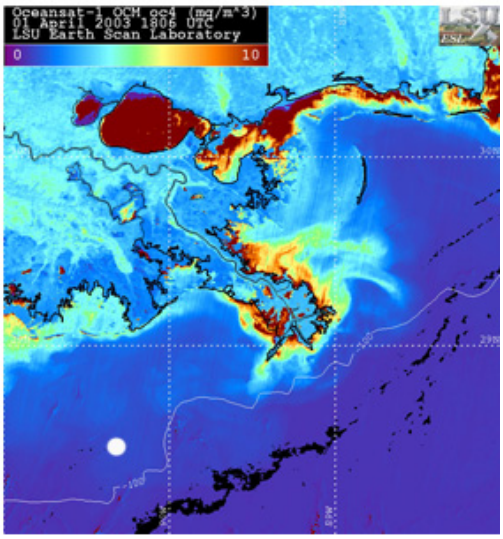

April 1 2003

Figure 2.5: Oceansat satellite images of surface chlorophyll *a* around the Mississippi River plume. The white dot is the location of ST151. Because of cloud coverage, these images are the only ones available which adequately show the extension of the Mississippi River plume in relation to ST151. During the periods of March 22 and 24 and May 29 and 31, the images show the Mississippi River plume likely had a strong influence on the study site. The remaining images indicate that the Mississippi River plume did not extend far enough to influence the study site. Figure continues on next page.

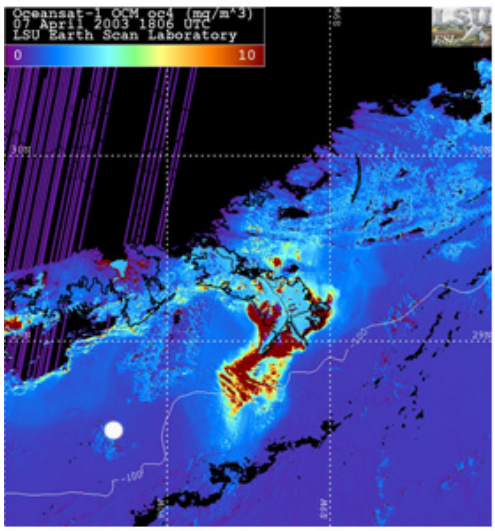

April 7 2003

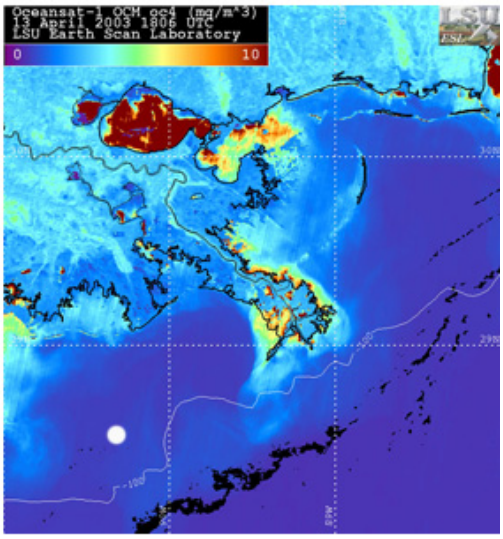

April 13 2003

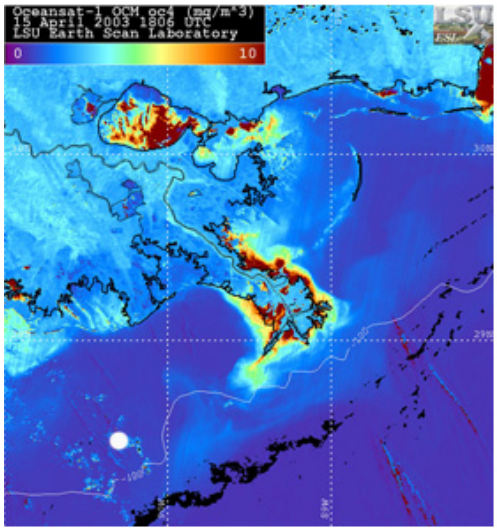

April 15 2003

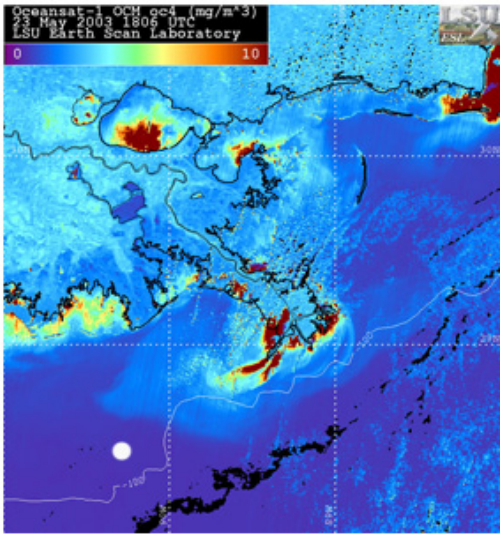

May 23 2003

Figure 2.5 (Continued)

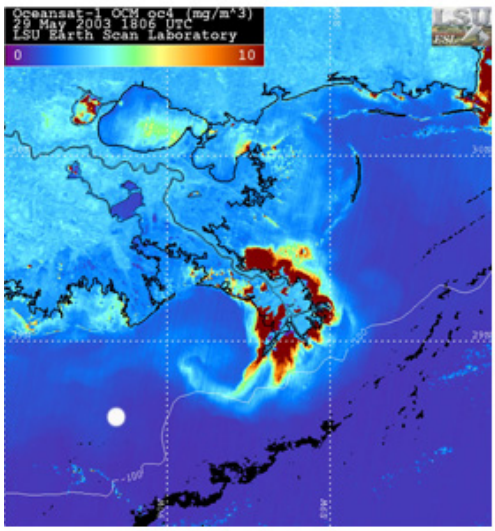

May 29 2003

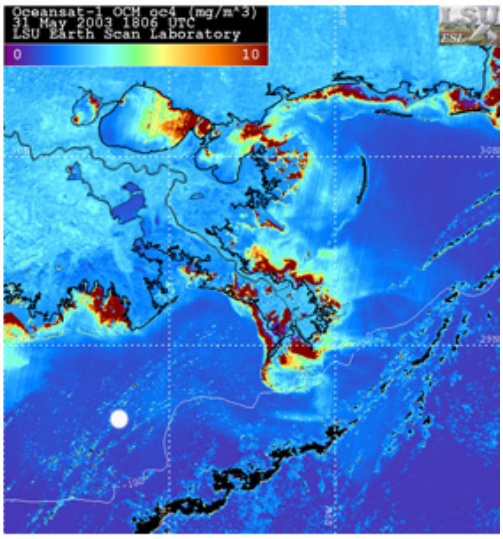

May 31 2003

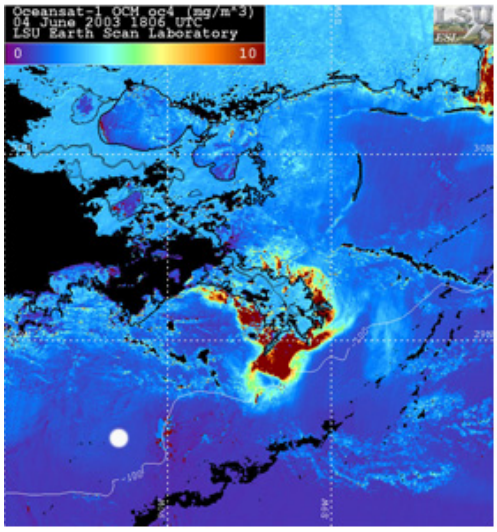

June 4 2003

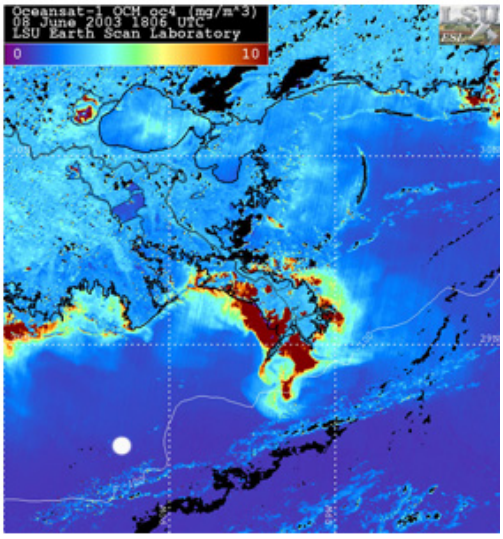

June 8 2003

Figure 2.5 (Continued)

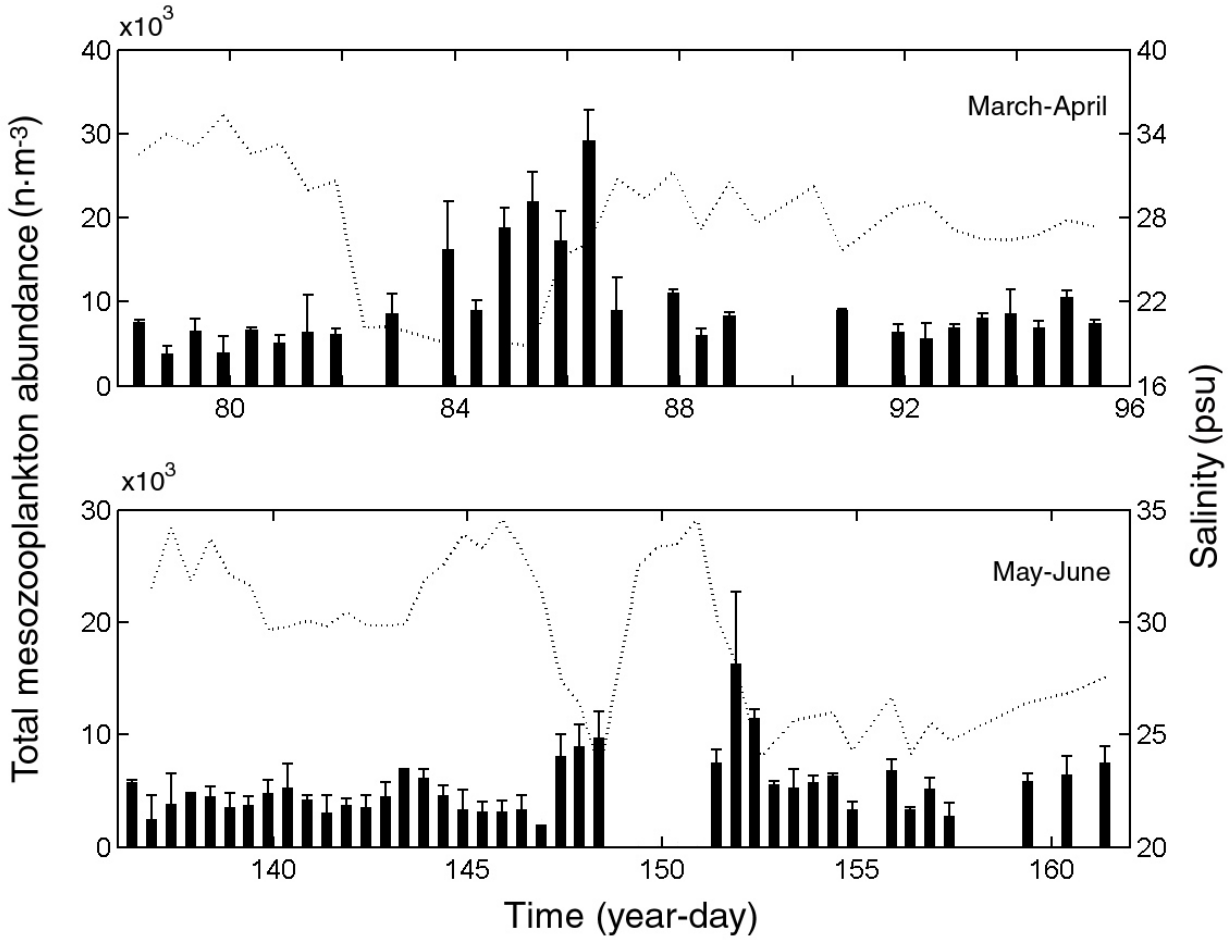

Figure 2.6: Mean abundance of mesozooplankton from the upper 15m of the water column over the study period. Each bar is the mean density from three replicate vertical tows and error bars represent one standard deviation. The dotted line shows surface salinity. The upper panel shows abundance in March–April and the lower panel shows abundance in May–June 2003.

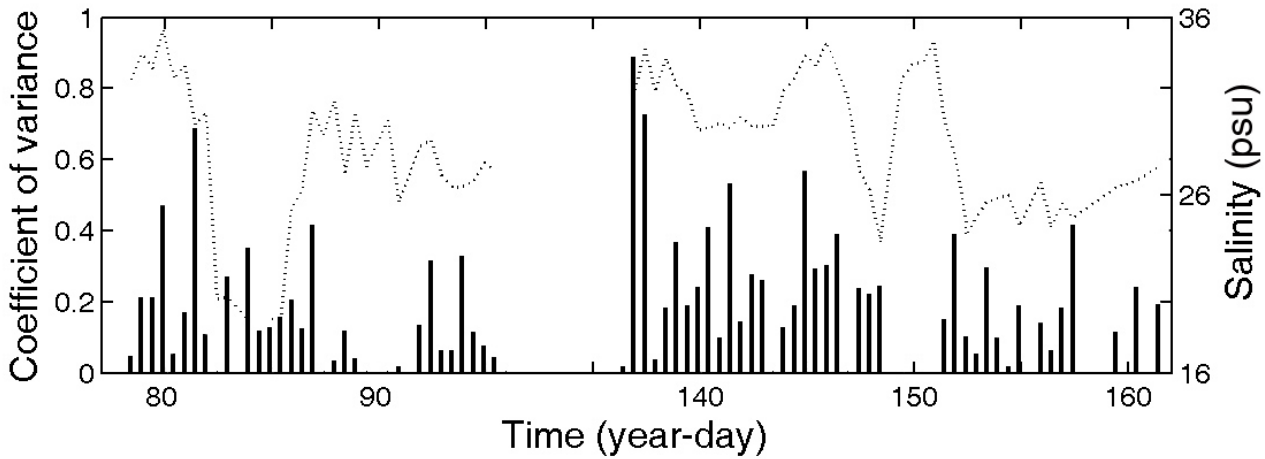

Figure 2.7: Coefficient of variation based on three replicates for each sample period. The bars represent the coefficient of variation and the dotted line represents surface salinity.

Table 2.1: Parameter estimates, *t*–test and *p*–values for the regression model with log–transformed total abundance as the dependent variable, and salinity and seasonality as independent variables.

Variable	DF	Parameter estimates	Standard error	*t*–value	*p*–value
Intercept	1	12.41	0.46	27.01	<0.01
Temperature	1	-0.06	0.01	-4.88	<0.01
Salinity	1	-.07	0.01	-6.07	<0.01

seasonality and salinity explained most of the variation ($F = 32.64$; $p < 0.01$; $R^2 = 0.50$) and both factors had significant effects on log total abundance (Table 2.1). The residual–by–predicted plot is provided in Appendix A and a Kolmogorov-Smirnov test indicated that the residuals did not violate the normality assumption ($p \geq 0.15$). The results of regression analysis indicated an inverse relationship between total abundance and salinity, i.e., the low salinity plume water tends to have a higher zooplankton abundance than the high salinity offshore water. Total abundance declined towards summer. Salinity appeared to have a larger influence on local abundance than seasonality (Table 2.1).

2.3.3 Species Richness and Species Composition

Twenty common copepod species and nine other taxonomic groups were counted during the study period and of these eleven taxa had mean densities >100 n m^{-3} (Table 2.2). Two distinct groups represented a coastal shelf assemblage and an oceanic assemblage. The coastal shelf assemblage was composed of the copepods *Acartia tonsa, Centropages furcatus, Corycaeus*

clausii, *Paracalanus quasimodo*, larvaceans *Oikopleura* sp. and the chaetognath *Sagitta enflata*. The second oceanic assemblage was composed of the copepods *Clausocalanus furcatus*, *Eucalanus attenuatus* and *Euchaeta marina*.

The abundance of the coastal shelf group was greater than the oceanic group during the overall study period (Figure 2.8). Coastal and shelf species increased their abundance when surface salinity declined and made up more than 70% of total abundance when low salinity riverine water dominated the study site. The abundance of oceanic species did not show a large fluctuation and they made up a relative larger proportion of the total sample during high salinity periods than during low salinity.

Approximately 25–28 species occurred in net samples during the entire study period. Bootstrap and first order jackknife species richness indices showed similar patterns (Figure 2.9). Species richness was relative low during the period when surface salinity was lower than 25 psu in the study area during the first study period (year–day 82–86). In May–June, there were consistently 26 species which occurred in net samples.

2.3.4 Tidal Effects

Total abundance of mesozooplankton did not show a clear diurnal pattern during the entire study period (Figure 2.10). Total abundance underwent large variations during the spring tide period in March–April and the second spring tide period in May–June. Total abundance peaks on March 24 (year day 83) and on May 31 (year day 152) were coincident with spring tides. The first peak was also coincident with prevailing southward wind. During neap tides, total abundance did not undergo large fluctuations.

Table 2.2: Ranked average abundance ($n \cdot m^{-3}$), standard error and maximum concentration for common taxa (>100 $n \cdot m^{-3}$) collected between March 18–April 6 and May 15–June 9, 2003 from vertical net samples above 15m. Taxa are ranked in order of decreasing average abundance and SE is the standard error. 'C' represents coastal/shelf species and 'O' stands for oceanic species. [a]

Taxa	Median	Mean	SE	Maximum
Acartia tonsa (C)	680.33	2278.32	452.68	20446.87
Oikopleura sp. (C)	953.91	1389.72	145.60	4762.31
Oncaea mediterranea [b]	399.32	582.15	51.02	1730.40
Conaea sp. [b]	332.77	474.81	50.89	2203.67
Corycaeus clausii (C)	244.03	318.57	25.31	1014.95
Centropages furcatus (C)	188.57	298.37	34.69	1120.33
Clausocalanus furcatus (O)	232.94	286.13	20.25	876.29
Eucalanus attenuatus (O)	192.97	279.52	29.03	1419.92
Sagitta enflata (C)	207.06	230.79	18.03	926.10
Paracalanus quasimodo(C)	40.26	109.5	29.03	608.95
Oithona plumifera [b]	73.95	103.72	12.58	502.85

[a] *Euchaeta marina* is a common oceanic species that occurred in the study area with relative low abundance.

[b] Unclear habitat type

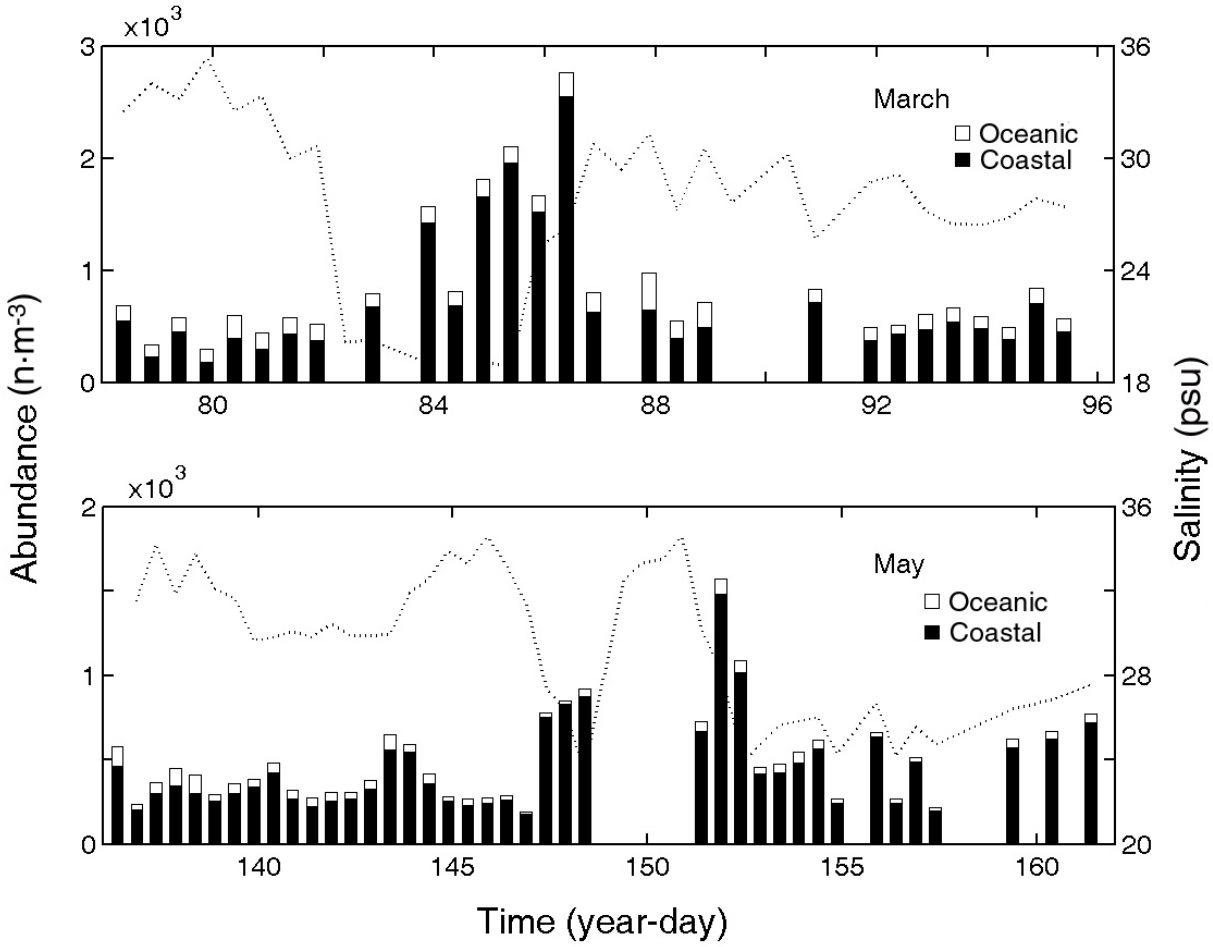

Figure 2.8: Abundance of coastal shelf and oceanic species in relation to surface salinity. The upper panel shows abundance and salinity (dotted line) in March–April, while the lower panel shows abundance and salinity in May–June.

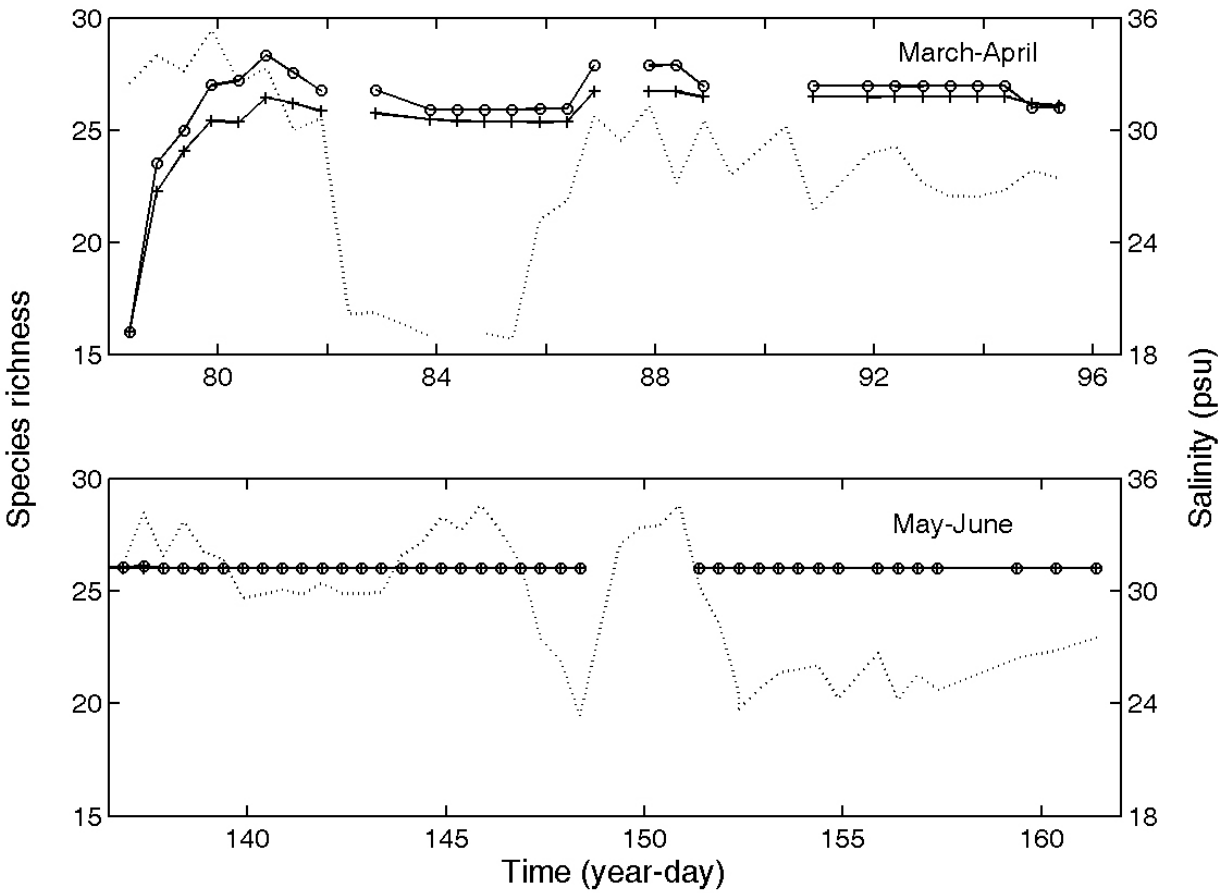

Figure 2.9: First order jackknife and bootstrap species richness indices during the study period: –+– represents the first order of the jackknife index; –o– represents the bootstrap index; and the dotted line represents surface salinity.

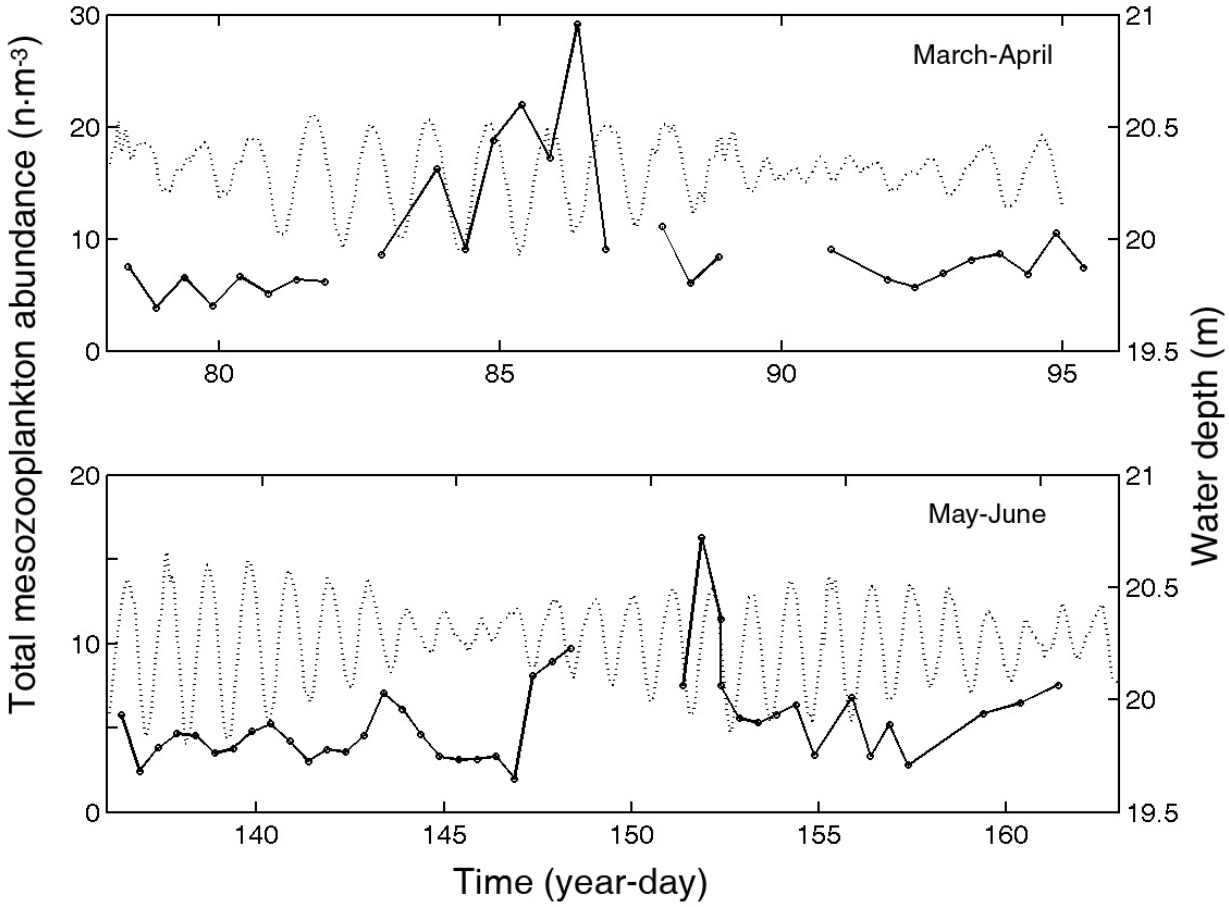

Figure 2.10: Total mesozooplankton abundance (solid line) and tidal pattern (dotted line) during the study period.

2.3.5 Shift of Community Structure

Salinity had a significant influence on community structure as indicated by multivariate analysis of variance (MANOVA; Table 2.3; $p < 0.01$). Low salinity samples (< 25 psu) and high salinity samples (> 30 psu) were well separated in a multidimensional scaling (MDS) plot (Figure 2.11). Samples from intermediate salinity (25–30 psu) spread among the two other groups. MANOVA analysis indicated that the high salinity group was different from both the intermediate and low salinity group (p <0.01 and 0.02, respectively) and there was no significant difference between the intermediate salinity and low salinity group ($p = 0.74$). Similarity among species suggested that *Acartia tonsa*, *Lucifer* sp. and hyperiid amphipods were responsible for differences between the low salinity and high salinity groups (Figure 2.11).

Table 2.3: Wilks' Lambda test statistics and p values for multivariate tests on zooplankton species abundance for the hypothesis of no difference among salinity groups.

Multivariate test	Num. DF	Denom. DF	Wilks' Lambda	F	p–value
Overall salinity effects	22	112	0.49	2.19	<0.01
Low vs. High	11	56	0.68	2.39	0.02
Low vs. Intermediate	11	56	0.88	0.69	0.74
Intermediate vs. High	11	56	0.69	2.39	<0.01

2.3.6 Factors Controlling Local Species Abundance

During the study period, salinity underwent large daily variation, whereas temperature was relatively stable within each of two sampling sub–periods. *Acartia tonsa*, *Labidocera nerri*,

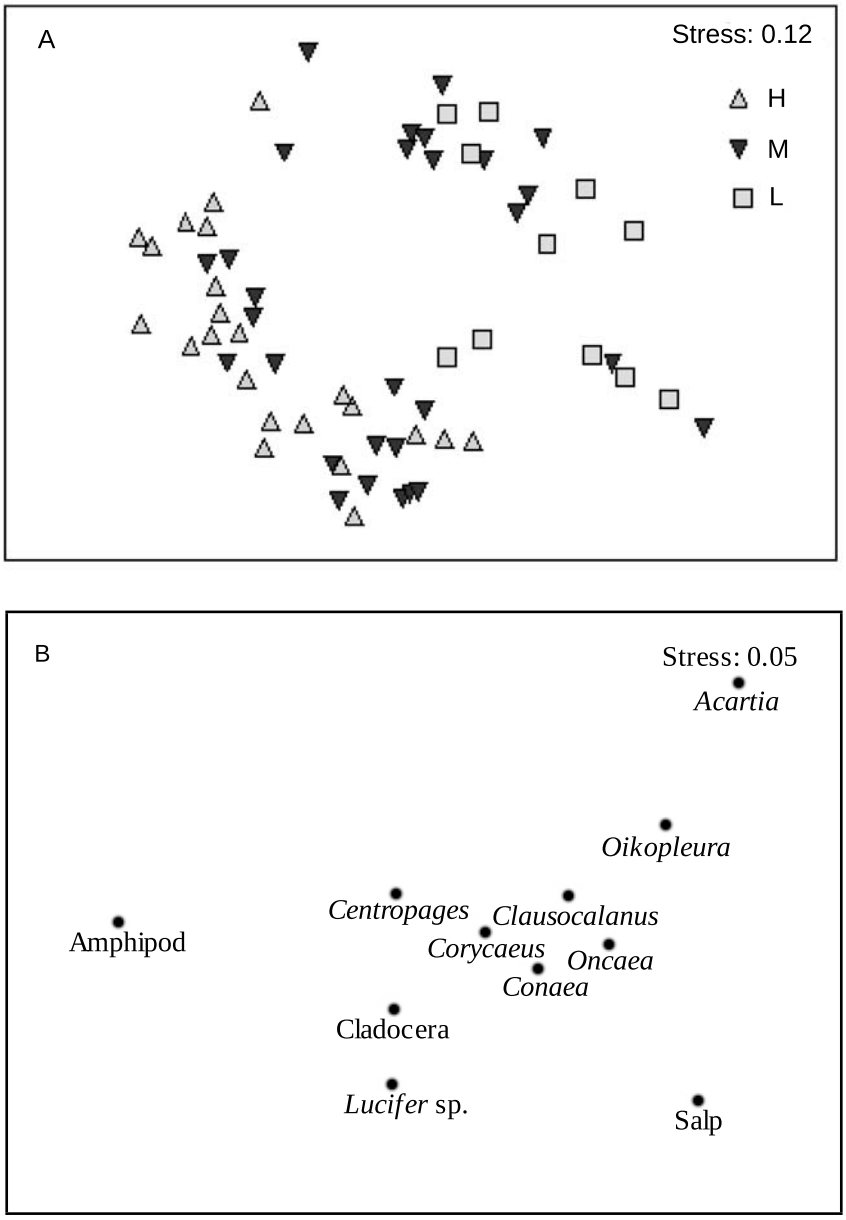

Figure 2.11: Multi–dimensional scaling (MDS) plots of mesozooplankton assemblages. Tight clustering of the data means high similarity. Stress indicates the quality of measurements with low stress suggesting good measurements: A) MDS for different samples categorized by salinity: H: high salinity; M: intermediate salinity; L: low salinity; B) MDS for species contributing more than 15% of the difference.

Eucalanus attenuatus and *Clausocalanus furcatus* appeared to respond strongly to salinity (Figure 2.12). *Acartia tonsa* and *L. nerri* had high abundances in low salinity riverine water and this was supported by a negative relationship between the log abundance and surface salinity from the regression analysis (Table 2.4). *Clausocalanus furcatus* increased their abundance with salinity, and *E. attenatus* appeared to have relative high abundance in low temperature and high salinity water (Figure 2.12). The peaks in abundance for *A. tonsa*, and *E. attenuatus* appeared to reflect the strong influence of the plume on March 24 (year day 83) and May 31 (year day 152), 2004 (Figure 2.13) which explained most of variability in total abundance. A positive relationship between the log abundance of *Cl. furcatus* and surface salinity was supported by the regression analysis (Table 2.4). Kolmogorov-Smirnov tests for the normality assumption indicated that linear regression analysis were not appropriate for some species (e.g., *Conaea* sp., Table 2.4). Results were only used when the normality assumption were satisfied. The R^2 from the regression analyses indicate that there are other factors influencing the species abundances (Table 2.4).

The abundance of *Oikopleura* sp., *Oncaea mediterranea*, *Centropages furcatus*, and *Paracalanus quasimodo*, appeared to respond to temperature (Figure 2.14). This group can be divided into two subgroups. Abundance increased with the temperature for *Centropages furcatus*, *Sagitta enflata*, and *Corycaeus clausi*, and regression analysis showed a positive relationship between temperature and species for *Ce. furcatus*, *C. clausi* and *S. enflata* (Table 2.4). Abundance of *Oikopleura* sp. and *Oncaea mediterranea* decreased with the increase of temperature, and regression analysis only supported result for *Oikopleura* (Table 2.4). The variation of species abundance over two study periods shown in Figure 2.15 can be mainly explained by temperature.

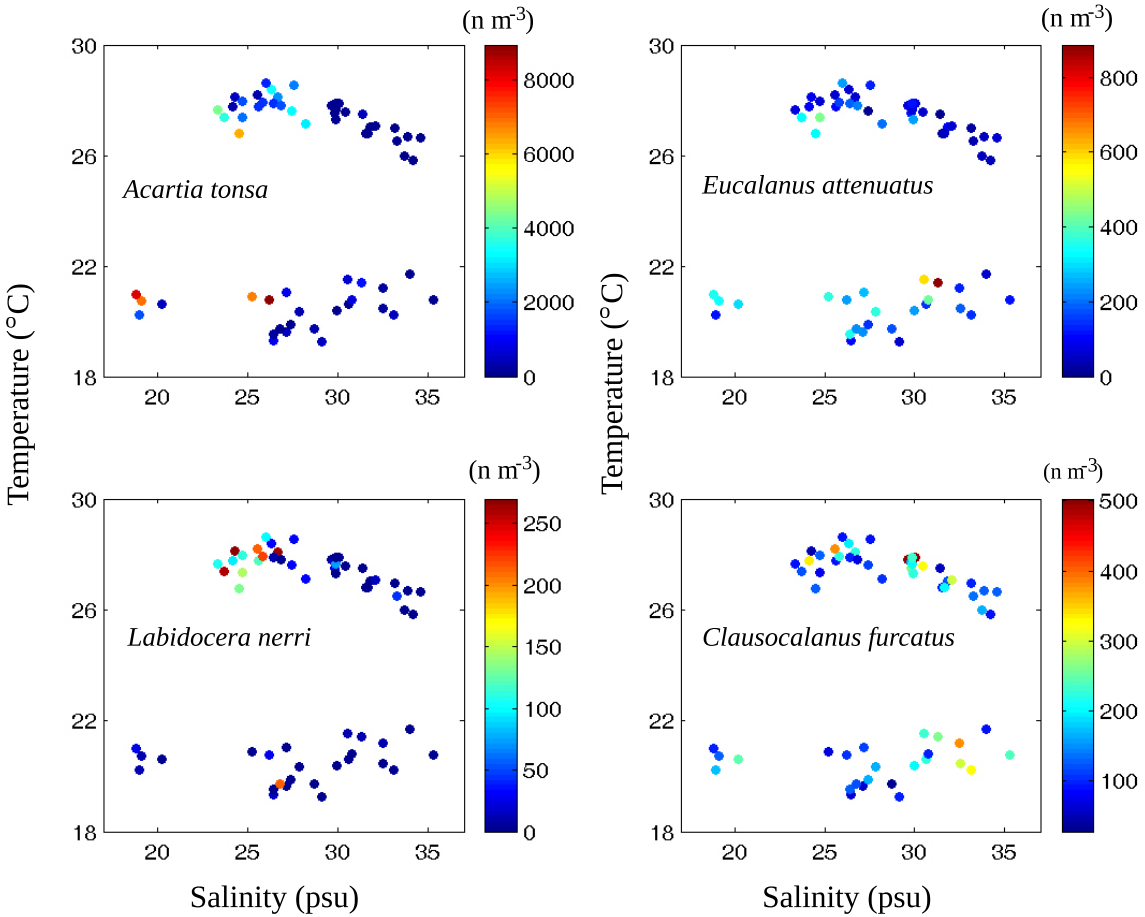

Figure 2.12: Scatter plot for species with abundance affected by salinity: abundance versus salinity and temperature. Color scale represents abundance (n m^{-3}).

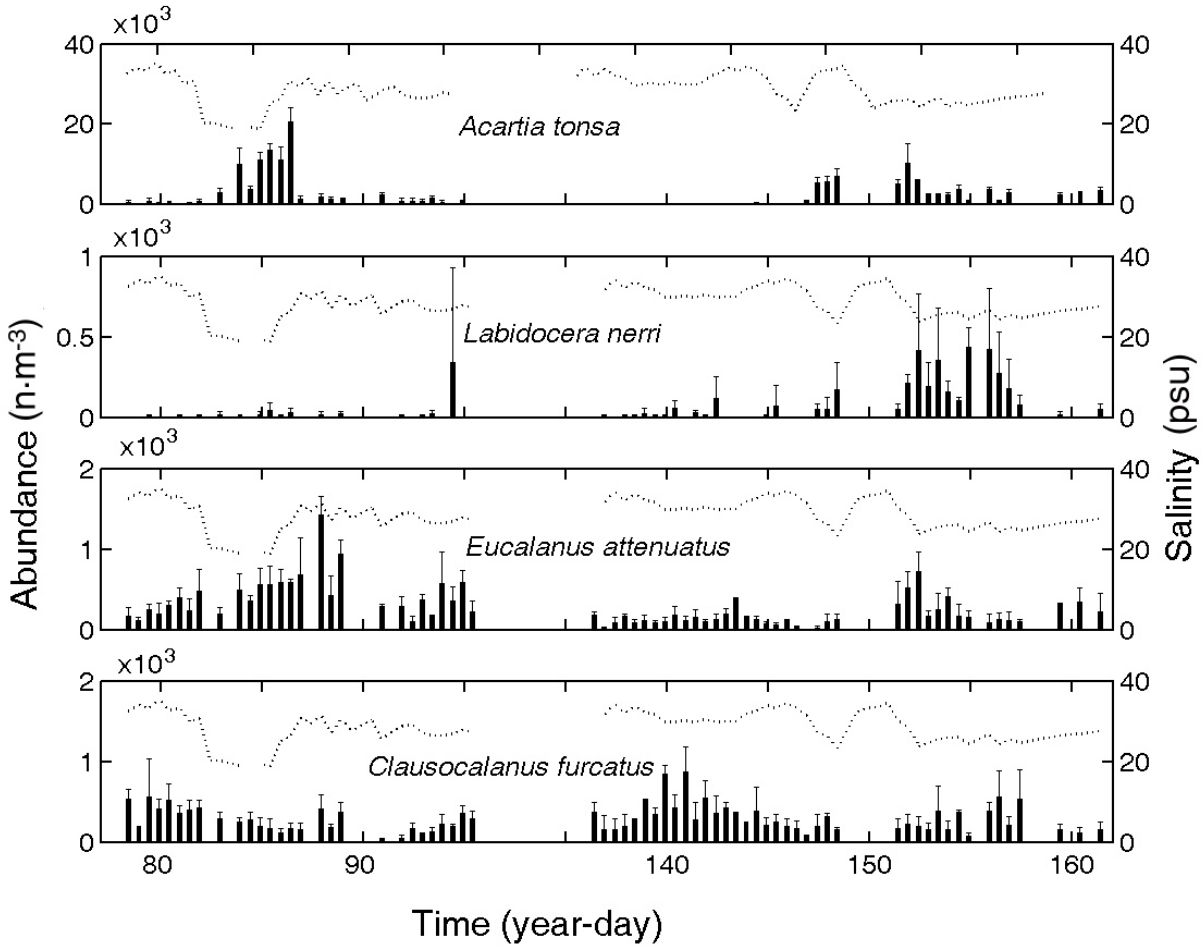

Figure 2.13: Abundance of species (histograms; 0–15m, mean value from 3 replicate net tows) that appeared to respond strongly to salinity (dotted line) during the study period. Error bars represent on standard error.

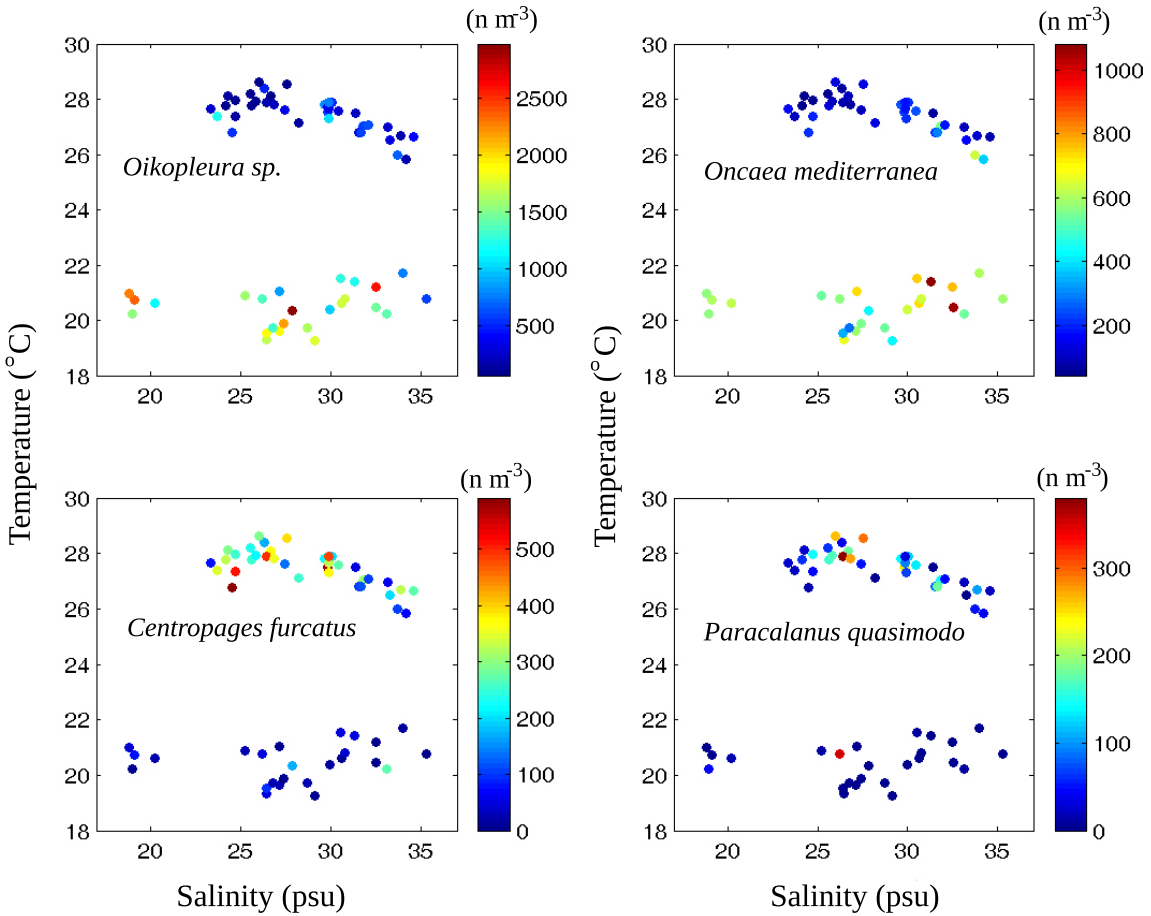

Figure 2.14: Scatter plot for species with abundance affected by temperature: abundance versus temperature and salinity. Color scale represents abundance (n m^{-3})

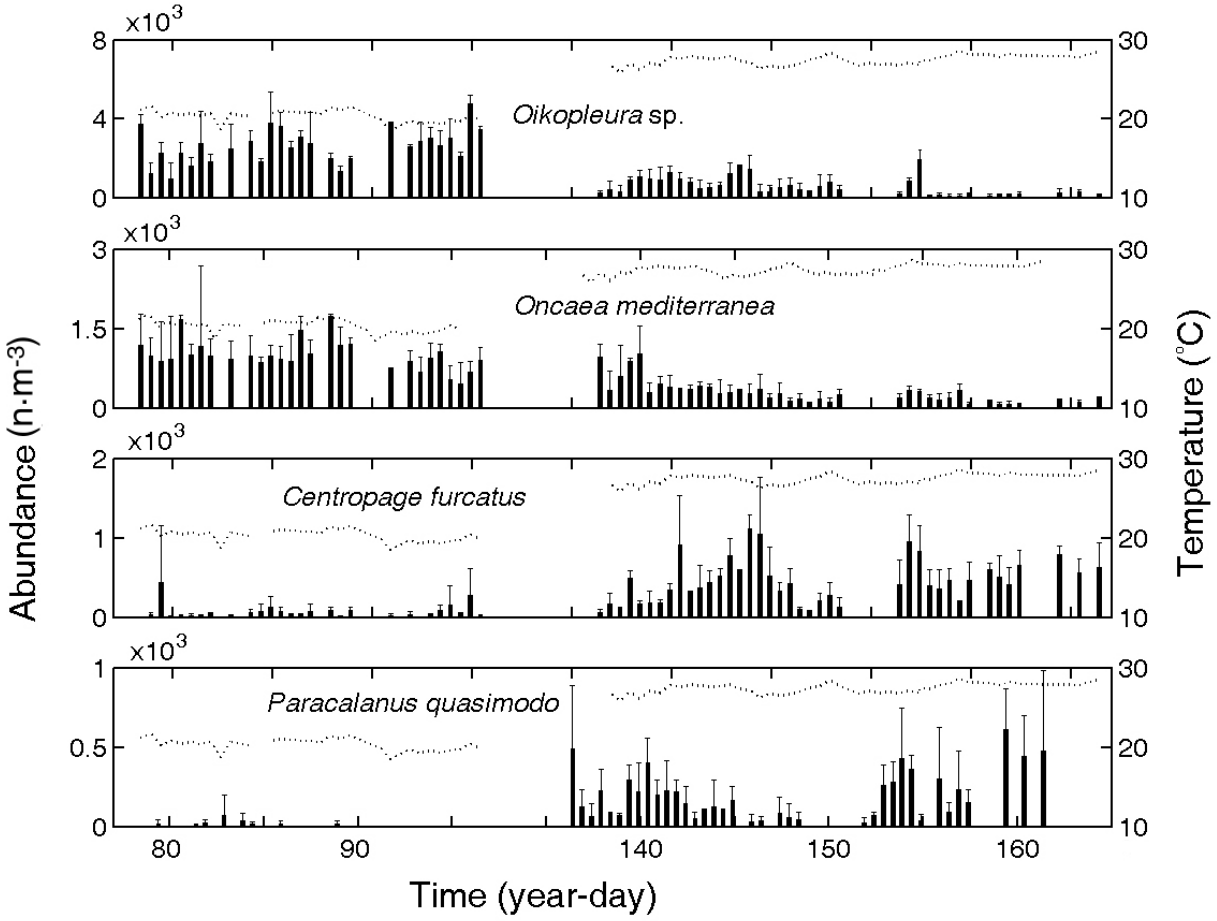

Figure 2.15: Abundance of species (histograms; 0–15m, mean value from 3 replicate net tows) that appeared to respond to temperature (dotted line) during the study period. Error bars represent one standard error.

Table 2.4: Regression results for species abundance versus time and salinity: log(Abundance) = a×[Temperature] + b×[Salinity] + C. The normality assumption for residuals were tested by Kolmogorov-Smirnov (K–S) test and residual–by–predicted plots are provided in Appendix A. §indicates violation of normality assumption.

Species	a		b		c		r^2	p–value	p_{K-S}
	estimate	p–value	estimate	p–value	estimate	p–value			
Acartia tonsa	-0.22	< 0.01	-0.47	< 0.01	24.57	< 0.01	0.45	< 0.01	0.11
Centropages furcatus	0.34	< 0.01	-0.04	0.18	-2.27	0.07	0.60	< 0.01	> 0.15
Oikopleura sp.	-0.27	< 0.01	0.02	0.38	12.71	< 0.01	0.66	< 0.01	> 0.15
Conaea sp. §	-0.14	< 0.01	0.01	0.83	9.05	< 0.01	0.20	< 0.01	0.01
Corycaeus clausii	0.06	< 0.01	0.07	0.13	3.26	< 0.01	0.19	< 0.01	> 0.15
Oithona plumifera §	-0.10	0.05	-0.01	0.99	6.366	< 0.01	0.06	0.14	< 0.01
Sagitta enflata	0.11	< 0.01	-0.01	0.95	2.58	< 0.01	0.31	< 0.01	> 0.15
Eucalanus attenuatus §	-0.13	< 0.01	-0.08	< 0.05	10.69	< 0.01	0.28	< 0.01	0.01
Oncaea mediterranea §	-0.20	< 0.01	-0.20	0.01	9.79	< 0.01	0.70	< 0.01	< 0.01
Labidocera nerri	0.26	< 0.01	-0.27	< 0.01	3.95	0.04	0.43	< 0.01	0.10
Temora stylifera	-0.14	< 0.01	-0.01	0.89	7.95	< 0.01	0.25	< 0.01	> 0.15
Clausocalanus furcatus	0.02	0.24	0.04	0.04	3.77	< 0.01	0.09	0.04	0.12

2.4 Discussion

2.4.1 Zooplankton Assemblages

A westward current flows along the inner and mid Louisiana–Texas shelf and a cyclonic gyre is well formed during most of the year (Wiseman et al. 1976). The study site was frequently influenced by the Mississippi River plume and mesozooplankton assemblages varied correspondingly. A coastal shelf group associated with the Mississippi River plume and an oceanic group from the Gulf of Mexico were found in the study area. A double-layered salinity structure with a low salinity surface layer and high salinity lower layer was found during most of the study period. Consequently, most samples contained both oceanic taxa from below the halocline and coastal/shelf taxa from the surface waters. The relative abundance of each group likely depends upon the halocline depth. Zooplankton associated with these groups had different dominant species that were consistent with distributional results from other studies (Ortner et al. 1989; Minello 1980; Marum 1974). *Acartia tonsa*, *Labidocera nerri*, and *Corycaeus clausi* have been reported as typical coastal species and are abundant in the Mississippi River plume. These species increased their abundance in the presence of low salinity plume water in the study area. The oceanic species associated with the high salinity offshore water, such as *Clausocalanus furcatus*, are more abundant when the high salinity water predominates the study area.

Shifts between the two assemblages reflected the influence of local physical forcing at different temporal scales. Tide introduced both diurnal and spring–neap cyclic components (Krumme and Liang 2004). Wind events influenced the time series variation by transporting Mississippi River plume to the study area.

Tides are an important mesoscale physical process in estuarine areas (Daly and Smith Jr. 1993). Tides can cause a periodic change in abundance and species composition by horizontal advection (Gagnon and Lacroix 1981). Peaks in zooplankton biomass and abundances have been reported to occur during either high tide (Robertson et al. 1988) or low tide periods (Krumme and Liang 2004). However, in the present study, total abundance did not show a clear diurnal pattern, which may reflect other factors related to the dynamic conditions in the study area. Tides did introduce a periodic component by way of the spring–neap cycle. Zooplankton abundance experienced large fluctuations during two of the spring tide periods and had relatively small variations during the neap tide period. By displacing the water mass in the upper water column, tidal currents can change vertical structure. As a result, a combination of oceanic and coastal assemblages occurred in the study area at a fixed location. The shifts in vertical structure caused by tidal currents might be important in restructuring vertical distribution for certain species (Kimmerer et al. 1998).

Wind driven currents were another important physical process in the study area that possibly causes large variations in total abundance. In the present study, total abundance maxima were coincident with the occurrence of a highly stratified water mass beneath the platform, suggesting that Mississippi River plume water dominated. Plume water is characterized by high nutrients, high primary production and high secondary production (Dagg and Whitledge 1991; Lohrenz et al. 1990). Prevailing southward winds likely forced more productive, surface plume water offshore directly influencing the study area. Thus total zooplankton abundance increased.

The community structure was also influenced by this wind driven current. When plume water dominated the study area, mesozooplankton community structure was dominated by coastal and shelf species such as *Acartia tonsa* and *Corycaeus clausi* . When high salinity oceanic

water predominated the study area, oceanic species such as *Eucalanus attenuatus* and *Clausocalanus furcatus* increased their abundance. The large variations for coastal shelf species explained most of the differences between communities of low salinity plume water and that of high salinity gulf water.

The control of mesozooplankton in the dynamic coastal area is a response to the combination of different physical processes. The Mississippi River plume was normally compressed against the coast by the Coriolis force, resulting in a well–defined, westward coastal current (Wiseman et al. 1976). However, when northerly winds prevailed, the plume water was transported to the study site. This northerly wind suppressed the inshore tidal movement (as shown in Figure 4 when the difference between high tide water level and mean water level was smaller than the difference between low tide water level and mean water level). The northerly wind, coincident with an ebb tide during the spring tide period, led to peaks of total abundance. Other factors, such as river discharge, may also have had strong impacts.

2.4.2 Factors Controlling Local Species Abundance and Mixing Process

In the present study, salinity was used as a proxy for the presence of different water masses. Three types of vertical profiles occurred during the study period and they indicated the mixing process between plume water and oceanic water: a low density of river plume water formed a thin lens on top of oceanic water, and then mixed with oceanic water by physical forcing, such as tidal advection and wind stress. In the mixing process, salinity underwent large variation and the influence of this change may not only vary from species to species, but also among different development stages (Lee and Peterson 2003).

Knowledge of copepod mortality rates is critical to understanding their spatial and temporal distribution. The inability of coastal species to acclimate to the high salinity oceanic water may cause a population decline. The abundance of *Acartia tonsa* and *Labdiocera nerri* was

negatively correlated to surface salinity. Even though *A. tonsa* has been considered capable of colonizing a wide range of environments (up to 52 psu; Rey et al. 1991), low abundance was observed in intermediate and high salinity water. This is consistent with its nearshore distribution (Ortner et al. 1989; Paffenhöfer and Sterns 1988). Laboratory experiments suggest species experiences high mortality if instantaneous variations in salinity are larger than 10–15 psu (Cervetto et al. 1999). In the field, other factors such as changes in food regime and the chemical composition of the ambient environment can explain *A. tonsa* being distributed in a narrower range than its tolerance. Temporal and spatial variations in mortality rates determine the species abundance and distribution.

The abundance of oceanic species in the upper 15m of the water column, such as *Cl. furcatus*, were positively related to the surface salinity. The vertical distribution of *Cl. furcatus* also indicated the species primarily utilized high salinity oceanic water, i.e., relative low abundance at 5m water depth corresponding to the strong plume (year–day: 82–86 and 151–160, Figure 2.16). Tidally oriented migration has been frequently observed for copepod species (Schabetsberger et al. 2000; Kimmerer et al. 1998). Samples collected at 5m depth with Niskin water bottles indicated this species can migrate to the upper water column. However, different species and different development stages may utilize different layers (Dagg et al. 1988; Paffenhöfer 1985). Vertical distribution information is necessary to facilitate understanding how oceanic species respond to this mixing process.

2.4.3 Summary

This study demonstrated the difficulty of studying zooplankton ecology, especially in highly advective coastal areas, given the variability introduced by physical processes on different temporal scales. Knowledge about how long the samples can represent a particular water mass

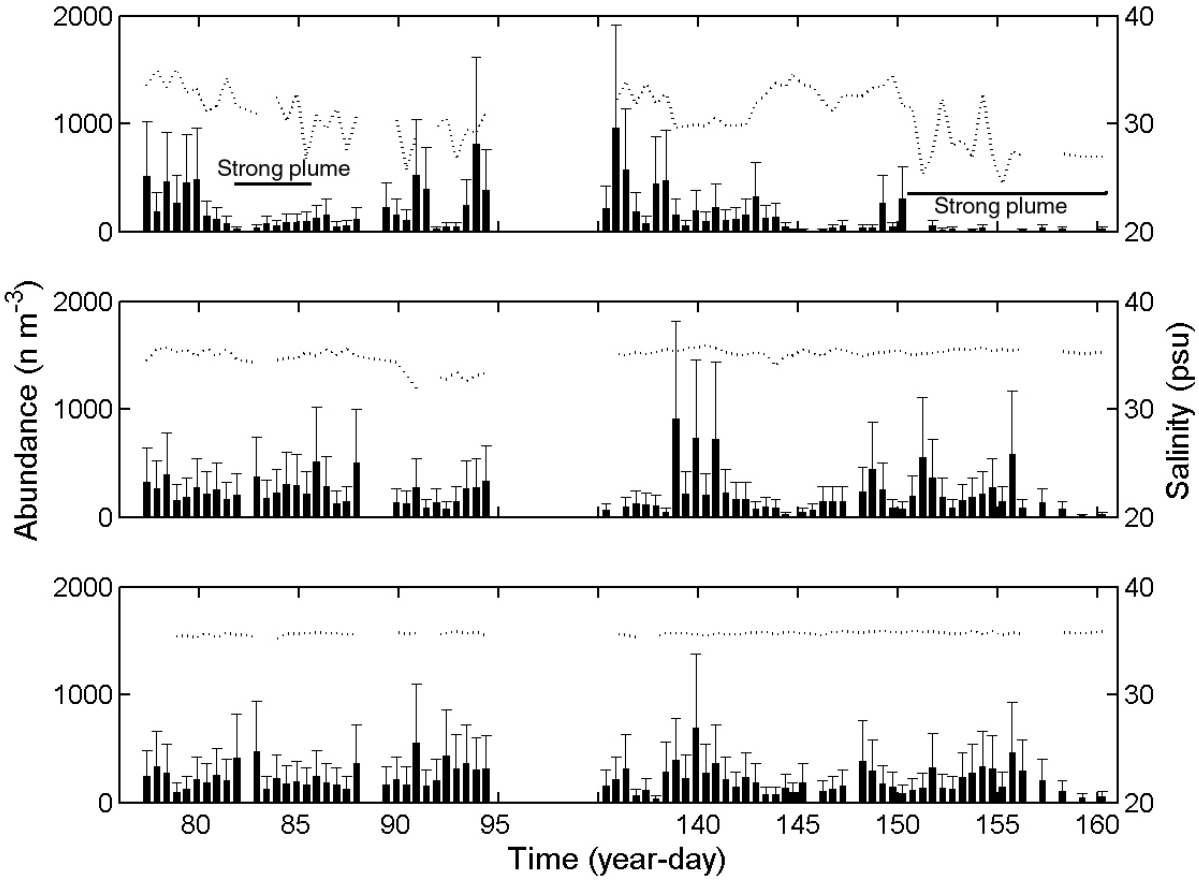

Figure 2.16: Abundance of *Cl. furcatus* in March–April and May–June at different water depth over the study period. Each bar is the mean density from three replicates; error bars represent one standard error; dotted lines indicate salinity.

and a zooplankton assemblage is essential to study biological processes, such as population dynamics, feeding behavior and vertical migration.

Clausocalanus furcatus is widely distributed in the oligotrophic oceanic waters around the world (Lo et al. 2004; Paffenhöfer 1985) and knowledge about its population dynamics is limited (Mazzocchi and Paffenhöfer 1998). In the present study, *Cl. furcatus* consistently occurred in the study area and made up a notable portion of the total mesozooplankton abundance. The abundance of *Cl. furcatus* appeared to be correlated with high salinity offshore water. Estimating population parameters, including egg production rates, stage duration and mortality rates, are the essential to understanding its population dynamics.

2.5 Bibliography

Bailey, K. M. and Houde, E. D. 1989. Predation on eggs and larvae of marine fishes and the recruitment problem. *Adv. Mar. Biol.*, 25:1–83.

Banse, K. 1986. Vertical distribution and horizontal transport of planktonic larvae of echinoderms and benthic polychaetes in an open coastal sea. *Bull. Mar. Sci.*, 39:162–175.

Cervetto, G., Gaudy, R., and Pagano, M. 1999. Influence of salinity on the distribution of *Acartia tonsa* (Copepoda, Calanoida). *J. Exp. Mar. Biol. Ecol*, 239:33–45.

Chelton, D. B., Bernal, P. A., and McGowan, J. A. 1982. Large scale internanual physical and biological interaction in the California Current. *J. Mar. Res.*, 40:1095–1125.

Clarke, K. R. and Warwick, R. M. 1994. *Change in marine communities: an approach to statistical analysis and interpretation*. Plymouth Marine Laboratory, Plymouth.

Dagg, M. J., Ortner, P. B., and Al-Yamani, F. 1988. Winter–time distribution and abundance of copepod nauplii in the Northern Gulf of Mexico. *Fish. Bull*, 86:219–230.

Dagg, M. J. and Whitledge, T. E. 1991. Concentration of copepod nauplii associated with the nutrient–rich plume of the Mississippi river. *Cont. Shelf Res.*, 11:1409–1423.

Daly, K. L. and Smith Jr., W. O. 1993. Physical–biological interactions influencing marine plankton production. *Annu. Rev. Ecol. Syst*, 24:555–585.

Dinnell, S. P. and Wiseman, W. J. 1986. Fresh water on the Louisiana and Texas Shelf. *Cont. Shelf Res*, 6:765–784.

Gagnon, M. and Lacroix, G. 1981. Zooplankton sample variability in a tidal estuary: An interpretative model. *Limnol. Oceanogr*, 26:401–413.

Hannan, C. A. 1984. Planktonic larvae may act like passive particles in turbulent near–bottom flows. *Limnol. Oceanogr*, 28:1108–1116.

Hassett, R. P. and Boehlert, G. W. 1999. Spatial and temporal distributions of copepods to leeward and windward of Oahu, Hawaiian Archipelago. *Mar. Biol.*, 134:571–584.

Haury, L. R., Yamazaki, H., and Wiebe, P. H. 1978. Patterns and processes in the time–space scales of plankton distribution. In Steele, J. H., editor, *Spatial pattern in plankton communities*, pages 77–327. Plenum Press, New York.

Hensen, V. 1887. Über die bestimmung des planktons oder de im Meere treibenden Materials an Pflanzen und. *Thieren Berichte der Kommssion wissenschaftlichen Untersuchung der dtschen Meere Kiel Ber.*, 50:1–107.

Huntley, M. E. and Lopez, M. D. G. 1992. Temperature–dependent production of marine copepods: A global synthesis. *Am. Nat.*, 140:201–242.

Huntley, M. E. and Niiler, P. P. 1995. Physical control of population dynamics in the Southern Ocean. *ICES J. Mar. Sci.*, 52:457–468.

Ibanez, F. 1976. Contribution à l'analyse mathématique des événements en écologie planctonique. *Bull. Inst. Oceaogr. Monaco*, 72:1–96.

Johnson, M. P. and Costello, M. J. 2002. Local and external components of the summertime plankton community in Lough Hyne, ireland a stratified marine inlet. *J. Plankton Res.*, 24:1305–1315.

Kimmerer, W. J., Burau, J. R., and Bennett, W. A. 1998. Tidally oriented vertical migration and position maintenance of zooplankton in a temperate estuary. *Limnol. Oceanogr.*, 43:1697–1709.

Krumme, U. and Liang, T. 2004. Tidal-induced changes in a copepod-dominated zooplankton community in a macrotidal mangrove channel in northern Brazil. *Zool. Stud.*, 43:404–414.

Lee, C. E. and Peterson, C. H. 2003. Effects of developmental acclimation on adult salinity tolerance in the freshwater–invading copepod *Eurytemora affinis*. *Physiol. Biochem. Zool*, 76:296–301.

Lo, W., Shih, C., and Hwang, J. 2004. Diel vertical migration of the planktonic copepods at an upwelling station north of Taiwan, western North Pacific. *J. Plankton Res.*, 26:89–97.

Lohrenz, S. E., Dagg, M. J., and Whitledge, T. E. 1990. Enhanced primary production at the plume/oceanic interface of the Mississippi River. *Cont. Shelf Res.*, 10:639–664.

Mackas, D. L., Denman, K. L., and Abbott, M. R. 1985. Plankton patchiness: biology in the physical vernacular. *Bull. Mar. Sci.*, 37:652–674.

Marum, J. P. 1974. *Spatial and temporal variations of zooplankton in relation to offshore oil drilling and estuarine–marine faunal exchange*. PhD thesis, Florida State University.

Mazzocchi, M. G. and Paffenhöfer, G. A. 1998. First observations on the biology of *Clausocalanus furcatus* (Copepoda, Calanoida). *J. Plankton Res.*, 20:331–342.

McKinney, M. L. 1997. Extinction vulnerability and selectivity: Combining ecological and paleontological views. *Annu. Rev. Ecol. Syst.*, 28:495–516.

Minello, T. J. 1980. *The neritic zooplankton of the northwestern Gulf of Mexico*. PhD thesis, Texas A&M University.

Orive, E., Iriarte, A., Madariaga, I., and Revilla, M. 1998. Phytoplankton blooms in the Urdaibai estuary during summer: physico–chemical conditions and taxa involved. *Oceanol. Acta*, 21:293–305.

Ortner, P. B., Hill, L. C., and Cummings, S. R. 1989. Zooplankton community structure and copepod species composition in the northern Gulf of Mexico. *Cont. Shelf Res.*, 9:387–402.

Paffenhöfer, G. A. 1985. The abundance and distribution of zooplankton on the southeastern shelf of the United States. In Atkinson, L. P., Menzel, D. W., and Bush, K. A., editors, *Oceanography of the Southeastern U.S. Continental shelf*, pages 104–117.

Paffenhöfer, G. A., Atkinson, L. P., Lee, T. N., Blanton, J. O., Sherman, B. K., and Stewart, T. B. 1994. Variability of particulate matter and abundant zooplankton off the southeastern United States during spring of 1984 and 1985. *Cont. Shelf Res.*, 14:629–654.

Paffenhöfer, G. A. and Sterns, D. E. 1988. Why is *Acartia tonsa* (Copepoda, Calanoida) restricted to nearshore environments? *Mar. Ecol. Prog. Ser.*, 42:33–38.

Postel, L., Fock, H., and Hagen, H. 2000. Biomass and abundance. In P, H. R. and et al., P. H. W., editors, *Zooplankton methodology manual*, pages 83–174. Academic Press, London.

Power, J. H. 1989. Sink or swim: growth dynamics and zooplankton hydromechanics. *Am. Nat.*, 133:706–721.

Rey, J. R., Kain, T., and Crossman, R. 1991. Zooplankton of impounded marshes and shallow areas of subtropical lagoon. *Florida Scientist*, 54:191–203.

Riley, G. A. 1937. The significance of the Mississippi River drainage for biological conditions in the northern Gulf of Mexico. *J. Mar. Res.*, 1:60–74.

Robertson, A. I., Dixon, P., and Daniel, P. A. 1988. Zooplankton dynamics in mangrove and other nearshore habitats in tropical australia. *Mar. Ecol. Prog. Ser.*, 43:139–150.

Roden, C. M., Rodhouse, P. G., Hensey, M. P., McMahon, T., Ryan, T. H., and Mercer, J. P. 1987. Hydrography and the distribution of phytoplankton in Killary Harbour: A fjord in western Ireland. *J. Mar. Biol. Ass. UK*, 67:359–371.

Schabetsberger, R., Brodeur, R. D., Ciannelli, L., Napp, J. M., and Swartzman, G. L. 2000. Diel vertical migration and interaction of zooplankton and juvenile walleye Pollock (*Theragra chalcogramma*) at a frontal region near the Pribilof Islands, Bering Sea. *ICES J. Mar. Sci.*, 57:1283–1295.

Smith, E. P. and Belle, G. V. 1984. Nonparmetric estimation of species richness. *Biometrics*, 40:119–129.

Steele, J. H. and Frost, B. W. 1977. The structure of plankton communities. *Philos. Trans. R. Soc. Ser. B*, 280:485–533.

Thompson, B. M. 1982. Growth and development of *Pseudocalanus elongates* and *Calanus* sp. in the laboratory. *J. Mar. Biol. Assoc. U. K.*, 62:359–372.

Vernberg, W. B. and Vernberg, F. J. 1972. *Environmental physiology of marine animals*. Springer-Verlag, NY.

Wiebe, P. H. and Benfield, M. C. 2003. From the Hensen net toward four-dimensional biological oceanography. *Prog. Oceanogr.*, 56:7–136.

Wiseman, W. J., Banes, J. M., Murray, S. P., and Tubman, M. W. 1976. Small scale temperature and salinity structure over the inner shelf west of the Mississippi River Delta. *Memoirs Royal Soci. Liege*, 6:277–285.

Wroblewski, J. W. 1980. A simulation of the distribution of *Acartia clausi* during Oregon upwelling, august 1973. *J. Plankton Res*, 2:43–68.

CHAPTER 3 EGG PRODUCTION RATES AND STAGE DURATIONS

3.1 Introduction

Clausocalanus furcatus (Figure 3.1) is a small, widespread, epipelagic, calanoid copepod (~0.8–1.7mm, total length) that occurs in a wide latitudinal range, i.e., 35°S– 40°N (Williams and Wallace 1975; Frost and Fleminger 1968; Vervoort 1963). The species has been reported as a dominant species in oceanic water off the southeastern USA (Bowman 1971). Subsequently *Cl. furcatus* has been reported to make up a notably large proportion of zooplankton communities in the northern Gulf of Mexico, where it has been reported to be abundant in late spring and early summer (Ortner et al. 1989; Minello 1980; Marum 1974).

Despite the circumglobal distribution of *Cl. furcatus*, only a few studies have been conducted on the population dynamics of this species. Mazzocchi and Paffenhöfer (1998) conducted the first laboratory observation on *Cl. furcatus* reproductive behavior and egg production rates. Their experiments indicate the species carries an egg mass with a clutch size of 6.5–17.5 eggs clutch^{-1} female^{-1} with a generation time of approximately 14–21 days.

Egg production rates and stage–specific development times are key variables to estimate population production and recruitment rates. The egg production rate sets the upper limit for population size and egg production also represents a potential food resource for fish larvae (Kiørboe et al. 1988). Egg production rates and stage durations respond to temperature (Hirst and Kiørboe 2002; Huntley and Lopez 1992; Thompson 1982), the concentration of appropriate food (Peterson and Kimmerer 1994; Ianora and Poulet 1993; Dagg et al. 1988; Harris and Paffenhöfer 1976), and salinity (Hall and Burns 2001; Miliou and Moraitou-Apostologpoulou 1991). Both egg production and growth rates increase with temperature and follow an exponential relationship within an optimum temperature range (Peterson 2001; Hirche 1990; Runge 1985). Food concentration (Peterson and Kimmerer 1994) and food quality (Miralto

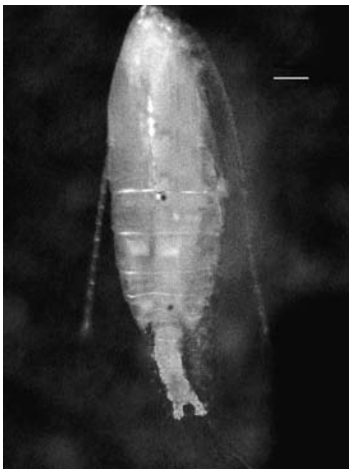

Figure 3.1: The adult female of *Clausocalanus furcatus,* from the dorsal side. Scale bar = 100 μm.

et al. 1999) can limit female fecundity and influence stage development time (Peterson 2001; Harris and Paffenhöfer 1976). Egg production rates can either increase (Hall and Burns 2001) or decrease (Miliou and Moraitou-Apostologpoulou 1991) when salinity is out of the optimum range.

Physical processes can influence egg production indirectly by altering the salinity, temperature or food regime. Dagg et al. (1988) speculated that *Acartia tonsa* and *Centropages furcatus* increased their egg production rates within hours after exposure to increased food availability associated with upwelling events caused by winter storms in the northern Gulf. Thus, copepod egg production rates could possibly respond to shifts in water masses caused by physical processes such as wind–induced currents.

In the northern Gulf, wind–induced currents and tidal currents frequently transport Mississippi River plume waters onto the inner shelf region (Smith 1980; Price 1976) forming a two layer system with plume water on top of oligotrophic Gulf water (Wiseman et al. 1976). Plume water is characterized by high nutrients and enhanced primary production (Lohrenz et al. 1997)

which could represent a potential food source for oceanic species such as *Clausocalanus furcatus* and *Eucalanus attenatus* located beneath the plume. The ability of *Cl. furcatus* to migrate to the upper water column has been observed (Lo et al. 2004; Paffenhöfer and Mazzocchi 2003) and the ascent to food–rich plume water could potentially increase egg production rates.

The aim of this part of the study was to estimate egg production and stage duration for *Clausocalanus furcatus*. The objectives were to:

- Measure egg production rates with both the *in situ* Edmonson egg ratio method (1960) and the laboratory incubation method;
- Investigate the response of egg production rates to the food–rich plume water; and
- Estimate the stage–specific development times.

3.2 Method

3.2.1 Study Site and Zooplankton Sampling

Sampling was conducted at South Timbalier 151 (ST151; 28°37'N, 90°15'W), a Chevron-Texaco offshore petroleum platform complex located 50 km south of Grand Isle Louisiana in 45m water depth (Figure 2.1). Zooplankton were collected at 12h intervals between March 18–April 6 and May 15–June 9, 2003 with a 30L Niskin water bottle at 5, 15, and 25m. Contents were filtered through 20μm mesh. Each collection consisted of 3 replicate water bottle samples from each depth.

Samples were fixed in 5% formalin and transferred to 70% ethanol in the lab before being sorted and identified under a stereo–microscope (50x) to the different development stages. Vertical profiles of temperature and salinity were taken every 12h with an YSI 6920 sonde.

3.2.2 Egg Production and Stage Duration Measurements

Incubation experiments for stage duration were conducted during May 28–29 (24.5°C), June 5–9 (26°C) and July 5–9 (28.5°C), 2002, March 20–21 (20°C) and June 5, 2003 (24°C), while incubation experiments for egg production rates were conducted during May 28–29 and June 5–9, 2002, March 20–21 and June 5, 2003. Live adult female *Clausocalanus furcatus* were collected with a 70cm zooplankton net (2.5m long, 153μm mesh) hauled vertically at a 20–25cm s^{-1} from 10m to surface. Net samples were diluted into a 15L bucket containing 63μm filtered seawater collected from 5m. Mature adult females were gently picked out under a stereoscope for egg production measurements. These individuals were randomly placed in 400ml incubation chambers (inverted spring water bottles). Chambers had a 3cm diameter opening covered with 63μm mesh, and a 100ml vial connected to the lower part to collect eggs. There was a 153μm mesh screen between the incubation chamber and the egg collection vial to avoid cannibalism. Each incubation chamber held 5 individuals and was held at ambient seawater surface temperature for 24h. Egg production rates were expressed as eggs $female^{-1}$ day^{-1}.

Estimates of egg production rates *in situ* were derived from Niskin water bottle samples using the Edmonson egg ratio method (Edmondson 1968; Edmondson 1960).

$$B_{ER} = \frac{E}{N_f D} \tag{3.1}$$

where, B_{ER} is the egg production rate, E is the egg concentration estimated from field samples, N_f is the female abundance, and D is the egg development time. Mean egg production rates were calculated from the three replicates taken at the three water depths (5, 15, and 25m).

Stage–specific development times were directly measured from incubation experiments with similar procedures as egg production experiments. 5–10 individuals of known stages

were picked out and incubated at ambient temperature (18–28 °C). The number of individuals reaching successive development stages was recorded every 7–10h.

3.2.3 Particulate Organic Carbon

Food availability was evaluated by measuring particulate organic carbon in the water column. Water samples were collected with polyethylene bottles and filtered through Whatman GF/F filters (0.45μm pore size) precombusted at 450°C. Water samples (1L) from 5, 15, and 25m were filtered every 12h during the study period. Filtered samples were stored frozen after collection. Prior to analysis, all filtered samples were dried at 90°C for 2h and weighed. Loss of filter dry weight on combustion at 500°C (4h) estimated particulate organic matter with half of the weight loss being considered to be available particulate organic carbon (POC; Peterson Jr. 1986).

3.2.4 Data Analyses

Mean *in situ* egg production rates was calculated by averaging measurements from the three water depths (5, 15 and 25m) during day or night for each sampling period. Day was defined as 6:00AM to 6:00PM, however, in all cases daytime samples occurred in early morning (5:00AM–11:00AM) and nighttime samples occurred in early evening (6:00PM–11:00PM). This yielded estimates of egg production for day and night for most of sample times, however, in some cases, either a day or night egg production estimate was missing due to adverse sampling conditions. A Kolmogorov-Smirnov test was applied to examine the normality of those data, and it indicated that those data violated the assumption of normality. A nonparametric Kruskal–Wallis (K–W) test was used to determine if there was a difference between daytime and nighttime egg production rates (NPAR1WAY procedure, SAS 1990). K–W tests were also applied to determine whether there were differences between mean *in situ* egg production rates

during March–April and May–June. Because the water column in study area frequently was stratified and temperature is known to influence the egg production rates, nonparametric K–W tests (due to violation of normality assumption) were applied to evaluate the hypothesis of no difference in egg production rates between the two study periods in the three water depths.

Nonparametric K–W tests were also applied to determine if there were depth effects on *in situ* egg production rates among the three water depths because data did not follow a normal distribution. Since the water column may have had different vertical structure during the two study periods, e.g., water column was more thermally stratified in May–June, the depth effects were tested for the two study periods separately. The test hypothesis was no difference among water depths.

Mean POC concentration for the water column was determined by averaging measurements from three water depths (5, 15 and 25m). A Kolmogorov-Smirnov test indicated these data did not have normal distributions. Nonparametric K–W tests were applied to evaluate potential differences between day and night POC concentrations, and the two study periods (March–April and May–June). Depth effects were also examined with nonparametric K–W tests. Spearman correlation coefficient was computed to examine the relationship between salinity and POC concentration for three water depths.

Scatter plots were applied to examine the relationship among mean *in situ* egg production rate, temperature and mean POC concentration. Spearman correlation coefficients were calculated for the *in situ* egg production rate and the mean POC concentration, the *in situ* egg production rate and the temperature, and the *in situ* egg production rate and salinity.

To estimate the stage–to–stage development times, individuals successfully reaching the next consecutive stage were coded as 1 when the observation occurred; otherwise, coded as 0. After creating this Bernoulli dataset, a logistic regression model (Equation 3.2) was applied to estimate the stage development times, which is defined as time required for 50% of individuals

to enter the next stage. The analysis was performed in SAS with a PROBIT procedure (SAS 8.0, 1990).

$$\ln\left(\frac{\pi_i}{1-\pi_i}\right) = \beta_0 + \beta_1 x_{ij} \tag{3.2}$$

where, π_i is the probability of individuals entering to next stage, β_0 and β_1 are coefficients, and x_{ij} is a dummy variable,

$$x_{ij} = \begin{cases} 1 & \text{if individual } i \text{ successfully entered the consecutive stage } (j = 1) \\ 0 & \text{if individual i stayed in the same stage } (j = 0). \end{cases}$$

3.3 Results

3.3.1 Observation of Reproductive Behavior

Clausocalanus furcatus females frequently carried their eggs as an egg mass mildly stuck together and attached to the ventral side of the genital somite. External stimuli can easily cause the egg mass to detach from the abdomen, as well as separate eggs from each other. A clutch of 12–18 eggs normally formed an egg mass; however, eggs were also observed extruded as a group of 4–7 eggs and discharged as a whole immediately. These eggs remained together after detachment from the abdomen and adult females resumed laying eggs after 15–90min. Eggs from the discharged groups and the attached egg masses were both observed to hatch normally.

The irregular egg masses were also observed in the preserved samples from both Niskin water bottle samples. Approximately 5–10% of eggs in water bottle samples occurred either in the form of complete egg masses or small groups. In net samples, no complete egg masses were observed.

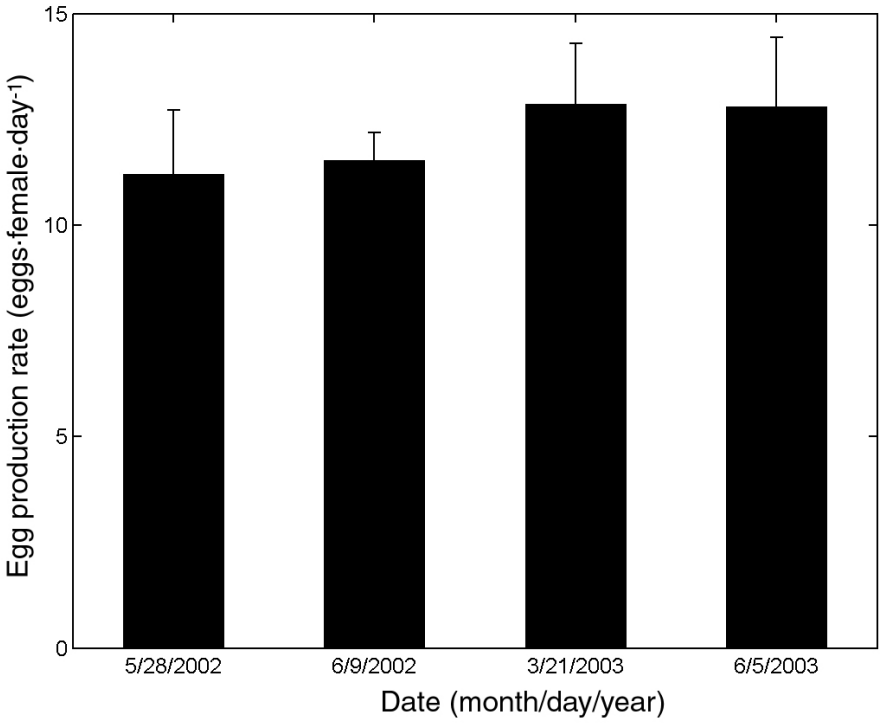

Figure 3.2: Egg production rate measured from incubation experiments. Each bar is the mean from three replicates and error bars represent one standard error.

3.3.2 Egg Production Rates

Egg production rates from incubation experiments did not show a large variation (Figure 3.2). Individual egg production rates from incubation experiments averaged 12.08 ± 1.40 (mean ± SE) eggs female^{-1} day^{-1}. *In situ* egg production rates estimated from Edmonson egg ratio method were lower than those from incubation experiments during the most of the study period and averaged 1.67 ± 0.27 eggs female^{-1} day^{-1}. Egg production rates in the daytime (early morning; 2.15 ± 0.29 eggs female^{-1} day^{-1}) were significantly higher than those in the nighttime (early evening; 1.15 ± 0.22 eggs female^{-1} day^{-1}; $\chi^2 = 6.18$, $p \leq 0.01$).

Mean *in situ* egg production rates showed a significant difference among the two study periods (Figure 3.3; $\chi^2 = 108.27$, $p < 0.01$). In March–April the mean egg production rate

(3.39 ± 0.34 eggs female^{-1} day^{-1}) was higher than in May–June (0.43 ± 0.17 eggs female^{-1} day^{-1}). In fact, at all three water depths (5, 15 and 25m; Table 3.1), egg production rates in March–April were consistently higher than those in May–June .

Kruskal–Wallis test results on depth effects are reported in Table 3.2. Even though the water column was stratified in the study area, there were no significant differences among mean *in situ* egg production rates at the three water depths during March–April, May–June or the entire study period (Table 3.2). The *in situ* egg production rates averaged 1.59 ± 0.16, 1.38 ± 0.13, and 1.88 ± 0.18 eggs female^{-1} day^{-1} for 5, 15, and 25m depths, respectively. The fluctuation of *in situ* egg production rates was consistent at three water depths over the course of the study (Figure 3.4).

3.3.3 Particulate Organic Carbon

The mean POC concentration in the water column ranged from 3.01–7.88 mg C L^{-1} (Figure 3.5). There was no significant difference between daytime POC concentration (5.27 ± 0.14 mg C L^{-1}, mean ± standard error (SE)) and nighttime POC concentration (5.13 ± 0.11 mg C L^{-1}; Kruskal–Wallis tests, $\chi^2 = 1.62$ and $p = 0.20$).

Mean POC concentrations were not significantly different between the two sampling periods as a whole: 5.26 ± 0.19 mg C L^{-1} in March–April and 5.11 ± 0.16mg C L^{-1} in May–June (χ^2=0.23, $p = 0.63$), nor across three water depths (5, 15, and 25m; Table 3.3.3).

The bottom layer had a higher POC concentration (5.50 ± 0.17 at 25m) than the mid and upper water column (4.98 ± 0.14 mg C L^{-1} at 15m and 5.10 ± 0.14 mg C L^{-1} at 5m). The difference was not significant ($p = 0.07$) over the entire study period (Table 3.4). In May–June, the POC concentration in the bottom layer was significantly higher than that in upper water column, whereas, no significant difference was detected in March–April.

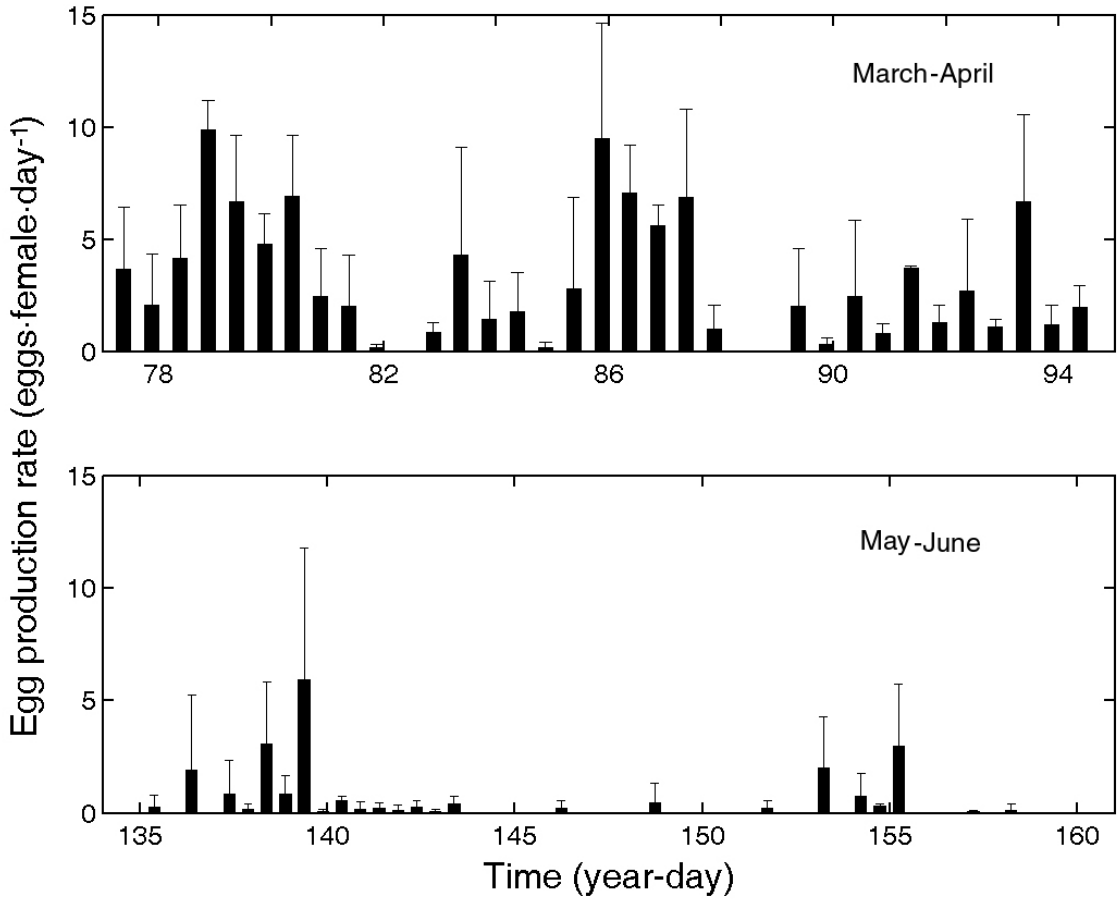

Figure 3.3: Mean *in situ* egg production rates averaged from samples taken from 5, 15 and 25m over the study period. Each bar is the mean from nine replicates; error bars represent one standard error.

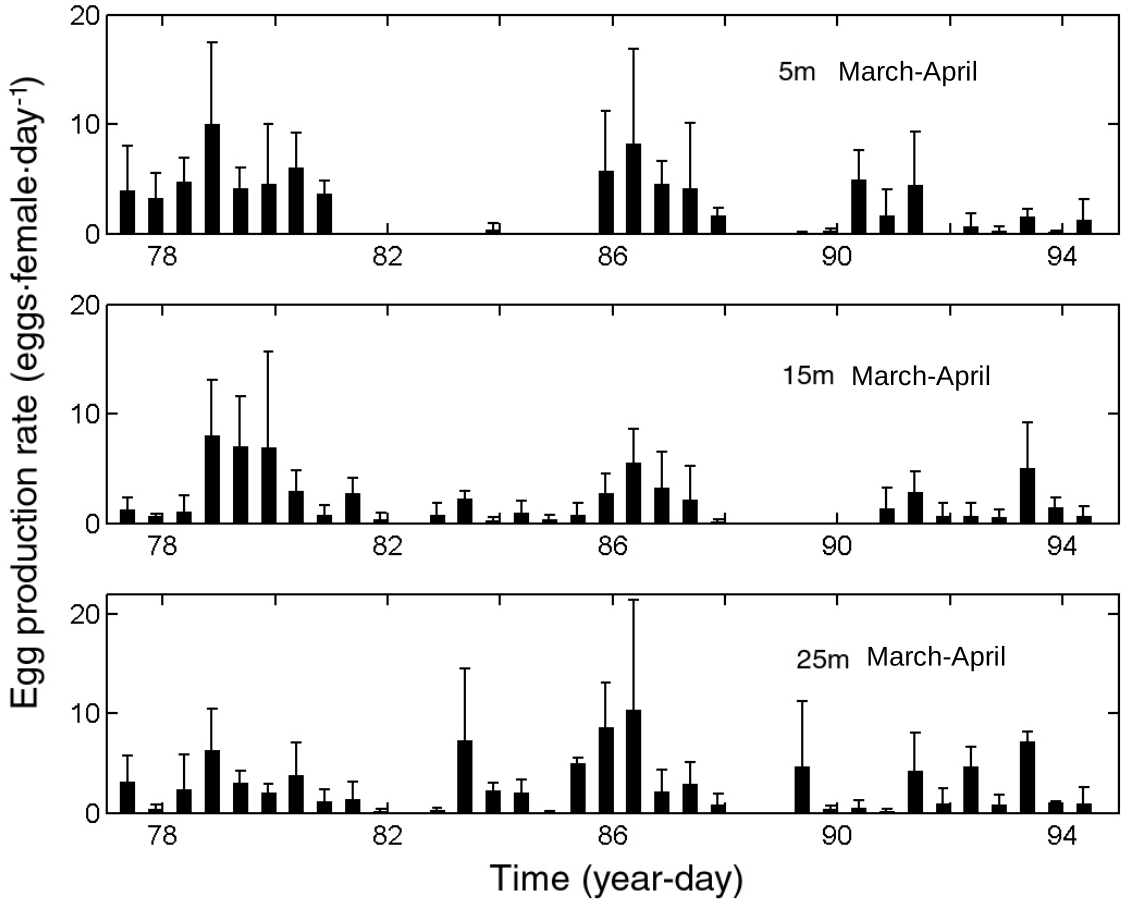

Figure 3.4: *In situ* egg production rates in March–April and May–June at different water depth over the study period. Each bar is the mean density from three replicates; error bars represent one standard error. Data are not available for 83.5, 91.5 and 157.3 (year–day). Figure continues on next page.

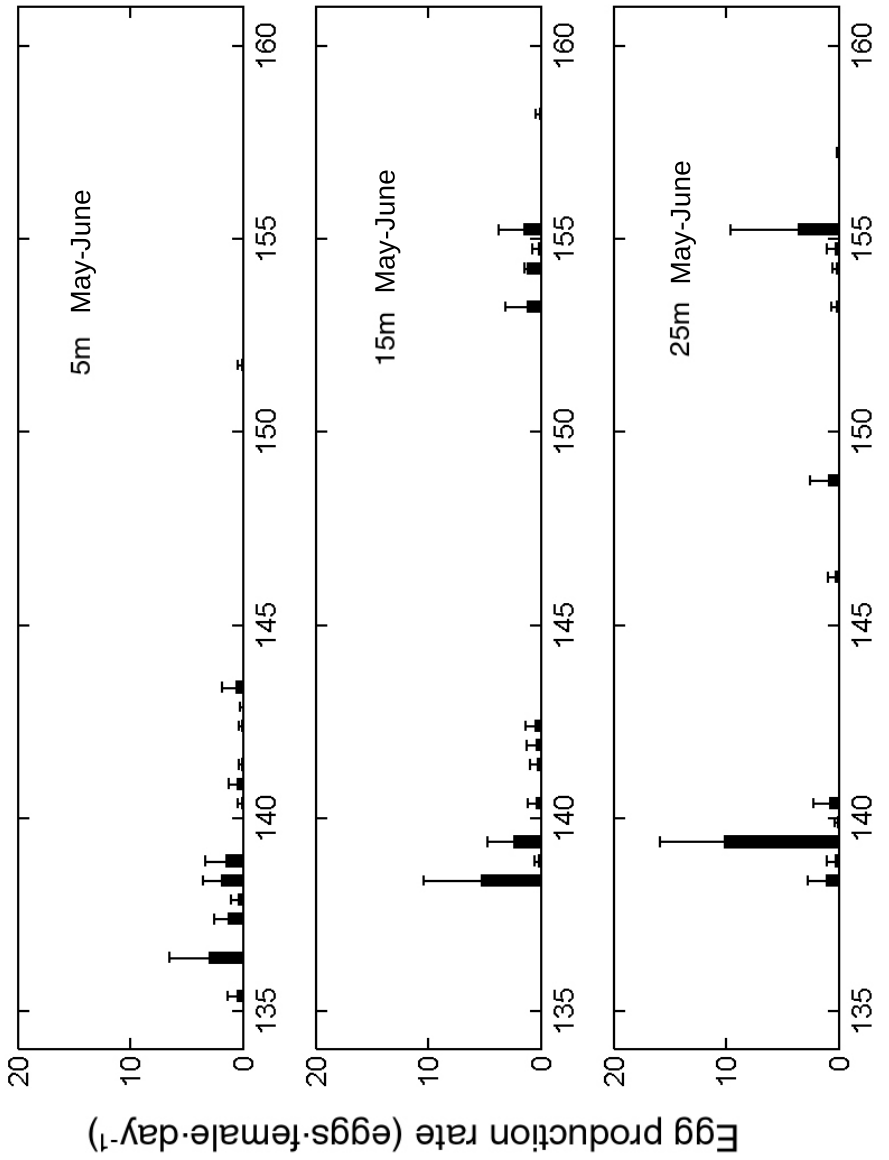

Figure 3.4 (Continued)

Table 3.1: Statistical results for mean *in situ* egg production rates (mean ± SE) in March–April and May–June, from nonparametric Kruskal–Wallis tests comparing mean egg production rate during two study periods at different water depths; n is sample size.

Water depth (m)	Egg production rate (eggs female^{-1} day^{-1})		χ^2	*p*–value
	March–April (n = 31)	May–June (n = 47)		
5	3.37 ± 0.64	0.50 ± 0.17	20.23	< 0.01
15	2.88 ± 0.52	0.41 ± 0.16	35.17	< 0.01
25	3.91 ± 0.62	0.50 ± 0.29	45.16	< 0.01

Table 3.2: Kruskal–Wallis results for *in situ* egg production rates testing the hypothesis of no difference among three different water depths accross three different time periods; n is sample size.

Test	Entire study period (n = 78)		March–April (n = 31)		May–June (n = 47)	
	χ^2	p–value	χ^2	p–value	χ^2	p–value
Overall depth effects	1.15	0.56	1.46	0.48	0.60	0.74
5m vs. 15m	0.69	0.40	0.51	0.47	0.19	0.66
5m vs. 25m	0.07	0.79	0.21	0.64	0.75	0.39
15m vs. 25m	1.02	0.31	1.52	0.22	0.01	0.91

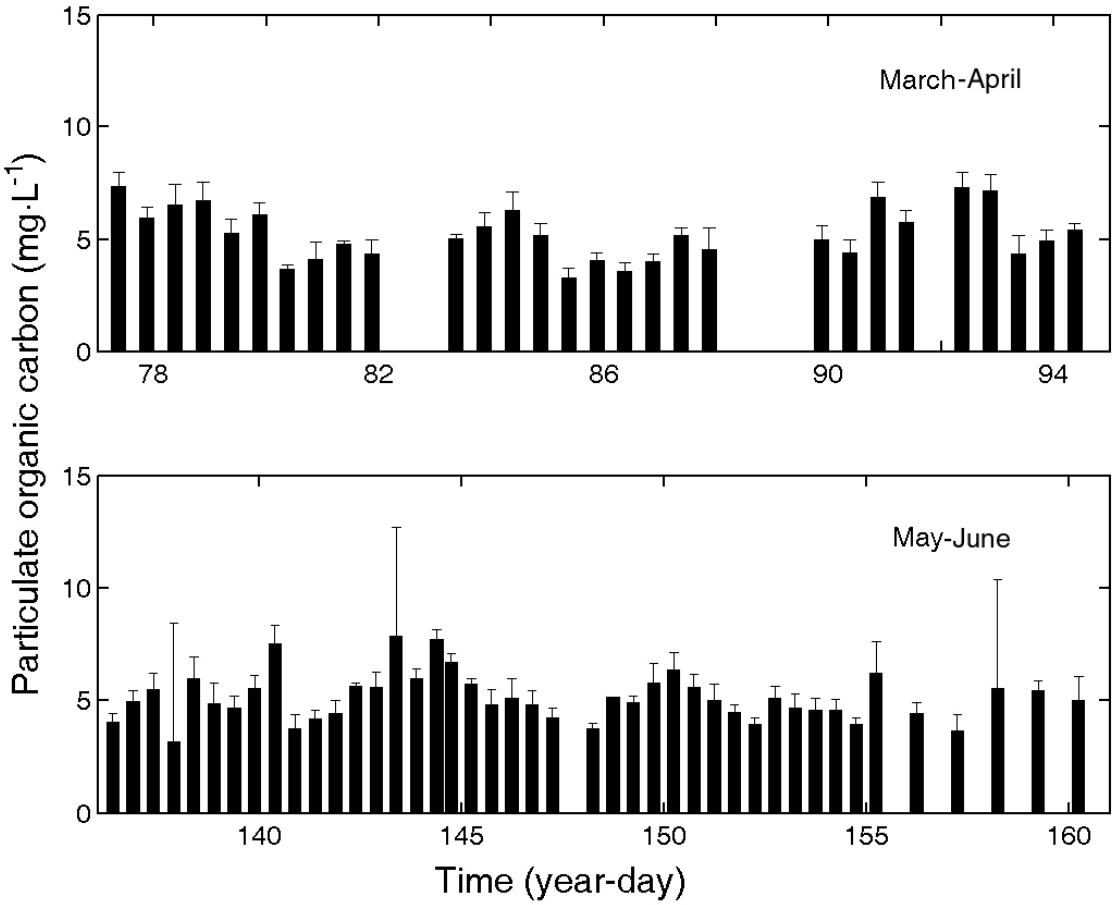

Figure 3.5: Mean particulate organic carbon (POC) concentrations. Each bar is the mean calculated by averaging from 5, 15, and 25m over the study period; error bars represent one standard error.

The POC concentration in the three layers underwent similar variations in the study period (Figure 3.6). The Spearman correlation coefficient between POC concentration and salinity was 0.29 (p = 0.01) at 5m water depth. There were no significant correlation between POC and salinity at 15m (p = 0.72) and 25m (p = 0.88) water depth.

3.3.4 Factors Influencing Egg Production Rates

In situ egg production rates did not show a clear response to the mean POC concentration (Figure 3.7). This is also supported by the Spearman correlation analysis (coefficient = 0.01, p = 0.86). *In situ* egg production rates, however, did appear to slightly respond to temperature (Figure 3.7). Egg production rates negatively correlated with temperature (coefficient = -0.34, $p < 0.01$). Spearman correlation indicated that the *in situ* egg production rates were positively correlated with salinity (coefficient = 0.32, $p < 0.01$).

3.3.5 Stage–specific Development Times

Logistic regression models were derived from incubations involving eggs, nauplii I–VI and copepodite I–IV (Figure 3.8). Parameter estimations for the regression model are reported in Table 3.5. Due to limited data points, goodness–of–fit tests were not available; however, fitness can be directly visualized from Figure 3.8. It appeared models for egg and nauplii fit better than those for copepodid stages.

Development times for *Cl. furcatus* from hatching to adulthood ranged from 13–15 days. *Clausocalanus furcatus* spent a relatively short time in the nauplii stages (4–7 days from egg through NVI and 8–12 days in copepodid stages; Figure 3.9). Stage duration generally increased with stage number, except nauplius VI, which had a shorter development time than previous stages.

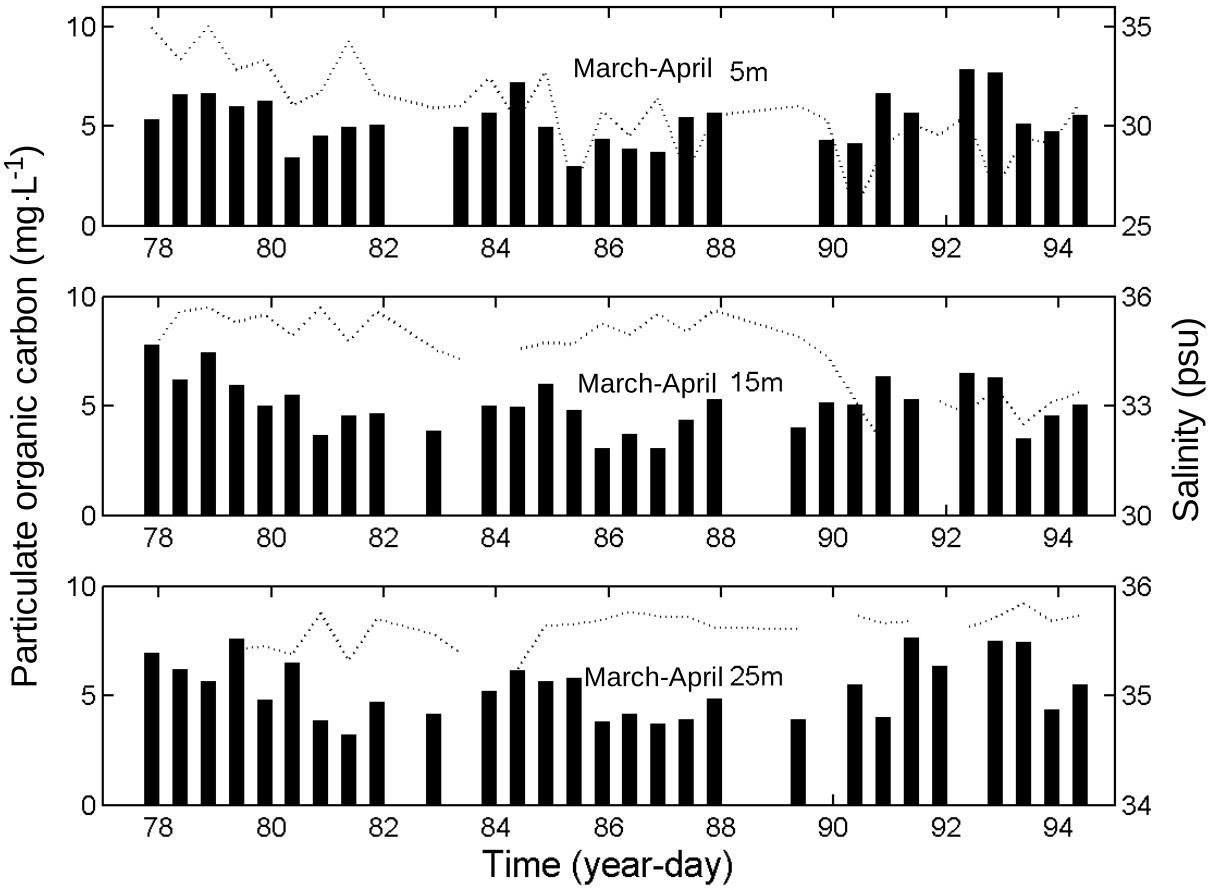

Figure 3.6: Mean particulate organic carbon (POC) concentrations (bars) in relation to salinity (dotted line) at different depths (5, 15 and 25m). Figure continues on next page.

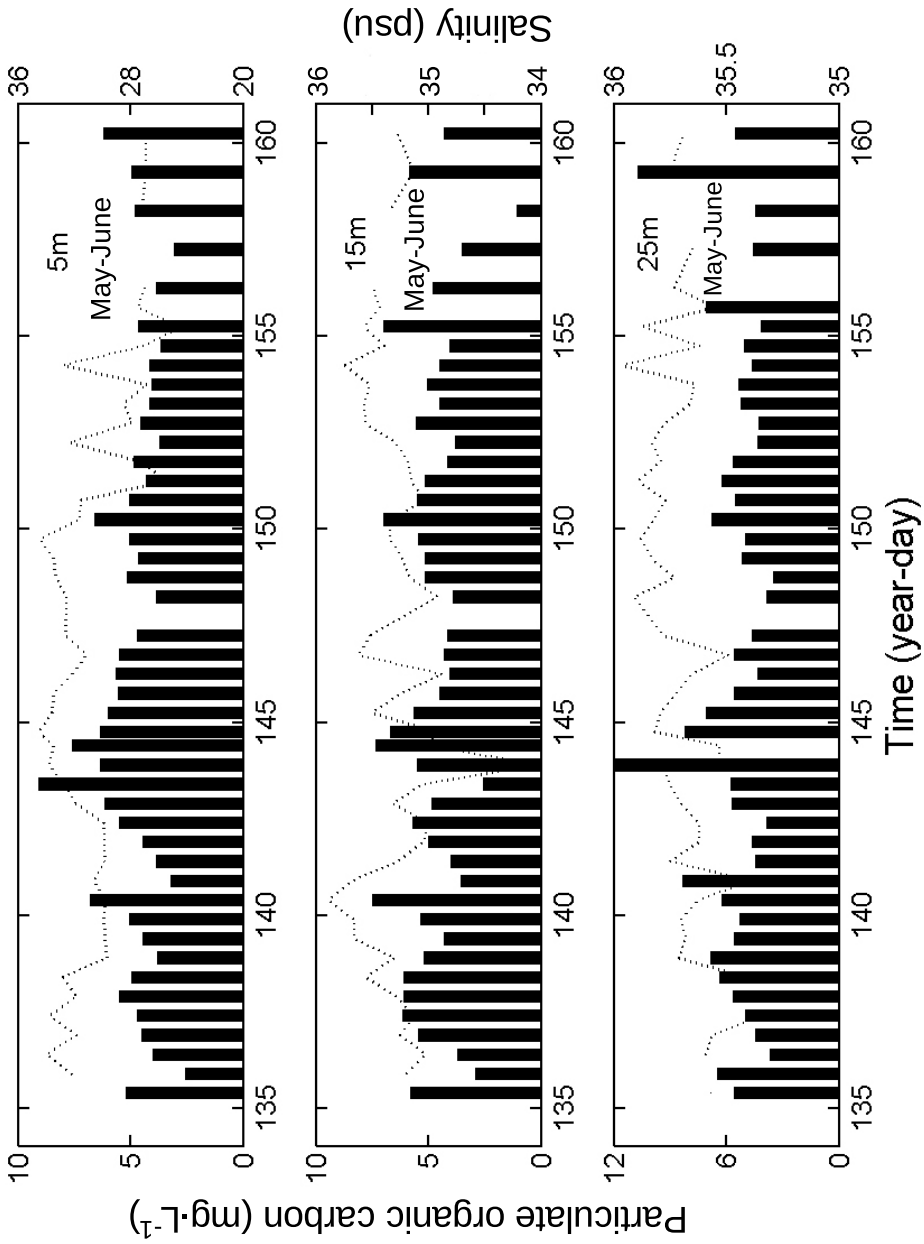

Figure 3.6 (Continued)

Table 3.3: Statistical results for mean particulate organic carbon (POC) concentrations (mean ±SE) in March–April and May–June from nonparametric Kruskal–Wallis tests comparing POC concentrations during two study periods at different water depths; n is the sample size.

Water depth (m)	POC ($mg \cdot L^{-1}$)		χ^2–test	*p*–value
	March–April (*n*= 31)	May–June (*n*= 47)		
5	5.33 ± 0.22	4.96 ± 0.18	2.21	0.14
15	5.05 ± 0.21	4.93 ± 0.18	0.05	0.83
25	5.33 ± 0.24	5.60 ± 0.24	0.16	0.69

Table 3.4: Kruskal–Wallis results on particulate organic carbon (POC) concentrations testing the hypothesis of no difference among three different water depths; n is the sample size.

Test	Entire study period (n = 78)		March–April (n = 31)		May–June (n = 47)	
	χ^2	p–value	χ^2	p–value	χ^2	p–value
Overall depth effects	5.38	0.07	1.08	0.58	5.47	0.06
5m vs. 15m	0.33	0.56	0.98	0.32	0.01	0.93
5m vs. 25m	2.60	0.11	0.05	0.82	3.91	0.04
15m vs. 25m	4.50	0.03	0.57	0.45	3.67	0.04

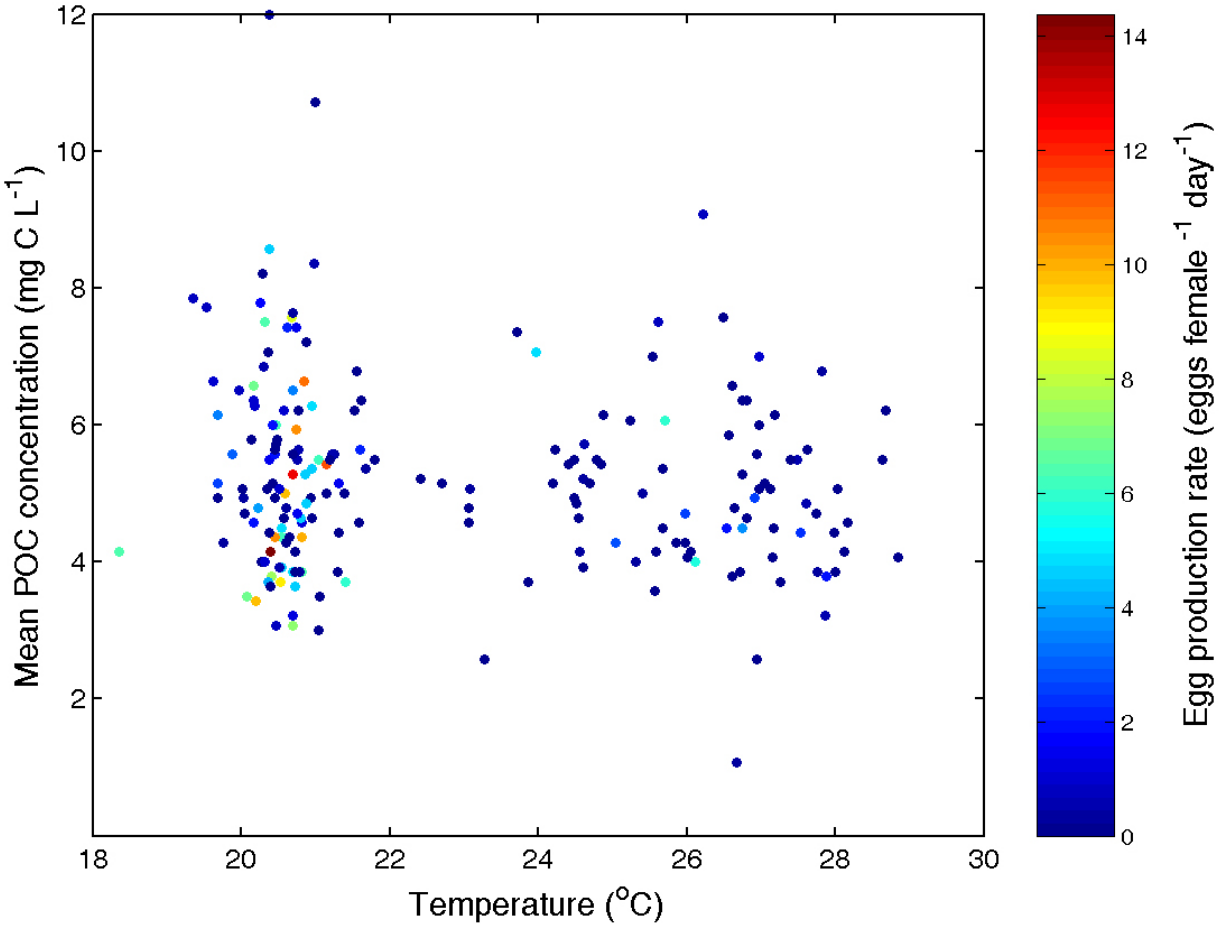

Figure 3.7: Scatter plot showing *in situ* egg production rates versus temperature and particulate organic carbon (POC) concentration.

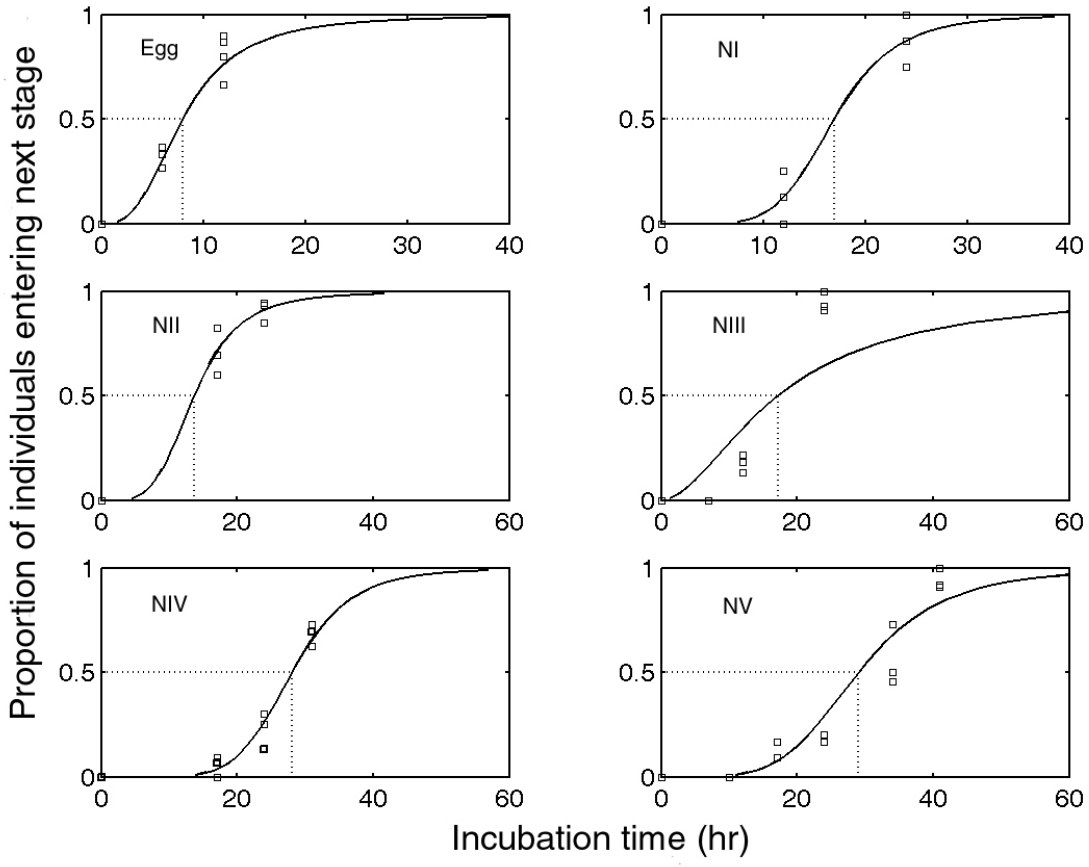

Figure 3.8: Estimating stage-specific developmental times for egg, nauplius I–VI and copepodite I–V by fitting logistic regression models to find when 50% of the individuals successfully enter the consecutive stage. Solid lines represent simulated development times; square boxes represent observation values; horizontal dotted lines show 50% individuals entering next stage; vertical dotted lines show the duration times for 50% individuals entering next stage. Figure continues on next page.

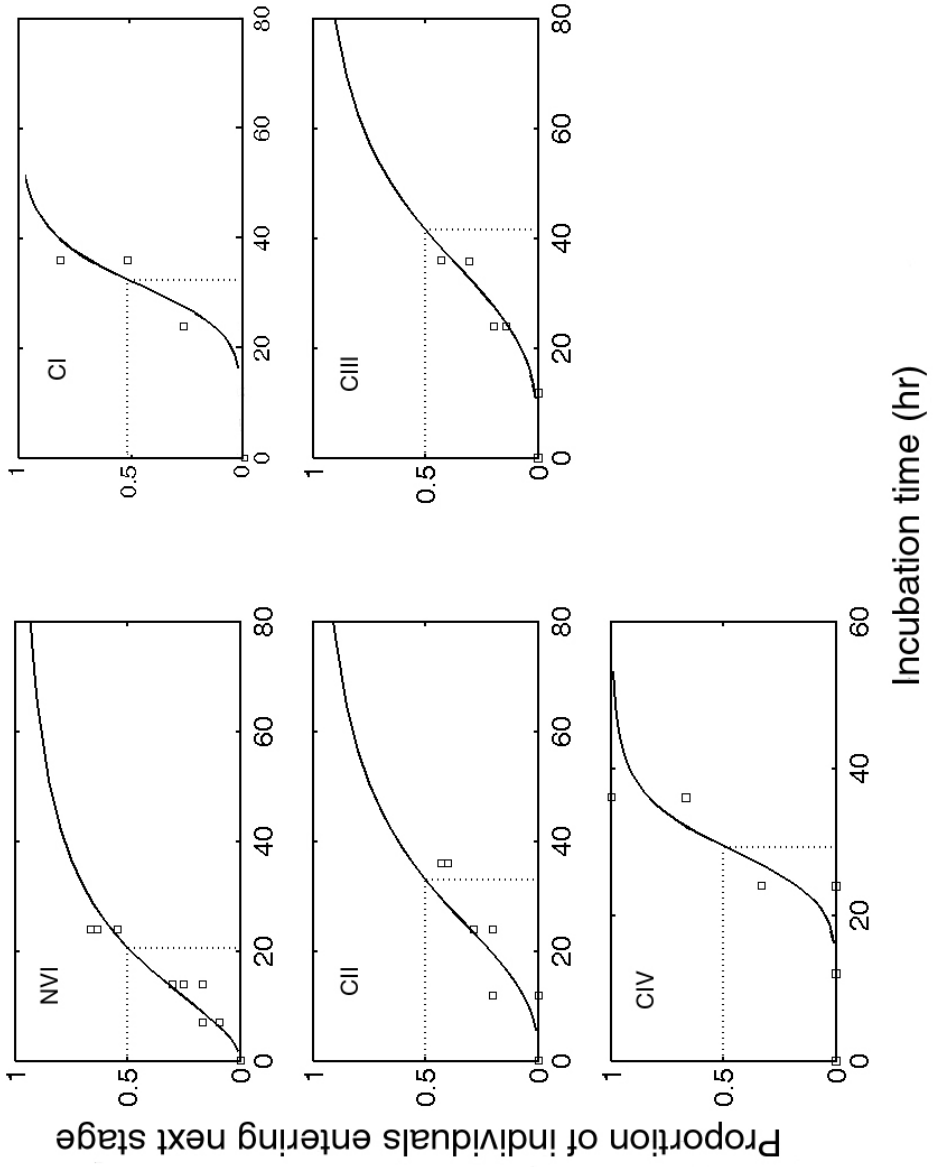

Figure 3.8 (Continued)

Table 3.5: Parameter information from logistic regression models estimating stage-specific developmental times for egg, nauplius I–VI and copepodite I–V: $\ln(\frac{\pi}{1-\pi}) = \beta_0 + \beta_1 \log_{10}(\text{Duration})$, where π is the probability of individual successfully entering the consecutive stage.

Developmental stage	Intercept			Log(Duration in h)		
	Parameter	χ^2	$p > \chi^2$	Parameter	χ^2	$p > \chi^2$
Egg	-5.93	65.23	<0.01	6.58	69.08	<0.01
NI	-15.90	19.59	<0.01	12.93	19.88	<0.01
NII	-10.92	4.22	0.04	9.53	5.32	0.02
NIII	-5.10	22.03	<0.01	4.12	23.54	<0.01
NIV	-21.70	20.95	<0.01	14.98	20.26	<0.01
NV	-15.77	35.10	<0.01	10.78	35.43	<0.01
CI	-23.45	5.27	0.02	15.51	5.20	0.02
CII	-9.13	5.82	0.02	6.00	5.19	0.22
CIII	-12.72	6.16	0.01	7.85	5.16	0.02
CIV	-26.12	4.48	0.03	17.80	4.49	0.03

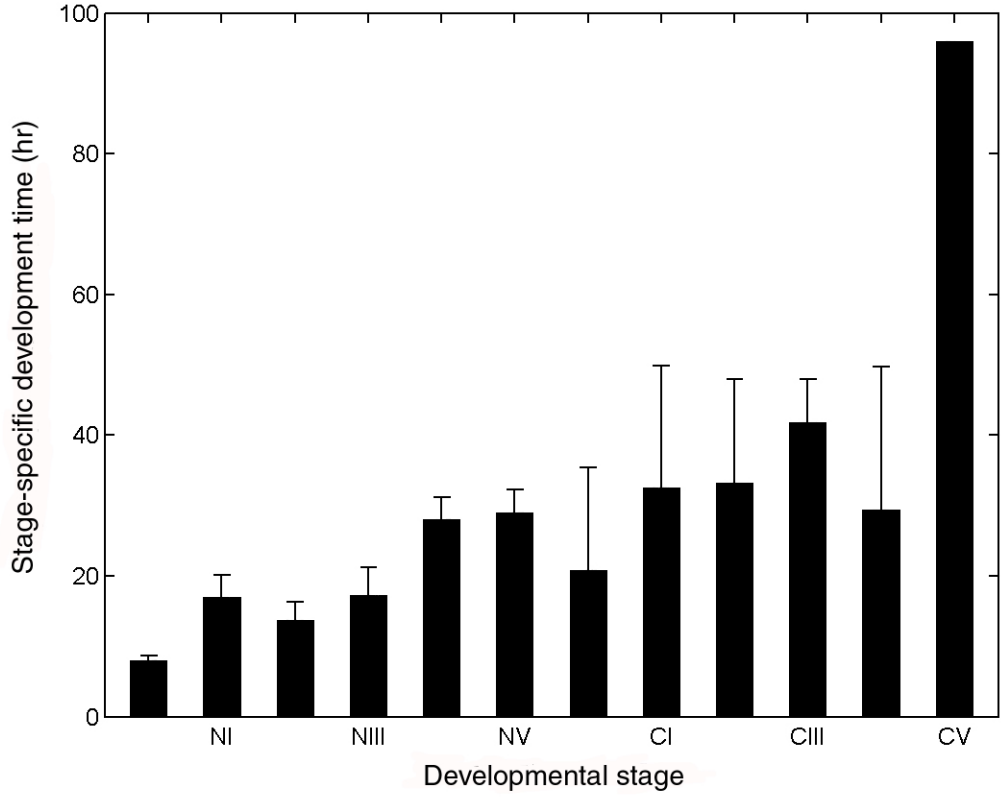

Figure 3.9: Stage–specific developmental times estimated from logistic regression models for egg, nauplius I–VI and copepodite I–V. Error bars represent 95% confidence intervals (upper limit). The developmental time for CV (copepodite stage V) is the result of direct observation on one (out of three) individual successfully entering the consecutive stage.

3.4 Discussion

3.4.1 Broadcast or Sac Spawner

Clausocalanus furcatus was first observed in the field as as egg carrying species (Webber and Roff 1995). Mazzocchi and Paffenhöfer (1998) observed eggs carried within a very fragile egg mass in a laboratory study, and they also found the remains of a thin membrane surrounding the eggs. In the present study, both regular egg masses and irregular egg masses were observed in the incubation experiments. Eggs stuck together in both complete and irregular cases, were easily separated by any disturbance. This irregular formation of egg mass has also been reported for many other genera such as *Euchaeta*, *Euchirella*, *Eurytemora*, *Paraeuchaeta*, *Paraugaptilus*, *Pseudocalanus*, *Pseudochirella*, *Psedudodiaptomaus* and *Valdiviella* (Mauchline 1998).

Fragile egg masses may be an adaptive life strategy to lower egg mortality, since masses can be easily detached when adult females are captured by predators (Svensson 1996). In Niskin water bottle samples, the presence of intact egg masses attached to the female genital somite reflected the occurrence of egg mass. Eggs were also found singly, or in groups of 2–9 eggs from Niskin water samples, suggesting the existence of irregular egg masses in the field.

Mazzocchi and Paffenhöfer (1998) found in a laboratory study on *Cl. furcatus* that only eggs in egg masses hatched successfully; however, in the present study, single eggs, irregular egg masses, and intact egg masses hatched normally. Development and hatching of the eggs appeared to be independent of parental care in the incubation experiments. In field samples from Niskin bottle, more than 90% of the eggs were single. If only eggs from intact egg masses hatch normally in the field, this would suggest heavy egg mortality. More direct *in situ* observations with cameras or optical imagery from the field are necessary for a better understanding of this strategy for *Cl. furcatus*.

3.4.2 Egg Production Rates

The occurrence of egg mass appeared to be confirmed by the egg production experiments. The clutch size of *Cl. furcatus* observed in this study ranged from ~12–18 eggs female^{-1} day^{-1}, which was similar to previous studies (Mazzocchi and Paffenhöfer 1998; Webber and Roff 1995; Szahina 1985). However, *in situ* egg production rates estimated from the Edmonson egg ratio method ranged from 0 to 11 eggs female^{-1} day^{-1} with an average of 3.38 (surface temperature ranged 18–24°C) in March–April and 0.47 eggs female^{-1} day^{-1} in May–June (surface temperature ranged 24–28°C). These results were lower than incubation experiments; however, they were more comparable to reported values from other egg–carrying species in the same family: *Clausocalanus* sp. (2.7–6.7 eggs female^{-1} day^{-1}at 17°C; Saiz et al. 1997) and *Pseudocalanus* spp. (0.5–5.3 eggs female^{-1} day^{-1}at 4.8–7.3°C; Paul et al. 1990).

Such a difference in egg production rates could possibly be caused by overestimation from incubation experiments and underestimation from the Edmonson egg ratio method. Overestimation of egg production rates in the present study may come from a higher visibility rates and subsequent capture/sampling rates for ovigerous females. The ovigerous females are easier to be visually perceived than non–ovigerous females (Bollens and Frost 1991; Winfield and Townsend 1983). The incubation experiments were conducted on an offshore petroleum platform, more females might have been picked due to the mechanical vibration. As a result, egg production rates estimated from incubation experiments were more likely to be a maximum egg production rate.

The underestimation of egg production rates might also be caused by the time lag between egg production and their accurate measurement in the field (Dam and Tang 2001; Tang et al. 1998). This underestimation may result from several causes: egg loss due to sinking processes

(Marcus 1996; Miller and Marcus 1994), egg loss due to predation (De Stasio Jr. 1993; Svensson 1992; Hairston et al. 1983), egg loss due to cannibalism (Ohman and Hirche 2001), and eggs hatching into nauplii.

Clausocalanus furcatus appeared to have a diel rhythm of egg laying, with a higher egg production rate during night and early morning than during day. Most daytime samples in the present study were taken from 5:00–9:00am local time, while nighttime samples were taken from 5:00–9:00pm. Given egg hatching time required 7–8 hours, eggs collected in daytime samples likely reflect spawning activities during the late night through early morning (7–8 hours prior to sampling time), while eggs collected at night would suggest spawning activities during the day. Egg production rates estimated from daytime samples were significantly higher than those from nighttime samples, suggesting more egg production during night than day.

In situ egg production did not show significant differences among the three different water depths. *Clausocalanus furcatus* has been reported to be abundant in the upper water column (~40m) in both daytime and nighttime (Paffenhöfer and Mazzocchi 2003; Sameoto 1986). *Clausocalanus furcatus* occur mainly in outer shelf areas (Minello 1980; Frost and Fleminger 1968) and it might be susceptible to low salinity plume water. However, it still remains unclear how salinity would affect the species (e.g., salinity tolerance).

3.4.3 Particulate Organic Carbon

Field POC concentration can be used as an indication for food that can be ingested by mesozooplankton (Wishner et al. 1995; Hamilton and Galat 1983). Legendre and Rassoulzadegan (1996) showed that zooplankton can directly or indirectly feed on phytoplankton, the microbial food web, and organic aggregates. Mazzocchi and Paffenhöfer (1998) successfully cultured *Cl. furcatus* for four consecutive generations with a diet mixture of dinoflagellate *Gymnodinium*

nelsoni (20μm) and the flagellate *Rohodomonas* sp. (5μm). In the present study, POC was collected with 0.45μm filters, which included particles within the known range that can be handled by *Cl. furcatus*. In terms of the lower size range, POC concentration was appropriate to evaluate food availability. However, the study area was frequently influenced by the Mississippi River plume water, the detritus transported by the plume water might mask the signal in POC. Further studies on feeding ecology of *Cl. furcatus* are necessary.

Concentrations of POC measured during this study were not comparable to previous estimates from the same area (Trefry et al. 1994) due to different laboratory methods, i.e., combustion method used in present study vs. the use of a Carlo Erba NA1500 NCS system. However, combustion measurements still show relative fluctuations of POC over time. The study area has been shown to have high POC concentrations in summer (Trefry et al. 1994) and high levels of primary production (Lohrenz et al. 1990). In the present study, relatively high POC concentrations were present for both March–April and May–June, and this may indicate food availability might not be a limiting factor for egg production. The wide range of *in situ* egg production rates may be caused by predation, sinking and cannibalism.

The POC concentrations in the upper water column was approximately similar to the lower water column, even though the Mississippi River plume frequently influenced the upper water column (Wiseman et al. 1976). This could be generally explained by high levels of primary productivity in the study area (Lohrenz et al. 1990).

3.4.4 Factors Influencing Egg Production Rates

Clausocalanus furcatus had an approximately 8–10 times higher egg production rate as measured by Edmonson egg ratio method in March–April than that in May–June. Egg production rates appeared to be a response to the strong plume indicated by low surface salinities during 82–86 (year–day) in March–April (Figure 2.3).

Egg production rates have been found to be limited by food availability in many cases (Peterson and Kimmerer 1994; Ianora and Poulet 1993; Runge 1985). In the present study, however, egg production rates did not show a clear relationship with POC concentration. The study area generally has high primary production (Lohrenz et al. 1990) and POC levels have been found to remain high during the entire summer (Trefry et al. 1994). Food availability did not appear to be a limiting factor for the egg production rate in the study area. Moreover, incubation–derived estimates egg production were very similar over the coverage of the study. These constant and high production rates support the hypothesis that food was not limiting.

Egg production rates appear to respond to temperature in many studies (Hirst and Kiørboe 2002; Hirche et al. 1997; Huntley and Lopez 1992; Runge 1985). In present study, the egg production rates of *Cl. furcatus* decreased with increasing temperature over the range of ~18–28˚C). The other factor that might influence egg production rate is salinity. Other studies have shown that egg production rates can either decline (Miliou and Moraitou-Apostologpoulou 1991) or increase (Hall and Burns 2001) when salinity is out of the optimum range. However, it still remains unclear how salinity would affect egg production rates for *Cl. furcatus*.

The egg production rates at three different water depths (5, 15 and 25m) underwent similar variations. Relative egg production rates were coincident with a strong Mississippi River plume (year–day:82–86; Figure 3.4). Assuming the adult females are producing eggs at the maximum rate and carrying their eggs without food limitation, the variations in the *in situ* egg production rate likely reflect differential mortality rates of eggs or adult females in the water column.

3.4.5 Stage-specific Development Times

The development times of *Cl. furcatus* from hatching to adulthood ranged from ~13–20 days and were consistent with a previously laboratory study (Mazzocchi and Paffenhöfer 1998). Compared with the generalized pattern for calanoid copepods summarized by Peterson (2001),

the development patterns of *Cl. furcatus* are: egg and nauplii stages I–III have a relatively short duration of ~17–24h; development in NIV and NV are prolonged and NVI has a relatively short duration; copepodite stages (I–IV) have similar durations to late naupliar stages; copepodite stage V has a prolonged duration, that is much longer than other early stages. In the present study, the first feeding stage (nauplii II or III) did not show a prolonged duration.

3.4.6 Summary

Clausocalanus furcatus is an common oceanic species. The mean egg production rate (± standard error) estimated from field samples was 1.67 ± 0.27 eggs female^{-1} day^{-1}, and was lower than 12.08 ± 1.40 eggs female^{-1} day^{-1} measured from incubation experiments. The *in situ* egg production rate showed large variations (0–14.6 eggs female^{-1} day^{-1}). The *in situ* egg production rate appeared to be influenced by the Mississippi River plume. When the plume water dominated the study area, the *in situ* egg production rate was relative low. The *in situ* egg production rate also appeared to influenced by temperature. The egg production rate in March–April was significantly higher than that in May–June.

Laboratory showed that the species carried eggs with an fragile egg mass. The variation of the *in situ* egg production rates may be caused by predation, cannibalism, sinking loss, differential hatching success and mortality in the adult females. Realistic egg production rates remain uncertain or somewhere between the two methods. More laboratory and field studies are necessary to ground truth the egg production rate and reproductive behavior of *Cl. furcatus*.

3.5 Bibliography

Bollens, S. M. and Frost, B. W. 1991. Ovigerity, selective predation, and variable diel vertical migration in *Euchaeta elongata* (Copepoda, Calanoida). *Oecologia*, 87:155–161.

Bowman, T. E. 1971. The distribution of calanoid copepods off the southern United States between Cape Hatteras and southern Florida. *Smithson. Contrib. Zool.*, 96:1–58.

Dagg, M. J., Ortner, P. B., and Al-Yamani, F. 1988. Winter–time distribution and abundance of copepod nauplii in the Northern Gulf of Mexico. *Fish. Bull,* 86:219–230.

Dam, H. G. and Tang, K. W. 2001. Affordable egg mortality: constraining copepod egg mortality with life history traits. *J. Plankton Res.*, 23:633–640.

De Stasio Jr., B. T. 1993. Diel vertical and horizontal migration by zooplankton: Population budgets and the diurnal deficit. *Bull. Mar. Sci.*, 53:44–64.

Edmondson, W. T. 1960. Reproductive rates of rotifers in natural populations. *Memorie Ist. Ital. Idrobiol.*, 12:21–77.

Edmondson, W. T. 1968. A graphical method for evaluating the use of the egg ratio technique for measuring birth and death rates. *Oecologica,* 1:1–37.

Frost, B. and Fleminger, A. 1968. A revision of the genus *Clausocalanus* (Copepoda: Calanoida) with remarks on distributional patterns in diagnostic characters. *Bull. Scripps Inst. Oceanogr.*, 12:1–235.

Hairston, N. G., Walton, W. E., and Li, K. T. 1983. The causes and consequences of sex–specific mortality in a freshwater copepod. *Limnol. Oceanogr.*, 28:935–947.

Hall, C. J. and Burns, C. W. 2001. Effects of salinity and temperature on survival and reproduction of *Boeckella hamata* (Copepoda: Calanoida) from a periodically brackish lake. *J. Plankton Res.,* 23:97–103.

Hamilton, K. and Galat, D. L. 1983. Seasonal variation of nutrients, organic carbon, ATP, and microbial standing crops in a vertical profile of Pyramid Lake, Nevada. *Hydrobiologia*, 105:27–43.

Harris, R. P. and Paffenhöfer, G. A. 1976. The effect of food concentration on cumulative ingestion and growth efficiency of two small marine planktonic copepods. *J. Mar. Biol. Assoc. UK,* 56:675–690.

Hirche, H. J. 1990. Egg production of *Calanus finmarchicus* at low temperature. *Mar. Biol.*, 106:53–58.

Hirche, H. J., Meyer, U., and Niehoff, B. 1997. Egg production of *Calanus finmarchicus*: effect of temperature, food and season. *Mar. Biol.*, 127:609–620.

Hirst, A. G. and Kiørboe, T. 2002. Mortality in marine planktonic copepods: Global rates and patterns. *Mar. Ecol. Prog. Ser.,* 230:195–209.

Huntley, M. E. and Lopez, M. D. G. 1992. Temperature–dependent production of marine copepods: A global synthesis. *Am. Nat.*, 140:201–242.

Ianora, A. and Poulet, S. A. 1993. Egg viability in the copepod *Temora stylifera*. *Limnol. Oceanogr*, 38:1615–1626.

Kiørboe, T., Møhlenberg, F., and Tiselius, P. 1988. Propagation of planktonic copepods: production and mortality of eggs. *Hydrobiologia*, 167/168:219–225.

Legendre, L. and Rassoulzadegan, F. 1996. Food–web mediated export of biogenic carbon in oceans: environmental control. *Mar. Ecol. Prog. Ser.*, 145:179–193.

Lo, W., Shih, C., and Hwang, J. 2004. Diel vertical migration of the planktonic copepods at an upwelling station north of Taiwan, western North Pacific. *J. Plankton Res.*, 26:89–97.

Lohrenz, S. E., Dagg, M. J., and Whitledge, T. E. 1990. Enhanced primary production at the plume/oceanic interface of the Mississippi River. *Cont. Shelf Res.*, 10:639–664.

Lohrenz, S. E., Fahnenstiel, G. L., Redalje, D. G., Lang, G. A., Chen, X., and Dagg, M. J. 1997. Variations in primary production of northern Gulf of Mexico continental shelf waters linked to nutrient inputs from the Mississippi River. *Mar. Ecol. Prog. Ser.*, 155:45–54.

Marcus, N. H. 1996. Ecological and evolutionary significance of resting eggs in marine copepods: past, present, and future studies. *Hydrobiologia*, 320:141–152.

Marum, J. P. 1974. *Spatial and temporal variations of zooplankton in relation to offshore oil drilling and estuarine–marine faunal exchange*. PhD thesis, Florida State University.

Mauchline, J. 1998. The biology of calanoid copepods. *Adv. Mar. Biol*, 33:710.

Mazzocchi, M. G. and Paffenhöfer, G. A. 1998. First observations on the biology of *Clausocalanus furcatus* (Copepoda, Calanoida). *J. Plankton Res.*, 20:331–342.

Miliou, H. and Moraitou-Apostologpoulou, M. 1991. Combined effects of temperature and salinity on the popualtion dynamics of *Tisbe holothuriae* Humes (Copepods: Harpacticoida). *Arch. Hydrobiol.*, 121:289–319.

Miller, D. D. and Marcus, N. H. 1994. The effects of salinity and temperature on the density and sinking velocity of eggs of the calanoid copepod *Acartia tonsa* Dana. *J. Exp. Mar. Biol. Ecol.*, 179:235–252.

Minello, T. J. 1980. *The neritic zooplankton of the northwestern Gulf of Mexico*. PhD thesis, Texas A&M University.

Miralto, A., Barone, G., Romano, G., Poulet, S. A., Ianora, A., Russo, G. L., Buttino, I., Mazzarella, G., Laabir, M., Carini, M., and Giacobbe, M. G. 1999. The insidious effect of diatoms on copepod reproduction. *Nature*, 402:173–176.

Ohman, M. D. and Hirche, H. J. 2001. Density–dependent mortality in an oceanic copepod population. *Nature*, 412:638–641.

Ortner, P. B., Hill, L. C., and Cummings, S. R. 1989. Zooplankton community structure and copepod species composition in the northern Gulf of Mexico. *Cont. Shelf Res.*, 9:387–402.

Paffenhöfer, G. A. and Mazzocchi, M. G. 2003. Vertical distribution of subtropical epiplanktonic copepods. *J. Plankton Res.*, 25:1139–1156.

Paul, A. J., Coyle, K. O., and Ziemann, D. A. 1990. Variation in egg production rates by *Pseudocalanus* spp. in a subarctic Alaskan bay during the onset of feeding by larval fish. *J. Crust. Biol.*, 10:648–658.

Peterson, W. T. 2001. Patterns in stage duration and development among marine and freshwater calanoid and cyclopoid copepods: a review of rules, physiological constraints, and evolutionary significance. *Hydrobiologia*, 453/545:91–105.

Peterson, W. T. and Kimmerer, W. J. 1994. Processes controlling recruitment of the marine calanoid copepod *Temora longicornis* in Long Island Sound: Egg production, egg mortality, and cohort survival rates. *Limnol. Oceanogr.*, 39:1594–1605.

Peterson Jr., R. C. 1986. In situ particle generation in a southern Swedish stream. *Limnol. Oceanogr.*, 31:432–437.

Price, J. F. 1976. Several aspects of the response of shelf waters to a cold front passage. *Memoirs of the Royal Society of Liege*, 6:201–208.

Runge, J. A. 1985. Egg production rates of *Calanus finmarchicus* in the sea of Nova Scotia. *Arch. Hydrobiolgia*, 21:33–40.

Saiz, E., Calbet, A., Trepat, I., Irigoien, X., and M, A. 1997. Food availability as a potential source of bias in the egg production method for copepods. *J. Plankton Res.*, 19:1–14.

Sameoto, D. D. 1986. Influence of the biological and physical environment on the vertical distribution of mesozooplankton and micronekton in the eastern tropical pacific. *Mar. Biol.*, 93:263–279.

Smith, N. P. 1980. Temporal and spatial variability in longshore motion along the Texas Gulf coast. *J. Geophys. Res.*, 85:1531–1536.

Svensson, J. E. 1992. The influence of visibility and escape ability on sex–specific susceptibility to fish predation in *Eudiaptomus gracilis* (Copepoda, Crustacea). *Hydrobiologia*, 234:143–150.

Svensson, J. E. 1996. Clutch detachment in a copepod after capture by a predator. *J. Plankton Res.*, 18:1369–1374.

Szahina, L. I. 1985. Fecundity and growth rate of copepods in different dynamic zones of equatorial counter current of the Indian Ocean. *Pol. Arch. Hydrobiol.*, 32:491–505.

Tang, K. W., Dam, H. G., and Feinberg, L. R. 1998. The relative importance of egg production rate, hatching success, hatching duration and egg sinking in population recruitment of two species of marine copepods. *J. Plankton Res.*, 20:1971–1987.

Thompson, B. M. 1982. Growth and development of *Pseudocalanus elongates* and *Calanus* sp. in the laboratory. *J. Mar. Biol. Assoc. U. K.*, 62:359–372.

Trefry, J. H., Nelsen, T. A., Trocine, R. P., and Eadie, B. J. 1994. Transport of particulate organic carbon by the Mississippi River and its fate in the Gulf of Mexico. *Estuaries*, 17:839–849.

Vervoort, W. 1963. Pelagic copepoda. Pt. I: Copepoda Calanoida of the families calanoidae up to and including Euchaetidea. *Atlantide Report*, 7:77–194.

Webber, M. K. and Roff, J. C. 1995. Annual biomass and production of the oceanic copepod community off Discovery Bay, Jamaica. *Mar. Biol.*, 123:481–495.

Williams, R. and Wallace, M. A. 1975. Continuous plankton records: a plankton atlas of the North Atlantic and North sea: supplement 1–The genus *Clausocalanus* (Crustacea: Copepoda, Calanoida) in 1965. *Bull. Mar. Ecol.*, 8:167–184.

Winfield, I. J. and Townsend, C. R. 1983. The cost of copepod reproduction: increased susceptibility to fish predation. *Oceanologia*, 60:406–411.

Wiseman, W. J., Banes, J. M., Murray, S. P., and Tubman, M. W. 1976. Small scale temperature and salinity structure over the inner shelf west of the Mississippi River Delta. *Memoirs Royal Soci. Liege*, 6:277–285.

Wishner, K. F., Ashjian, C. J., Gelfman, C., Gowing, M., Kann, L., Levin, L. A., Mullineaux, L. S., and Saltzman, J. 1995. Pelagic and benthic ecology of the lower interface of the Eastern tropical Pacific oxygen minimum zone. *Deep–Sea Res.*, 42:93–115.

CHAPTER 4 ESTIMATING STAGE–SPECIFIC MORTALITY RATES

4.1 Introduction

Copepods are the most abundant mesozooplankton in pelagic ecosystems (Longhurst 1985) and knowledge of their vital rates is essential to understand population processes (Eiane et al. 2002; Twombly and Lewis Jr. 1989). Temporal and spatial variations in mortality rates determine the species abundance and distribution. Small changes in mortality rates can have order of magnitude effects on copepod population abundance. How mortality is apportioned among their 13 distinctive development stages affects the population growth rate and reproductive output (Aksnes et al. 1997; McCauley and Murdoch 1990). Furthermore, copepod grazing often regulates primary production and copepods are important food sources for higher trophic levels. Knowledge of zooplankton mortality rates is, therefore, necessary to understand the trophic linkage between primary production and higher trophic levels (Eiane et al. 2002; Aksnes et al. 1997).

Estimation of mortality rates from natural copepod populations is complicated for a number of reasons. In the pelagic environment, organisms are often patchily distributed (Aksnes et al. 1997). Field samples may be biased towards certain development stages depending upon gear selectivity and their vertical distribution (Wood and Nisbet 1991). Other factors that can influence mortality rates in the field include: advection, predation (Aksnes et al. 1997; Ohman 1986), cannibalism (Ohman and Hirche 2001; Peterson and Kimmerer 1994), food availability (Kleppel et al. 1998) food quality (Paffenhöfer 2002; Ianora and Poulet 1993; Ianora et al. 1990), reproduction method (Ohman et al. 2002), and interrelationships among population parameters (e.g., high mortality in adult females will lead to a low egg production rate; Ohman and Wood 1996; Hairston and Twombly 1985).

Cannibalism and predation have been considered among the main causes for copepod mortality. Predator–prey interactions are important factors in regulating seasonal and spatial distributions (Kiørboe and Nielsen 1994; Ianora et al. 1990). Predation pressure from visual predators, such as fish, can cause high mortality rates (Möllmann and Köster 2002; Verheye and Richardson 1998). As the major nonvisual predators, chaetognaths (Ohman 1986) and jellyfish (Brodeur et al. 2002; Purcell et al. 1994) can also regulate copepod populations. Hirst and Kiørboe (2002) attributed about 66–75% of the adult copepod mortality to predation and Tarling et al. (2004) attributed over 80% of the mortality of *Calanoides acutus* during winter to predation. Predation pressure from visual and nonvisual predators may vary seasonally (Ohman 1986). Cannibalism has been considered the main cause of high egg mortality rates (Ohman and Hirche 2001; Peterson and Kimmerer 1994).

Several methods have been proposed to estimate copepod mortality rates. Methods such as the horizontal life table (Manly 1990; Gehers and Roberston 1975; Rigler and Cooley 1974), quadratic programming method (Wood 1994), and regression method (Caswell 2000) depend on an intensive time series of samples. Alternative approaches such as the vertical life table (Aksnes and Ohman 1996; Mullin 1991) can infer mortality from snapshot samples. The underlying assumptions for these methods have been reviewed by Aksnes et al. (1997) and are not discussed here. Providing that samples are taken from the same population over one generation within a short time interval (shorter than the shortest stage duration), all of these methods, in theory, can be used to obtain estimates of stage–specific mortality rates (Torres-Sorando et al. 2003; Ohman and Hirche 2001; Ohman and Wood 1996; Rigler and Cooley 1974).

In reality, organisms drift with ocean currents in the pelagic environment and mortality is likely different in the various patches being sampled. Consequently the assumption of sampling from the same population is unlikely to hold and demographical noise attributed to factors other

than mortality–induced population variability is inevitable (Aksnes and Ohman 1996; Huntley and Niiler 1995). Such noise has different consequences for the effectiveness of the different mortality estimation methods. When time series data from a fixed observation point fail to reflect well–defined population changes in the field, the horizontal life table method will likely generate negative estimates (Caswell 2000; Hairston and Twombly 1985). The vertical life table method attempts to reduce noise in different ways either by estimating mortality based on snapshot samples (Aksnes and Ohman 1996), or averaging samples between generations or years (Brinton 1976). However, in an advective environment, vertical life tables may not be able to reduce the noise sufficiently to yield meaningful results. By fitting a smooth surface to the observation data, the quadratic programming method (also referred as the surface smooth method) proposed by Wood (1994) can avoid demographic instabilities to some extent (Ohman et al. 2004; Ohman and Wood 1996; Wood 1994). However, it remains unclear how well this method can be applied to samples collected from a highly advective environment.

Mathematical population models not only provide the ability to predict and simulate zooplankton populations measured from field data, they also provide a powerful tool for estimating population parameters to look at factors and processes that determine the population's trajectory (Carlotti et al. 2000). Stage–structured matrix projection models have been widely applied to simulate zooplankton populations (Torres-Sorando et al. 2003; Lo et al. 1995; Caswell and Twombly 1989; Levin et al. 1987), as well as vital rate estimation (Twombly 1994; Hiby and Mullen 1980). By fitting the model to field data with a standard nonlinear Gauss–Marquardt–Levenburg algorithm to minimize the difference between modeling data and observed data (Carlotti et al. 2000), the inverse matrix modeling method has the potential to estimate mortality rates from samples collected in a dynamic environment.

Clausocalanus furcatus has been reported as one of the dominant copepods in oceanic water off the southeastern USA (Bowman 1971). Subsequent studies have shown *Cl. furcatus* to

make up a large proportion of zooplankton communities in the northern Gulf of Mexico (Ortner et al. 1989; Minello 1980; Marum 1974). The species is widely distributed in oligotrophic oceanic waters (Lo et al. 2004; Paffenhöfer 1985); yet, knowledge about their population dynamics and underlying population parameters is limited (Mazzocchi and Paffenhöfer 1998).

The aim of this part of the study was to estimate the mortality rates for *Cl. furcatus* in the northern Gulf of Mexico. The specific objectives were to:

- Estimate mortality with horizontal life table method, vertical life table method, Wood's quadratic programming method, and inverse matrix modeling;
- Compare the suitability of different methods; and
- Examine factors influencing mortality rates.

4.2 Method

4.2.1 Study Site and Zooplankton Sampling

Sampling was conducted at South Timbalier 151 (ST151), a ChevronTexaco offshore petroleum platform complex located 50 km south of Grand Isle, Louisiana (28°37'N, 90°15'W) in 45m water depth (Figure 2.1). Zooplankton were collected at 12h intervals from 18 March–6 April and from 15 May– 9 June, 2003 with a 30L Niskin water bottle and a 70cm diameter ring plankton net (2.5m long, 153 μm mesh). Niskin water bottles were deployed at 5, 15, and 25m and the contents were filtered through 20μm mesh. Each sample consisted of 3 replicate water bottle samples from each depth. Vertical net tows were made from approximately 15m and were hauled to the surface at a retrieval rate 20–25 cm s^{-1} using an electrical winch. The net was lowered into the water from a point on ST151 located approximately 20m above the surface. The depth to be sampled was determined by premeasured mark on the cable, verified with a VEMCO temperature and depth data logger calibrated against pressure readings from

a YSI 6920 sonde. The average filtered water volume for each net tow was 5.75 m^3. At each sample period, three replicate net tows were collected within 30 min.

Samples were fixed in 5% formalin and transferred to 70% ethanol in the lab before being sorted and identified. Samples were sorted and *C. furcatus* were identified and staged under a stereo–microscope (50x).

4.2.2 Data Analysis

4.2.2.1 Numerical Abundance Data Calibration

Given the oceanic nature of *Cl. furcatus*, the species favors high salinity waters. At ST151 the water column is frequently stratified with low salinity coastal water overlying oceanic water. Thus the volume filtered by vertical net tows is likely an overestimate of the true volume occupied by *Cl. furcatus*. To determine the lower boundary of the optimum salinity for *Cl. furcatus*, the stage abundance data (n m^{-3}) from Niskin water bottles were categorized by salinity from 18–36 psu with 1 psu increments for each development stage. A cumulative sums procedure (CUSUM; SAS Institute, 1990) was applied to detect the salinity point when the abundance significantly increased based on equation 4.1 and equation 4.2.

$$z_t = \frac{\overline{X_i} - \mu_0}{\frac{\sigma}{\sqrt{n_i}}} \tag{4.1}$$

where, z_t is the deviation from the expected mean value, $\overline{X_i}$ is mean of the i^{th} salinity group, n_i is the sample size for i^{th} salinity group, μ_0 is the mean estimated by the whole population, and σ is the standard deviation estimated from the entire population.

$$S_i = S_{i-1} + z_i \tag{4.2}$$

where, S_i is the sum of deviation from 0 to i^{th} group ($S_0 = 0$).

In a CUSUM plot, a segment of the CUSUM chart with an upward slope indicates a period where the abundance tended to be above the overall mean abundance. Likewise a segment with a downward slope indicates a period of time where the abundance tended to be below the mean abundance. A sudden change in direction of the CUSUM indicates a sudden shift or change in the mean. Periods where the CUSUM chart follows a relatively straight path indicate where the mean abundance did not change.

After the lower boundary of optimum salinity was determined, the water depths below which salinities were favorable for *Cl. furcatus* was estimated from the vertical salinity profile. The numerical density was then corrected with a coefficient defined by 4.3.

$$k = \frac{D}{D - d_s} \tag{4.3}$$

where, k is the calibration coefficient for the volume, D is the sampling water depth, and d_s is the water depth of the salinity shift point. This calibration was only made for vertical net tows data.

4.2.2.2 Sample Comparison

The mean abundance from Niskin water bottle samples was determined by averaging all samples collected from 5, 15, and 25m. A scatter plot was applied to display the relationship among the abundance of each stage estimated from three replicated net samples and Niskin water bottles collected at close intervals to each other throughout the study period. Then, paired *t*–tests were used to test whether there were differences between abundances estimated from nets and those estimated from the Niskin bottles.

4.2.3 Estimating Mortality Rates

4.2.3.1 Horizontal Life Table

A time–specific life table was applied to obtain a detailed description of mortality (Carey 1993). In the life table, the proportion of a cohort surviving from egg to stage x is denoted as l_x. The difference in number of survivors for successive stage x and $x + 1$ is designated d_x:

$$d_x = l_x - l_{x+1} \tag{4.4}$$

Thus the periodic mortality rates (q_x) that represent the probability of dying over these respective stage periods can be defined by:

$$q_x = \frac{d_x}{l_x} \tag{4.5}$$

To obtain nonnegative estimation, the abundance of stage $i+1$ at time $t+1$ has to be lower than the abundance of stage i at time t. In the present study, estimates were made only when the the data met this assumption, i.e., yielded positive results, and then the mean of all positive values were calculated for each stage.

4.2.3.2 Vertical Life Table

Assuming that the mortality rates of stage i and $i + 1$ can be considered equal for a period corresponding to the duration of two consecutive stages, mortality of stage i can be determined from equation 4.6 and equation 4.7 (Aksnes and Ohman 1996).

$$\frac{n_i}{n_{i+1}} = \frac{[\exp(m \times d_i) - 1]}{[1 - \exp(-m \times d_{i+1)}]} \tag{4.6}$$

$$\frac{n_{q-1}}{n_q} = \exp(m_{q-1}) - 1 \tag{4.7}$$

where, n_i is the number of individuals in stage i, q is the adult stage, m is the mortality rate for stage i, and d_i is the stage duration determined from incubation experiment (Table 4.1). In

the present study, the vertical life table method was applied to mean stage densities for two sampling periods respectively.

4.2.3.3 Quadratic Method

The quadratic method (see surface smooth method by Wood (1994) for details) was applied to estimate stage-specific mortality rates. This method first uses a smoothing spline technique to reduce the variation in the field data and to create equal time interval samples (Curve fitting toolbox 2.0 in Matlab 6.5, Mathworks Inc. Natick, MA, 2002). Then it finds the best fit mortality rates by minimizing the quadratic term, defined by 4.8.

$$z = p \sum_i w_i (y_i - s(x_i))^2 + (1 - p) \int \left[\frac{d^2 s}{dx^2} \right]^2 dx \tag{4.8}$$

where, p is a smooth parameter between 0 and 1, w_i is the specified weights, $s(x_i)$ is the spline function, x_i is sampling time, and y_i is the observed abundance.

Caswell (2000) implemented this method by using *QuadProg* in the Optimization toolbox in Matlab 6.5 (Mathworks Inc. Natick, MA, 2002). To perform quadratic programming, a $s \times s$ transitional matrix A containing population parameters was defined by equation 4.9, where s is the number of development stages. In this study, I combined egg and NI as one stage to meet the requirement of sample interval has to be shorter than the shortest stage duration, thus $s = 12$.

$$A = \begin{bmatrix} P_1 & 0 & \cdots & \cdots & F \\ G_1 & P_2 & 0 & & 0 \\ 0 & G_2 & \ddots & & \vdots \\ \vdots & & \ddots & \ddots & \vdots \\ 0 & \cdots & \cdots & G_{s-1} & P_s \end{bmatrix} \tag{4.9}$$

where, P_s is the probability of individuals surviving and staying in the same stage, G_s is the probability of individuals surviving and entering the next stage, and F is the recruitment rate from the adult stage, i.e., egg production rate.

Next, a vector P_t was created by eliminating zero elements in A. M_t was created by removing the corresponding columns in $n(s)^t \bigotimes I_{s\times s}$, where $n(s)$ is a vector holding the abundance of stage s and I is identity matrix. P_t and M_t satisfied 4.10.

$$\begin{pmatrix} n_1(t) \\ \vdots \\ n_s(t) \end{pmatrix} = M_t \times \begin{pmatrix} P_1 \\ G_1 \\ \vdots \\ F \\ P_s \end{pmatrix} \tag{4.10}$$

where, $n_s(t)$ is the abundance of stage s at time t.

The parameters in matrix A are nonnegative and the column sum of diagonal and subdiagonal elements can not exceed 1. Z, M and P are defined as:

$$Z = \begin{bmatrix} \begin{pmatrix} n_1(1) & \cdots & n_s(1) \end{pmatrix} & \cdots & \begin{pmatrix} n_1(t) & \cdots & n_s(t) \end{pmatrix} \end{bmatrix}^T \tag{4.11}$$

$$M = \begin{bmatrix} M_0 & 0 & \cdots & \cdots & 0 \\ 0 & \ddots & & & \vdots \\ \vdots & & \ddots & & \vdots \\ \vdots & & & \ddots & \vdots \\ 0 & \cdots & \cdots & 0 & M_{T-1} \end{bmatrix} \tag{4.12}$$

$$P = \begin{pmatrix} P_0 & \cdots & P_t \end{pmatrix}^T \tag{4.13}$$

P_t can be estimated by minimizing the quadratic terms $||Z - M'P'||^2$. Then mortality rates can be estimated from equation 4.14. An example of the Matlab code I used to implement the

Quadratic method is provided in Appendix B.

$$P_s(t) + G_s(t) = 1 - m_s(t) \tag{4.14}$$

where, $P_s(t)$ is the probability of survival and staying in same stage for stage s at time t, $G_s(t)$ is the probability of survival and entering the consecutive stage of stage s at time t, and $m_s(t)$ is the mortality rate for stage s at time t.

4.2.3.4 Inverse Matrix Method

The stage–structured matrix population model is defined by equation 4.15.

$$n_{t+1} = A \times n_t \tag{4.15}$$

where, n is a vector which contains the numbers of individuals at each stage, t is the sampling time, and A is the transitional matrix defined by equation 4.9. To formulate the transitional matrix, egg production rates (F) were estimated from Niskin water bottle samples using the Edmonson egg ratio method (Edmondson 1960) discussed in Chapter 3. The probability of surviving and staying in the same stage is calculated from the stage duration listed in Table 4.1.

Table 4.1: Stage–specific development times measured from incubation experiments with 50% individuals entering next stage. Individuals of known stage were incubated 16–20°C with natural food filtered with 63μm mesh.

Stage	Egg	NI	NII	NIII	NIV	NV	NVI	CI	CII	CIII	CIV	CV
Duration (h)	8	17	14	17	28	29	20	33	33	42	29	96

An automated model-independent parameter estimation procedure (PEST, Doherty 2004) was applied to obtain the estimates for stage-specific mortality rates. PEST minimizes the

discrepancies between the pertinent model-generated data and the corresponding observations by implementing the Gauss-Marquardt-Levenberg algorithm. PEST linearizes the model parameters and model-generated observations by formulating a Taylor expansion, and then the derivatives of observations with respect to all parameters are calculated. PEST computes the partial derivatives using central differences. The parameters are varied by small amounts in both positive and negative directions and the model is rerun twice, and the derivatives are computed. PEST then finds a better parameter set from the linearized problem, and the new parameters are tested by running the model again. By comparing parameter changes and objective function, i.e., the improvement achieved through the current iteration and the improvement achieved in previous iterations, PEST can determine whether it is worthwhile undertaking another optimization iteration.

The field data that constituted the stage distribution vectors contain a large amount of variability. To allow PEST to properly estimate the stage-specific mortality rates, the sampling window has to contain enough samples. In the present study PEST was run for two study periods (24 samples collected in approximately two weeks during March–April and 45 samples in approximately three weeks during May–June).

4.2.4 Comparison Between the Quadratic Method and the Inverse Matrix Method

The horizontal life table method and the vertical life table method did not provide an estimated mortality rate for the adult stage and simulations could not be performed, consequently the simulation comparisons were only made for the quadratic method and the inverse matrix method. To compare the difference between the quadratic method and PEST, a simulated population with known mortality rates was presented as observed data, and then the quadratic method and PEST were applied respectively. Secondly, the population was simulated with estimated parameters for the study periods by Equation 4.15.

4.2.5 Predation Effects

Regression analysis was used to detect the possible predation effects from chaetognaths and larger copepods, *Eucalanus attenuatus* and *Euchaeta marina*. The response variable in the model was the stage abundance of *Cl. furcatus* and the regressor was the abundance of chaetognaths or larger copepods. The normality assumption for residuals was examined by Kolmogorov-Smirnov test. The preliminary test showed the normality assumption for residuals was violated, hence the stage abundances of *Cl. furcatus* were log transformed to satisfy the normality assumption. In the cases where the log transformation could not satisfy the normality assumption, nonparametric Spearman correlation coefficients were computed.

4.3 Results

4.3.1 Salinity Shift Point

Clausocalanus furcatus increased its abundance with increasing salinity for all development stages (left panel of Figure 4.1). Nauplii appeared to increase their abundance at 30–31 psu salinity and copepodids appeared to be more abundant when salinity was higher than 27–29 psu. Cumulative sum control charts for abundance versus salinity (Figure 4.1) appear to take upward turns in direction around 31 psu for nauplii and early copepodite stages (CI–CIII). Stages CV and CVI took the upward turn at 27–29 psu. This suggested the existence of a salinity shift point for the increasing abundance of *Clausocalanus furcatus*, allowing salinity to be broken into two separate regimes. In this study, 30 psu was considered the salinity shift point that delineated waters favorable to *Cl. furcatus* from those overlying low salinity waters.

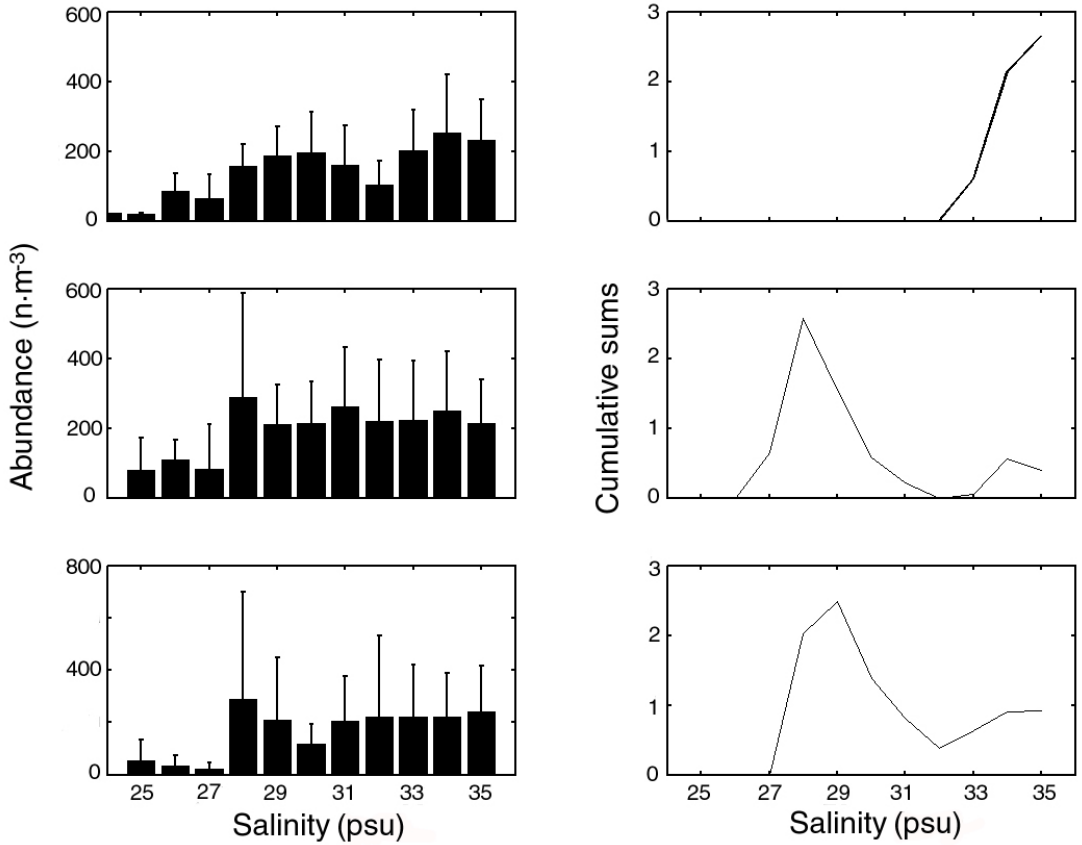

Figure 4.1: Left panel shows histograms of mean abundances for different development stages of *Cl. furcatus* over the salinity range during the entire study period and error bars stand for one standard error. Right panel shows CUMSUM procedure to find the corresponding salinity shift point for increasing abundance (positive slope). Figure continues on next page.

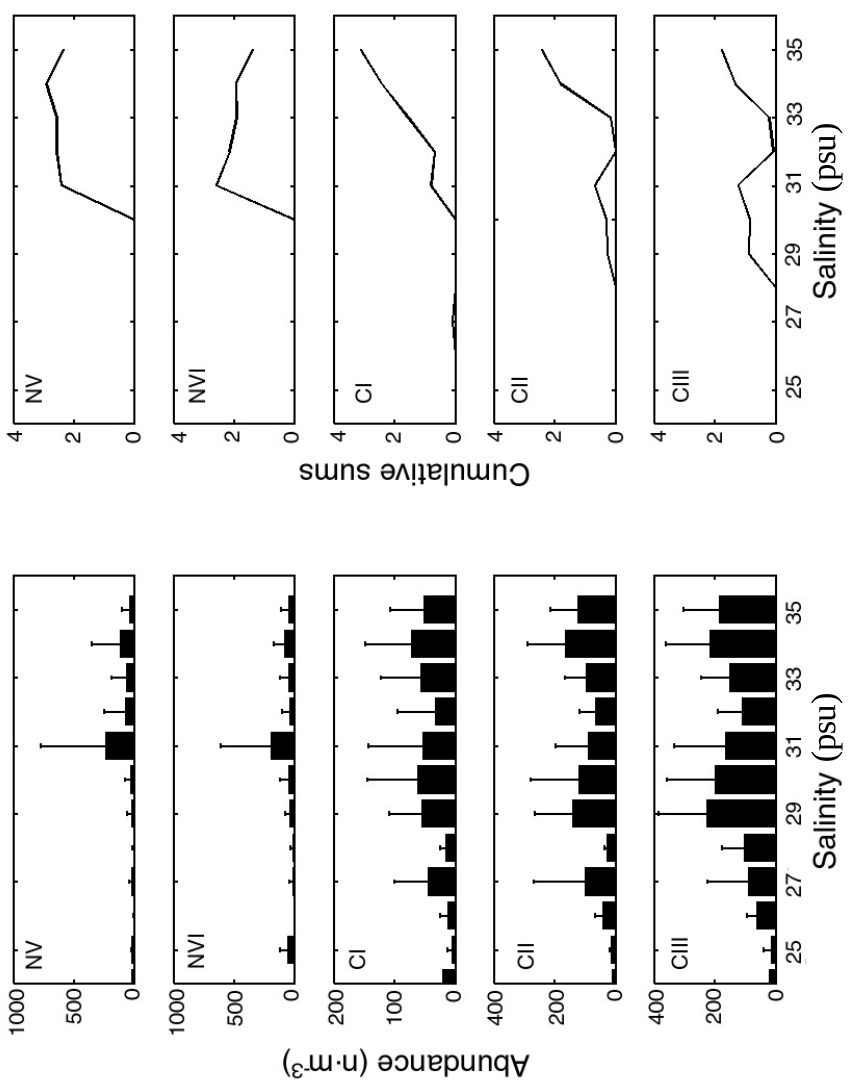

Figure 4.1 Continued

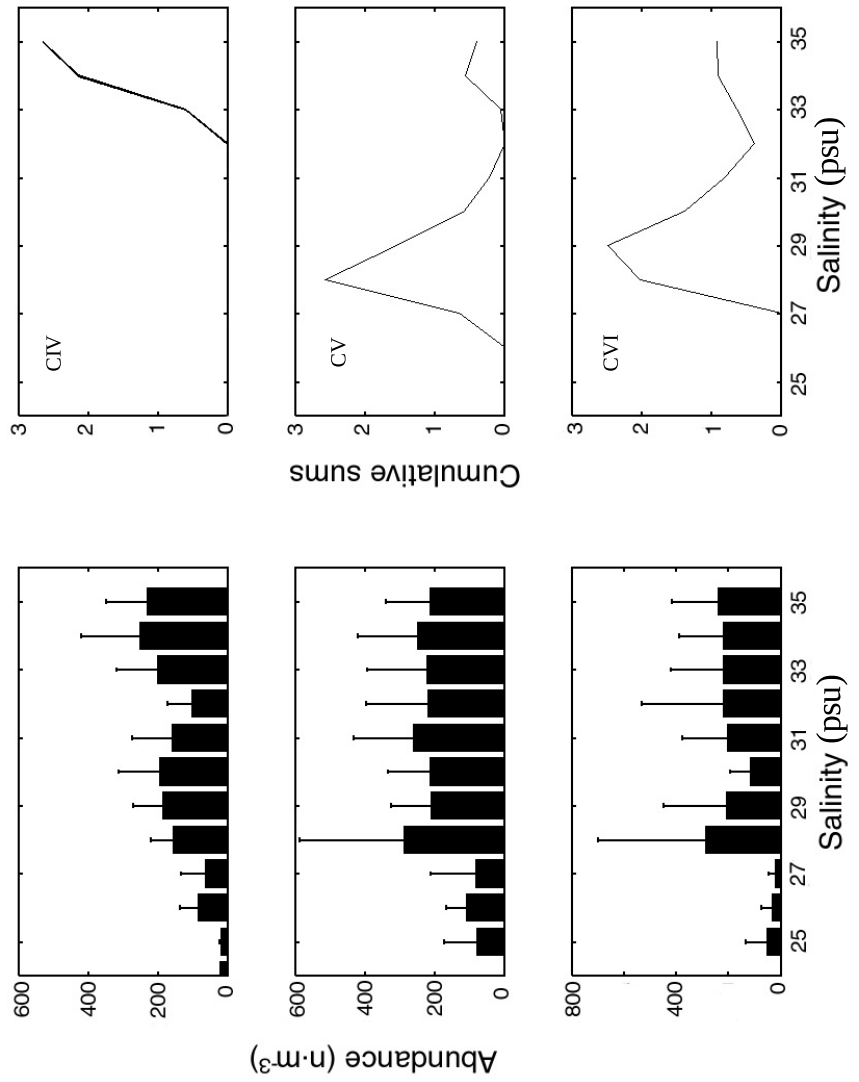

Figure 4.1 Continued

4.3.2 Comparison between Net Samples and Niskin Bottle Samples

Clausocalanus furcatus was continuously present in the study area with all development stages represented throughout the study period. Nauplii had higher abundance in March–April than in May–June. Copepodite stages did not exhibit such a difference.

There was no significant difference between net samples and Niskin bottle samples for late nauplii stages (NIII–NVI, Table 4.2). However, a significant difference was detected between net samples and Niskin water bottle samples for copepodids ($p < 0.05$, Table 4.2). Niskin water bottle samples consistently produced lower abundance estimates than net samples for copepodite stages during both study periods (Figure 4.2). Niskin water bottle samples provided higher abundance estimates for nauplii stages than net samples during the early part of the first sampling period, whereas net samples had a higher abundance than Niskin samples during the period (year-day 85-90) when lower salinity plume water predominated the upper water column (Figure 2.5).

4.3.3 Stage–specific Mortality Rate Estimation

4.3.3.1 Horizontal Life Table

The copepodite stages were more abundant than early nauplii stages for both collection gears (Table 4.2). Higher abundances of later stages than the younger stages at the previous sampling period were frequently encountered during the study period (e.g., $\mathrm{NIII}_{t+1} > \mathrm{NII}_t$), and this led to negative mortality rate estimates.

By constraining nonnegative mortality rates, periodic mortality rates were estimated from samples with 12 h intervals during the entire study period (Table 4.3). Less than 5% of samples yielded meaningful mortality rate estimates for all development stages simultaneously. Mortality rates for NVI and CI could be only estimated from less than 15% of samples. Mortality

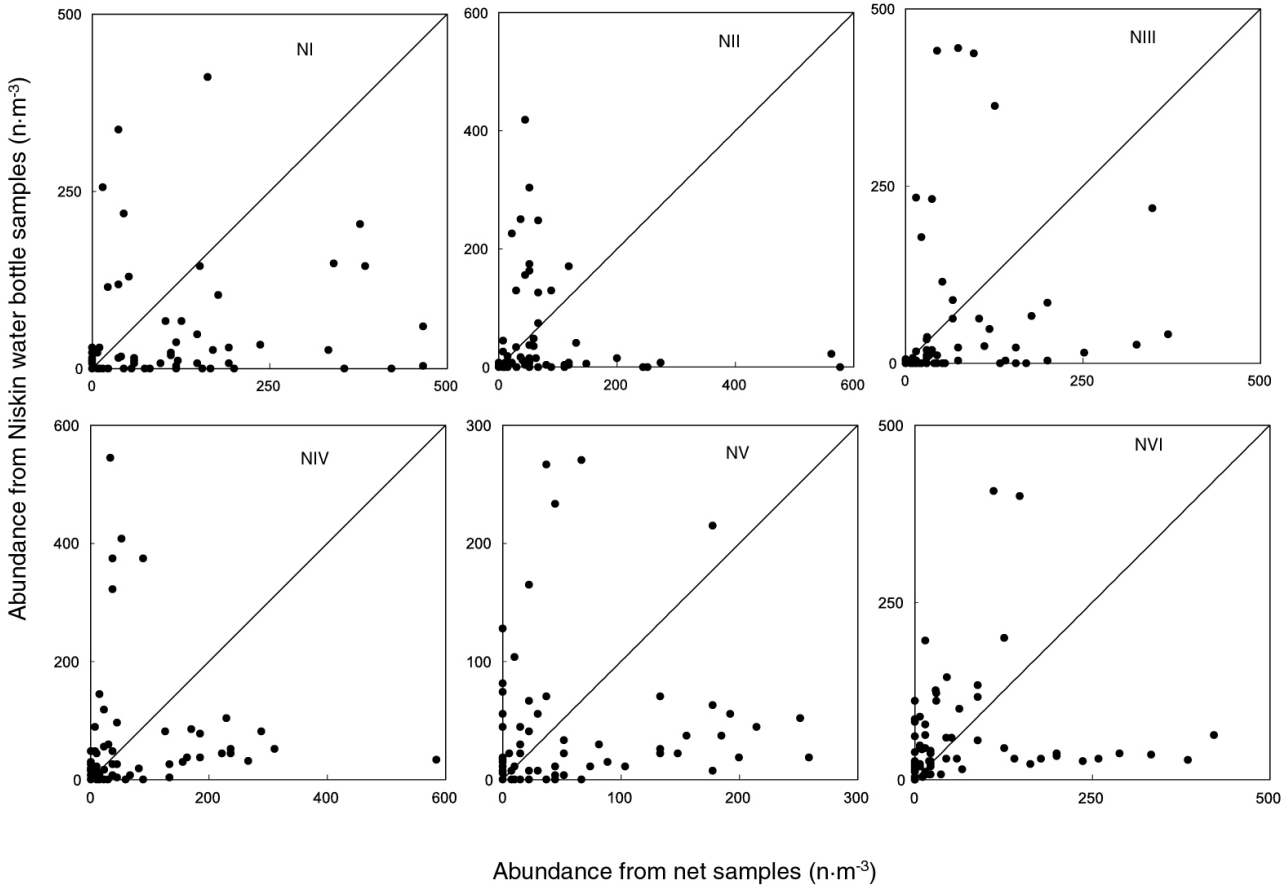

Figure 4.2: Scatter plots showing *Cl. furcatus* abundances from net versus Niskin water bottle samples for each stage. Mean abundances for net samples were calculated from three replicate net tows (0–15m) and mean Niskin water bottle abundances were averaged from samples at 5, 15 and 25m with three replicates for each depth. Figure continues on next page.

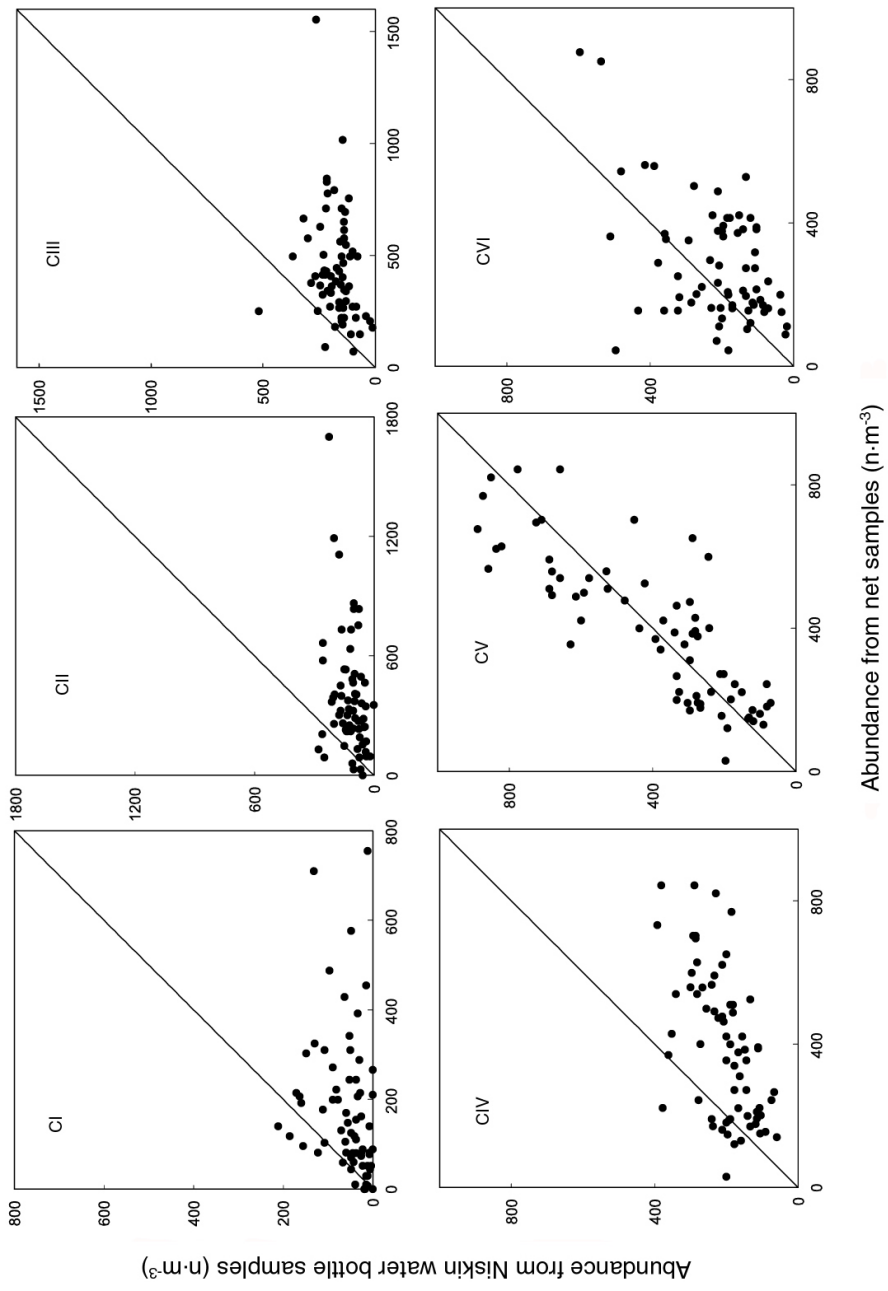

Figure 4.2 Continued

Table 4.2: Statistical results for mean abundance (n· m^{-3}, mean± standard error (SE)) from paired *t*–tests for each development stage comparing net and Niskin water bottle samples over the entire study period. N is the number of samples.

Stage	Net samples (mean ± SE) $N = 67$	Niskin bottle samples (mean ± SE) $N = 67$	*t*-value	*p*-value
NI	104.76 ± 15.03	46.72 ± 9.96	3.69	< 0.01
NII	94.90 ± 19.99	62.99 ± 15.6	2.15	0.04
NIII	117.00 ± 31.01	73.01 ± 14.64	1.52	0.13
NIV	70.63 ± 12.48	59.56 ± 12.23	0.01	0.99
NV	58.32 ± 8.41	59.53 ± 8.45	0.13	0.89
NVI	64.24 ± 11.72	55.08 ± 5.69	0.36	0.72
CI	174.50 ± 19.26	119.08 ± 7.35	6.25	<0.01
CII	379.91 ± 35.62	178.99 ± 9.06	7.74	< 0.01
CIII	437.79 ± 29.25	207.21 ± 8.86	9.11	< 0.01
CIV	398.47 ± 25.07	219.09 ± 11.82	8.95	< 0.01
CV	410.48 ± 30.35	214.01 ± 14.12	7.79	< 0.01
CVI	286.13 ± 20.40	37.47 ± 6.08	3.59	< 0.01

rates for other development stages could be estimated from 40–60% of samples. As a result, it was not feasible to obtain mortality rate estimation for each sample interval and the average mortality rates were compared among different methods in the present study.

Average mortality rates (over 12 h intervals) based on available samples indicated that a higher mortality rate occurred in naupliar stages than in copepodid stages (Figure 4.3). Stages with similar sizes generally appeared to have similar mortality rates (e.g., copepodids). In March, the highest morality rate occurred for eggs (70%), and then decreased when individuals passed through subsequent development stages. Mean mortality rates for naupliar and copepodid stages were 51% ± 6% (mean ± 95% confidence level (CL)) and 34% ± 8%, respectively. In May, the highest mortality rate occurred in NVI stage(83%). The egg mortality rate in May was 17% higher than in March. The mean mortality rate for naupliar stages also increased 28%. The mean mortality rate for copepodite stages was about 3% higher in May than in March.

Table 4.3: Mortality rates ($\times$100% in $12h^{-1}$) calculated from horizontal life tables over the entire study period: – stands for negative value; empty space stands for no available estimation, and SE is the standard error.

Year–day	NI	NII	NIII	NIV	NV	NVI	CI	CII	CIII	CIV	CV
78.88	–	–	0.17	–	0.67	–	–	–	0.51	0.52	0.80
79.38	0.17	0.29	0.50	0.40	–	–	–	–	–	–	–
79.88	0.69	–	–	–	–	–	–	–	–	0.08	0.50
80.38	–	0.50	0.53	0.29	0.96	–	–	–	–	–	0.13
80.88	0.86	–	0.38	–	–	–	–	–	–	–	0.48
81.38	–	–	0.65	0.20	–	–	–	0.10	0.01	0.16	0.45
81.88	0.56	0.50	–	–	–	–	–	–	–	–	0.29
82.88											
83.88											
84.38	–	–	–	–	–	–	–	0.25	0.10	–	–
84.88	–	–	–	–	0.57	–	–	–	0.48	0.31	0.31
85.38	–	–	0.80	0.77	–	–	–	–	0.04	–	0.39

continued on next page

– continued from previous page

Year–day	NI	NII	NIII	NIV	NV	NVI	CI	CII	CIII	CIV	CV
85.88	–	0.36	0.76	0.52	0.50	–	–	0.41	0.35	–	0.63
86.38	–	–	0.36	0.72	–	–	–	0.60	–	–	0.73
86.88	0.80	0.60	0.77	0.25	–	–	–	–	–	0.14	0.75
87.88	0.83	–	0.23	0.13	–	–	–	–	0.07	–	0.02
88.38	0.75	–	–	0.86	0.82	0.19		0.53	0.67	0.11	0.80
88.88	0.59	–	–	–	–	–	–	0.21	0.32	–	0.46
90.88											
91.88											
92.38	0.71	0.71	0.57	0.92	0.83	0.59	0.27	0.72	0.66	0.31	0.42
92.88	–	–	–	–	–	–	–	–	–	–	0.65
93.38	–	0.73	0.40	–	0.00	–	–	0.17	0.24	0.35	0.64
93.88	–	–	–	–	–	–	–	0.22	0.06	0.24	0.24
94.38	0.25	–	–	–	0.23	0.76	–	0.25	0.45	0.52	0.33
94.88	0.82	–	–	0.22	0.08	0.04	–	–	–	–	–
95.38	0.86	0.56	0.78	0.22	0.33	0.42	–	0.53	0.13	–	0.66
136.38											
136.88	–	–	–	–	1.00	–	–	0.50	–	0.28	0.54
137.38	1.00	1.00	1.00	–	0.00	–	–	–	–	0.00	0.45
137.88	–	–	–	–	–	–	–	0.45	–	–	0.50
138.38	0.27	–	–	1.00	1.00	–	–	–	0.01	0.09	0.43
138.88	0.71	1.00	1.00	1.00	–	–	–	–	0.31	–	–
139.38	0.96	–	–	–	–	–	–	–	0.13	–	0.41
139.88	–	–	0.50	–	0.00	–	–	–	0.28	–	–
140.38	–	–	1.00	0.00	1.00	–	–	–	–	0.10	0.63
140.88	–	0.00	0.50	–	0.00	–	–	–	–	0.19	–
141.38	0.00	–	0.67	0.00	0.60	–	–	–	–	0.19	0.59
141.88	0.47	–	0.75	–	–	–	0.26	–	–	–	–
142.38	0.13	–	0.17	–	0.50	–	–	–	–	0.07	0.58
142.88	0.13	0.00	0.89	0.40	1.00	–	–	–	0.41	0.26	0.20
143.38	–	–	–	–	1.00	–	–	–	0.74	0.02	0.00
143.88	0.81	0.77	0.67	0.50	0.50	–	0.45	–	0.43	–	0.30
144.38	0.93	0.63	1.00	–	0.67	–	–	–	0.21	–	–
144.88	–	–	0.11	–	0.92	–	0.66	–	0.13	–	0.23
145.38	0.44	0.50	0.00	0.75	–	–	–	0.05	0.72	0.38	0.14
145.88	–	–	–	–	–	0.67	–	–	–	0.42	–

continued on next page

– continued from previous page

Year–day	NI	NII	NIII	NIV	NV	NVI	CI	CII	CIII	CIV	CV
146.38	–	–	0.43	0.38	0.25	–	–	–	–	–	–
146.88	–	0.75	0.87	0.50	1.00	–	–	–	0.00	–	0.70
147.38	0.71	0.33	–	0.33	0.67	–	–	0.42	–	0.11	0.44
147.88	–	0.33	0.50	0.36	–	–	–	–	0.25	0.07	–
148.38	0.96	0.69	–	0.40	0.71	–	–	–	0.71	0.14	0.25
151.88	–	–	–	–	–	–	–	–	–	–	–
152.38	–	–	–	1.00	1.00	1.00	–	–	0.33	0.47	–
152.88	–	–	–	1.00	–	–	–	–	0.84	–	–
153.38	–	–	–	–	–	–	–	–	0.34	–	0.37
153.88	–	1.00	0.00	1.00	–	–	–	–	0.41	0.53	0.50
154.38	–	0.67	–	0.00	–	–	–	–	–	–	–
154.88	–	0.00	1.00	0.00	0.00	–	0.26	0.63	0.41	0.61	0.52
155.38	0.88	1.00	0.63	–	–	–	0.23	0.64	0.83	0.03	–
155.88	–	–	–	1.00	–	–	0.83	0.17	–	–	0.64
156.38	–	0.92	1.00	1.00	–	–	–	–	0.24	0.56	–
156.88	1.00	–	–	–	–	–	–	0.19	–	–	–
157.38	–	–	1.00	1.00	–	–	–	0.07	0.49	0.62	0.13
Mean	0.64	0.58	0.61	0.53	0.58	0.52	0.42	0.36	0.35	0.26	0.41
SE	0.06	0.06	0.05	0.06	0.07	0.13	0.09	0.04	0.05	0.04	0.04

4.3.3.2 Vertical Life Table Method

Clausocalanus furcatus had different population structures in March and May (Figure 4.4). Egg and naupliar stages were more abundant relative to copepodids in March than in May. Late copepodid stages were abundant in both study periods. Constraining nonnegative mortality rates, available mortality estimates are shown in Figure 4.5. Egg mortality was higher in March than May. The NIII stage appeared to experience relative high mortality in both study periods; however, the estimates were only available for some stages.

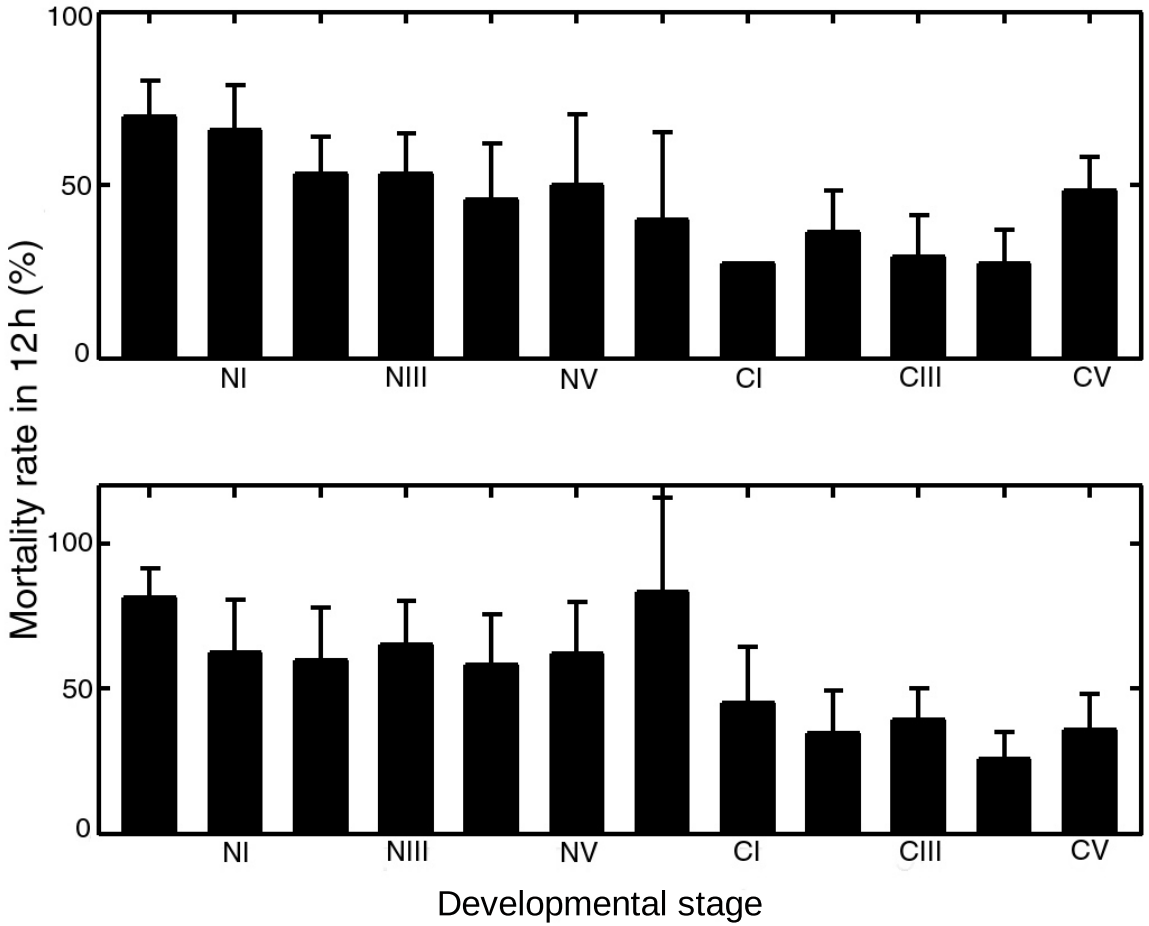

Figure 4.3: Mean stage–specific mortality rates for *C. furcatus* estimated from horizontal life tables with errorbars indicating one standard error. The top panel shows mortality rates in March–April and lower panel shows mortality rates in May–June.

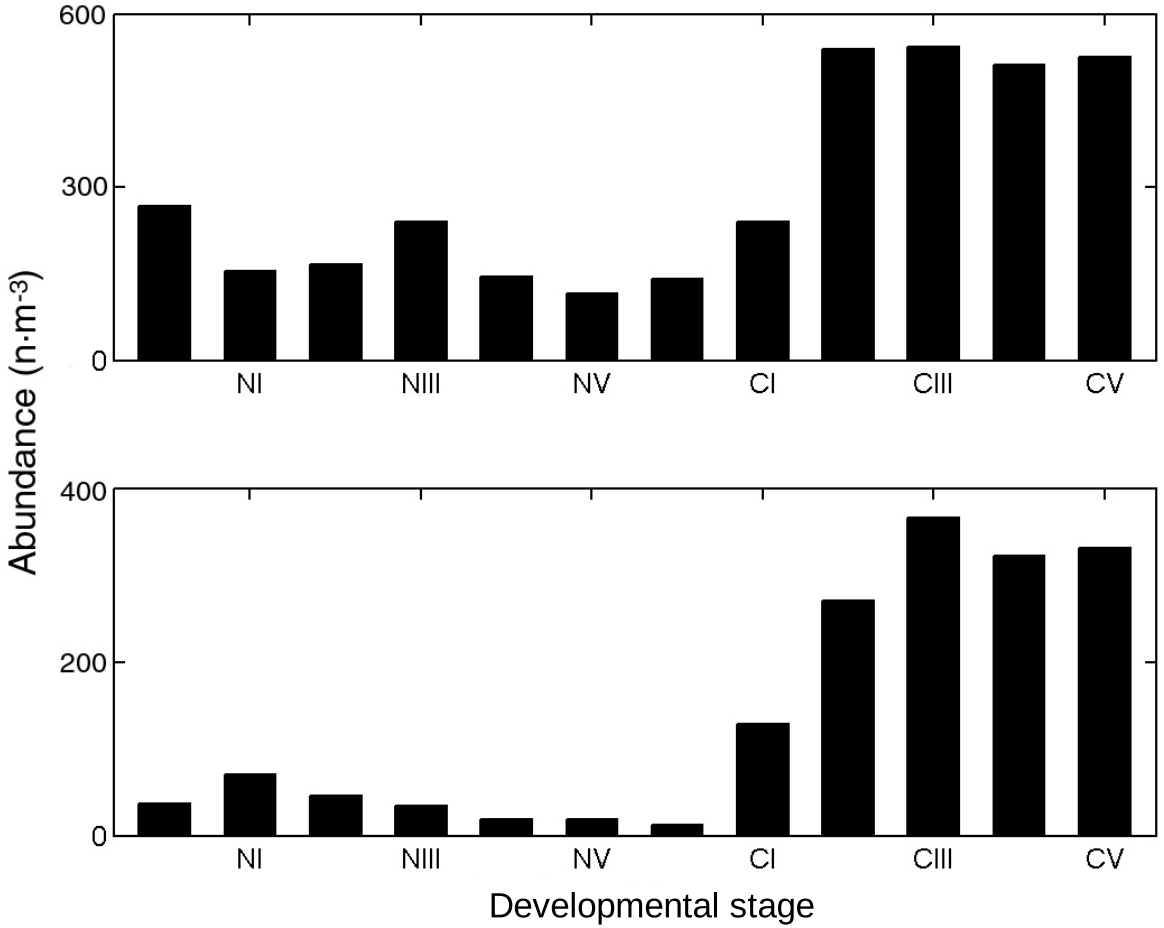

Figure 4.4: Development stage composition of *Cl. furcatus* during the two study periods. Mean abundance was calculated for each stage during each study period. Upper panel shows the mean population structure in March–April and lower panel shows population structure in May–June.

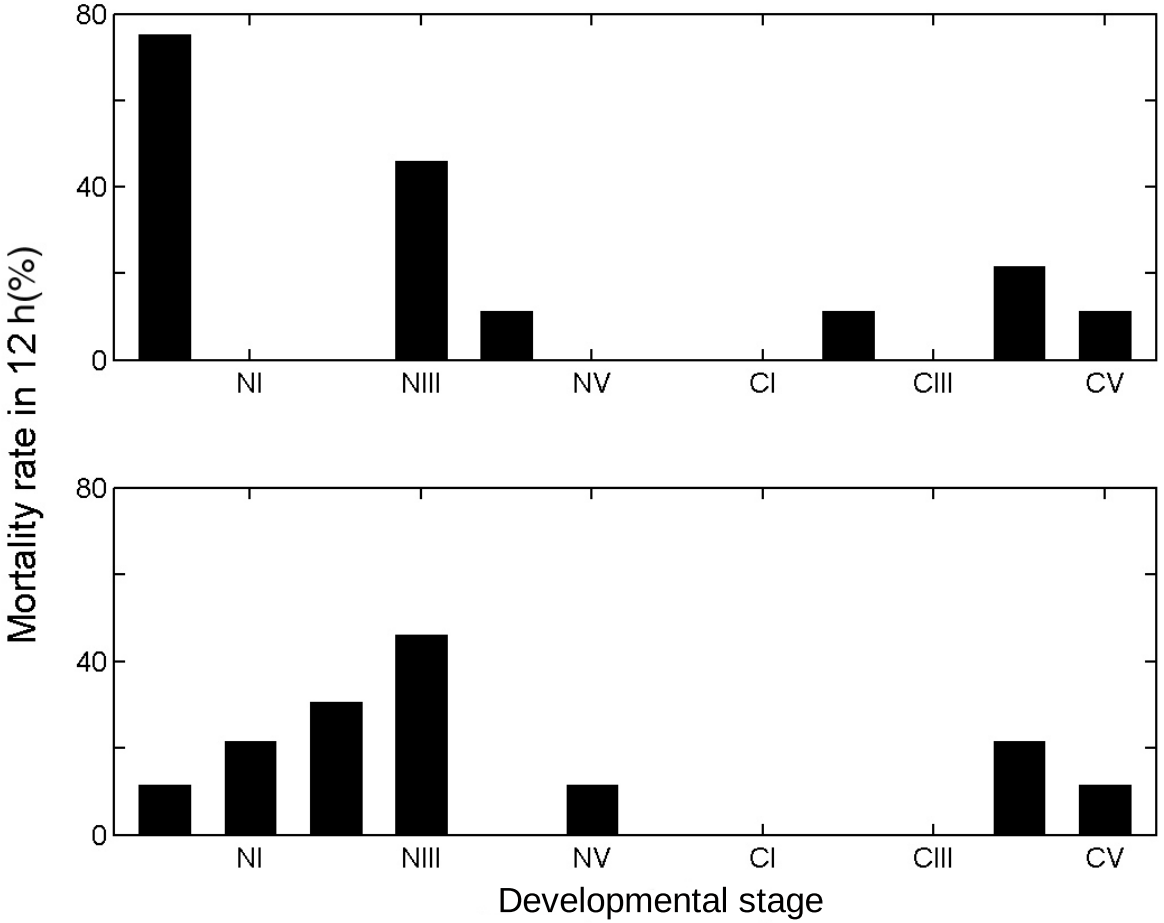

Figure 4.5: Stage–specific mortality rates for *Cl. furcatus* estimated from vertical life tables. Upper panel shows the mortality rates in March–April and lower panel shows mortality rates in May–June.

4.3.3.3 Quadratic Method

Field data frequently showed high variability, which led to negative mortality estimation as shown in the horizontal life table method. The smoothing spline effectively characterized the variations in field data (Table 4.4), reduced the noise in stage-frequency data from net samples, and effectively allowed interpolation of missing data (Figure 4.6, smoothing parameter was near $\frac{1}{1+h^3/6}$, chosen by Curve fitting toolbox in Matlab, where h is the average spacing of data points. In the present study, the smoothing parameters ranged from 0.78–0.80).

Table 4.4: Goodness–of–fit test (R^2) of the smoothing spline fitting for the stage frequency data from net samples. The smoothing parameter was $\frac{1}{1+h^3/6}$, where h is the average spacing of data points.

	NI	NII	NIII	NIV	NV	NVI	CI	CII	CIII	CIV	CV	CVI
March	0.74	0.82	0.82	0.89	0.78	0.70	0.85	0.88	0.88	0.75	0.87	0.85
May	0.75	0.71	0.83	0.78	0.81	0.84	0.81	0.87	0.82	0.93	0.92	0.75

High mortality rates (over 12 h intervals) for *Cl. furcatus* in March occurred in early naupliar stages. The average mortality rate for naupliar stages was 36% and higher than for copepodid stages (10%). The highest mortality occurred in NI (96%) and followed by NIII (37%) and NII (32%; Figure 4.7). Mortality rates for late naupliar stages and early copepodid stages through CIV showed small fluctuations ranging from 7%–16%. The mortality rate for adults increased slightly to 15%.

The average mortality rates (in 12 h intervals) in May were more variable than those in March (Figure 4.7), peaking at NI (74%) and then decreased through NIII (31%). The mortality rates in NIV through CI ranged from 30%–43% in May, and appeared to experience higher

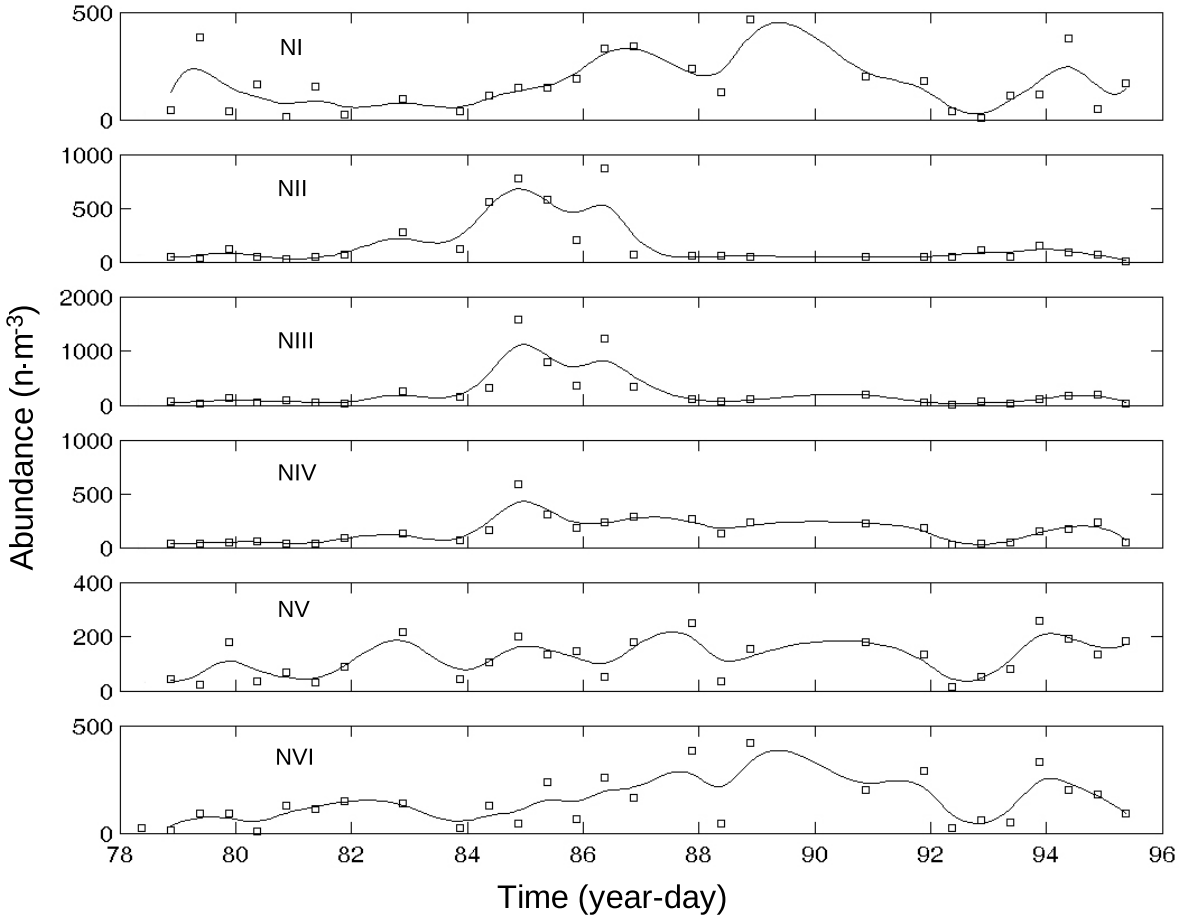

Figure 4.6: Smoothing spline applied to mean abundances data for each stage in both study periods. The smoothing parameter was $\frac{1}{1+h^3/6}$, where h is the average spacing of data points. Figure continues on next page.

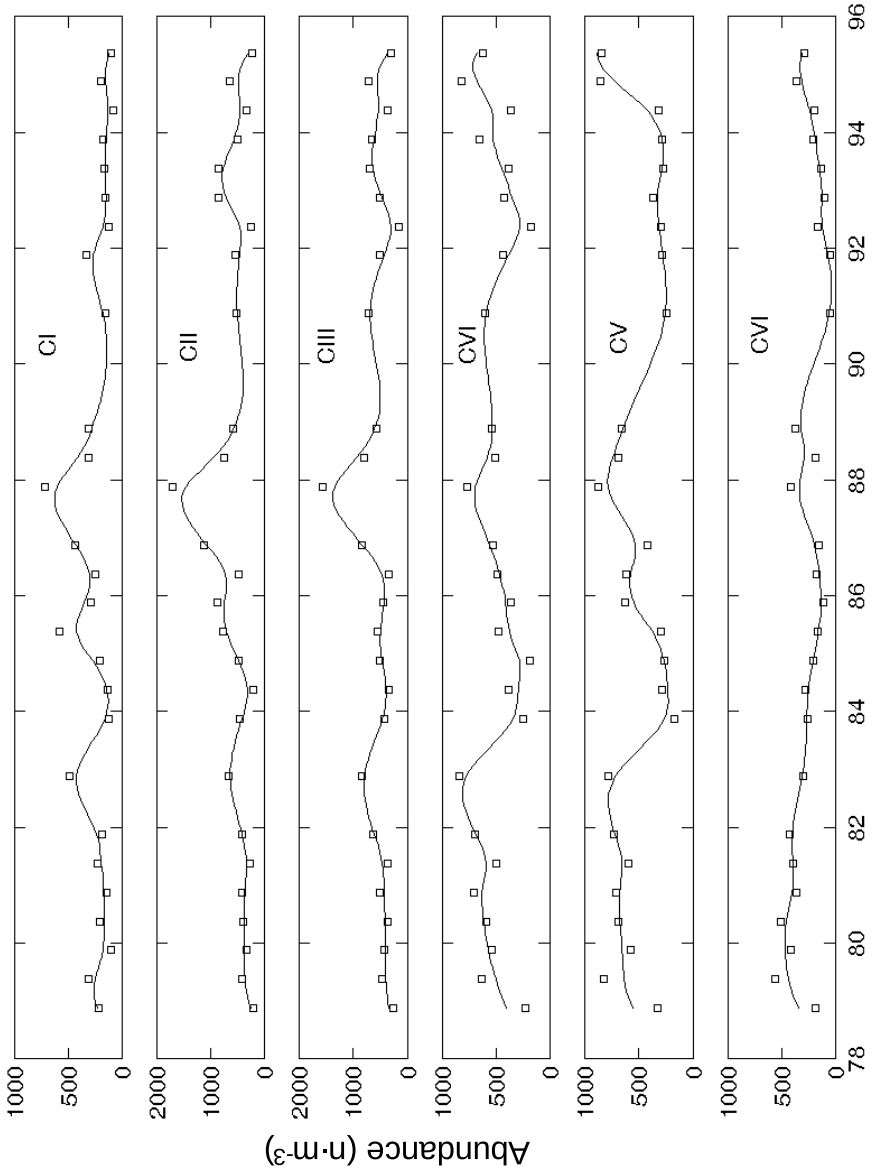

Figure 4.6 Continued

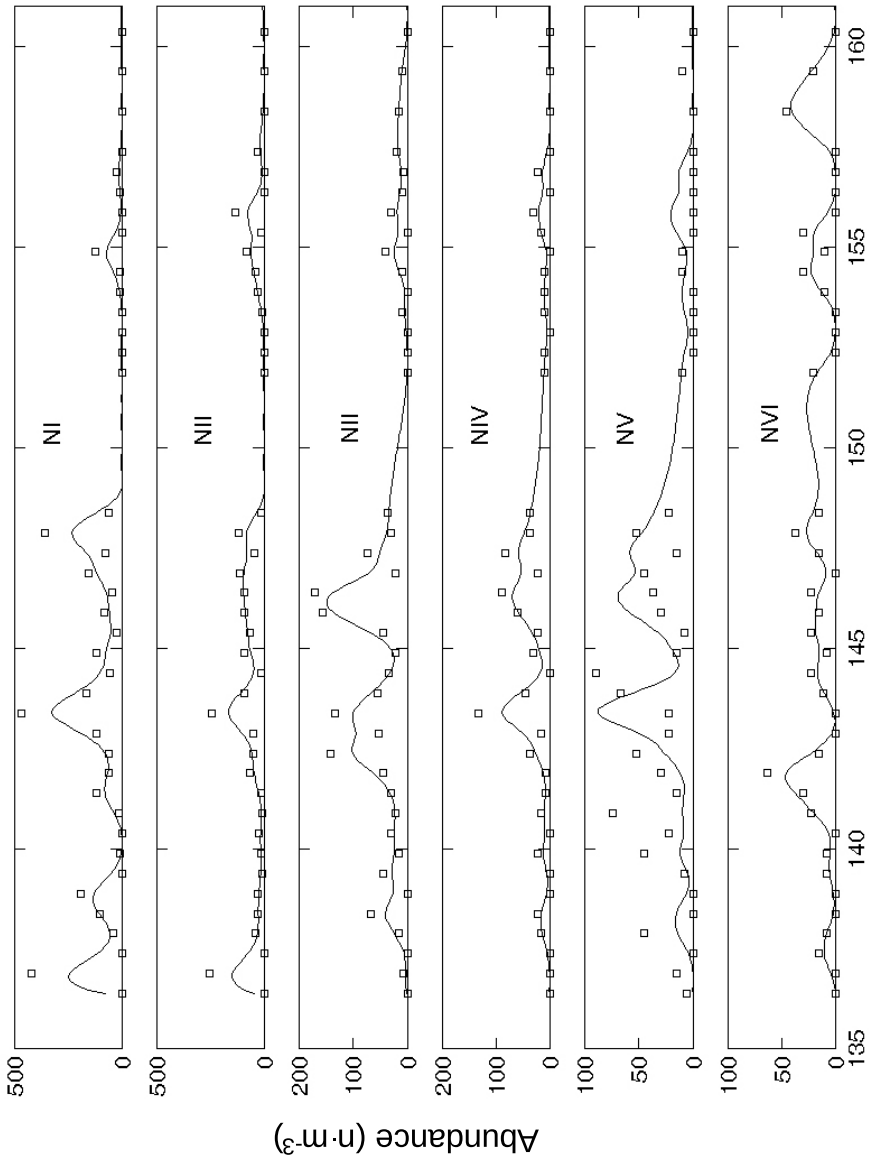

Figure 4.6 Continued

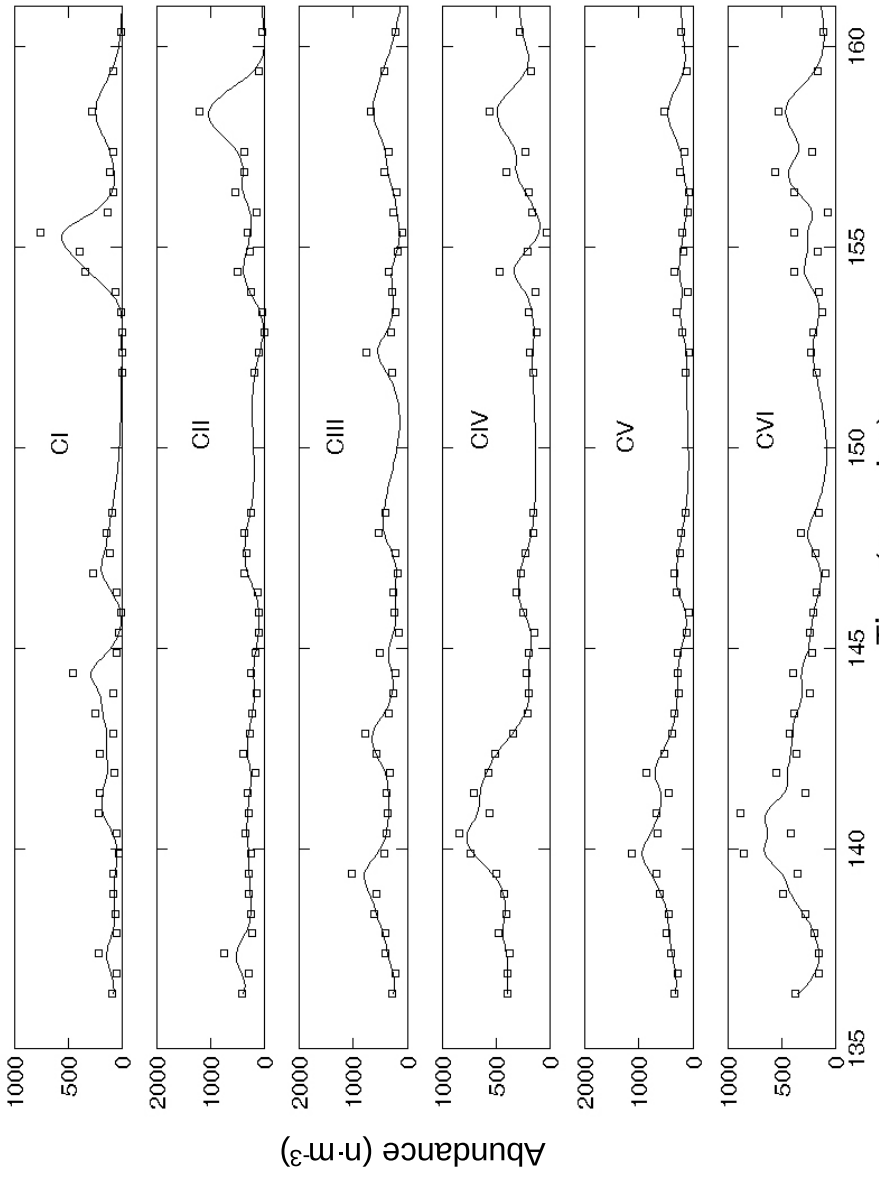

Figure 4.6 Continued

mortality rates than that in March. The May mortality rate for the adult stage (22%) was slightly higher than for late copepodid stages (CIV 6% and CV 12%).

4.3.3.4 Inverse Matrix Method Using PEST

Clausocalanus furcatus experienced relatively higher mortality in March than in May (Figure 4.8). The average mortality rates (in 12h) in March showed a large fluctuation with highest mortality in eggs (47%), followed by CV (32%), CVI (17%) and NIII (11%). Mortality rates for other stages were similar and relatively low (1%). The average mortality rates in May showed a similar pattern, being highest in eggs (55%), followed by CVI (15%) while the other stages ranged from 1–3%.

4.3.4 Comparison between the Quadratic Method and the Inverse Matrix Method

The simulations were not available for the horizontal life table method and the vertical life table method, because both methods did not provide an estimated mortality rate for the adult stage. The available mortality rate estimation for (NI–CV) from the horizontal life table method and the vertical life table method were higher than the quadratic method. If the quadratic method overestimated mortality rates, it is reasonable to conclude that the horizontal life table method and the vertical life table method also overestimated mortality rates.

When the inverse matrix method and the quadratic programming method were applied on a simulated population with known preset mortality rates, PEST recovered the preset values precisely and the quadratic method also generated reasonable estimation (Figure 4.9). The quadratic method appeared to overestimate mortality for NI (combining egg and NI) and slightly underestimate mortality rates for NII through NIV, CV and adult stages.

When the population was simulated with fixed mortality rates estimated from PEST and the quadratic method for the two study periods, i.e., March–April and May–June (Figure 4.10),

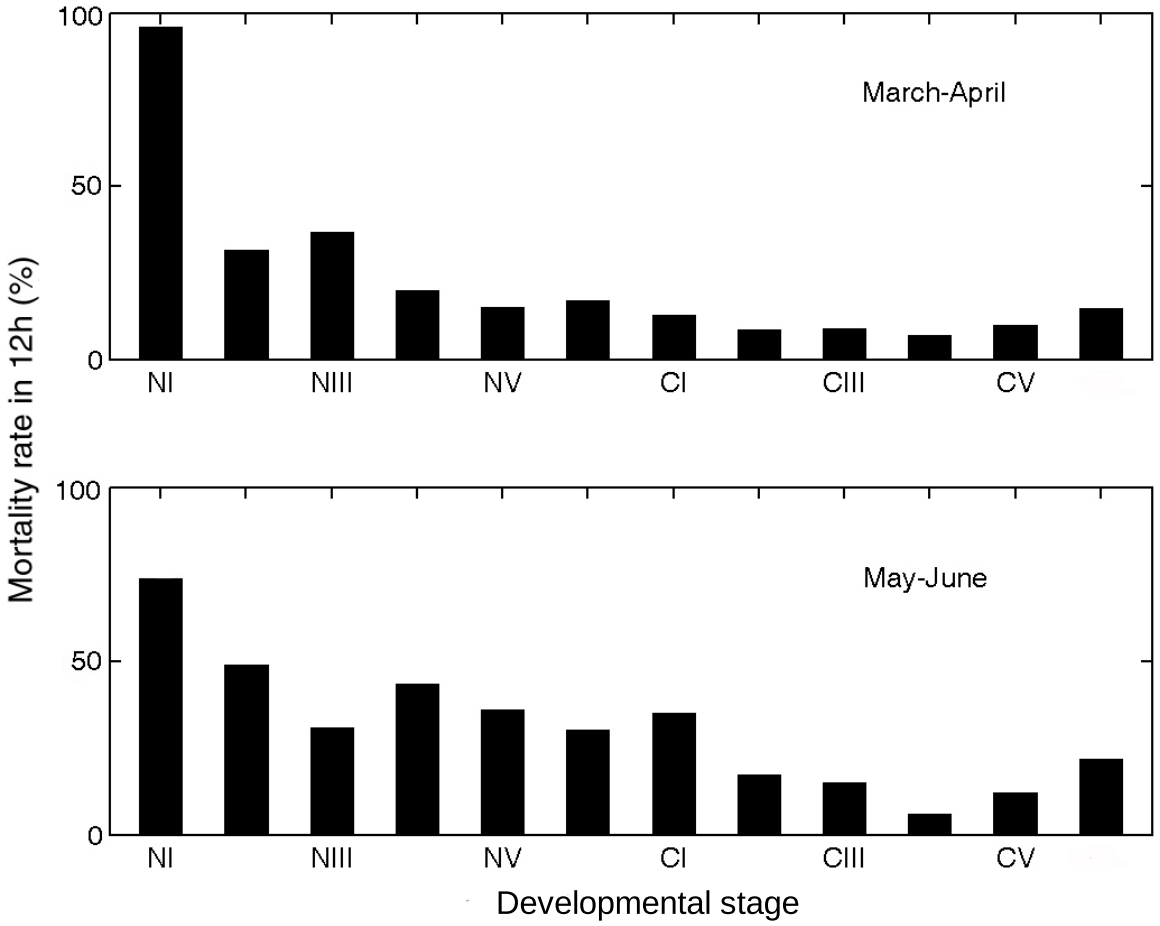

Figure 4.7: Estimated stage-specific mortality rates (% in 12h) of *Cl. furcatus* from the quadratic method.

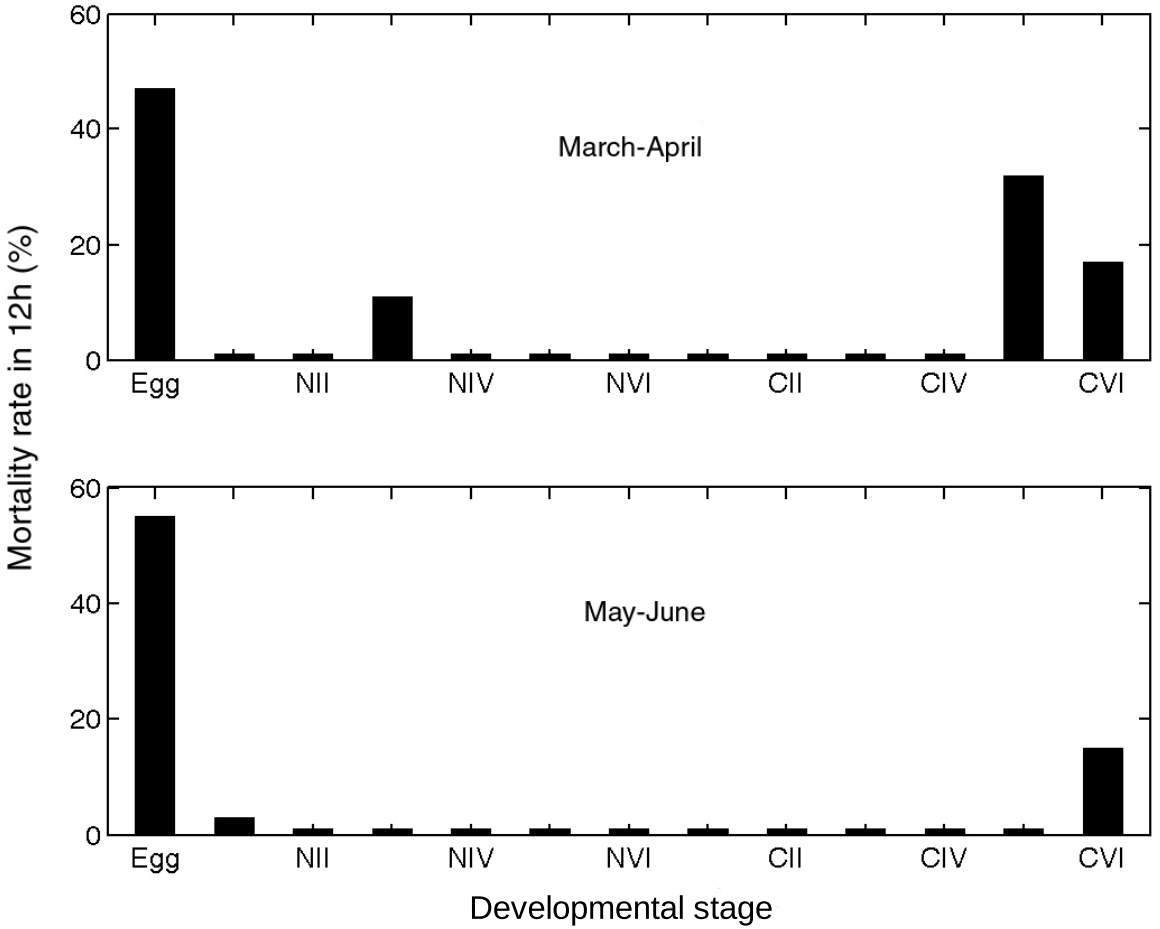

Figure 4.8: Estimated stage-specific mortality rates (% in 12h) of *Cl. furcatus* from the inverse matrix method using the automated model–independent parameter estimation.

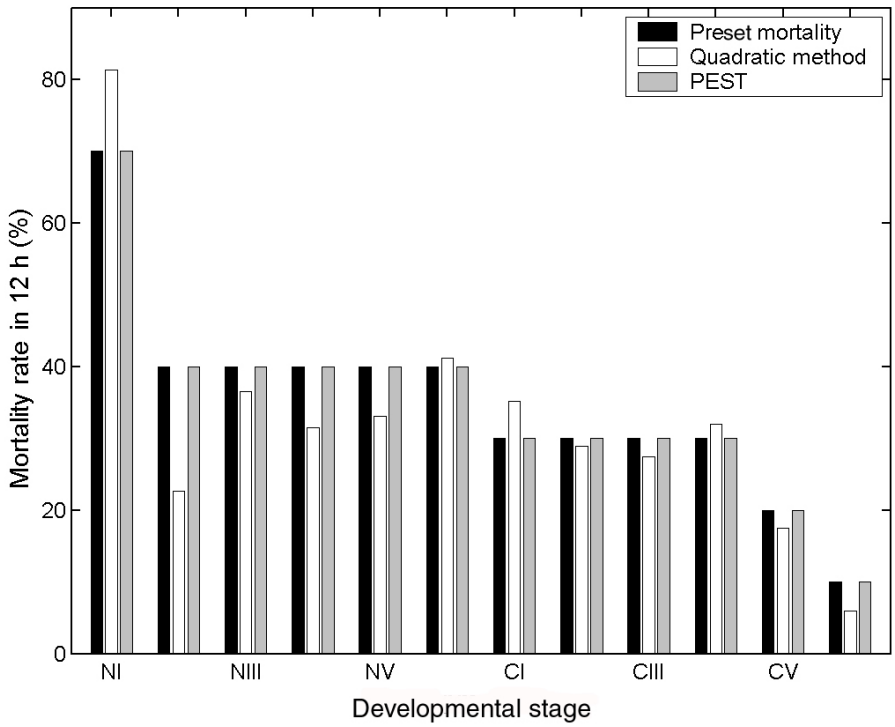

Figure 4.9: Mortality estimated by the quadratic method and the inverse matrix method using PEST for a simulated population with known preset mortality rates

the simulated results could not describe the subtle changes in field data. When the population was simulated with mortality rates estimated from the quadratic method, the population abundance decreased as projected over time, particularly in later stages (NVI–CVI; Figure 4.11 and 4.12). This indicated an overestimation of mortality rates for both March–April and May–June. Simulations with mortality rates estimated from the inverse matrix method using PEST produced total abundance estimates that appeared to be more consistent with field data (Figure 4.10). During March–April, the population simulated with mortality rates from inverse matrix method showed a similar pattern with field data for most development stages (Figure 4.11). From May–June, the population appeared to be relative stable when simulated with mortality rates from the inverse matrix method using PEST, but appeared to overestimate the abundance of naupliar stages and underestimate the abundance of copepodid stages (Figure 4.12).

4.3.5 Predation Effects on Mortality

Chaetognaths were present at high to moderate densities (0–1109.5 n·m^3 with an average 207.5 n·m^3) throughout both study periods: March–April and May–June. The log total abundances of naupliar stages and log total abundances of copepodite stages were both negatively correlated with the abundance of *Sagitta* spp. (Table 4.5; Figure 4.13). The abundances of NI through CV were negatively correlated with chaetognath abundance (Table 4.5). Chaetognath abundance had an influence on all developmental stages except CVI. The chaetognath abundance was 139.97 n·m^3 in March–April and 292.81 n·m^3 in May–June. The mean abundance of all nauplii stages for *Cl. furcatus* were 160.39 and 33.64 n·m^3 in March–April and May–June, the estimated mortality rate caused by chaetognath predation was about 1.34 day^{-1} in March–April and 2.81 May–June (assuming a linear relationship between chaetognath predation and prey abundance with a feeding rate at 0.02 day^{-1} for prey size less than 350μm, Saito and Kiørboe 2001). The mean abundance of copepodite stages were 438.17 and 286.22 n·m^3

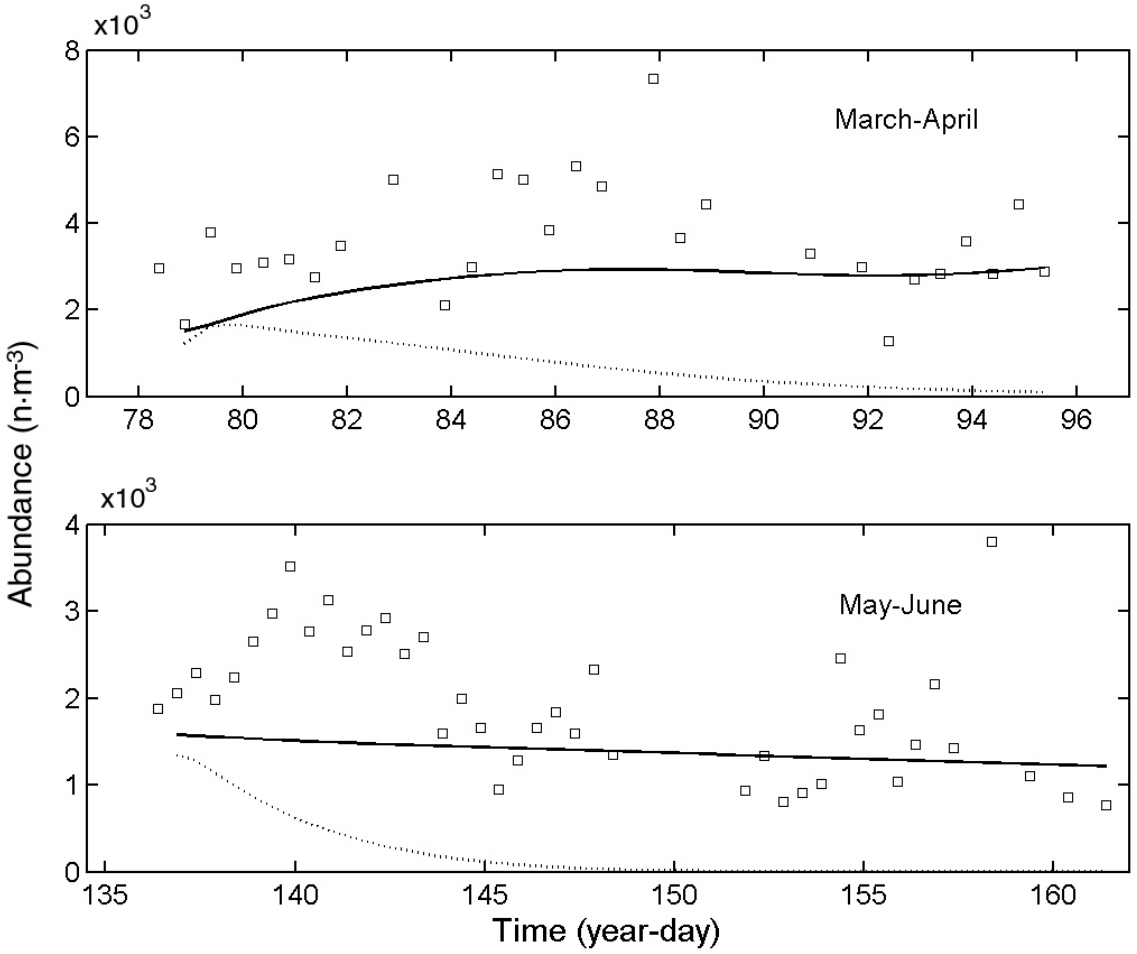

Figure 4.10: Comparison of total abundances between simulated populations and field data. The dotted line represents population simulated with mortality rates estimated from the quadratic method; solid line represent population simulated with mortality rates from PEST; and rectangles represents field data.

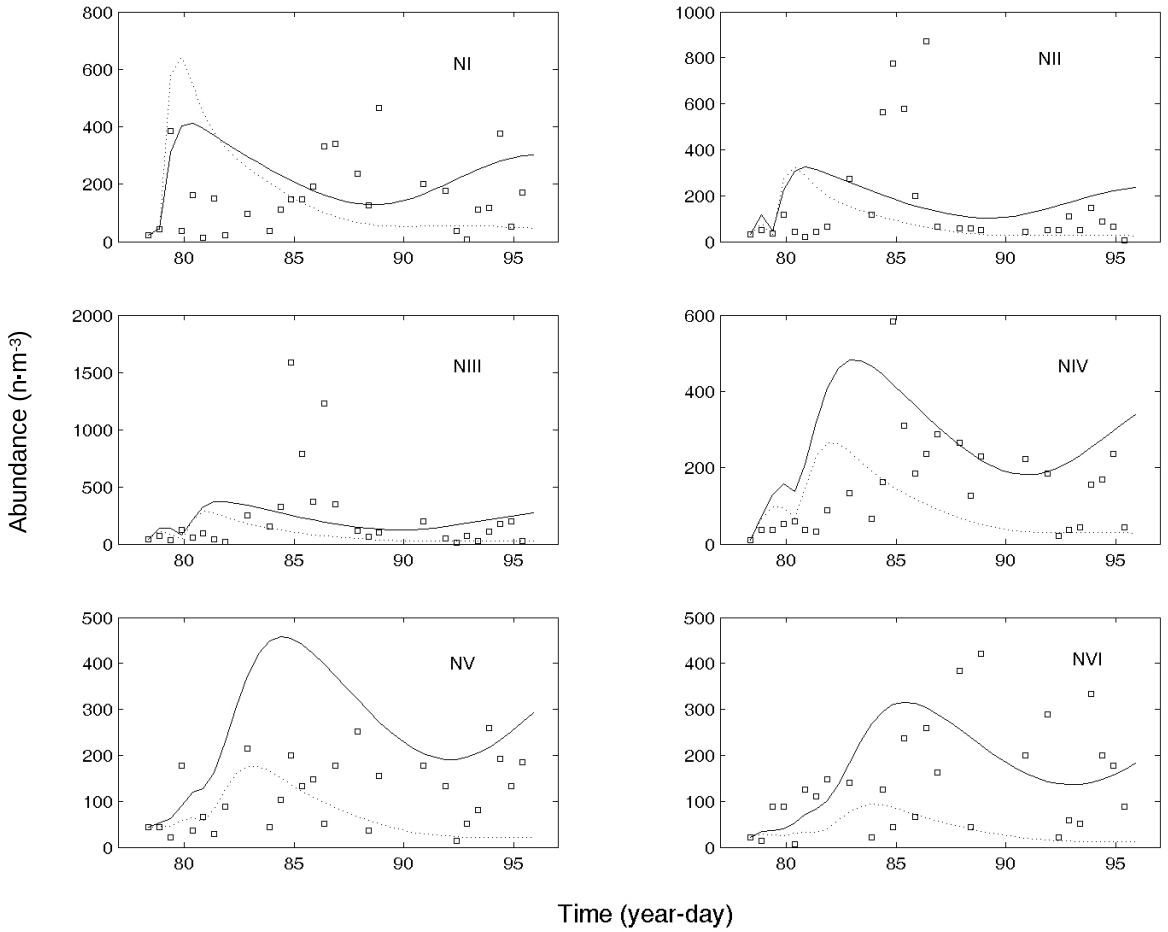

Figure 4.11: Comparisons of stage abundances between simulated population and field data in March–April. The dotted line represents a population simulated with mortality rates estimated from the quadratic method; solid line represents a population simulated with mortality rates from PEST; and rectangles represent field data. Figure continues on next page.

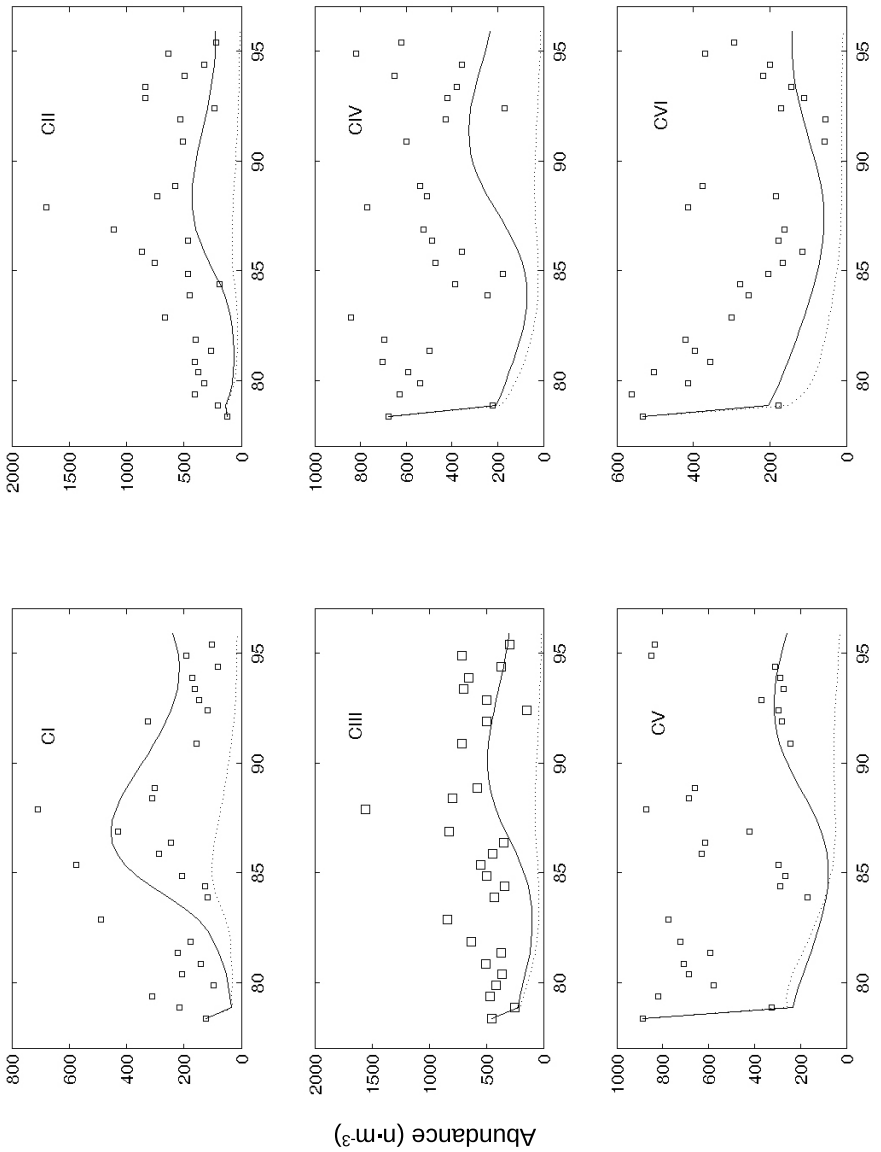

Figure 4.11 Continued.

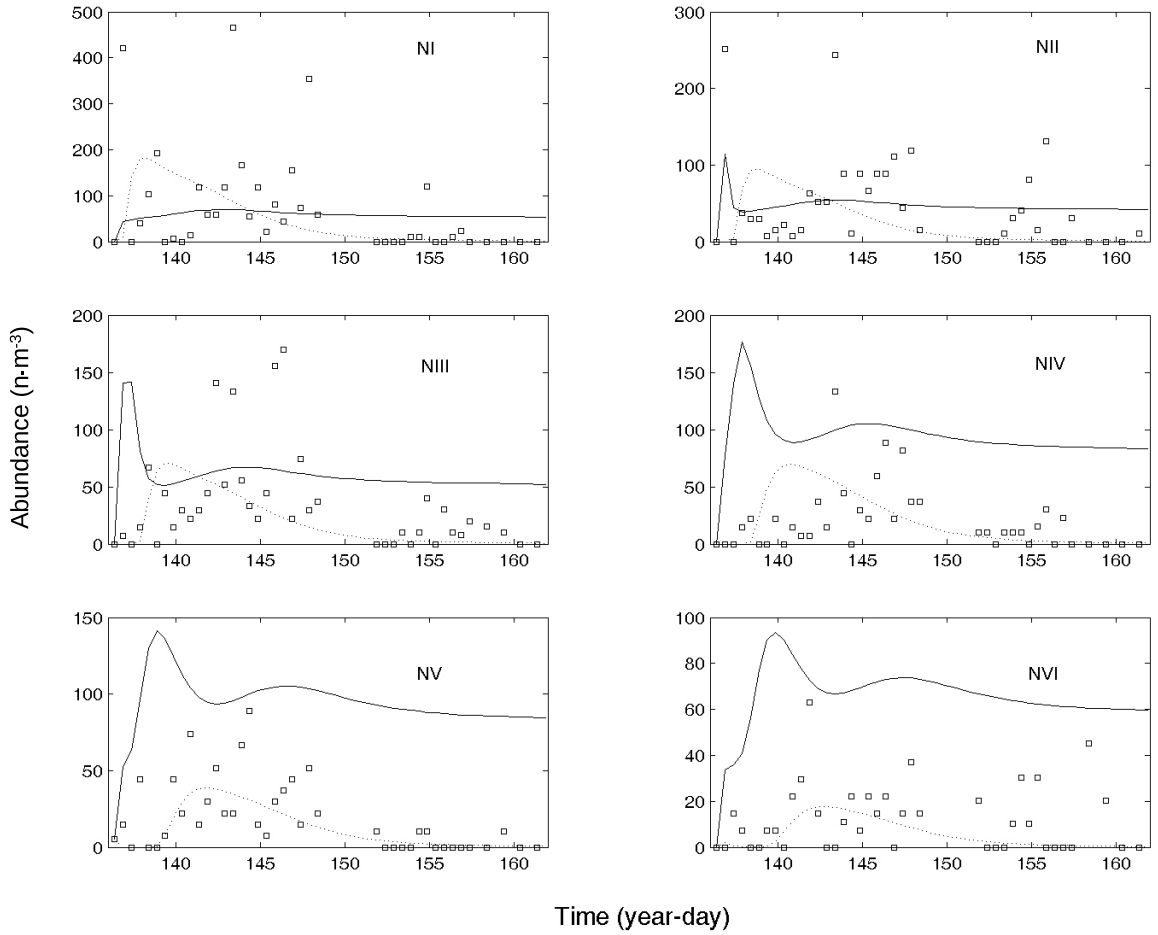

Figure 4.12: Comparisons of stage abundances between a simulated population and field data in May–June. Dotted line represents a population simulated with mortality rates estimated from the quadratic method; solid line represents a population simulated with mortality rates from PEST; and rectangles represent field data. Figure continues on next page.

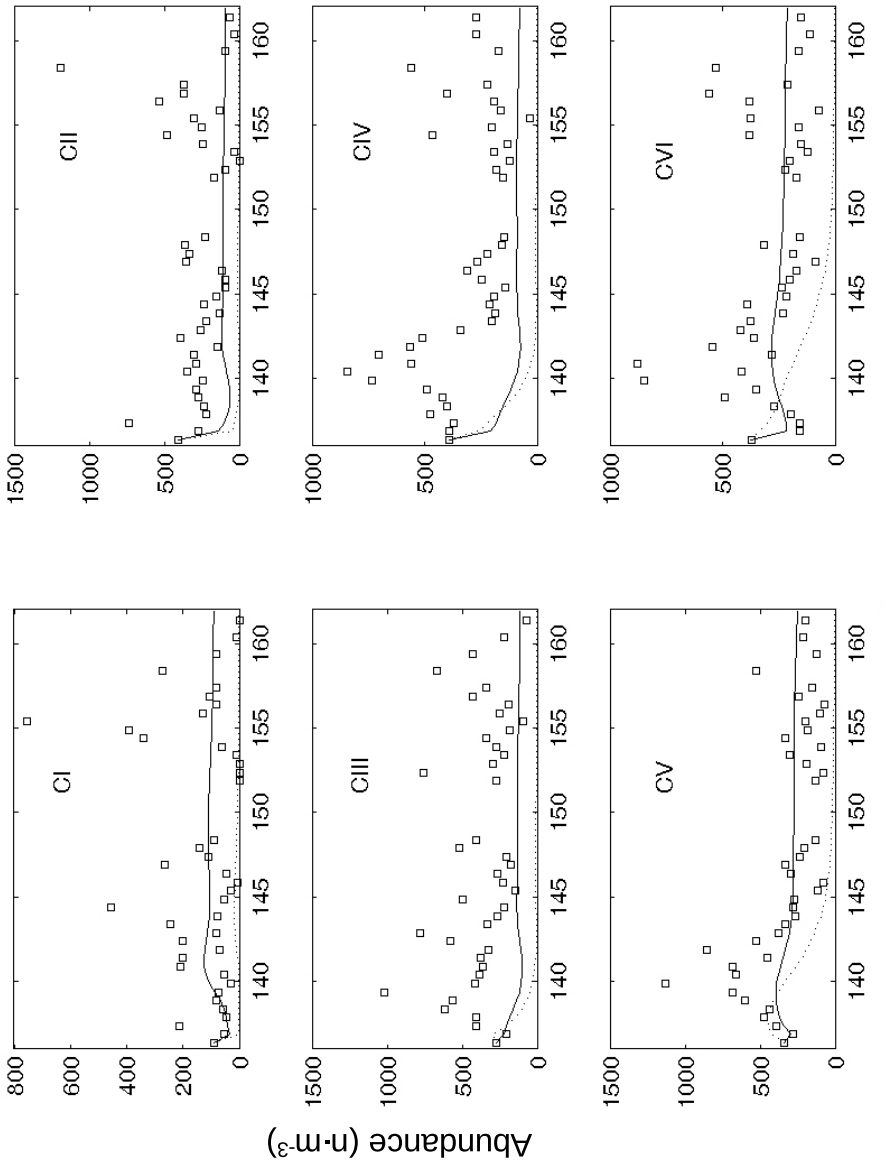

Figure 4.12 Continued.

in March–April and May–June, the estiamted mortality rate caused by chaetognath predation was 1.34 day^{-1} in March–April and 2.81 May–June (feeding rate was 0.02 day^{-1} for prey size ranged from 500–750μm at concentration of ~300–400, Saito and Kiørboe 2001). Chaetognath predation would only explained 7%–11% of the mortality rates in *Cl. furcatus*. Potential predation from larger copepods, such as *Eucalanus attenuatus* and *Euchaeta marina*, and cannibalism from adult *Cl. furcatus* did not show a significant affects on egg or nauplii abundance (Table 4.6).

4.4 Discussion

4.4.1 Sampling Variability

The fundamental problem of estimating mortality lies in sampling variability. Field data reflect not only statistical sampling errors but also variability imposed by other factors, such as sampling techniques (Miller and Tande 1993; Miller and Judkins 1981), the influence of a dynamic physical environment (Herman et al. 1991; Aksnes and Magnesen 1983) and complicated biological processes such as vertical migrations and predation (Hall et al. 1976). The present study was conducted from a fixed point within a highly dynamic environment, which frequently was influenced by the Mississippi River plume. Thus, sampling variability is a great concern in these mortality estimates.

Biased samples caused by differential gear selectivity have long been a concern in estimating mortality, because older stages are more mobile and more sensorially developed than younger stages (Aksnes et al. 1997; Wood and Nisbet 1991). If the mesh size is matched to the target stage size (e.g., egg or nauplii), net clogging will be more of a problem for both smaller and larger stages (Miller and Tande 1993) or reducing net efficiency thereby leading to avoidance by larger motile stages. However, in this study there was no indication that net samples underestimated the early development stages compared to Niskin water bottle samples.

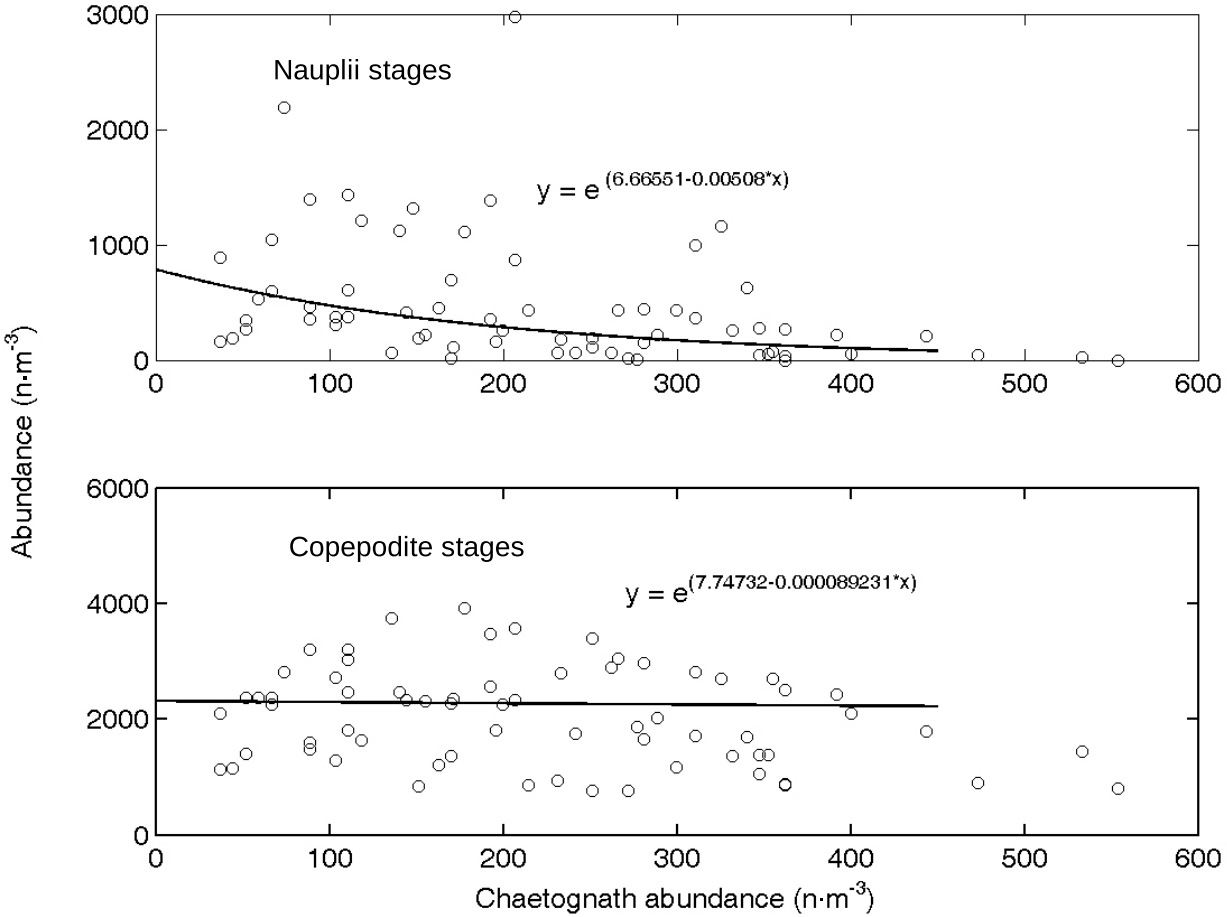

Figure 4.13: Scatter plot for abundance of *Sagitta* sp. versus total abundance of nauplii and copepodite stages during the entire study period. Line indicates the best fit regression line.

Table 4.5: Parameter information for the regression analysis with chaetognath abundance as regressor and log stage abundance as the dependent variable: $\log y = a + bx$. The normality assumption for residuals was examined by Kolmogorov-Smirnov (K–S) tests. Due to the violation of normality assumption, the Spearman correlation coefficient was calculated for the abundance of nauplii I versus the chaetognath abundance.

Stage	F	p	R^2	Intercept			Coefficient			p_{K-S}
				Par.	t	p	Par.(10^{-2})	t	p	
NI–NVI	24.98	< 0.01	0.28	6.67	24.61	< 0.01	-0.51	-5.00	< 0.01	> 0.15
CI–CVI	6.02	0.02	0.08	7.74	77.63	< 0.01	-0.01	-2.45	0.02	> 0.15
NI							-37.95		< 0.01	
NII	3.37	0.05	0.06	4.53	14.95	< 0.01	-0.25	-1.84	0.05	> 0.15
NIII	6.35	0.01	0.11	4.73	15.29	< 0.01	-0.33	-2.52	0.01	> 0.15
NIV	9.97	< 0.01	0.16	4.52	18.15	< 0.01	-0.32	-3.16	< 0.01	0.09
NV	6.74	0.01	0.11	4.46	16.03	< 0.01	-0.32	-2.60	0.01	> 0.15
NVI	6.32	0.02	0.11	4.47	13.81	< 0.01	-0.37	-2.51	0.02	> 0.15
CI	6.71	0.01	0.10	5.40	22.85	< 0.01	-0.26	-2.59	0.01	> 0.15
CII	10.70	< 0.01	0.14	6.14	37.56	< 0.01	-0.20	-3.27	< 0.01	0.09
CIII	0.39	0.53	0.01	6.01	48.98	< 0.01	-0.02	-0.62	0.53	> 0.15
CIV	7.08	0.01	0.10	6.12	46.63	< 0.01	-0.13	-2.66	0.01	0.09
CV	8.71	< 0.01	0.12	6.17	43.32	< 0.01	-0.15	-2.95	< 0.01	> 0.15
CVI	2.95	0.09	0.04	5.29	39.56	< 0.01	0.01	1.72	0.09	> 0.15

Table 4.6: Statistical results from the regression analysis with with larger copepods abundance (*Clausocalanus furcatus, Eucalanus attenuatus* and *Euchaeta marina*) as regressor and egg (or nauplii) abundance as the dependent variable: $y = a + bx$. Due to the violation of normality assumption, the Spearman correlation coefficients were computed for the abundance of nauplii abundance and the abundances of the adult *Cl. furcatus, E. attenuatus* and *E. marina*.

	R^2	F	p	Intercept			Coefficient			p_{K--S}
				Par.	t	p	Par.(10^{-2})	t	p	
Egg *vs Cl. furcatus*	<0.01	0.10	0.75	4.38	9.60	<0.01	-0.01	-0.31	0.75	>0.15
Nauplii *vs Cl. furcatus*							0.02	0.99		
Egg *vs E. attenuatus*	0.02	0.85	0.36	4.17	17.18	<0.01	-0.54	-0.92	0.36	> 0.15
Nauplii *vs E. attenuatus*							15.01		0.21	
Egg *vs E. marina*	0.05	2.34	0.05	3.85	11.19	<0.01	0.13	1.53	0.14	> 0.15
Nauplii *vs E. marina*							40.00		<0.01	

In this study, the net was only deployed down to 15m and this relative short sampling depth (duration) was unlikely to reduce net efficiency significantly. The higher abundance estimates of copepodites from net samples relative to Niskin water bottle samples is therefore likely due to avoidance of the bottles by the large more motile copepodites.

Interactions between water mass transport by physical processes and vertical migration or swimming ability may also cause bias in the sampled stage composition (Aksnes et al. 1997). Different development stages may utilize different vertical strata (Huang et al. 1993) and experience different physical conditions. Naupliar stages were normally confined to the near surface and likely were subjected to greater dispersion than later stages (Aksnes et al. 1997; Herman et al. 1991; Aksnes and Magnesen 1983), consequently the depth–integrated net samples may be skewed towards later stages. The present study indicated that most stages of *Cl. furcatus* were present in low abundances when the salinity was lower than 30 psu and this is consistent with its outer–shelf distribution (Minello 1980; Frost and Fleminger 1968). The Mississippi River plume frequently influences the study area advecting low salinity plume water at the surface (Wiseman et al. 1976). If younger stages primarily stay in the upper water column, they may experience higher dispersion rates than later copepodid stages, which are more motile and capable of vertical migrating. Therefore, the depth–integrated samples may underestimate nauplii abundance.

4.4.2 Suitability of Different Methods

Table 4.7 summarized the difference among four methods. A life table is a detailed description of the mortality of a population giving the probability of dying and various other statistics at each stage (Pressat 1985). Horizontal life tables might be appropriate for a population with discrete cohorts when the sample interval is shorter than the shortest stage–specific development time and samples satisfy complete temporal coverage (Aksnes et al. 1997; Manly 1990).

In present study, samples were taken every 12h for 2–3 weeks, which is approximately one generation time for *Cl. furcatus*. In the present study, samples were taken a fixed location within an area under the influence of the Mississippi River plume, therefore, data may not adequately reflect a well–defined, closed population. Consequently, the horizontal life table method frequently yielded negative mortality estimates due to the large sampling variability. Since the negative mortality rates are not possible, the substantial negative mortality rate reflects the large sampling variability in the present study. When the constraints of nonnegative mortality rates were applied, this method overestimated mortality rates. The mortality rates produced by this method should be used cautiously with validation from other methods are recommended.

Vertical life tables assume a steady population (Aksnes and Ohman 1996) and can be applied to either snapshot data, or data averaged over time (Brinton 1976). By averaging the data over a period and taking stage duration into consideration, this method can reduce the demographic noise to some extent. In the present study, the stage–frequency data indicated that the population structure varied quickly over short time periods suggesting that the population did not reach steady state. When mortality rates were constrained to be nonnegative, the vertical life table method could not reduce the noise in the data adequately to produced mortality estimates for all development stages. This also occurred in the study of Aksnes and Ohman (1996), where negative mortality rates were produced for copepodite II.

The quadratic method has been applied to simulate population dynamics and give robust mortality estimates even in presence of moderate sampling variability (Ohman and Wood 1996; Wood 1994). My study also indicated that the quadratic method could recover the mortality rates from a population simulated with known preset mortality rates. When this method was applied to field data, it generated mortality estimates for most stages except that the egg stage

Table 4.7: Comparisons among the horizontal life table, vertical life table, quadratic and inverse matrix methods.

	Horizontal life table (HLT)	Vertical life table	Quadratic method	Inverse matrix method
Sample period	Approximately one generation	Not required	Not required	Not required
Sample interval	Less than the shortest stage duration	Not required	Same as HLT	Same as HLT
Closed population?	Yes	No	Yes	Yes
Need stage duration?	No	Yes	Yes	Yes
Need egg production rate?	No	No	Yes	Yes
Estimate the adult stage mortality?	No	No	Yes	Yes
Produced negative mortality rates	Yes	Yes	No	No
Reduce variability?	No	Average over time	Minimize quadratic term between the modeled and observed data	Minimize the difference between model and observed data
Need steady–state population?	No	Yes	No	No

was combined with naupliar I. When the population was simulated with those estimates, however, the population quickly decreased to very low abundances after a short period of time in both March–April and May–June. In the present study, samples were taken an area under the influence of the Mississippi River plume, and large sampling variability occurred. As indicated by the simulation study, the quadratic method does not guarantee the continuous existence of the population.

The inverse matrix method uses PEST to minimize the difference between observed data and simulated data by using the Gauss–Marquardt–Levenburg algorithm (Doherty 2004). The inverse matrix method can recover the preset mortality rates for the simulated population precisely. When the inverse matrix method was applied to field data, the mortality pattern was different from the quadratic and both life table methods. When the population was presented with mortality rates estimated by PEST, the simulated results were more consistent than the simulated population with values from the quadratic method. PEST appears to have more flexibility for overall control of the differences between simulated data and observed data.

The inverse matrix method and the quadratic method used different algorithms to minimize the differences between modeled data and observed data. Which method works better for data with large variability is still uncertain and more studies are necessary. Both methods have the ability to provide temporal resolution for stage–specific mortality rates, e.g., estimate mortality rates with a small number of samples. However, sampling variability is a problem for both methods with a small sample window. The quadratic program method will have difficulty finding a solution satisfying all constraints and PEST will have difficulty finding a unique solution (i.e., PEST can find several solutions depending on initial conditions). If the sampling period lasts too long, the physical and biological conditions cause changes within this period, therefore, there may be no point to obtaining one set of fixed mortality rates for such a dynamic

environment. To apply PEST properly, one has to have enough samples for a unique solution and not over extend the sampling period.

4.4.3 Mortality Rates

The key question in this study is which method yielded mortality rates that were more realistic? The horizontal life table method yielded the highest mortality rates (less than 1% of the individuals entered the adult stage in both March–April and May–June). The vertical life table only yielded mortality estimates for a few stages, and it is not comparable with other methods. The quadratic method produced the next highest mortality estimates (less than 1% survival to the adult stage in both March–April and May–June). The inverse matrix method produced the lowest mortality with 29% of the individuals entering the adult stage in March–April and 39% in May–June without considering the mortality in the adult stage. As shown by the simulation, the quadratic programming method overestimated mortality rates leading to a progressive population decline and it is reasonable to conclude that the horizontal life table also overestimate stage–specific mortality rates.

The stage–specific mortality rates estimated by the inverse matrix method are consistent with other studies. High mortality rates occurred in early stages (egg through NI) and relative low mortality rates occurred in subsequent stages. Few studies have investigated copepod stage–specific mortality rates. Kiørboe (1997) summarized studies before 1997 and Table 4.8 shows additional and more recent studies. Estimates from different studies vary up to one order of magnitude. Eggs normally have a higher mortality rate than other stages. Previously calculated instantaneous mortality rates are as high as 21 d^{-1} for eggs, 0–0.34 d^{-1} for naupliar stages, and 0–0.30 d^{-1} for copepodite stages. Compared to these reported estimates, the quadratic programming method (NII–NV ranged from 0.35–1.31 d^{-1} and CI–CVI ranged from

0.08–0.83 d^{-1}) and the horizontal life table method (NI–NVI ranged from 0.63–3.50 d^{-1} and CI–CVI ranged from 0.63–1.31 d^{-1}) appear to overestimate mortality.

Did PEST yield reasonable estimates? Ohman et al. (2004) estimated stage–specific mortality rates for *Calanus finmarchicus* using the quadratic programming method at different locations. They also found a high instantaneous mortality rate in eggs (1.70d^{-1}) and very low mortality rates for N2–CIV at a North Sea station, an ocean station and a Lurfjorden station in the Norwegian Sea. In the present study, the instantaneous egg mortality rate was 1.30d^{-1} in March–April and 1.60d^{-1} in May–June, and the instantaneous mortality rates for NI–CIV ranged from 0.02 to 0.18d^{-1}. Eiane and Ohman (2004) and Eiane et al. (2002) also reported similar mortality patterns for *C. finmarchicus*, *Oithona similis* and *Calanus* spp.

Both the inverse matrix method and the quadratic method indicated that adults had a higher mortality rate than most other copepodite stages (except CV in March for the inverse matrix method and CI in May for the quadratic method). This may reflect higher predation risks for adult females, e.g., ovigerous females are more likely to be perceived by visual predators (Bollens and Frost 1991; Winfield and Townsend 1983). *Clausocalanus furcatus* has been reported as a species that carries its eggs for a transitional or extended period. Other studies have documented higher predation risk for females with eggs than those without eggs (Svensson 1995; De Stasio Jr. 1993; Hairston et al. 1983).

Predation is often believed to be the major cause of copepod mortality (Steele and Henderson 1995; Purcell et al. 1994; Ohman 1986). Chaetognaths frequently are important predators on copepods (Kehayias 2003; Froneman et al. 1998, Ohman 1986). In the eastern Mediterranean Sea, chaetognaths predation on copepod standing stock ranged from ~0.3–7.8% (Kehayias 2003). In Lurefjorden, Norway, the chaetognath *Eukrohnia hamata* accounted for an appreciable part of the mortality of late naupliar stages (Eiane et al. 2002). In present study, the abundance of most naupliar stages and early copepodid stages were negatively correlated

Table 4.8: Reported stage–specific mortality rates for *Acartia omnori*, *Centropages abdominalis*, *Calanus finmarchicus*, *Calanus* spp., *Pseudocalanus elongatus*, *P. newmani*, *P. marinus*, *Oithona similis*, *O. amazonica*, *Paracalanus* sp., *Diaptomus negrensis*, *D. clavipes* and from the present study *Clausocalanus furcatus*.

Species	Location	Egg	NI	NII	NIII	NIV	NV	NVI	CI	CII	CIII	CIV	CV	CVI	Author
C. finmarchicus [a]	Georges Bank	0.5		0.08	0.03	0.14	0.17	0.15	0.11	0.06	0.10	0.09	0.10		Ohman et al. (2004)
	North Sea		0.34	0.26	0.02	0.01	0	0	0	0	0	0.04	0.14	0	
	Ocean Station M	1.78	0.01	0.01	0.01		0.03		0.04	0.05	0.06	0.13			
	Lurefjorden		0.33	0.36	0.16	0.07	0.03	0.01	0.02	0	0	0.01	0.17		
	Sørfjorden				0.05				0.11	0.12	0.1	0.07	0.11		
C. finmarchicus	North Sea		0.34	0.26	0.02	0	0	0	0	0	0	0.04	0.1	0	Eiane and Ohman (2004)
P. elongatus			0.11	0.09	0.03	0.02	0	0.01	0.11	0	0	0	0.01		
O. similis			0.07	0.03	0.01	0.01	0.01	0.01	0.01	0.02	0.01	0.01	0.01	0.01	
C. finmarchicus [b]	Scotia Sea										0.06				Tarling et al. (2004)
Calanus spp.	Lurefjorden	0.18	0.32	0.35	0.14	0.05	0.01	0.0	0.01	0	0	0	0.12		Eiane et al. (2002)
	Sørfjorden				0.05				0.1	0.11	0.08	0.04	0.06		
Broadcasting [c]		1.36						0.14							Hirst and Kiørboe (2002)
Egg–carrying [c]		0.17						0.17							
C. finmarchicus	Norwegian Sea	1.76													Ohman and Hirche (2001)
P. marinus [d]	Japan				5–10% eggs entering the adult stage										Liang and Uye (1997)
Paracalanus sp. [d]					5% eggs entering the adult stage										
C. abdominalis [d]					1.5% eggs entering the adult stage										
A. omnori [d]					1.5% eggs entering the adult stage										
P. newmani [e]	Dabob Bay, US	0.05			0.10				0.12	0.06	0.05	0.07	0.12	0.04	Ohman and Wood (1996)
	Same	0.07			0.12				0.17	0.08	0.03	0.03	0.07	0.04	
P. newmani [de]	Dabob Bay, US								0.19	-0.01	0.03	0.12	0.06		Aksnes and Ohman (1996)
	Same								0.15	0.06	0	0.06	0.05		
D. negrensis [f]	Venezuela		0.11		0.69		0.79		0.09		1.38	2.04	0.79	0.80	Twombly (1994)
O. amazonica					0.11				1.46		0.69	0.36	0.25	1.2	
D. clavipes	Laboratory study		1.26			0.10	0.03	0.07	0	0.04	0	0	0.03	0.23	Gehers and Roberston (1975)
Cl. furcatus	Gulf of Mexico		6.44	0.74	0.89	0.45	0.33	0.35	0.28	0.17	0.19	0.15	0.21	0.32	Quadratic March (2003)
			3.03	1.31	0.71	1.12	0.86	0.71	0.83	0.37	0.33	0.08	0.26	0.49	May
	Same	1.27	0.02	0.02	0.23	0.02	0.02	0.02	0.02	0.02	0.02	0.02	0.77	0.37	PEST March (2003)
		1.6	0.06	0.02	0.02	0.02	0.02	0.02	0.02	0.02	0.02	0.02	0.02	0.32	May

[a] The stage-combinations were: egg–N1 at Georges Bank, NI–II and NIV–VI at ocean station, average nauplii mortality at Søfjorden.

[b] Average mortality rate for copepodid.

[c] Egg mortality and the average mortality for post–hatch staged was calculated from regression model at 20°C.

[d] Negative mortality rate occurred.

[e] Average mortality for nauplii.

[f] Maximum mortality rates were presented. Nauplii were combined as NI–II, NIII–IV and NV–VI for *D. negrensis* and NI–VI for *O. amazonica*.

with chaetognath abundance, which may suggest a predator–prey relationship. However, feeding studies are necessary to quantify the impact of predation. Cannibalism and predation from other larger size copepods also likely exists, however, correlations are hard to detect due to the large sampling variability in this dynamics environment. Juvenile fish predation may also impact on mortality, and further studies are needed to quantify such impacts.

4.4.4 Summary

The fundamental problem for mortality rate estimation was sampling variability caused by both physical processes and biological processes. Different methods yielded widely varying results. The horizontal life table and vertical life table methods frequently produced unrealistic negative estimation. Results from the quadratic method and the inverse matrix method using PEST indicated that egg–NI had high mortality followed by low mortality from late nauplii through early copepodid stages and higher mortality rates for adults relative to other copepodid stages. However, the quadratic method overestimated mortality rates as indicated by simulation results.

Mortality rates are critical to the understanding of copepod population dynamics. For an ideal closed population, changes in stage composition can be explained by population parameters; however, in the field the variability due to patchiness, migration and advections frequently cause large demographic noise in stage composition data. As a result the effectiveness and accuracy of mortality estimates depend upon how well the estimating techniques can handle the demographic noise.

Changes in stage composition data could be caused by either population parameters, such as egg production rate, stage duration and mortality, or sampling variability due to avoidance, patchiness, migration and advections. The inverse matrix method using PEST appeared to have the potential to estimate mortality rates from samples with large variability; however, further

studies are necessary to correctly estimate mortality rates. Estimating mortality also depends upon the knowledge of other population parameters, such as egg production rates.

Clausocalanus furcatus experienced high morality in eggs. The instantaneous egg mortality was $1.30d^{-1}$ in March–April and $1.60d^{-1}$ in May–June. The adult stage had a higher mortality rate than other copepodite stages (copepodite I–IV), i.e., $0.37d^{-1}$ in March–April and $0.32d^{-1}$ in May–June. Copepodite V had a relative high mortality in March–April ($0.70d^{-1}$). Other nauplii stages and copepodite stages had similar mortality rates in March–April and May–June ($0.02d^{-1}$), except nauplii III, which had a relative high mortality rate in March–April ($0.23d^{-1}$).

4.5 Bibliography

Aksnes, D. L. and Magnesen, T. 1983. Distribution, development, and production of *Calanus finmarchicus* (Gunnerus) in Lindåpollene, Western Norway, 1979. *Sarsia*, 68:195–208.

Aksnes, D. L., Miller, C. B., Ohman, M. D., and Wood, S. N. 1997. Estimation techniques used in studies of copepod population dynamics — A review of underlying assumptions. *Sarsia*, 82:279–296.

Aksnes, D. L. and Ohman, M. D. 1996. A vertical life table approach to zooplankton mortality estimation. *Limnol. Oceanogr.*, 41:1461–1469.

Bollens, S. M. and Frost, B. W. 1991. Ovigerity, selective predation, and variable diel vertical migration in *Euchaeta elongata* (Copepoda, Calanoida). *Oecologia*, 87:155–161.

Bowman, T. E. 1971. The distribution of calanoid copepods off the southern United States between Cape Hatteras and southern Florida. *Smithson. Contrib. Zool.*, 96:1–58.

Brinton, E. 1976. Population biology of *Euphausia pacifica* off Southern California. *Fish. Bull.*, 74:733C–762.

Brodeur, R. D., Sugisaki, H., and Hunt Jr, G. L. 2002. Increases in jellyfish biomass in the Bering Sea: implications for the ecosystem. *Mar. Ecol. Prog. Ser.*, 233:89–103.

Carey, J. R. 1993. *Applied Demography for Biologist with Special Emphasis on Insects*. Oxford University Press, Oxford.

Carlotti, F., Gikse, J., and Werners, F. 2000. Modeling zooplankton dynamics. In Harris, R. P., Wiebe, P. H., Lenz, J., Skjoldal, H. R., and Huntley, M., editors, *ICES Zooplankton Methodology Manual*, pages 571–667. Academic Press, London.

Caswell, H. 2000. *Matrix Population Models: Construction, Analysis, and Interpretation*. Sinauer Associates Inc.

Caswell, H. and Twombly, S. 1989. Estimation of stage–specific demographic parameters for zooplankton populations: methods based on stage–classified matrix projection models. In McDonalds, L. L., Manly, B., Lockwood, J., and Logan, J., editors, *Estimation and analysis of insect populations*, volume 55 of *lecture notes in statistics*, pages 93–107. Springer–Verlag.

De Stasio Jr., B. T. 1993. Diel vertical and horizontal migration by zooplankton: Population budgets and the diurnal deficit. *Bull. Mar. Sci.*, 53:44–64.

Doherty, J. 2004. *PEST: Model independent parameter estimation user manual*. Watermark Numerical Computing, Brisbane, Australia, 5 edition.

Edmondson, W. T. 1960. Reproductive rates of rotifers in natural populations. *Memorie Ist. Ital. Idrobiol.*, 12:21–77.

Eiane, K., Aksnes, D. L., Ohman, M. D., Wood, S., and Martinussen, M. B. 2002. Stage-specific mortality of *Calanus spp.* under different predation regimes. *Limnol. Oceanogr.*, 47:636–645.

Eiane, K. and Ohman, M. D. 2004. Stage-specific mortality of *Calanus finmarchicus, Pseudocalanus elongatus* and *Oithona similis* on Fladen Ground, North Sea, during a spring bloom. *Mar. Ecol. Prog. Ser.*, 268:183–193.

Froneman, P. W., A, P. E., Perissinotto, R., and Meaton, V. 1998. Feeding and predation impact of two chaetognath species, *Eukrohnia hamata* and *Sagitta gazellae*, in the vicinity of Marion Island (Southern Ocean). *Mar. Biol.*, 131:95–101.

Frost, B. and Fleminger, A. 1968. A revision of the genus *Clausocalanus* (Copepoda: Calanoida) with remarks on distributional patterns in diagnostic characters. *Bull. Scripps Inst. Oceanogr.*, 12:1–235.

Gehers, W. C. and Roberston, A. 1975. Use of life tables in analyzing the dynamics of copepod populations. *Ecology*, 56:665–672.

Hairston, N. G. and Twombly, S. 1985. Obtaining life table data from cohort analysis: a critique of current methods. *Limnol. Oceanogr.*, 30:431–435.

Hairston, N. G., Walton, W. E., and Li, K. T. 1983. The causes and consequences of sex–specific mortality in a freshwater copepod. *Limnol. Oceanogr.*, 28:935–947.

Hall, D. J., Threlkeld, S. T., Burns, C., and Crowley, P. H. 1976. The size–efficiency hypothesis and the size structure of zooplankton communities. *Annu. Rev. Ecol. Syst.*, 7:117–208.

Herman, A. W., Sameoto, D. D., Shunnian, C., Mitchell, M. R., Petrie, B., and Cochrane, N. 1991. Sources of zooplankton on the Nova Scotia Shelf and their aggregation with deep–shelf basins. *Cont. Shelf Res.*, 11:211–238.

Hiby, A. R. and Mullen, A. J. 1980. Simultaneous determination of fluctuating age structure and mortality from field data. *Theor. Popul. Biol.*, 18:192–203.

Hirst, A. G. and Kiørboe, T. 2002. Mortality in marine planktonic copepods: Global rates and patterns. *Mar. Ecol. Prog. Ser.*, 230:195–209.

Huang, C., Uye, S., and Onbe, T. 1993. Ontogenetic diel vertical migration of the planktonic copepod *Calanus sinicus* in the Inland Sea of Japan. *Mar. biol.*, 117:289–299.

Huntley, M. E. and Niiler, P. P. 1995. Physical control of population dynamics in the Southern Ocean. *ICES J. Mar. Sci.*, 52:457–468.

Ianora, A., Mazzocchi, M. G., and Grottoli, R. 1990. Seasonal fluctations in fecundity and hatching success in the planktonic copepod *Centropages typicus*. *J. Plankton Res.*, 14:1483–1494.

Ianora, A. and Poulet, S. A. 1993. Egg viability in the copepod *Temora stylifera*. *Limnol. Oceanogr*, 38:1615–1626.

Kehayias, G. 2003. Quantitative aspects of feeding of chaetognaths in the eastern Mediterranean pelagic waters. *J. Mar. Biol. Ass. U.K.*, 83:559–569.

Kiørboe, T. 1997. Population regulation and role of mesozooplankton in shaping marine pelagic food webs. *Hydrobiologia*, 363:13–27.

Kiørboe, T. and Nielsen, T. G. 1994. Regulation of zooplankton biomass and production in a temperate, coastal ecosystem. 1. Copepods. *Limnol. Oceanogr.*, 39:393–507.

Kleppel, G. S., Burkart, C. A., and Houchin, L. 1998. Nutrition and the regulation of egg production in the calanoid copepod *Acartia tonsa*. *Limnol. Oceanogr.*, 43:1000–1007.

Levin, S. A., Caswell, H., DePatra, K. D., and Creed, E. L. 1987. Demographic consequences of larval development mode: planktontrophy vs. lecithotrophy in *Streblospio benedicti*. *Ecology*, 68:1877–1886.

Liang, D. and Uye, S. 1997. Population dynamics and production of the planktonic copepods in a eutrophic inlet of the Inland Sea of Japan IV. *Pseudodiaptomus marinus*, the egg-carrying calanoid. *Mar. Biol.*, 128:415–421.

Lo, N. C. H., Smith, P. E., and Butler, J. L. 1995. Population growth of northern anchovy and Pacific sardine using stage–specific martic models. *Mar. Ecol. Prog. Ser.*, 127:15–26.

Lo, W., Shih, C., and Hwang, J. 2004. Diel vertical migration of the planktonic copepods at an upwelling station north of Taiwan, western North Pacific. *J. Plankton Res.*, 26:89–97.

Longhurst, A. R. 1985. The structure and evolution of plankton communities. *Prog. Oceanogr.*, 15:1–35.

Manly, B. F. 1990. Stage-structured populations: sampling, analysis, and simulation. In *Population and community biology series*, page 187. Chapman and Hall, London; New York.

Marum, J. P. 1974. *Spatial and temporal variations of zooplankton in relation to offshore oil drilling and estuarine–marine faunal exchange*. PhD thesis, Florida State University.

Mazzocchi, M. G. and Paffenhöfer, G. A. 1998. First observations on the biology of *Clausocalanus furcatus* (Copepoda, Calanoida). *J. Plankton Res.*, 20:331–342.

McCauley, E. and Murdoch, W. W. 1990. Predator–prey dynamics in environments rich and poor in nutrients. *Nature*, 343:455–457.

Miller, C. B. and Judkins, D. C. 1981. Design of pumping systems for sampling zooplankton, with descriptions of two high-capacity samplers for coastal studies. *Biol. Oceanogr.*, 1:29–56.

Miller, C. B. and Tande, K. S. 1993. Stage duration estimation for *Calanus* populations, a modelling study. *Mar. Ecol. Prog. Ser.*, 102:15–34.

Minello, T. J. 1980. *The neritic zooplankton of the northwestern Gulf of Mexico*. PhD thesis, Texas A&M University.

Möllmann, C. and Köster, F. W. 2002. Population dynamics of calanoid copepods and the implications of their predation by clupeid fish in the Central Baltic Sea. *J. Plankton Res.*, 24:959–977.

Mullin, M. M. 1991. Relative variability of reproduction and mortality in two pelagic copepod populations. *J. Plankton Res.*, 13:1381–1387.

Ohman, M. D. 1986. Predator–limited population growth of the copepod *Pseudocalanus* sp. *J. Plankton Res.*, 8:673–713.

Ohman, M. D., Eiane, K., Durbin, E. G., Runge, J. A., and Hirche, H. J. 2004. A comparative study of *Calanus finmarchicus* mortality patterns at five localities in the North Atlantic. *ICES J. Mar. Sci.*, 61:687–697.

Ohman, M. D. and Hirche, H. J. 2001. Density–dependent mortality in an oceanic copepod population. *Nature*, 412:638–641.

Ohman, M. D., Runge, J. A., Durbin, E. G., Field, D. B., and Niehoff, B. 2002. On birth and death in the sea. *Hydrobiologia*, 480:55–68.

Ohman, M. D. and Wood, S. N. 1996. Mortality estimation for planktonic copepods: *Pseudocalanus newmani* in a temperate fjord. *Limnol. Oceanogr.*, 41:126–135.

Ortner, P. B., Hill, L. C., and Cummings, S. R. 1989. Zooplankton community structure and copepod species composition in the northern Gulf of Mexico. *Cont. Shelf Res.*, 9:387–402.

Paffenhöfer, G. A. 1985. The abundance and distribution of zooplankton on the southeastern shelf of the United States. In Atkinson, L. P., Menzel, D. W., and Bush, K. A., editors, *Oceanography of the Southeastern U.S. Continental shelf*, pages 104–117.

Paffenhöfer, G. A. 2002. An assessment of the effects of diatoms on planktonic copepods. *Mari. Ecol. Prog. Ser.*, 227:305–310.

Peterson, W. T. and Kimmerer, W. J. 1994. Processes controlling recruitment of the marine calanoid copepod *Temora longicornis* in Long Island Sound: Egg production, egg mortality, and cohort survival rates. *Limnol. Oceanogr.*, 39:1594–1605.

Pressat, R. 1985. *The Dictionary of Demography*. Bell and Bain, Ltd., Glasgow.

Purcell, J. E., R, W. J., and Roman, M. R. 1994. Predation by gelatinous zooplankton and resource limitation as potential controls of *Acartia tonsa* copepod populations in Chesapeake Bay. *Limnol. Oceanogr.*, 39:263–278.

Rigler, F. H. and Cooley, J. M. 1974. The use of field data to derive population statistics of multivoltine copepods. *Limnol. Oceanogr.*, 19:636–655.

Saito, H. and Kiørboe, T. 2001. Feeding rates in the chaetognath *Sagitta elegans*: effects of prey size, prey swimming behavior and small scale turbulence. *J. Plankton Res.*, 23:1385–1398.

Steele, J. H. and Henderson, E. W. 1995. Predation control of plankton demography. *ICES J. Mar. Sci.*, 52:565–573.

Svensson, J. E. 1995. Predation risk increases with clutch size in a copepod. *Funct. Ecol.*, 9:774–777.

Tarling, G. A., Shreeve, R. S., Ward, P., Atkinson, A., and Hirst, G. A. 2004. Life–cycle phenotypic composition and mortality of *Calanoides acutus* (Copepoda: Calanoida) in the Scotia Sea: a modelling approach. *Mar. Ecol. Prog. Ser.*, 272:165–181.

Torres-Sorando, L. J., Zacarias, de Roa, E. Z., and Rodríguez 2003. Population dynamics of *Oithona hebes* (Copepoda: Cyclopoida) in a coastal estuarine lagoon of Venezuela: a stage-dependent matrix growth model. *Ecol. Model.*, 161:159–168.

Twombly, S. 1994. Comparative demography and population dynamics of two coexisting copepods in a Venezuelan floodplain lake. *Limnol. Oceanogr.*, 39:234–247.

Twombly, S. and Lewis Jr., W. M. 1989. Factors regulating cladoceran dynamics in a Venezuelan floodplain lake. *J. Plankton Res.*, 11:317–333.

Verheye, H. M. and Richardson, A. J. 1998. Long–term increase in crustacean zooplankton abundance in the southern Benguela upwelling region (1951–1966): bottom–up or top–down control? *ICES J. Mar. Sci.*, 55:803–807.

Winfield, I. J. and Townsend, C. R. 1983. The cost of copepod reproduction: increased susceptibility to fish predation. *Oceanologia*, 60:406–411.

Wiseman, W. J., Banes, J. M., Murray, S. P., and Tubman, M. W. 1976. Small scale temperature and salinity structure over the inner shelf west of the Mississippi River Delta. *Memoirs Royal Soci. Liege*, 6:277–285.

Wood, S. N. 1994. Obtaining birth and mortality patterns from structured population tragjectories. *Ecol. Monogr.*, 64:23–44.

Wood, S. N. and Nisbet, R. M. 1991. Estimation of mortality rates in stage-structured populations. In *Lecture Notes in biomathematics*, volume 90, pages 1–101. Springer–Verlag.

CHAPTER 5 FACTORS INFLUENCING MORTALITY RATE ESTIMATION

5.1 Introduction

Egg production rates, stage–specific development times and mortality rates are the essential parameters to describe a copepod population (Wood and Nisbet 1991). Studies have shown that these population parameters are interrelated with each other (Ohman et al. 1996; Ohman and Wood 1995; Roff 1992). For example, changes in mortality rates can generate substantial temporal variation in measured fecundity (Ohman et al. 1996) and fast growth rates may lead to higher survival rates for the vulnerable early life stages (Roff 1992).

In a closed population, changes in stage abundance can be directly attributable to population parameters. Conversely field samples collected at a fixed location frequently failed to reflect the stage composition of underlying population due to patchiness, immigration, emigration and other dynamic processes (Huntley and Niiler 1995). Consequently sampling variability and errors can lead to unrealistic estimation of population parameters, such as negative mortality rate (Aksnes and Ohman 1996), greater than 100% survival rates (Twombly 1994), or higher abundance of latter life stages than earlier stages in a growth curve (Liang and Uye 1997). To properly estimate population parameters, particularly stage–specific mortality rates, estimation techniques must have the ability to extract useful information in spite of the variability induced by a less than optimal sampling designs or project logistics. Besides sampling variability, variations in population parameters, such as the egg production rate and stage duration, should also be considered within the context of population dynamics.

Studies have observed large variability in copepod egg production rates caused by different abiotic and biotic factors (Plourde and Runge 1993; Mullin 1993; Paul et al. 1990; Peterson 1988). Abiotic factors include temperature (Hirst and Kiørboe 2002; Hirche et al. 1997; Huntley and Lopez 1992), salinity (Hall and Burns 2001; Miliou and Moraitou-Apostologpoulou

1991) and water quality. Biotic factors include food availability (Peterson and Kimmerer 1994; Ianora and Poulet 1993), food quality (Paffenhöfer 2002; Miralto et al. 1999), and morphological and life–history attributes (Stearns 1992; Båmstedt 1988). Variation in the egg production rate can be as large as an order of magnitude (Plourde and Runge 1993) and such a large variation can alter population growth trends (declining *vs* growing).

Stage–specific development times may vary by a factor of two in the field due to environmental conditions (Halsband-Lenk et al. 2002; Hirche et al. 2001; Diel and Klein Breteler 1986). Temperature appears to be a controlling factor for stage duration (Bělehrdek 1935). Unfavorable temperature conditions may lead to longer stage durations (Halsband-Lenk et al. 2002; Hirche et al. 2001; Takahasshi and Ohno 1996; Landry 1983). Unfavorable food condition can also increase stage development times (Hirche et al. 2001).

Mortality rates also show large variation across different regions (Ohman et al. 2004), predator regimes (Eiane and Ohman 2004), and life traits, i.e., egg–carrying versus egg–broadcasting species (Ohman 1986). Predation is another major factor contributing to the high mortality during early life stages (Hirche et al. 2001; Ohman and Wood 1996; Peterson and Kimmerer 1994; Kiørboe and Nielsen 1994; Ohman 1986). Mortality patterns among different development stages affect the population production and reproduction (McCauley and Murdoch 1990; Aksnes et al. 1997).

Among these population parameters, the egg production rate and stage duration can be estimated either from field data or laboratory experiments. Stage–specific mortality rates are also important to know, but difficult to measure. To properly estimate mortality rates, the egg production rate and stage duration are critical information. As a result, not only the erratic fluctuations in stage composition data, but also the variations in egg production rates and stage durations can influence mortality rate estimation.

The current inverse techniques for estimating mortality rates, such as the surface smooth method (Wood 1994) and the inverse matrix method (Caswell 2000), find a set of stage–specific mortality rates that best fit the data by using different algorithms to minimize differences between modeled and observed data. Both methods require knowledge of egg production rates and the stage–specific development times in order to obtain estimation for mortality rates. Experiments and field samples indicated that the egg production rate for *Clausocalanus furcatus* ranged from 0–18 eggs female^{-1} day^{-1} and stage–specific development time also varied among individuals. Thus knowledge of the egg production rate and stage–specific development times directly influences the accuracy of mortality estimates in these two techniques.

The aim of this part of the study was to test how mortality rate estimation responds to changes in egg production rates and sampling variability. The specific objectives were to:

- Examine how mortality rate estimation responded to changes in egg production rates;
- Examine how sensitive mortality rate estimations are to the sampling variability; and
- Compare the quadratic method and the inverse matrix method with respect to prediction of the stage–specific mortality rates under varying rates of egg production and sampling variability.

5.2 Methods

The validity of any estimates of copepod stage-specific, mortality rates depends upon factors such as: (1) the adequacy of population parameter estimates other than mortality rates (e.g. egg production rates and stage durations); (2) the degree to which samples reflect the underlying population stage and abundance structure; and (3) the effectiveness of the mortality estimation techniques under conditions of unknown egg production rates, stage duration and

uncertain stage abundance estimates. In Chapter 4, I showed that the quadratic method, referred to as the surface smooth method by Wood (1994) and the inverse matrix method were the most useful techniques for estimating mortality rates.

In this study, a population of *Clausocalanus furcatus* was simulated by a matrix projection model through daily processes of development, mortality and reproduction. The model is briefly described here and fully described in Caswell (2000). The model assumed that all individuals in the same development stage experience the same mortality risk and development chance. The quadratic method and the inverse matrix method were applied on this simulated population to test how the estimated mortality rates varied in response to changes in the egg production rate and the variability in the stage composition data.

5.2.1 Model Description

The applied model is a stage structured matrix model. The model contains a vector N_t, which holds stage composition at time t, and a transitional matrix A (Equation 5.2) which holds population parameters.

$$N_{t+1} = A \times N_t \tag{5.1}$$

$$A = \begin{bmatrix} P_1 & 0 & \cdots & \cdots & F \\ G_1 & P_2 & 0 & & 0 \\ 0 & G_2 & \ddots & & \vdots \\ \vdots & & \ddots & \ddots & \vdots \\ 0 & \cdots & \cdots & G_{s-1} & P_s \end{bmatrix} \tag{5.2}$$

where, s is the number of development stages, P_s is the probability of individuals surviving and staying in the same stage, G_s is the probability of individuals surviving and entering next stage, and F is the recruitment rate from the adult stage, i.e., egg production rate.

5.2.2 Matrix Analysis

In the stage structured population model, the population growth rate is defined as the largest positive eigenvalue of transitional matrix A. The sensitivity of the eigenvalues to changes in the element a_{ij} of matrix A can be calculated from Equation 5.3.

$$\frac{\partial \lambda}{\partial a_{ij}} = \frac{\overline{v_i} \times w_j}{\langle \mathbf{w}, \mathbf{v} \rangle} \tag{5.3}$$

where, λ is the eigenvalue of matrix A, a_{ij} is the element in i^{th} row and j^{th} column in matrix A, $\mathbf{w}$ and $\mathbf{v}$ are the right and left eigenvectors, $\overline{v_i}$ is the complex conjugate of v_i, and $\langle \mathbf{w}, \mathbf{v} \rangle$ is the scalar product of right and left eigenvectors. See Caswell (2000) for details.

5.2.3 Experiment Design

Two simulation experiments were conducted to investigate how changes in egg production rates and increased noise in population samples influenced stage–specific mortality rate estimates provided by two methods, i.e., quadratic programming method (QPM) and inverse matrix method (IMM).

The population parameters chosen in this study were estimated from data derived from field sampling and incubation experiments conducted in March–April 2003. The egg production rate was calculated from the *in situ* Edmonson egg ratio method and the stage–specific development times were estimated from incubation experiments described in Chapter 3. The stage–specific mortality rates were estimated from the inverse matrix method as described in Chapter 4.

5.2.3.1 Influence of Egg Production Rates on Mortality Rate Estimation

This experiment examined how varying the egg production rate influenced mortality rate estimation using the QPM and IMM methods. Both methods were applied to the simulated

Table 5.1: Initial population parameters for the simulated *Clausocalanus furcatus* population.

Parameter	Egg	NI	NII	NIII	NIV	NV	NVI	CI	CII	CIII	CIV	CV	CVI
Egg production rate (eggs female $^{-1}$ day^{-1})													2.66
Stage duration (h)	7.99	16.97	13.67	17.25	28.07	29.05	20.78	32.51	33.23	41.74	29.34	96.00	
Mortality rates	0.47	0.01	0.01	0.11	0.01	0.01	0.01	0.01	0.01	0.01	0.01	0.32	0.17
Abundance (n m^{-3})	155.10	44.32	51.83	73.94	36.91	44.38	14.71	214.42	207.41	251.41	221.83	325.38	177.47

population. Results enabled determination of which method (QPM or IMM) was most capable of recovering known mortality rates from a simulated population when the estimated egg production rate deviated from the true egg production rate.

When mortality rates were estimated from field data, egg production rates and stage duration were necessary to properly estimate mortality rates. As discussed in Chapter 3, the egg production rate for *Clausocalanus furcatus* showed a large variation in the field, ranging from 0 to 18 eggs female^{-1} day^{-1}. In Chapter 4, I simulated a population with an egg production rate of 2.66 eggs female^{-1} day^{-1}, which was derived from the *in situ* Edmonson egg ratio method (Table 5.1). The present experiment examined the effects of varying the egg production rate on mortality rate estimation using simulated data. A simulated population in which all mortality rates are known was used as inputs for the QPM and IMM methods. The simulated population provided an ideal (closed) population where changes in abundance were directly attributable to assigned population parameters (fecundity, stage duration, mortality). Table 5.2 lists the simulations in this experiment. Estimated stage–specific mortality rates from the IMM and QPM were compared to evaluate of the two methods when inputs are known.

5.2.3.2 Influence of Sampling Variability on Mortality Rate Estimation

The effectiveness of mortality rate estimation largely depends upon how well the samples reflect the stage composition of the underlying population. In a closed population, the changes in stage composition are directly attributed to population parameters, such as fecundity, stage duration and mortality rates, whereas, analyzed field samples in Chapter 4 showed large demographic noise, which reflected to the erratic fluctuation of stage abundance due to patchiness, immigration and emigration (e.g., the abundances of early stages at time t were lower than the abundances of later stages at time $t + \Delta t$). The present experiment examines how the stage–specific mortality rate estimation are effected by demographic noise. Results should enable the determination of which method (QPM or IMM) is most capable of recovering known mortality rates from simulated populations with different levels of demographic noise.

In this experiment, a closed population was simulated by the baseline model using initial conditions listed in Table 5.1, which were estimated from samples taken in March–April, 2003. Then the abundance for each stage at each time step was generated from a normal distribution $N_{(ti)} \sim N(s_{(ti)}, \sigma^2)$, where $N_{(ti)}$ is the abundance of stage i at time t, $s_{(ti)}$ is the abundance of stage i at time t from baseline model, and σ is the standard deviation calculated from $s_{(ti)} \times CV$, and CV is the coefficient of variation. The generated abundances were constrained to be positive values. The CV indicated the demographic noise, which in the field was attributed to patchiness, immigration and emigration. In this experiment, 6 levels of demographic noise were introduced by taking different CVs (0.05, 0.10, 0.15, 0.25, 0.5, and 1). When CV was small, the stage abundances for the simulated population would generally show a small deviation from the baseline population, i.e., the changes in stage abundance could largely be explained by population parameters. By varying the level of CV for the normal distribution, different levels of demographic noise were generated (Figure 5.1). Then the QPM and IMM were applied to these simulated populations to obtain stage–specific mortality rates. The procedure

Table 5.2: The inverse matrix method (IMM) and the quadratic method (QPM), inputs and outputs for simulations in the experiments.

Experiment	Method	Input	Egg production rate (eggs female^{-1} day^{-1})	Output
I	IMM	Stage composition data from simulated population	0, 1.3, 2.6, 4, 5, 10 15, 20	Mortality rates
	QPM			
II	IMM	Stage composition data simulated with variance at 0.05, 0.10, 0.15 0.25, 0.50 and 1	1.3	Mortality rates
	QPM			

was repeated 100 times for each treatment, and then the mean stage–specific mortality rates and unbiased variance (Equation 5.4) were calculated to compare the QPM and IMM methods.

$$V = \frac{1}{n}\sum(x_{ij} - X_i)^2 \tag{5.4}$$

where x_{ij} is the estimated mortality rate for i^{th} stage in j^{th} replicate, and X_i is the known mortality rate for i^{th} stage.

5.3 Results

5.3.1 Sensitivity Analysis

The growth rate of the simulated population of *Clausocalanus furcatus* was 0.99 under the conditions listed in Table 5.1, indicating a relative stable population (Figure 5.2). The population growth rate increased to 1.10 when the egg production rate increased from 0 to 25 eggs female^{-1} day^{-1} holding all other parameters constant. When the egg production rate was less ~4 eggs female^{-1} day^{-1}, the population declined. The sensitivity of population growth rate

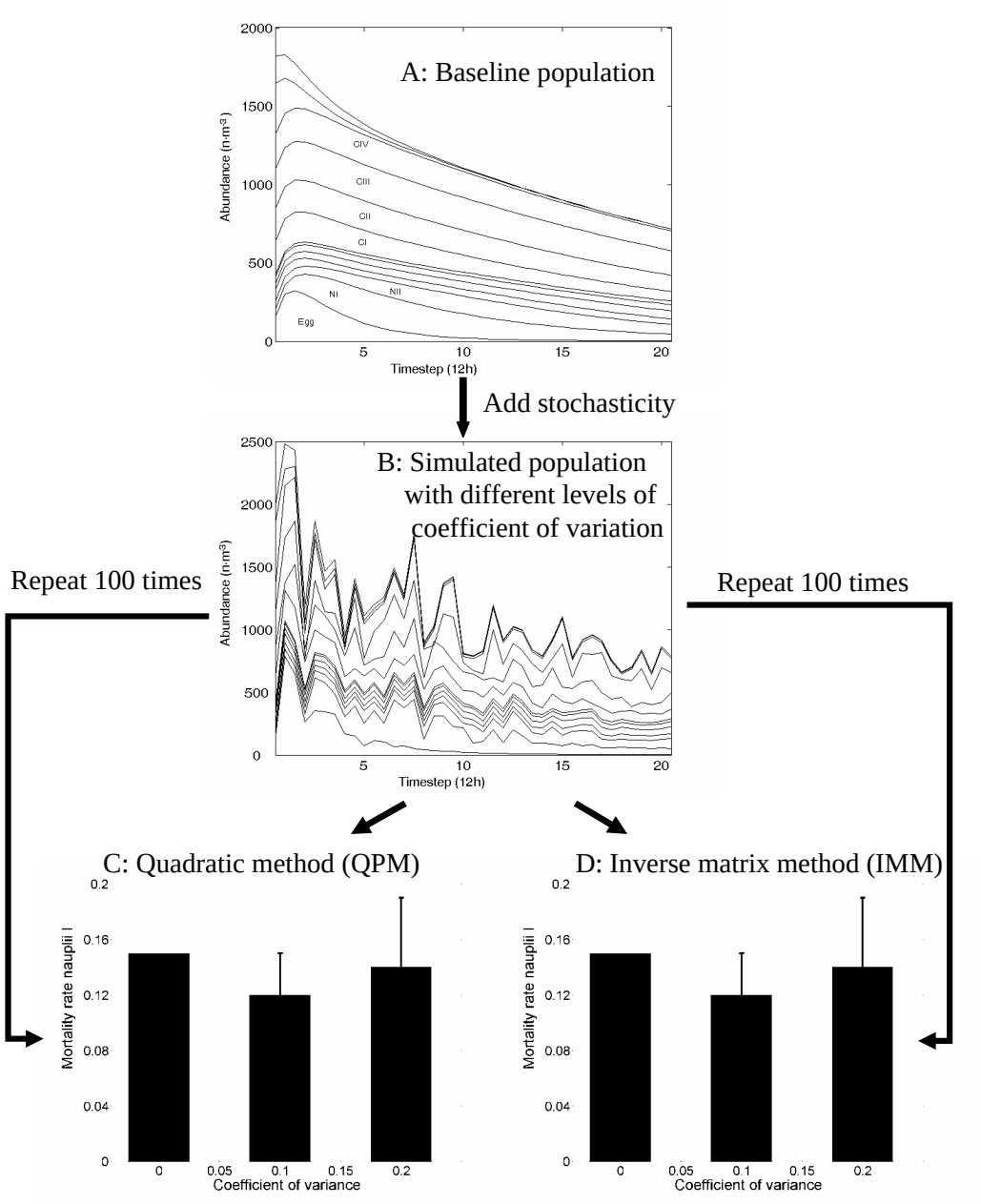

Example of mortality rates estimated from population B with QPM.

Example of mortality rates estimated from population B with IMM

Figure 5.1: Flowchart for experiment II to illustrate the procedure used to study how sampling variability influenced mortality esimtation.

(λ) to changes in the egg production rates was 0.02, i.e., when the egg production rate increased by 2 egg female^{-1} day^{-1}, λ would increase about 2%. The sensitivity of λ appeared to decrease exponentially with an increase of egg production rate (Figure 5.3).

The sensitivities of λ in relation to the stage–specific survival probability (P_i staying in the same stage i were higher in later nauplii stages (NIV–NVI) and copepodite stages (CI–CVI) than early nauplii stages (NI–NIII) and eggs (Figure 5.4). The population growth rate was most sensitive (0.18) to the survival rate in the adult stages. The sensitivities of λ to the changes in the stage–specific development rate (G_i, Figure 5.4) were consistent with the stage–specific development times listed in Table 5.1. The sensitivities of λ generally increased with the stage number except nauplii VI and copepodite IV, and the sensitivity of λ in copepodite V (0.36) was much higher than other stages.

5.3.2 Influence of Egg Production Rates on Mortality Estimation

When presented a simulated population with a known egg production rate (2.66 eggs female^{-1} day^{-1}) as observation data, the stage–specific mortality estimates for nauplii I–copepodite VI provided by the quadratic method were not altered by changes in the input egg production rate. The egg mortality rate appeared to increase in response to an increase in the egg production rate within a range of 0–5 eggs female^{-1} day^{-1} (Figure 5.5). When the egg production rate was ~5–10 eggs female^{-1} day^{-1}, the estimated egg mortality plateaued at 61% (this value depends on the constraints for the quadratic method as described in Chapter 4). If the provided egg production rate was higher than ~18 eggs female^{-1} day^{-1}, the quadratic method could not yield a mortality rate estimation.

When mortality rates were estimated for the same simulated population using the inverse matrix method, the mortality estimates for nauplii II, IV–VI and copepodite I–III provided by the inverse matrix method were not altered by changes in the input egg production rate. The

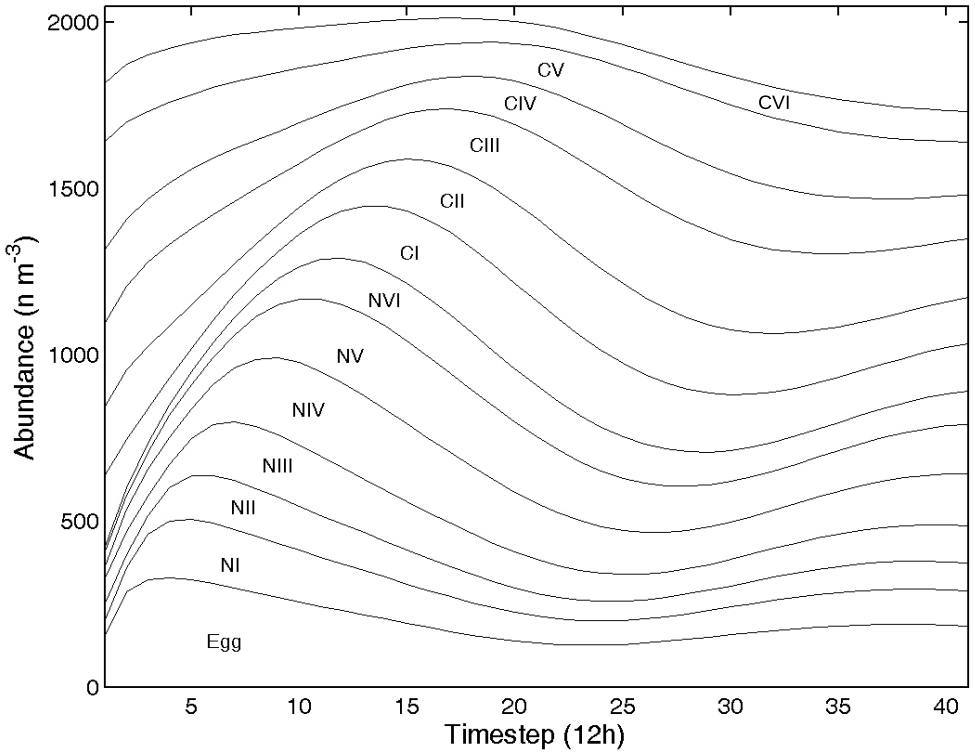

Figure 5.2: The stage (egg, nauplii I–VI and copepodite I–VI) composition of the baseline population simulated with the parameters estimated from field and laboratory data collected in March–April 2003.

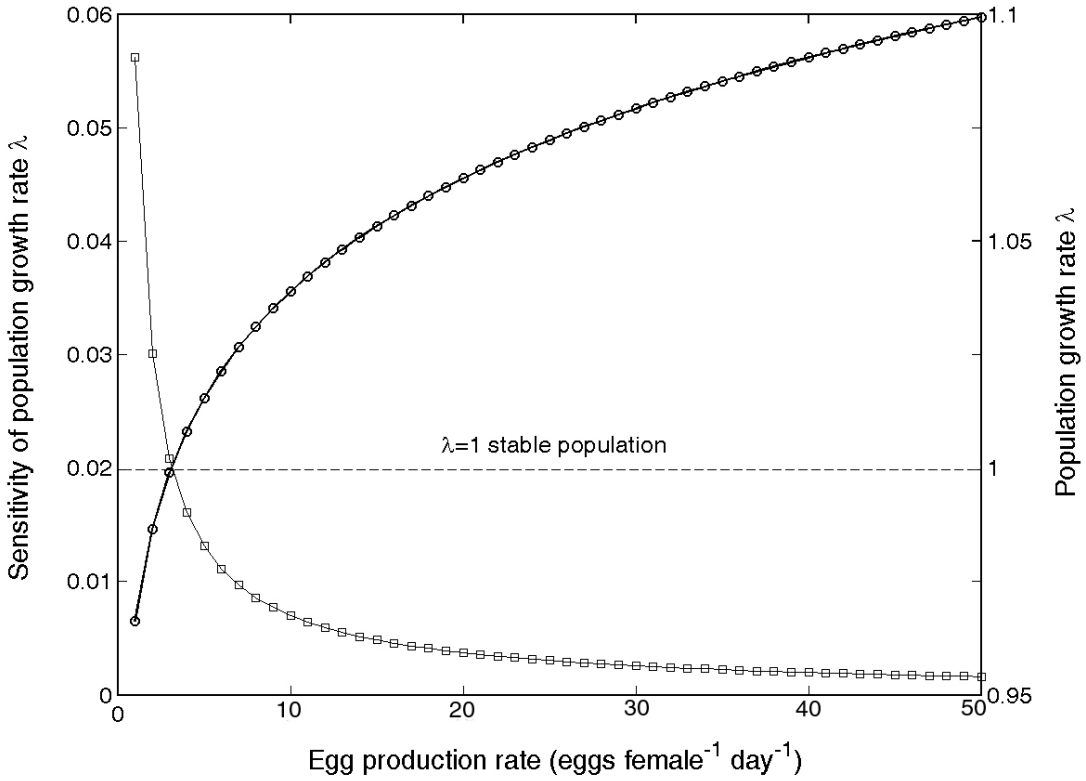

Figure 5.3: The population growth rate (λ, indicated by solid line with squares) and the sensitivity of λ (represented by solid line with circles) as a function of the egg production rate, holding all other parameters constant.

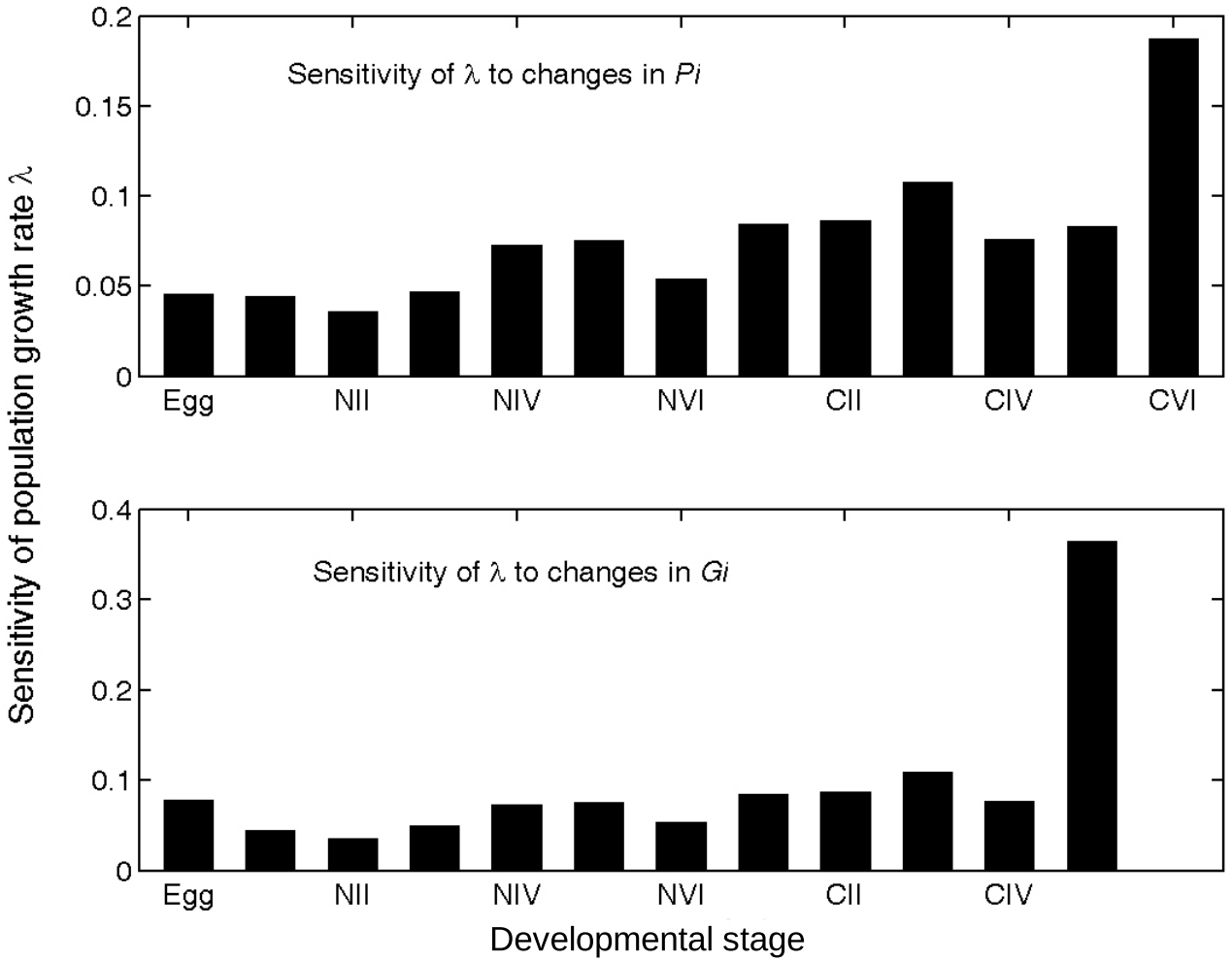

Figure 5.4: The sensitivity of population growth rate (λ) to changes in the probability of individuals surviving and staying in the same stage i (P_i, the upper panel) and the probability of individuals surviving and entering the consecutive stage (G_i, the lower panel) for *Cl. furcatus*.

egg mortality rate increased from 1% to 85% as the egg production rate increased from 1–20 eggs female^{-1} day^{-1} (Figure 5.5). At the same time, the mortality rates for the adult stage increased from 11% to 100%. The mortality rate for copepodite V first decreased from 37% to 8% as the egg production rate increased to 10 eggs female^{-1} day^{-1}, and then it increased to 41% as the egg production rate increased to 50 eggs female^{-1} day^{-1}. Mortality estimates for copepodite IV were also higher than the known value (1%) when the egg production ranged from 8–20 eggs female^{-1} day^{-1}. Mortality estimates for nauplii III were lower than the known value (11%).

5.3.3 Influence of Sampling Variability on Mortality Estimation

When the population was simulated without or with low levels of variability (e.g., CV = 0.05), the structure of the simulated population (Figure 5.6) had a slightly lower abundance than the baseline population as the population was progressively projected over time (Figure 5.2). At high levels of variability (e.g., CV = 1.00), the simulated population (Figure 5.6) had a higher abundance than the baseline population.

Both the quadratic method and the inverse matrix method recovered the underlying true mortality rates successfully (Figure 5.7), when the presented with populations that had low levels of variability (e.g., CV = 0.05). Levels of variability higher than a CV of 0.05 caused both methods to experience difficulty recovering the known mortality rates and the two methods performed quite differently. In the same simulations, the quadratic method appeared to slightly overestimate the egg mortality rate and it consistently overestimated mortality rates for early nauplii stages and copepodite stages. Estimated stage–specific mortality rates generally deviated further from the known values as CV increased from 0.10 to 1.00 (Table 5.3). The deviations occurred at all development stages, but the mortality rate pattern remained the same, i.e., high mortality rates in the egg, low mortality rates in the subsequent stages (nauplii

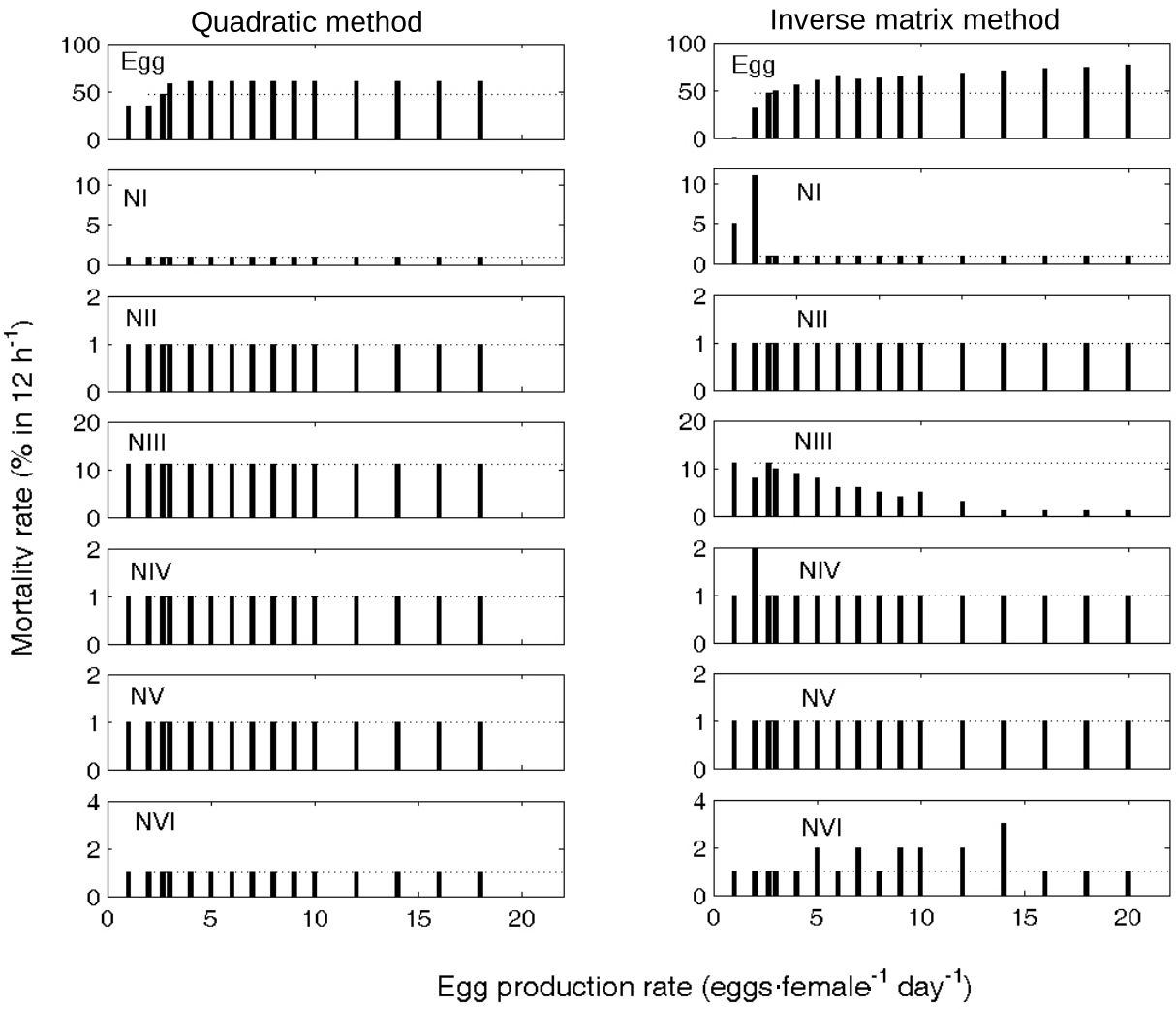

Figure 5.5: Stage–specific mortality rate estimates using a varied egg production rate, and the simulated population with parameters estimated from samples taken in March–April was presented as observation data. Dotted lines represent the preset known mortality rates. Figure continues on next page.

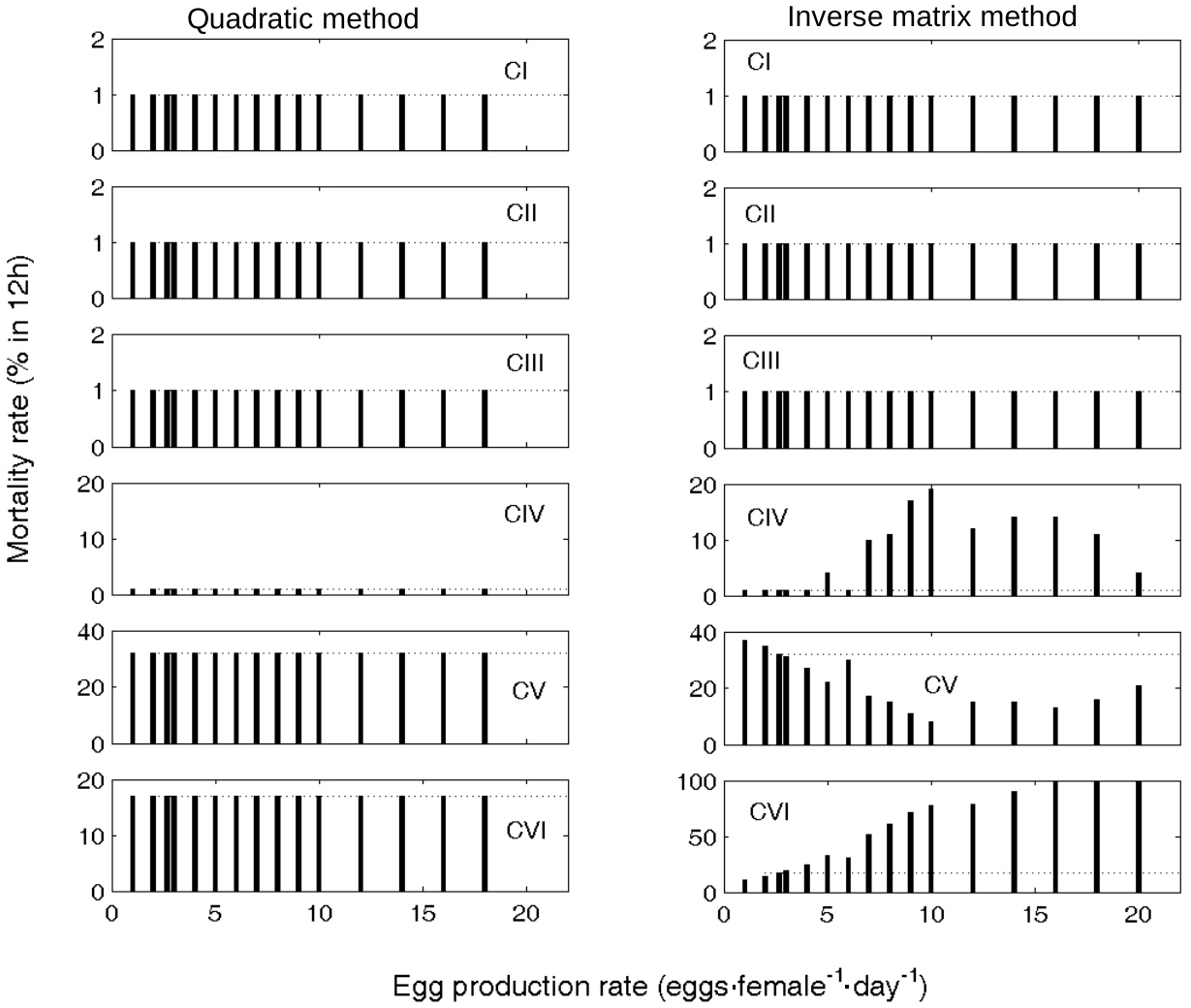

Figure 5.5 (continued)

I–copepodite VI), and high mortality rates in copepodite V and VI. The inverse matrix method provided low mortality rates for all stages at high levels of CV (mortality rates were close to 0 as the CV approached to 1.00). The estimates for late nauplii stages (NI–NVI) and early copepodite stages (CI–CIII) were close to the known preset values when the *CV* was less than 1.0. Estimates for egg and copepodite stage IV–VI deviated further from the known preset values as the CV increased (Table 5.3). The inverse matrix method produced estimates that were closed to known preset values when *CV* was less than 0.10.

5.4 Discussion

5.4.1 Sensitivities of Growth Rate to Changes in Population Parameters

Egg production is the only recruitment process for a closed copepod population, and establishing an accurate estimate of the egg production rate is a critical component of population dynamics studies. The population growth rate is very sensitive to changes in the egg production rate and a relatively small increase in the egg production rate may be sufficient to alter the population growth trend. For example, in the present study the population switched from a declining, to an increasing population, as the egg production rate increased from 2.6 to 3 eggs female^{-1} day^{-1}. Egg production rates have been studied for many species (Hirst and Kiørboe 2002; Mauchline 1998). In the field, egg production rates exhibit large spatial and temporal variation (Runge et al. 1997; Paul et al. 1990). Consequently, obtaining an accurate estimate of the egg production rate at the population level remains a problem. The egg production rate could be measured either by laboratory incubations or the Edmondson egg ratio method, and these two methods may yield different estimates. In Chapter 3, I have shown that the egg production rate for *Cl. furcatus* were quite different for incubation experiments (12.08 eggs female^{-1} day^{-1}) and field samples (2.66 eggs female^{-1} day^{-1}). If the population increases its egg production rate to 12.08 eggs female^{-1} day^{-1} without changing stage–specific

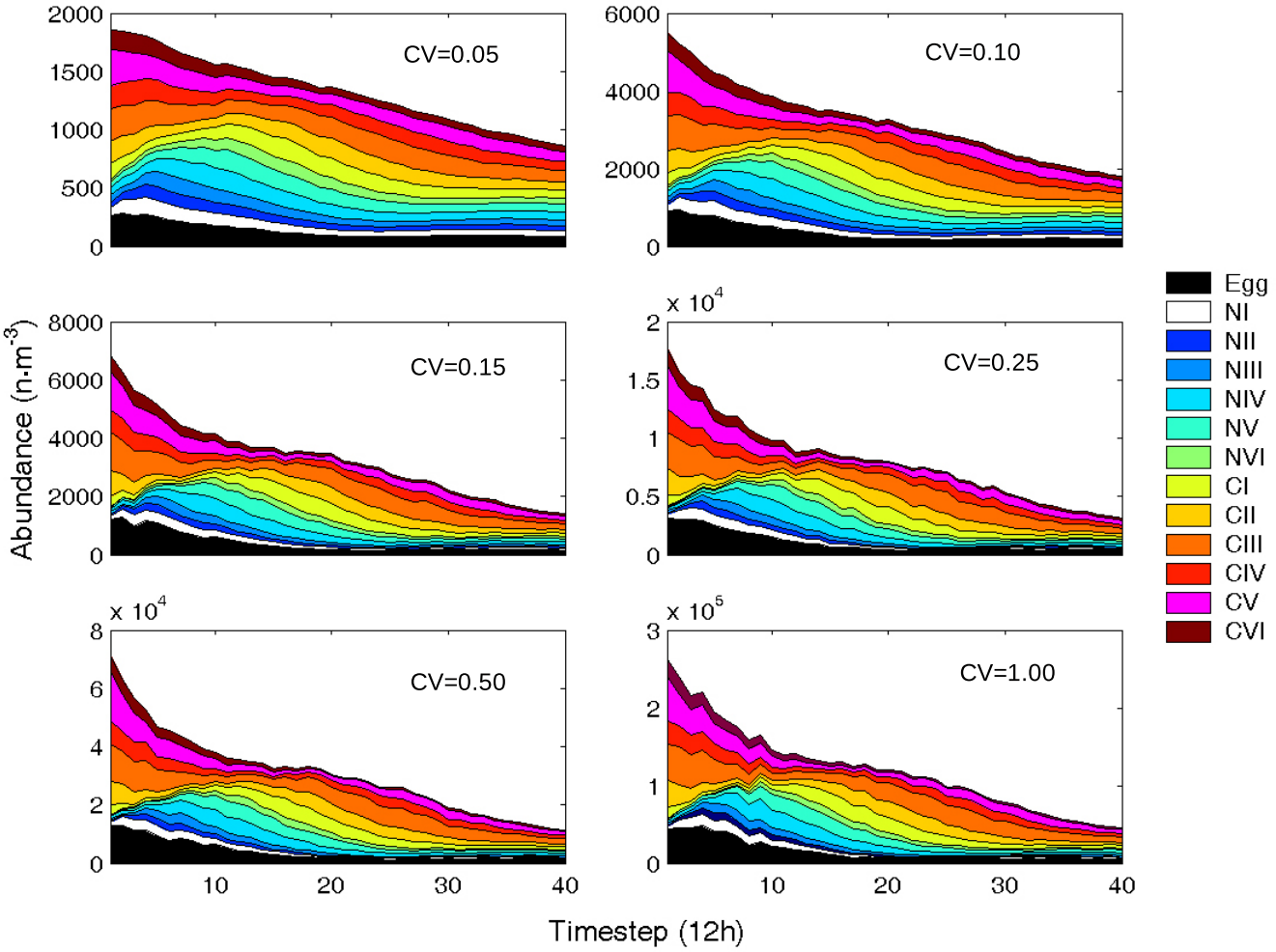

Figure 5.6: Mean stage composition of populations simulated with different levels of coefficient of variation (CV) based on the baseline population. From the bottom to top (egg, nauplii I–VI and copepodite I–VI), the area that is covered under each line indicates its abundance. There were 100 replicates in each CV level.

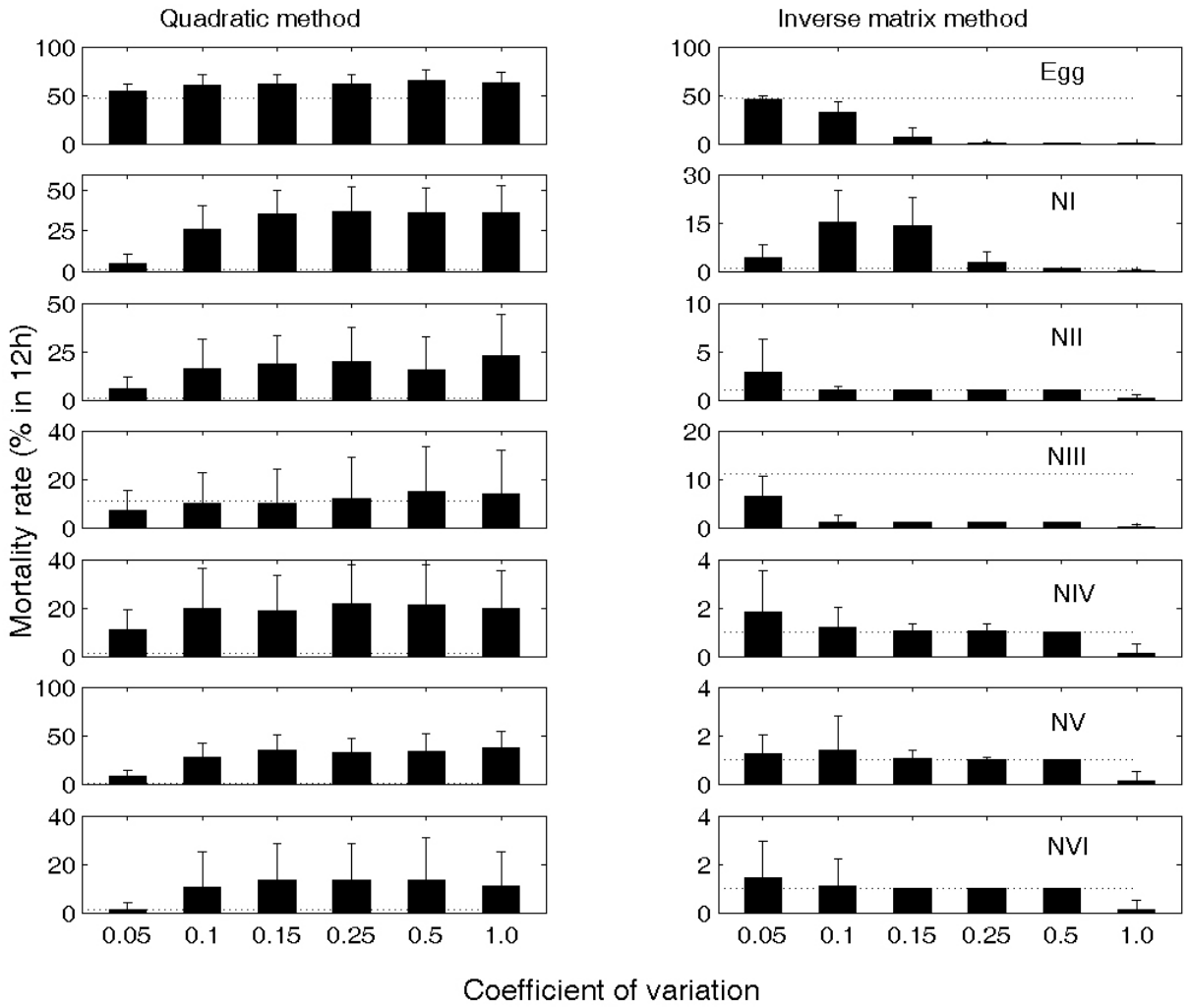

Figure 5.7: Stage–specific mortality rate estimates for the simulated population with different coefficients of variation using parameters estimated from samples taken in March–April. Error bars represent one standard error and dotted lines represent the preset known mortality rates. Figure continues on next page.

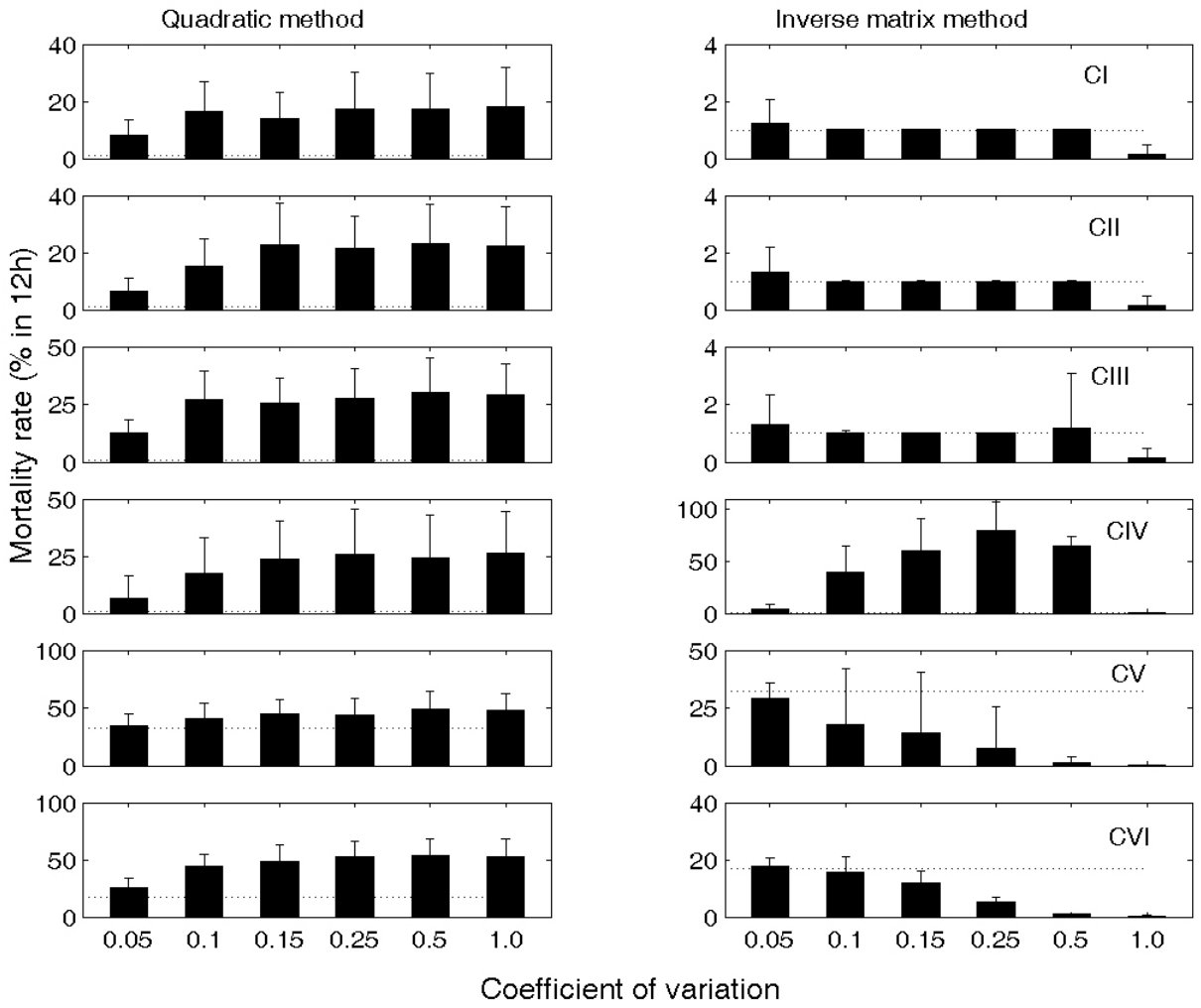

Figure 5.7 (continued)

Table 5.3: The unbiased variance of estimated stage–specific mortality rates for simulated populations with different coefficients of variation from the inverse matrix method and the quadratic method.

Variation	Method	Development stages												
		Egg	NI	NII	NIII	NIV	NV	NVI	CI	CII	CIII	CIV	CV	CVI
0.05	Inverse matrix method	<0.01	<0.01	<0.01	<0.01	<0.01	<0.01	<0.01	<0.01	<0.01	<0.01	<0.01	<0.01	<0.01
	Quadratic method	0.01	<0.01	<0.01	<0.01	0.02	<0.01	<0.01	<0.01	<0.01	0.02	0.01	0.01	0.01
0.10	Inverse matrix method	0.04	0.03	<0.01	0.01	<0.01	<0.01	<0.01	<0.01	<0.01	<0.01	0.10	0.08	<0.01
	Quadratic method	0.03	0.08	0.05	0.02	0.06	0.09	0.03	0.03	0.03	0.08	0.05	0.02	0.08
0.15	Inverse matrix method	0.17	0.02	<0.01	<0.01	<0.01	<0.01	<0.01	<0.01	<0.01	<0.01	0.44	0.09	<0.01
	Quadratic method	0.03	0.14	0.05	0.02	0.05	0.14	0.04	0.03	0.07	0.07	0.08	0.03	0.12
0.25	Inverse matrix method	0.21	<0.01	<0.01	<0.01	<0.01	<0.01	<0.01	<0.01	<0.01	<0.01	0.70	0.09	0.01
	Quadratic method	0.03	0.15	0.07	0.03	0.07	0.12	0.04	0.04	0.05	0.09	0.10	0.03	0.14
0.50	Inverse matrix method	0.21	<0.01	<0.01	<0.01	<0.01	<0.01	<0.01	<0.01	<0.01	<0.01	0.41	0.09	0.03
	Quadratic method	0.04	0.15	0.05	0.04	0.07	0.14	0.05	0.04	0.07	0.11	0.09	0.05	0.15
1.00	Inverse matrix method	0.22	<0.01	<0.01	<0.01	<0.01	<0.01	<0.01	<0.01	<0.01	<0.01	<0.01	0.10	0.03
	Quadratic method	0.04	0.15	0.09	0.03	0.06	0.16	0.03	0.05	0.06	0.10	0.10	0.05	0.15

mortality rates and development times, then the population growth rate would be increased to 1.04, which indicates a growing population. However, the population of *Cl. furcatus* was relative stable over March–April as discussed in Chapter 4 (Figure 4.10), and this suggested that incubation experiments might have overestimated the true egg production rate.

The adult stage is the only stage capable of reproducing. Consequently, a low survival rate in the adult stage will cause a low recruitment rate for the population at fixed levels of egg production. As a result, the population growth rate is sensitive to the adult survival rate and recruitment rate from the previous stage (copepodite V). Many studies have shown that copepod mortality is heavily concentrated in the egg or early nauplii stages (Ohman et al. 2004; Eiane et al. 2002; Peterson and Kimmerer 1994). Compared to the egg and early nauplii stages, the importance of the survival rate of the adult stage has not been emphasized. In the present study, the simulated baseline population had an egg mortality of 47% in 12h, which is comparable to the reported studies (Eiane and Ohman 2004; Ohman et al. 2004; Eiane et al. 2002; Ohman et al. 2002), and the adult stage had a mortality of 17% in 12h. The population growth rate is four times more sensitive to changes in the survival rate of the adult stage than to changes in the survival rate of the egg and early nauplii stages (I-III). Thus knowledge of survival rate in the adult stage is critical to understand copepod population dynamics.

5.4.2 Influence of Egg Production Rates on Estimated Mortality Rates

The accuracy of egg mortality rate estimation largely depends upon the egg production rate. Changes in the inputted egg production rates also could influence the mortality rate estimation for the adult stage, or even the copepodite stage V, depending how much the inputted egg production rate deviated from the true value, and which method was used. As a result, the high egg mortality rates could be a result of overestimating the egg production rate and should be used cautiously.

The large temporal and spatial variations in the egg production rate raised problems in addition to those associated with estimating stage–specific mortality rates. As noted, a small variation in the egg production rate could change a declining population into a growing one. The egg production rate has been measured for many species (Hirst and Kiørboe 2002; Mauchline 1998) primarily by incubation experiments. However, accurate knowledge of the egg production rate is still in a great demand in order to properly understand the population dynamics.

When the true egg production rate remains uncertain, the quadratic method should be able to recover the stage–specific mortality rates because it only changed its egg mortality rate estimates as a response to the changes in the input egg production rate. The inverse matrix method was relatively sensitive to changes in the measured egg production rate because it varied the mortality rate estimates in late copepodite stages to accommodate the changes in the egg production rate. The quadratic method could be used to approximate the maximum egg production rate. By increasing the measured egg production rate, the quadratic method first increased the egg mortality rate, then the estimated egg mortality rate remained stable. The value that started to stabilize the egg mortality rate estimation could be approximate the maximum egg production rate.

5.4.3 Influence of Sampling Variability on Estimated Mortality Rate

Sampling variability due to gear avoidance, patchiness, emigration and immigration, and dynamic physical processes is a key issue in the study of stage–specific mortality rates. Stage–specific mortality rate estimation depends on how well the stage composition data from the samples represent the underlying population. This uncertainty may mask the changes in stage composition due to reproduction, development and mortality. In the present study, this sampling variability was simulated by adding noise using different *CV* levels. The population

abundance showed progressively larger deviation from the baseline population as the *CV* increased.

The inverse matrix method performed better than the quadratic method when the population showed low variability (*CV* ranges from 0–0.10). When the population showed relatively high variability (*CV* = 0.15–0.5), both methods had difficulty obtaining estimates that were close to the true rates (original baseline rates). The inverse matrix method generally performed better than the quadratic method for most of the stages as indicated by the unbiased variance (Table 5.3). In extreme conditions where the coefficient of variation equaled one, the quadratic method produced mortality rates much higher than the true values and the inverse matrix method produced rates much lower than the true values. This information could be used as an indication of the validity of the mortality rate estimation.

To validate the mortality rate estimation, an estimate of sampling variability is critical. As discussed in Chapter 2 and Chapter 4, the zooplankton samples were taken from a fixed location in a highly dynamic environment. The changes in stage abundances (Figure 5.8) for *Cl. furcatus* were not only caused by the reproduction, development, and mortality, but likely also caused by tidal currents, wind–induced currents, mixing processes between oceanic water and the Mississippi River plume, vertical migration, gear avoidance and size selective predation. The field variability is inevitable (Figure 5.9), and the variabilities occurring in different stages were also different (Figure 5.10). The *CV* calculated from field data was lower than 1 during most of the study period for all the development stages. Copepodite stages showed smaller variation (*CV* =0.31–0.56) than nauplii stages (0.55–0.76). The *CV* in the present study was computed from 3 replicates and increasing sample size might lower *CV* considerably. Extending from the field data, a minimum of ~16 replicates was needed to reach 95% confidence interval at a *CV* level of 0.10, assuming the maximum difference between

the observed sample mean and the population mean was ~5 times.[1] In light of the variability observed in the field data, results imply that the absolute mortality rates estimated from the quadratic method and the inverse matrix method are uncertain.

The quadratic method did not change mortality estimates for nauplii I–copepodite VI, when the input egg production rate deviated from the true value. It overestimated the stage–specific mortality rates for all the stages to a similar extent when variability was high (Table 5.3). However, the mortality patterns over the stages obtained from the quadratic method appeared to remain the same as the true mortality patterns. The simulation experiments also indicated that the inverse matrix method could obtain reasonable estimates for most of stages (NII–CVI) when *CV* was lower than one. The inverse matrix method responded to changes in the egg production rate and the sample variability mostly by increasing or decreasing the mortality estimates in the egg, copepodite V and VI. A consistency in the mortality patterns estimated by the quadratic method and the inverse matrix method could be used as a validation for the stage–specific mortality rate estimation. In Chapter 4, I have discussed that the mortality rates estimated by the quadratic method and the inverse matrix method were consistent, i.e., high mortality rate in the egg, relative low mortality rate in the subsequent stages, and relative high mortality rates in copepodite V and CVI. The simulations in Chapter 4 (Figure 4.10) indicated that the population simulated with the estimated mortality rates from the inverse matrix method was consistent with observed field data.

5.5 Summary and Recommendations for Future Work

Stage–specific mortality rate estimation is complicated not only due to the sampling variability caused by patchiness, emigration, immigration, other biological processes and dynamic

[1]The minimum sample size was calculated by $n = (\frac{1.96 \cdot \bar{X} \cdot CV \cdot 100}{E})^2$, where $\bar{X}$ is the population mean abundance, *CV* is the coefficient of variation, and *E* is the maximum difference between the observed sample mean and the population mean.

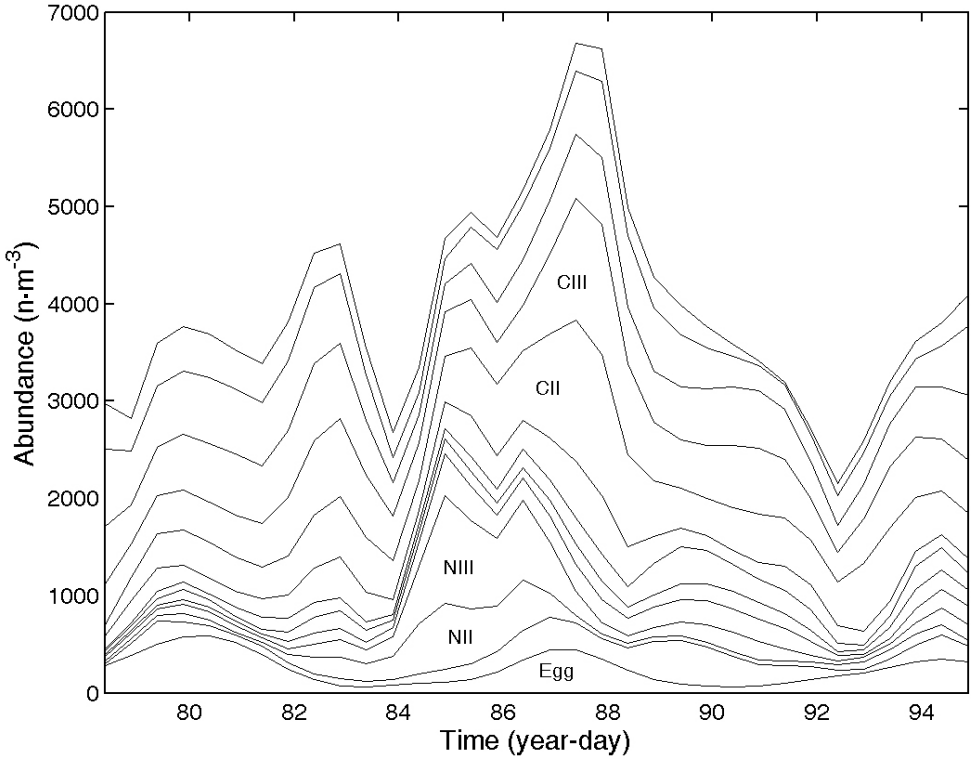

Figure 5.8: The stage composition estimated from field samples taken in March–April 2003. The egg abundance was estimated from Niskin water bottle samples taken during the sample period.

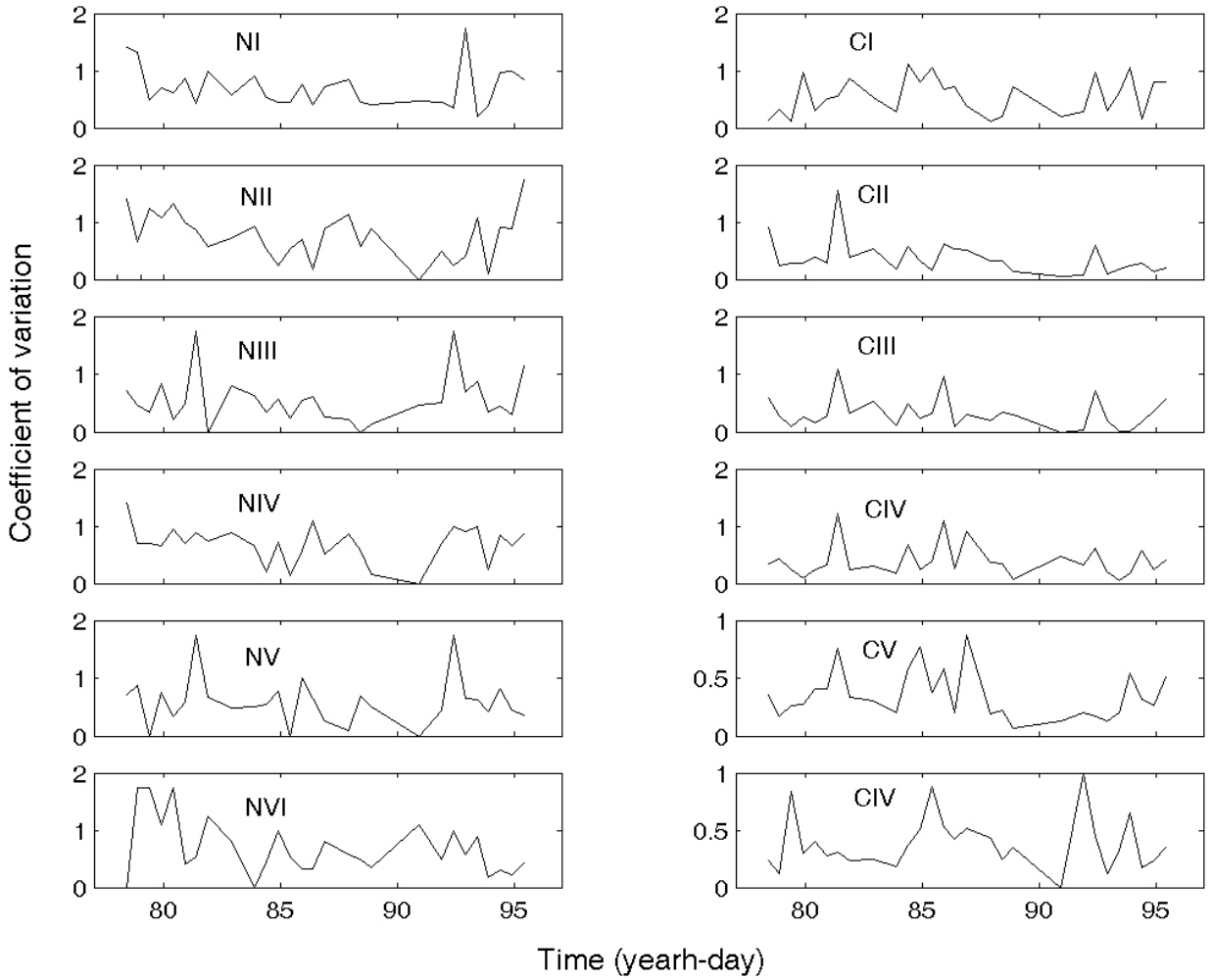

Figure 5.9: The coefficient of variation calculated from a time series of three replicate net samples taken in March–April 2003 for nauplii I–copepodite VI.

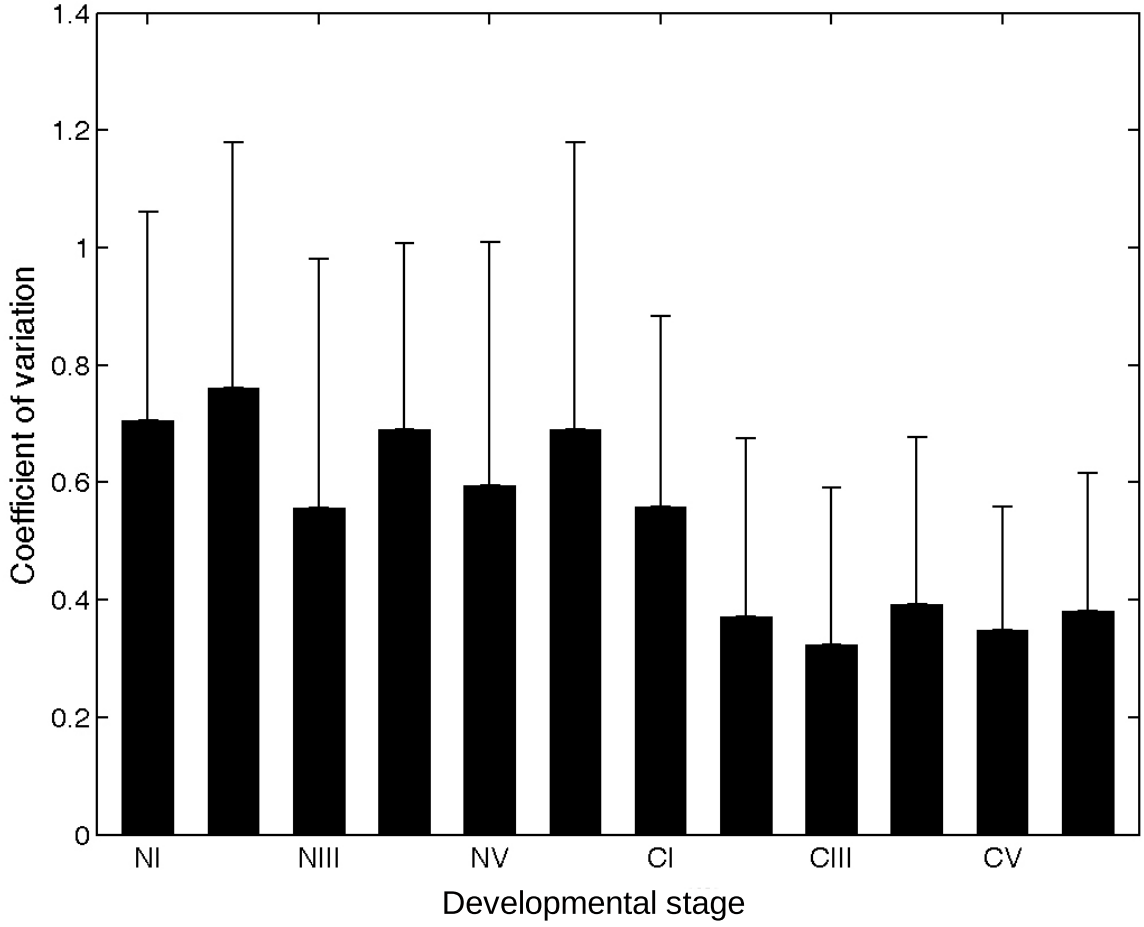

Figure 5.10: The mean coefficient of variation for nauplii I–copepodite VI during March–April 2003. Error bars represent one standard error.

physical processes, but also due to the uncertainty in the estimation of the population parameters, such as the egg production rate and stage–specific development times. The validity of the mortality rate estimation largely depends on the sampling variability, i.e., how well the data actually represent changes in stage composition for the underlying population. If high variability occurs, results should be interpreted with caution, e.g., the overestimation of mortality rates by the quadratic method. When samples had low variability, both the quadratic method and the inverse matrix method performed well in estimating stage–specific mortality rates. When samples had a relatively high variability, the inverse matrix method appeared to more suitable.

To properly estimate stage–specific mortality rates, particulary egg mortality rates, knowledge of the egg production rate at the population level is necessary. As shown in the present study, the accuracy of the egg production rate not only determines the accuracy of egg mortality rate, but also influences mortality rates for the adult stage and copepodite V for the inverse matrix method depending how much the provided rate deviated from the realistic value. The egg production rate is important not only for estimating mortality rate, but also for the understanding of population dynamics. Slight changes in egg production rate could also shift a declining population to a growing population. As a result the information on egg production rate at the population level should be emphasized.

Studies of copepod stage–specific mortality rates have focused on egg and early nauplii stages since the 1980s; however, the mortality rate in the adult stage should not be neglected. As indicated in Chapter 4, *Cl. furcatus* had a relative higher mortality rate at the adult stage than other copepodite stages (copepodite I–IV). Compared to egg and early nauplii stages, the population growth rate of *Cl. furcatus* is more sensitive to the survival rate and the recruitment rate for the adult stage. To validate the stage–specific mortality rates, it is necessary to continue to compare the estimates from the quadratic method and the inverse matrix method.

Further comparison between the quadratic method and the inverse matrix method under different conditions is warranted. The followings are some aspects that need to be addressed:

- How do the quadratic method and the inverse matrix perform with different mortality patterns, e.g., uniform patterns versus negative exponential patterns?
- How do the mortality estimates from these methods respond to the variability in development rates?
- How do the quadratic method and the inverse matrix method perform if the variability in stage composition followed different distributions, e.g., normal distribution or skewed distribution? and
- How do the quadratic method and the inverse matrix method perform when there is variability in both egg production rates and stage abundances?

5.6 Bibliography

Aksnes, D. L., Miller, C. B., Ohman, M. D., and Wood, S. N. 1997. Estimation techniques used in studies of copepod population dynamics — A review of underlying assumptions. *Sarsia*, 82:279–296.

Aksnes, D. L. and Ohman, M. D. 1996. A vertical life table approach to zooplankton mortality estimation. *Limnol. Oceanogr.*, 41:1461–1469.

Båmstedt, U. 1988. Ecological significance of individual variablity in copepod bioenergetics. *Hydrobiologia*, 167/168:43–59.

Bělehràdek, J. 1935. Temperature and living matter. *Protoplasma Monogr.*, 8:1–277.

Caswell, H. 2000. *Matrix Population Models: Construction, Analysis, and Interpretation*. Sinauer Associates Inc.

Diel, S. and Klein Breteler, W. C. M. 1986. Growth and development of *Calanus* sp. (Copepoda) during the spring phytoplankton succession in the North Sea. *Mar. Biol.*, 113:21–31.

Eiane, K., Aksnes, D. L., Ohman, M. D., Wood, S., and Martinussen, M. B. 2002. Stage-specific mortality of *Calanus spp.* under different predation regimes. *Limnol. Oceanogr.*, 47:636–645.

Eiane, K. and Ohman, M. D. 2004. Stage-specific mortality of *Calanus finmarchicus, Pseudocalanus elongatus* and *Oithona similis* on Fladen Ground, North Sea, during a spring bloom. *Mar. Ecol. Prog. Ser.*, 268:183–193.

Hall, C. J. and Burns, C. W. 2001. Effects of salinity and temperature on survival and reproduction of *Boeckella hamata* (Copepoda: Calanoida) from a periodically brackish lake. *J. Plankton Res.*, 23:97–103.

Halsband-Lenk, C., Hirche, H. J., and Carlotti, F. 2002. Temperature impact on reproduction and development of congener copepod populations. *J. Exp. Mar. Biol. Ecol.*, 271:212–153.

Hirche, H. J., Brey, T., and Niehoff, B. 2001. A high–frequency time series at Ocean Weather Ship Station M (Norwegian Sea): population dynamics of *Calanus finmarchicus*. *Mar. Ecol. Prog. Ser.*, 219:205–219.

Hirche, H. J., Meyer, U., and Niehoff, B. 1997. Egg production of *Calanus finmarchicus*: effect of temperature, food and season. *Mar. Biol.*, 127:609–620.

Hirst, A. G. and Kiørboe, T. 2002. Mortality in marine planktonic copepods: Global rates and patterns. *Mar. Ecol. Prog. Ser.*, 230:195–209.

Huntley, M. E. and Lopez, M. D. G. 1992. Temperature–dependent production of marine copepods: A global synthesis. *Am. Nat.*, 140:201–242.

Huntley, M. E. and Niiler, P. P. 1995. Physical control of population dynamics in the Southern Ocean. *ICES J. Mar. Sci.*, 52:457–468.

Ianora, A. and Poulet, S. A. 1993. Egg viability in the copepod *Temora stylifera*. *Limnol. Oceanogr*, 38:1615–1626.

Kiørboe, T. and Nielsen, T. G. 1994. Regulation of zooplankton biomass and production in a temperate, coastal ecosystem. 1. Copepods. *Limnol. Oceanogr.*, 39:393–507.

Landry, M. R. 1983. The development of marine calanoid copepods with comment on the isochronal rule. *Limnol. Oceanogr.*, 28:614–624.

Liang, D. and Uye, S. 1997. Population dynamics and production of the planktonic copepods in a eutrophic inlet of the Inland Sea of Japan IV. *Pseudodiaptomus marinus*, the egg-carrying calanoid. *Mar. Biol.*, 128:415–421.

Mauchline, J. 1998. The biology of calanoid copepods. *Adv. Mar. Biol*, 33:710.

McCauley, E. and Murdoch, W. W. 1990. Predator–prey dynamics in environments rich and poor in nutrients. *Nature*, 343:455–457.

Miliou, H. and Moraitou-Apostologpoulou, M. 1991. Combined effects of temperature and salinity on the popualtion dynamics of *Tisbe holothuriae* Humes (Copepods: Harpacticoida). *Arch. Hydrobiol.*, 121:289–319.

Miralto, A., Barone, G., Romano, G., Poulet, S. A., Ianora, A., Russo, G. L., Buttino, I., Mazzarella, G., Laabir, M., Carini, M., and Giacobbe, M. G. 1999. The insidious effect of diatoms on copepod reproduction. *Nature*, 402:173–176.

Mullin, M. M. 1993. Reproduction by the oceanic copepod *Rhincalanus nasutus* off southern California, compared to that of *Calanus pacificus*. Technical report.

Ohman, M. D. 1986. Predator–limited population growth of the copepod *Pseudocalanus* sp. *J. Plankton Res.*, 8:673–713.

Ohman, M. D., Aksnes, A. J., and Runge, J. A. 1996. The interrelationship of copepod fecundity and mortality. *Limnol. Oceanogr.*, 41:1470–1477.

Ohman, M. D., Eiane, K., Durbin, E. G., Runge, J. A., and Hirche, H. J. 2004. A comparative study of *Calanus finmarchicus* mortality patterns at five localities in the North Atlantic. *ICES J. Mar. Sci.*, 61:687–697.

Ohman, M. D., Runge, J. A., Durbin, E. G., Field, D. B., and Niehoff, B. 2002. On birth and death in the sea. *Hydrobiologia*, 480:55–68.

Ohman, M. D. and Wood, S. N. 1995. The inevitability of mortality. In *Zooplankton production*, volume 52 of *Proceedings of a symposium held in Plymouth, England, 15–19 AUGUST 1994.*, pages 517–522, LONDON (UK). ACADEMIC PRESS.

Ohman, M. D. and Wood, S. N. 1996. Mortality estimation for planktonic copepods: *Pseudocalanus newmani* in a temperate fjord. *Limnol. Oceanogr.*, 41:126–135.

Paffenhöfer, G. A. 2002. An assessment of the effects of diatoms on planktonic copepods. *Mari. Ecol. Prog. Ser.*, 227:305–310.

Paul, A. J., Coyle, K. O., and Ziemann, D. A. 1990. Variation in egg production rates by *Pseudocalanus* spp. in a subarctic Alaskan bay during the onset of feeding by larval fish. *J. Crust. Biol.*, 10:648–658.

Peterson, W. T. 1988. Rates of egg production by the copepod *Calanus marshallae* in the laboratory and in the sea off Oregon, USA. *Mar. Ecol. Prog. Ser.*, 47:229–237.

Peterson, W. T. and Kimmerer, W. J. 1994. Processes controlling recruitment of the marine calanoid copepod *Temora longicornis* in Long Island Sound: Egg production, egg mortality, and cohort survival rates. *Limnol. Oceanogr.*, 39:1594–1605.

Plourde, S. and Runge, J. A. 1993. Reproduction of the planktonic copepod *Calanus finmarchicus* in the lower St. Lawrence estuary: Relation to the cycle of phytoplankton production and evidence for a *Calanus* pump. *Mar. Ecol. Prog. Ser.*, 102:217–227.

Roff, D. 1992. *The evolution of life histories: theory and analysis*. Chapman & Hall.

Runge, J. A., Durbin, E., Plourde, S., and Gratton, Y. 1997. Spatial and temporal variation in egg production of *Calanus finmarchicus* on Georges Bank: implications of the productivity of prey of cod and haddock larvae. In *GLOBEC: Results from Interdisciplinary Programs in the North Atlantic*, Baltimore. ICES Annual Meeting.

Stearns, S. C. 1992. *The evolution of life histories*. Oxford University press.

Takahasshi, T. and Ohno, A. 1996. The temperature effect on the development of calanoid, copepod, *Acartia tsuensis*, with some comments to morphogensis. *J. Oceanogr.*, 52:125–137.

Twombly, S. 1994. Comparative demography and population dynamics of two coexisting copepods in a Venezuelan floodplain lake. *Limnol. Oceanogr.*, 39:234–247.

Wood, S. N. 1994. Obtaining birth and mortality patterns from structured population tragjectories. *Ecol. Monogr.*, 64:23–44.

Wood, S. N. and Nisbet, R. M. 1991. Estimation of mortality rates in stage-structured populations. In *Lecture Notes in biomathematics*, volume 90, pages 1–101. Springer–Verlag.

CHAPTER 6 CONCLUSION

6.1 Zooplankton Communities

Interactions between physical and biological processes are important in structuring zooplankton communities. In the present study, the Mississippi River plume frequently influenced the local zooplankton community in the study site ST151. Tidal currents introduced two periodic components to changes in total zooplankton abundance: a daily fluctuation associated with the change from high tide to low tide; and a 14 day fluctuation associated with the transition from spring to neap tides. Strong river plume events were identified during the study period indicating the presence of a low salinity riverine water mass within at the platform. Total zooplankton abundance was inversely correlated with surface salinity and experienced up to an order of magnitude variation. Estuarine copepod species, such as *Acartia tonsa* and *Labidocera nerri*, explained most of the variations in total abundance.

A low salinity assemblage and a high salinity assemblage were identified. The low salinity group was characterized by estuarine species, such as *A. tonsa* and *L. nerri*. The high salinity group was characterized by oceanic species, such as *Clausocalanus furcatus*. Salinity was used as a proxy for different water masses and shifts between two assemblages were associated with the presence or absence of Mississippi River plume water. The abundances of the copepods *A. tonsa*, *L. nerri*, *Eucalanus attenatus* and *Cl. furcatus* mainly responded to changes in salinity. The copepods *Centropages furcatus*, *Corycaeus clausii* and the chaetognath *Sagitta enflata* increased in abundance with increasing water temperature, while the density of larvaceans *Oikopleura* spp. and the copepod *Oncaea mediterranea* decreased in abundance with increasing temperature. Other factors, such as changes in food regime and chemical composition of ambient water may also influence the changes in species abundance.

6.2 Population Dynamics of *Cl. furcatus*

Clausocalanus furcatus was a common oceanic species and made up a notable portion of total mesozooplankton abundance at the study site. The species gradually increased its abundance through the entire study period (March–June) and its local abundance was influenced by the Mississippi River plume. Knowledge about the population dynamics of *Cl. furcatus* is limited. Egg production rates, stage–specific development times and stage specific mortality rates are essential parameters to describe population dynamics and the estimation of secondary production.

6.2.1 Egg Production Rates

Laboratory incubations showed that *Cl. furcatus* females frequently carried their eggs within a fragile egg mass of 12–18 eggs. Eggs were also extruded in clutches of 4–7 eggs by adult females. Field evidence indicated that most of the eggs collected with Niskin water bottles were solitary (90%) or in groups of 2–9 eggs. The present study supported the occurrence of a fragile and irregular egg mass. This research also indicated that the development and hatching of eggs appeared to be independent of parental care.

The mean egg production rate (± standard error), estimated from field samples, was 1.67 ± 0.27 eggs female^{-1} day^{-1}, and was lower than the mean of 12.08 ± 1.40 eggs female^{-1} day^{-1}, measured from incubation experiments. Spawning activities appeared to be higher during night than day based on field samples. The Edmonson egg ratio method may provide lower estimates of the production rate due to time lag, sinking loss and predation, and the incubation method appeared to overestimate the egg production rate. Such a difference in the egg production rate could alter the population trajectories because simulations revealed that population growth rates were very sensitive to changes in the egg production rates. More field data and incubation experiments are necessary to determine the realistic egg production rate.

Particulate organic carbon (POC) concentrations did not show large variation during the two study periods: March-April and May-June. Neither POC concentrations nor the egg production rates showed significant differences among 5, 15, and 25m depth. The egg production rate in March–April was significantly higher than that in May–June. Food availability did not appeared to be a limiting factor for the egg production rate in the study area. Moreover, incubation–derived estimates egg production were very similar over the coverage of the study. Since egg production rates were generally thought to be indicators of food availability, these constant and high production rates support the hypothesis that food was not limiting.

6.2.2 Stage–specific Development Times

The development times of *Cl. furcatus* from hatching to adulthood ranged from ~13–20 days. The development patterns of *Cl. furcatus* are: egg and naupliar stages I–III have a relatively short duration of ~17–24h; development in NIV and NV are prolonged and NVI has a relatively short duration; copepodite stages (I–IV) have similar durations to late naupliar stages; copepodite stage V has a prolonged duration, that is much longer than other early stages.

6.2.3 Stage–specific Mortality Rates

Knowledge of copepod stage–specific mortality rates is essential to understand copepod population dynamics. However, estimating mortality rates is complicated by the gear selection, the mobility of different stages, and sampling variability caused by patchiness, immigration and emigration. Field samples in the present study were taken from a fixed location in a dynamic environment and the stage composition data may not reflect a well defined population.

The horizontal life table could not produce realistic estimates in many cases due to the variability in the stage composition data. By constraining nonnegative mortality rates, the horizontal life table overestimated stage–specific mortality rates. The vertical life table was

applied to the averaged stage composition in March–April and May–June. The vertical life table also produced negative mortality rates. Neither the horizontal life table method nor the vertical life table method could provide an estimate of mortality for the adult stage.

The quadratic method estimates the stage–specific mortality rates by minimizing the quadratic term for the difference between the modeled data and observed data. The inverse matrix method uses a Gauss–Marquardt–Levenburg algorithm to minimize the difference between the modeled data and observed value. Simulations indicated that the quadratic method overestimated mortality rates in the present study. The mortality rates estimated by the inverse matrix method appeared to be more consistent with the field data.

The mortality rates estimated by the inverse matrix method were comparable with other studies as discussed in chapter 5. The highest mortality rate occurred in eggs (1.27 day^{-1} in March–April and 1.6 day^{-1} in May–June), with relative low mortality rates for the subsequent stages (NII–CVI), while the adult stage had a relative high mortality rate (0.37 day^{-}1 in March–April and 0.32 day^{-1} in May–June). In March–April, the copepodite stage V experienced a higher mortality rate than other copepodite stages (0.77 day^{-1}).

6.2.4 Factors Influencing Mortality Rate Estimations

In a closed population, changes in stage composition can be explained by population parameters (the egg production rate, stage–specific development times and stage–specific mortality rates. When estimating mortality rates from field data, the accuracy of the egg production rate and how well the sample reflects the underlying population.

The egg mortality estimate was influenced by the changes in the provided egg production rate. When the provided egg production rate deviated slightly from the true egg production rate, the quadratic method only changed the egg mortality estimate while estimates for other stages remained unchanged. If the provided egg production rate deviated substantially from

the true egg production rate (by 100% or more), the egg mortality rate estimation remained the same, as well as estimates for other development stages. When the provided egg production rate deviated from the realistic egg production rate, the inverse matrix method changed the estimate for egg mortality and it also changed the estimate for the adult stage accordingly. For example, when the provided egg production rate was higher than the true egg production rate, it increased the estimate for egg mortality and at the same it also increased the mortality estimate for the adult stage.

Both the quadratic method and the inverse matrix method were sensitive to the variability in the stage composition data, which was indicated by the coefficient of variation (CV) in the present study. When the variability was low ($CV = 0.05$), both methods could recover the stage–specific mortality rates. As the CV increased, the quadratic method consistently over-estimated stage–specific mortality rates ($CV > 0.05$), but the mortality patterns remained the same as the known patterns. The inverse matrix method appeared to have the ability to recover the stage–specific mortality when CV was less than 0.10. The inverse matrix method responded to the changes in variability by changing the mortality estimates for eggs and copepodites IV–VI. A consistency between the quadratic method and the inverse matrix method could be used as a validation for estimated mortality rates.

The importance of the adult stage mortality should be emphasized. As the only stage capable of producing eggs, the population growth rate of *Cl. furcatus* appeared to be more sensitive to the survival rate and recruitment rate for the adult stages than other development stages. Accurate estimation of the egg production rate at population level is important, because it determined not only the accuracy of egg mortality estimate, but also the population growth rate. Slight changes in the egg production rate could alter a declining population to a growing one.

6.3 Estimation of Production of *Clausocalanus furcatus*

The total body length for each developmental stage can be derived from Equation 6.1(Mauchline 1998).

$$\log TL = a \times N_s - b \tag{6.1}$$

where, TL is total body length, N_s is the stage number, and a and b are coefficients (a = 0.1902, b = 2.0228).

Dry weights for copepodite stages can be calculated from prosome body length using a length–weight model (Equation 6.2, Ara 2001). Carbon content was assumed to be 44.6% of dry weight (Ara 2001). In this study, I used the mean stage abundance estimated from three replicate net tows from 15m to surface to derive the standing stock and the carbon flux for each developmental stage.

$$DW = 1.471 \times 10^{-8} \times PL^{3.064} \tag{6.2}$$

where, DW is dry weight, and PL is prosome length.

Assuming all the individuals within each stage either developed into the consecutive stage or died, the biomass of *Cl. furcatus* gradually increased from eggs to copepodite IV in March–April and May–June (Figure 6.1). Copepodite stages (I–IV) appeared to gain more carbon than nauplii stages. Later copepodite stages (IV–VI) lost carbon to the environment and the carbon loss due to mortality in March–April (187.92 μg m^{-3}) was two times higher than in May–June (85.30 μg m^{-3}). The carbon flow corresponding to the reproduction in March–April was about an order of magnitude higher than in May–June. The net carbon increment from egg to the adult stage was slight higher in March–April (64.11 μg m^{-3}) than May–June (47.62 μg m^{-3}). The increment of carbon content for each stage can be estimated from the standing biomass and input from the previous stage. The carbon budget was unbalanced in the adult stage in both periods, in nauplii V in March–April and in copepodite II in May–June. These unbalanced

carbon budgets might be associated with (1) sampling variability; (2) stage composition at the initial and terminal samples; and (3) copepodite V had a relative long stage duration, which suggested some of the survivals might not develop into the adult stage.

6.4 Bibliography

Ara, K. 2001. Length–weight relationships and chemical content of the planktonic copepods in the Cananéia Lagoon estuarine system, São Paulo, Brazil. *Plankton Biol. Ecol.*, 48:121–127.

Mauchline, J. 1998. The biology of calanoid copepods. *Adv. Mar. Biol*, 33:710.

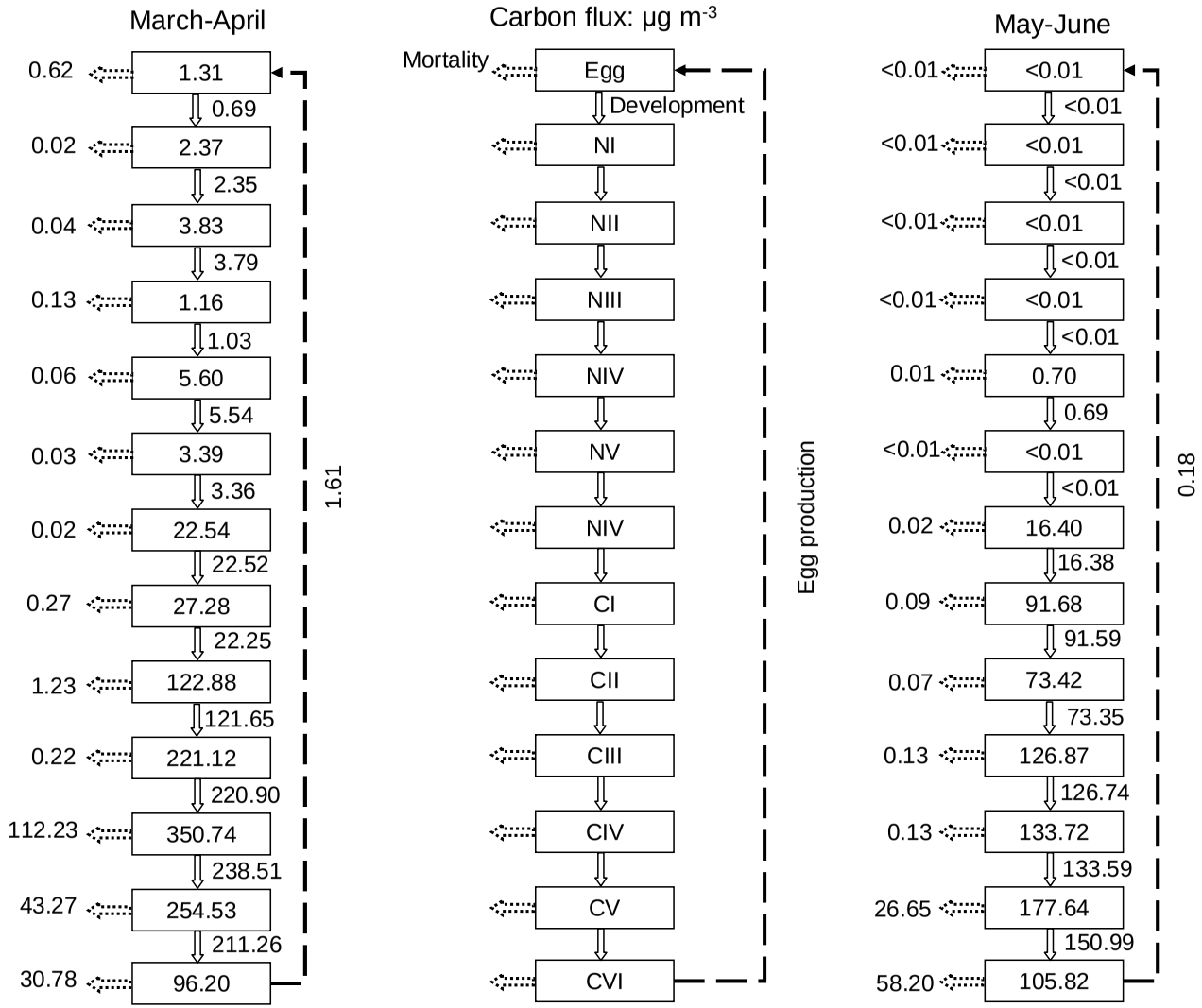

Figure 6.1: A schematic diagram showing the standing stock and carbon flux among different developmental stages (eggs, nauplii I–VI, and copepodite I–VI) in March–April and May–June.

APPENDIX A RESIDUAL PLOTS FOR REGRESSION ANALYSIS

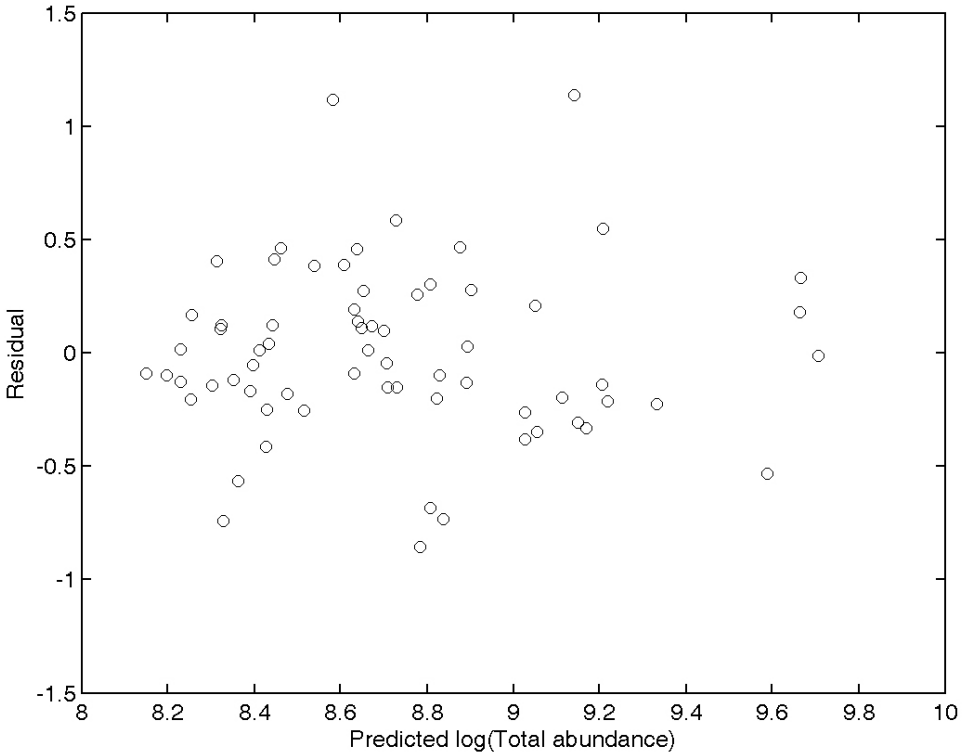

Figure A.1: The residual–by–predicted plot for the regression model in Chapter 1: Total abundance = 37382 - 497.14 × temperature -630.06 × salinity. Residuals were calculated from by the difference between the predicted and the observed value.

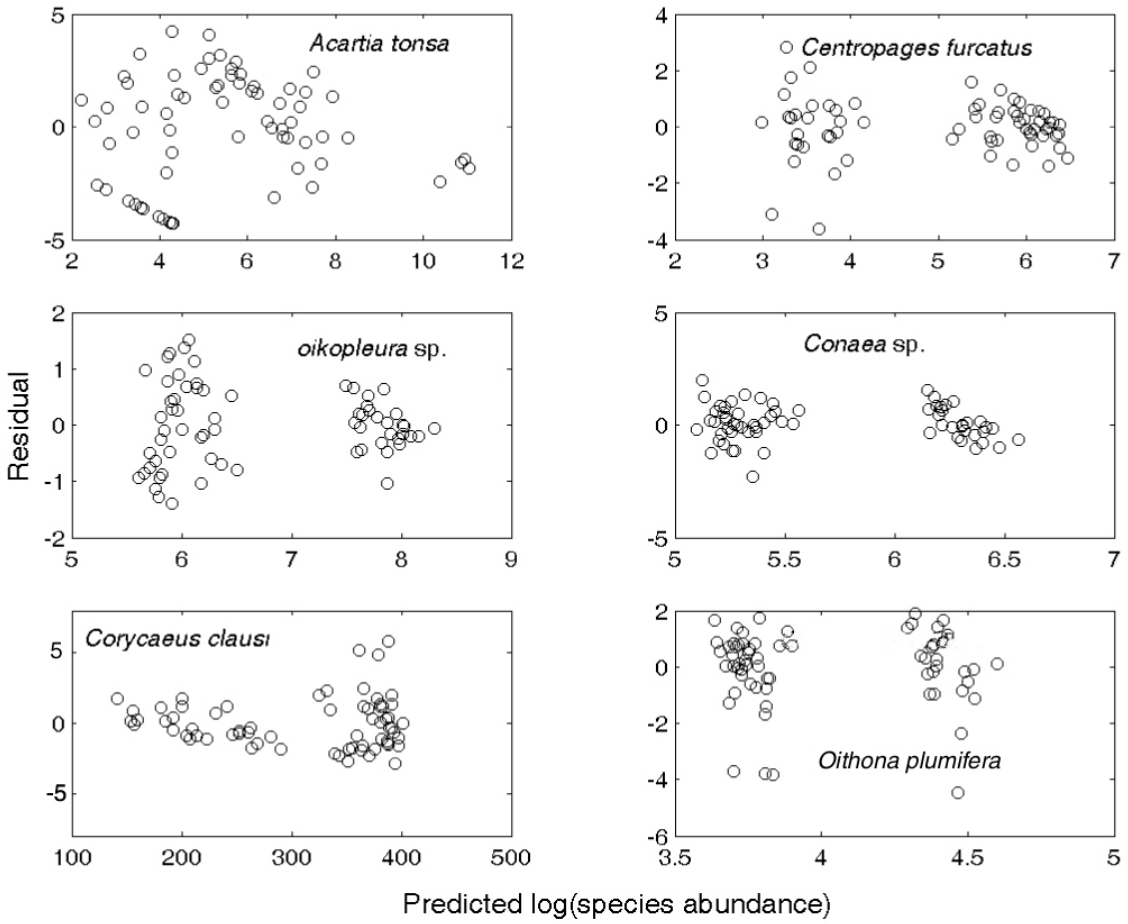

Figure A.2: The residual–by–predicted plots for the regression model in Chapter 1: Species abundance = $A \times$ *temperature* + $B \times$ *salinity* + C. Residuals were calculated from by the difference between the predicted and the observed value.

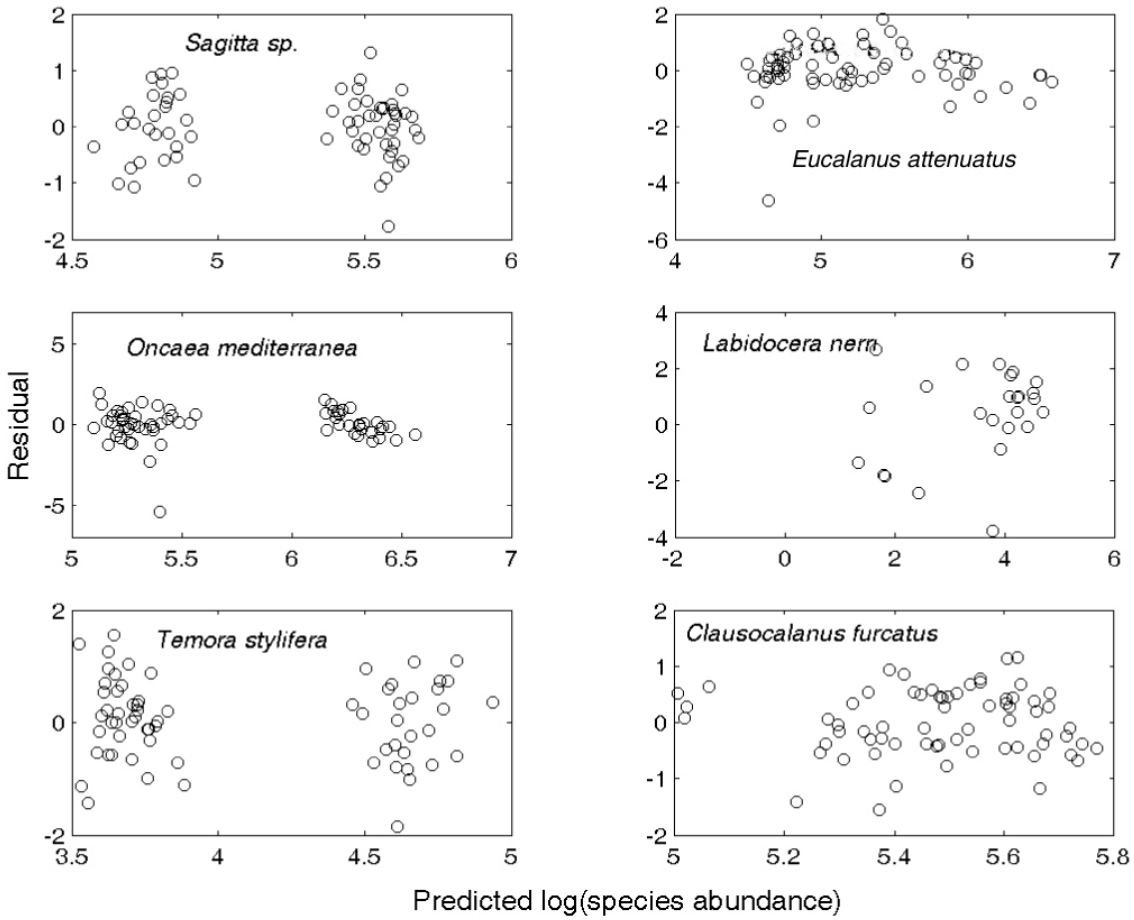

Figure A.2 Continued

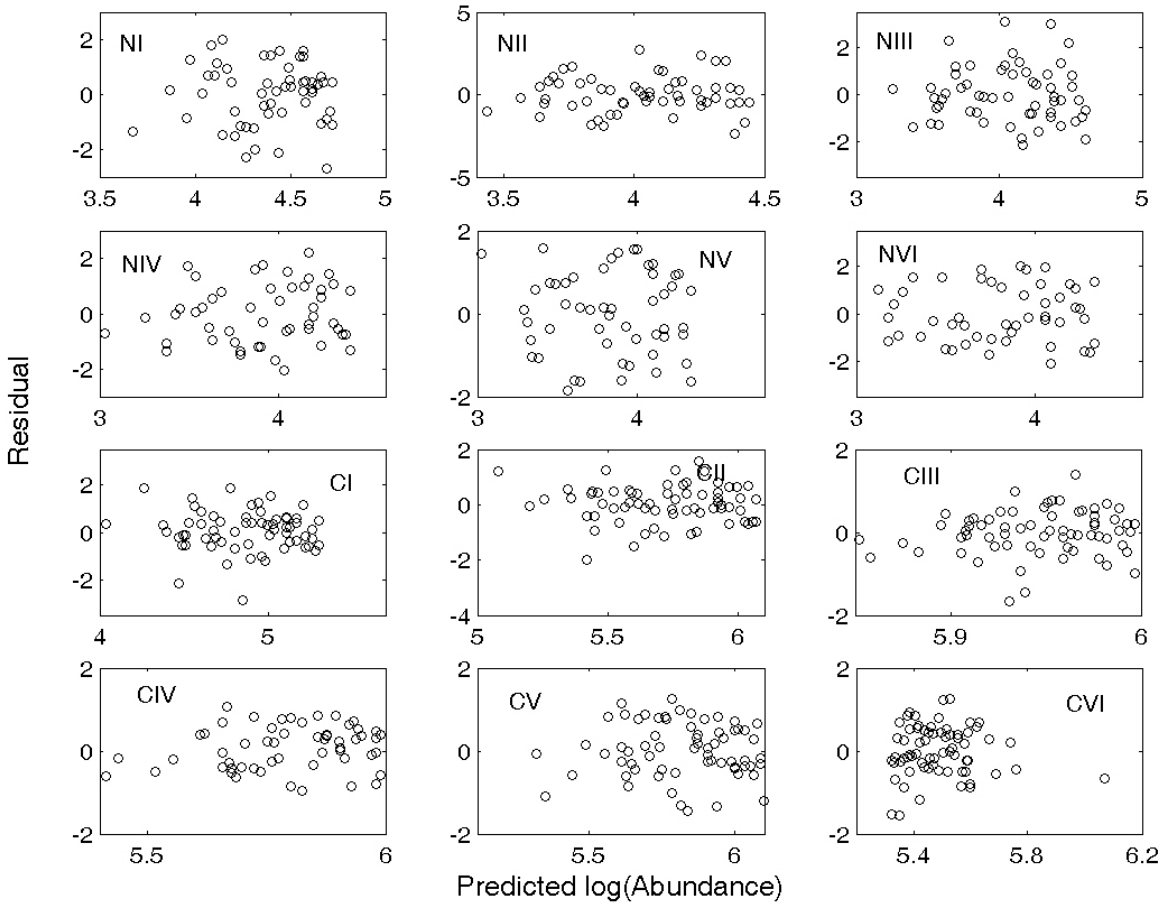

Figure A.3: The residual–by–predicted plots for the loglinear model in Chapter 4: log (Stage abundance) = $\beta_0 + \beta_1 \times$ (Chaetognath abundance). Residuals were calculated from by the difference between the predicted and the observed value.

APPENDIX B EXAMPLE CODE FOR QUADRATIC IN MATLAB

The following is an example m–file containing code to estimate mortality from net tows samples taken during March–April 2003. A cubic spline fit was first applied to get equal time intervals.

```
%pop is a matrix (41 by 13) hold the stage composition data.
nout=pop';
z=nout(:, 2:41);
z1=z(:);
% The following part formulates a vector that contains the nonzero elements in the 13 by 13 % transitional matrix.
nonzero=[1 2 15 16 29 30 43 44 57 58 71 72 85 86 99 100 113 114...
127 128 141 142 155 156 157 169];
M=[];
for i=1:40;
N=kron(nout(:,i)',eye(13));
m=N(:,nonzero);
M=[M;m];
end;
% Generate matrix G and vector f for the quadprog in the optimization toolbox.
G=M'*M;
f=-M'*z1;
b=zeros(39, 1);
for i=27:39;
b(i, 1)=1;
end;
```

```
c=zeros(39,26);
for i=1:26
c(i,i)=-1;
end;
for k=27:39;
j=(k-26)*2;
c(k,j)=1;
c(k,j-1)=1;
end;
c(39, 25)=0;
lb=zeros(26, 1);
ub=ones(26,1);
% Set lower boundary for the nonzero elements.
for i=1:12;
lb(2*i-1,1)=0;
lb(2*i, 1)=bb1(i,1);
end;
lb(25, 1)=1.33;
% Set upper boundary for the nonzero elements.
for i=1:12;
if(temp2¿1) temp2=0.75; end;
ub(2*i-1,1)=1-temp2;
temp2=12.0/duration(1, i);
ub(2*i, 1)=temp2;
end;
```

```
ub(25, 1)=1.33;
phat=quadprog(G,f, c, b,[],[],lb, ub);
a=zeros(169,1);
a(nonzero)=phat;
a=reshape(a, 13, 13);
for i=1:12;
death(1, i)=1-a(i, i)-a(i+1,i);
end;
death(1,13)=1-a(13, 13);
```

VITA

Hongsheng was born in Rongcheng, Shandong Province, People's Republic of China, on September 27, 1971. He graduated from Dongshan High School in 1990. He then attended Ocean University of Qingdao, where he received a Bachelor of Science degree in marine aquaculture. Hongsheng then entered Institute of Oceanography Chinese Academy of Sciences and received a Master of Science degree in marine ecology in 1996. After working for two years as a research associate in the Institute of Oceanography Chinese Academy of Sciences, he attended the University of Georgia to study organic chemistry in 1998. Shortly thereafter, he transferred into the doctoral program in the Department of Oceanography and Coastal Sciences at Louisiana State University in 1999.